IMMUNE RESPONSE AND ESSENTIAL OIL ACTIVITY AGAINST PATHOGENIC *CANDIDA* SPECIES

Lotte MATHÉ

Supervisors:
Prof. dr. P. Van Dijck
Prof. dr. A. Liston

Members of the Examination Committee:
Prof. dr. P. Cos
Dr. S. Kucharíková
Prof. dr. K. Lagrou
Prof. dr. L. Moons
Prof. dr. J. Thevelein

Dissertation presented in partial fulfillment of the requirements for the degree of Doctor of Science (PhD): Biology

October 2017

Uitgegeven in eigen beheer, Lotte Mathé, Kessel-Lo

Acknowledgements

After several months of writing and editing, today is the day to put the finished touch to my thesis by writing this section. It has been a very interesting and challenging period of learning. Not only about the wonderful world of *Candida*, but also on a personal level. However, I could not have reached this point if it wasn't for the help of so many people.

I would first like to thank my supervisor Prof. Patrick Van Dijck. Thanks for your guidance and for giving me the opportunity to do my research in your lab. You were always willing to listen to any research-issues, to look for solutions, and to give feedback on my work. I would like to thank my co-supervisor Prof. Adrian Liston and my assessors Prof. Katrien Lagrou, Dr. Soňa Kucharíková, and Dr. Hélène Tournu. Thank you for your valuable input into steering my research in the right direction and for training me in the lab. I would like to thank Prof. Paul Cos, Prof. Lieve Moons, and Prof. Johan Thevelein for allocating time to being part of my examination committee, and for worthy remarks on my preliminary thesis and defense. I would like to thank Dr. Erwin Swinnen and Dr. Michelle Holtappels for proofreading parts of this thesis. I would like to thank KU Leuven, VIB and all other financing sources for making this research possible.

The two projects presented in this thesis could not have been what they are today without Jossy and Adam. Jossy, thank you for making the countless hours in the lab more fun with your stories, for always being willing to answer my questions, and for your input on several parts of this thesis. Adam, thank you for giving me the opportunity to work with you on the essential oil project, for the interesting discussions about our research, and for the small talk during lunch. Thank you both for the pleasant collaboration!

I would like to thank Cindy, Celia and Ilse. Thank you for your excellent assistance in the lab, for answering all my questions, for always being willing to help, and for cheering up the *Candida* lab. Thank you, Martine, Renata, and Thomas for sharing your qPCR expertise, providing strains from the stock, and for making sure that enough plastic ware was available. Thanks to Hilde, Leni, Jan, Timmy and Nico for logistic support, for organizing the retreats to Blankenberge, and for all the help with technical issues. Without all of you, the lab would not run so smoothly. Thanks to Dr. Françoise Dumortier for arranging the lab meetings and as such giving us an opportunity to get feedback on our research.

Thanks to Liesbeth, Sanne, Bea, Winnie, Yuke, Floris, Ana, and all other (former) *Candida* and MCB lab members for the fun atmosphere inside and out of the lab. Thanks to the members

of the Translational Immunology lab for being so welcoming. Thanks to my (former) office mates for fun times in the office, and particularly to Paul for advice on parts of this work.

I would like to thank my family, family in law and friends for asking about my research, but also for helping me take my mind of my research. Thank you so much mama, papa and Nele for your continuous interest and unconditional support. You are the best! Finally, thank you Jef for your endless patience and support, for always making me smile, and so much more. In short, for being the best husband I could wish for!

September 10, 2017 – Kessel-Lo

Summary

Candida albicans biofilms on medical implant devices are a major risk factor for the development of systemic candidiasis. In the first part of this thesis, we research why *C. albicans* biofilms on medical implant devices are not readily cleared by the host immune system. Using a subcutaneous catheter model system in mice that was first optimized to fit our goal, we could detect efficient immunization in response to subcutaneous biofilms. This was evidenced by a higher survival rate after a lethal systemic challenge in mice immunized with subcutaneous biofilms compared to naïve mice. This proves that biofilms on subcutaneous catheters are detected by the immune system, and that immunological silence *i.e.* a total incapability of the immune system to detect the biofilms, is not responsible for the immune evasion of biofilms. Moreover, the efficient immunization mounted in response to the biofilm, which fails to eradicate the biofilm, can be interpreted as immunoresistance, rendering the biofilm resistant to an efficient immune response. Other results obtained were not sufficient to confirm nor reject the hypothesis of immunomodulation, which claims that the biofilm steers the immune response towards an ineffective one. These results lay a foundation for future experiments that can aim at establishing the importance of immunomodulation and immunoresistance in the clinical setting and at uncovering immune cell types involved in these processes. Gaining this knowledge is needed for the development of immunotherapies against *C. albicans* biofilms.

Not only the high resistance of *Candida* biofilms, but also the fact that more and more *Candida* infections are caused by intrinsically resistant (and multi-resistant) *Candida* isolates makes that the search for new ways of treating infections is urgent. In the second part of this thesis, we developed the vapor-phase-mediated patch and susceptibility assays for the detection and quantification, respectively, of the vapor-phase-mediated activity of volatiles. When testing a collection of 175 essential oils and 37 highly enriched essential oil components for their growth inhibitory effect against *C. albicans* and *C. glabrata* using the vapor-phase-mediated susceptibility assay, we observed growth inhibitory vapor-phase-mediated antimicrobial activity for approximately half of the essential oils and components tested. Moreover, *C. glabrata* showed a higher overall susceptibility to the essential oils and components than *C. albicans*. This was particularly true for essential oils rich in the essential oil component citronellal and citronellal itself. Being able to assess the vapor-phase-mediated antimicrobial activity in a reliable manner will help in the search for novel antimicrobials and will broaden the application potential of currently existing ones.

Samenvatting

Biofilmen gevormd door *Candida albicans* op medische implantaten zijn een belangrijke risicofactor voor een systemische *Candida* infectie. In het eerste deel van deze thesis onderzoeken we waarom *C. albicans* biofilmen op medische implantaten niet verwijderd worden door het immuunsysteem van de gastheer. Door gebruik te maken van een subcutaan katheter modelsysteem in muizen, dat eerst geoptimaliseerd werd met ons doel voor ogen, observeren we een toegenomen overleving van muizen geïmmuniseerd met subcutane biofilmen, na een hierop volgende systemische injectie met een lethale dosis *C. albicans,* vergeleken met muizen die niet geïmmuniseerd werden. Dit bewijst dat biofilmen op subcutane katheters worden gedetecteerd door het immuunsysteem, en dat het immuunsysteem dus niet volledig blind is voor de aanwezigheid van een biofilm. Verder ondersteunt het onze hypothese van immunoresistentie door aan te tonen dat een efficiënte immuunrespons wordt geïnduceerd in respons op de biofilmen, maar dat de biofilm zelf hiertegen resistent is. Andere resultaten zijn niet voldoende om de hypothese van immunomodulatie door de biofilm (= het actief sturen van de immuunrespons naar een minder efficiënte) te ondersteunen of te verwerpen. Deze resultaten leggen een basis voor toekomstige experimenten die de rol van immunomodulatie en immunoresistentie in een klinische setting verder kunnen onderzoeken en die verder licht kunnen werpen op de rol van verschillende celtypes in de immuunrespons tegen biofilm infecties op medische implantaten.

Naast de hoge resistentie van *Candida* biofilmen, zorgt ook de toename van (multi-)resistente klinische *Candida* isolaten ervoor dat de zoektocht naar nieuwe antischimmelproducten belangrijk is. In het tweede deel van de thesis ontwikkelen we daarom de vapor-phase-mediated patch en susceptibility assays, die kunnen gebruikt worden voor de detectie en de kwantificatie, respectievelijk, van dampfase-gemedieerde activiteit van volatiele moleculen. Van de 175 geteste essentiële oliën en de 37 geteste, hoog aangereikte essentiële olie componenten vertonen ongeveer de helft een groei-inhiberende activiteit tegen *C. albicans* en/of *C. glabrata* wanneer getest met behulp van de vapor-phase-mediated susceptibility assay. Verder tonen we aan dat *C. glabrata* een hogere algemene gevoeligheid vertoont aan de essentiële oliën en componenten dan *C. albicans*. Dit was vooral het geval voor essentiële oliën rijk aan de component citronellal, en citronellal zelf. De geïntroduceerde assays bieden de mogelijkheid om de dampfase-gemedieerde activiteit van volatiele bioactieve moleculen op een betrouwbare manier te onderzoeken. Dit zal helpen in de zoektocht naar nieuwe antimicrobiële middelen en de toepassingsmogelijkheden van bestaande middelen verhogen.

Abbreviations

ABC	ATP binding cassette
AmB	Amphotericin B
ANOVA	Analysis of variance
BSI	(*Candida*) Bloodstream infection
C. albicans	*Candida albicans*
C. glabrata	*Candida glabrata*
cAMP	Cyclic adenosine monophosphate
CC	Clean catheter
CFU	Colony forming unit
CLR	C-type lectin receptor
CLSI	Clinical Laboratory Standards Institute
CMC	Chronic mucocutaneous candidiasis
ct	Chemotype
DC	Dendritic cell
ECM	(Biofilm) Extracellular matrix
eDNA	Extracellular DNA
EO(C)	Essential oil (component)
EUCAST	European Committee on Antimicrobial Susceptibility Testing
FDA	Food and Drug Administration
Foxp3	Forkhead box P3
G-CSF	Granulocyte colony-stimulating factor
GM-CSF	Granulocyte-macrophage colony-stimulating factor
GPI	Glycosylphosphatidylinositol
HBF	High biofilm forming isolate
i.v.	Intravenous
IC	Immunocompetent / Mice immunized with infected catheter pieces
IFN	Interferon
IL	Interleukin
IS	Immunosuppressed
IV	Mice immunized with low dose i.v. injection
iVMAA	Inhibitory vapor-phase-mediated antimicrobial activity
KO	Knockout
LBF	Low biofilm forming isolate

MALDI-TOF MS	Matrix assisted laser desorption/ionization-time of flight mass spectrometry
MAPK	Mitogen-activated protein kinase
MBL	Mannose-binding lectin
MIC	Minimal inhibitory concentration
MRD	Modified robbins device
NAC	Non-*albicans Candida*
NET	Neutrophil extracellular trap
NLR	NOD-like receptor
NLRP3	NOD-, LRR- and pyrin domain-containing 3
OPC	Oropharyngeal candidiasis
PAMP	Pathogen-associated molecular pattern
PBMC	Peripheral blood mononuclear cell
PKA	Protein kinase A
PMN	Polymorphonuclear leukocyte
PRR	Pattern recognition receptor
(R)VVC	(Recurrent) Vulvovaginal candidiasis
RNS	Reactive nitrogen species
ROS	Reactive oxygen species
S. aureus	*Staphylococcus aureus*
S. cerevisiae	*Saccharomyces cerevisiae*
SD	Standard deviation
SEM	Standard error of the mean
SPME-GC-MS	Solid phase microextraction-gas chromatography-mass spectrometry
ssp	Species
Th	helper T-cell
TLR	Toll-like receptor
TNF	Tumor necrosis factor
Treg	Regulatory T-cell
var	variety
VM(A)A	Vapor-phase-mediated (antimicrobial) activity
VMP	Vapor-phase-mediated patch (assay)
VMS	Vapor-phase-mediated susceptibility (assay)
XTT	2,3-bis-(2-methoxy-4-nitro-5-sulfophenyl)-5-[(phenylamino)carbonyl]-2H-tetrazolium-hydroxide

Table of contents

1. Literature review

Parts of this introduction are based on and may contain text from: Mathé, L. & Van Dijck, P. Recent insights into *Candida albicans* biofilm resistance mechanisms. *Curr Genet* **59**, 251-264 (2013).

Unraveling the large communities of microorganisms inhabiting our body surfaces has gained increasing attention over the past decades. It is known that these so-called microbiomes greatly influence our metabolic processes and the functioning of our immune system[1]. At first, research focused mainly on the bacterial microbiome, which is now largely characterized, as it is the major part of our microbiome[2]. Lately however, our fungal inhabitants, the mycobiome, have been gaining attention because also they can have a significant impact on our health[1,3]. An example are species belonging to the *Candida* genus which can act as human pathogens.

The *Candida* genus is classified in the kingdom of the Fungi and the phylum Ascomycota and diverged approximately 200 to 800 million years ago from the model organism *Saccharomyces cerevisiae*[4,5]. Only a small number of species within the *Candida* genus are adapted to living inside a human host and are as such able to cause disease[6]. Among these, *Candida albicans* is most often the causative species, frequently followed by *Candida glabrata* although this depends on the geographical region (figure 1.1) and infection niche[7-13].

Figure 1.1: Distribution of the *Candida* species most frequently isolated from patients with symptomatic colonization, excluding *Candida albicans*. In case of *Candida dubliniesis*, indicated regions report more than two percent of isolates corresponding to this species. From Quindos (2014).

C. albicans is a diploid organism, that only rarely occurs as haploid[14], while *C. glabrata* is a haploid that is phylogenetically more closely related to *S. cerevisiae* than to *C. albicans*[15]. *C. albicans* exhibits a parasexual mating cycle and its mating type is determined by the alleles (**a** and/or α) present in a genetic locus on chromosome five, called the mating-type-like (*MTL*) locus, alluding to its resemblance with the mating-type (*MAT*) locus in *S. cerevisiae*[16]. Mating only occurs between a strain of mating type **a/a** and a strain of mating type α/α, meaning that only strains homozygous at the *MTL* locus are able to mate[16-18]. Moreover, the strain must be in an epigenetic state called 'opaque'[19]. Both hardly ever occur in clinical isolates which makes mating a cumbersome process requiring both the loss of (the *MTL* locus containing part of) chromosome five and an epigenetic switch[20]. The genome of *C. glabrata* also contains *MTL* loci with most genes necessary for mating in *S. cerevisiae* being conserved, but no sexual cycle has been observed in this pathogenic yeast[21,22].

Both *C. albicans* and *C. glabrata* are a dominant part of the mycobiome in the oral cavity[23], the gastrointestinal tract[24] and the female urogenital tract[25]. In a healthy host, growth of both species is confined by other players of the microbiome[26] and by the host immune system. However, when our natural microbiome is disturbed, *e.g.* by the use of antibiotics, or when a patient is immunocompromised, commensal *Candida* species can behave as pathogens[27].

1.1. *Candida albicans* and *Candida glabrata* as pathogens

C. albicans and *C. glabrata* can cause a variety of diseases in different host niches. These diseases can be divided into two groups: superficial infections which are not life-threatening but cause discomfort to the patient, and systemic infections with *Candida* cells present in circulation and/or vital organs. Systemic infections are associated with severe morbidity, and death of the patient is reported to be between 20% and 50%[7,28,29]. The causative species influences the survival rate, with disseminated candidiasis caused by *C. albicans* being associated with lower survival compared to infections caused by Non-*albicans Candida* (NAC) species[11].

1.1.1 Superficial infections

Because *C. albicans* and *C. glabrata* are commensals, they can be isolated from different mucosal niches mostly indicating asymptomatic colonization rather than infection. Mucosal epithelial cells have evolved a delicate detection cascade crucial in distinguishing colonization

from infection. The latter results in an immune response aimed at defending the host against fungal invasion[27,30] (discussed in section 1.4.3, p. 32). Superficial *Candida* infections can occur in patients with immune system statuses covering the whole spectrum of immunology, ranging from patients that are immunosuppressed which causes increased susceptibility, to patients with an over-active immune system that contributes to morbidity[31]. Here, this will be shortly illustrated while the immune response to *Candida* infections will be discussed elaborately in section 1.4 (p. 27).

Especially in the oropharyngeal tract, the importance of an intact host immune system in protection against oropharyngeal candidiasis (OPC) is evident. OPC is characterized by white or red patches on mucosa in the oral cavity. It hardly ever occurs in healthy humans while being the most common oral infection in HIV+ patients[32]. Before the discovery of efficient antiretroviral therapy, up to 90% of all HIV+ patients were confronted with at least one episode of OPC[31,33], indicating the involvement of cell-mediated immunity in protection against OPC. This is further evidenced by the fact that patients receiving chemotherapy, which results in a diminished immune response, also regularly suffer from OPC[31]. In contrast, vulvovaginal candidiasis (VVC) does not affect immunocompromised patients proportionally more than it does the healthy population[33]. VVC affects approximately 75% of all women in their reproductive ages. In five to eight percent of the cases these infections are recurrent (RVVC), meaning that the patient experiences four or more episodes of VVC annually. VVC is characterized by redness, itching, pain and burning of the vulvovaginal region[34,35]. These symptoms are primarily caused by massive immune cell infiltration into the vaginal mucosa[36]. Predisposing factors for VVC are diabetes, hormone replacement therapy, the use of oral contraceptives and the use of antibiotics[34]. All of these severely affect the natural vaginal microbiome thereby creating a niche for *Candida* species to fill. Denture stomatitis occurs in patients independent of their immune status. The causative agent is a very persistent infection of a denture by *Candida*, leading to constant exposure of the oral mucosa to the pathogen while the denture is being worn. Denture stomatitis can be a very painful condition and is rather common, with studies reporting this infection in up to 70% of all denture wearers[31,37].

1.1.2 Systemic infections

In contrast to superficial infections, systemic *Candida* infections are life-threatening. The prevalence of candidemia (a bloodstream infection caused by *Candida*) is variable between countries and numbers reported range between 1.1 and 14.4 cases per 100 000 capita, annually[11]. However, it is not clear whether these numbers reflect actual global differences in

candidemia prevalence or are reflective of variation in the efficacy of diagnostics or reporting between countries. In Belgium, a recent multi-center study reported an incidence rate of candidemia of 0.44 per 1 000 hospital admissions. The numbers reported in this study correspond to approximately three cases per 100 000 capita over the course of one year. In this study, *C. albicans* (50%) was the most prevalent cause of candidemia, followed by *C. glabrata* (27%) and *C. parapsilosis* (10%)[13]. Previous studies in Belgium reported *C. albicans* as the causative agent in 55 to 76% of cases[38,39]. This possibly indicates that the prevalence of *C. albicans* in bloodstream infections in Belgium is decreasing in favor of more resistant Non-*albicans Candida* (NAC) species. A similar trend has been reported in other countries, and has been attributed to the prophylactic use of azoles and echinocandins [11,40-43].

Even though *Candida* is known to infect distant organs such as liver and kidneys in deep-seated infections[44], a study in mice has shown that death is to be attributed to progressive sepsis rather than organ failure due to presence of *Candida* in the bloodstream and organs[45]. However, only part of the *Candida* bloodstream infections (BSI) cause sepsis in patients. While the associated mortality is much higher in BSIs with sepsis compared to BSIs without sepsis[46], sepsis can thus not be the only cause of death in patients and organ failure is likely involved as well. It is not clear from literature which *Candida* cell wall component is responsible for inducing sepsis.

Candida cells can end up in the bloodstream via two main routes. Either they gain access to the bloodstream, for example during the implantation of a catheter[47] or they break through the intestinal wall after it is weakened *e.g.* by chemotherapy[48]. The latter is mostly seen in neutropenic and immunocompromised patients. A catheter present in a central vein can act as a substrate for a biofilm (discussed in section 1.2.3, p. 12) which represents a resistant reservoir of cells. In such cases clearance of the infection is often problematic due to resistance, making removal of the catheter enclosing the biofilm the only solution[49,50]. Primary diagnosis of candidemia is always via positive blood culture even though false negative results are obtained in approximately 25 to 50% of candidemia cases[51]. Moreover, it takes 24 to 48 hours to obtain results for a blood culture test[13,52], while it has been shown that delayed treatment is a risk factor for patient mortality[11]. Therefore, alternative diagnostic procedures, such as detection of *Candida* cell wall components in serum[51], PCR based detection[52] and MALDI-TOF MS techniques[53] are being optimized to allow for early diagnosis and commencement of antifungal therapy.

The successful commensal lifestyle of *C. albicans* and *C. glabrata* is attributed to a repertoire of factors that allows the colonization of a human host and facilitates the fungus's survival in this ever-changing environment. However, these virulence factors can result in *Candida* causing systemic infections in weakened patients possibly leading to mortality which leaves the fungus without a host[54,55].

1.2. *Candida albicans* and *Candida glabrata* virulence factors

Virulence factors of *Candida* species range from simply being able to grow at the human body temperature to complex stress response pathways. Rather than discussing all known virulence factors, we will highlight the ones that are most important for this work. As such we will discuss morphogenesis, focusing on the yeast-to-hyphae switching observed in *C. albicans*, and adhesion and biofilm formation exhibited by both species.

1.2.1. Candida albicans morphogenesis

C. albicans is a pleomorphic organism that grows as budding yeast cells, pseudohyphae, which are elongated yeast cells, and true hyphae with parallel cell walls[56,57] (figure 1.2). Several environmental factors can trigger the switch between yeast and hyphal cells. Growth as yeast cells occurs in the lab at low temperature and pH, whereas a temperature of 37°C and a neutral pH favor hyphae formation[58]. An exception is growth embedded within a matrix, which can result in a switch to hyphal cell growth at temperatures as low as 25°C[59]. Hyphae formation can also be triggered by environmental stimuli such as the presence of serum, N-acetylglucosamine and environmental CO_2[58,60-63], all reminiscent of growth in a mammalian host.

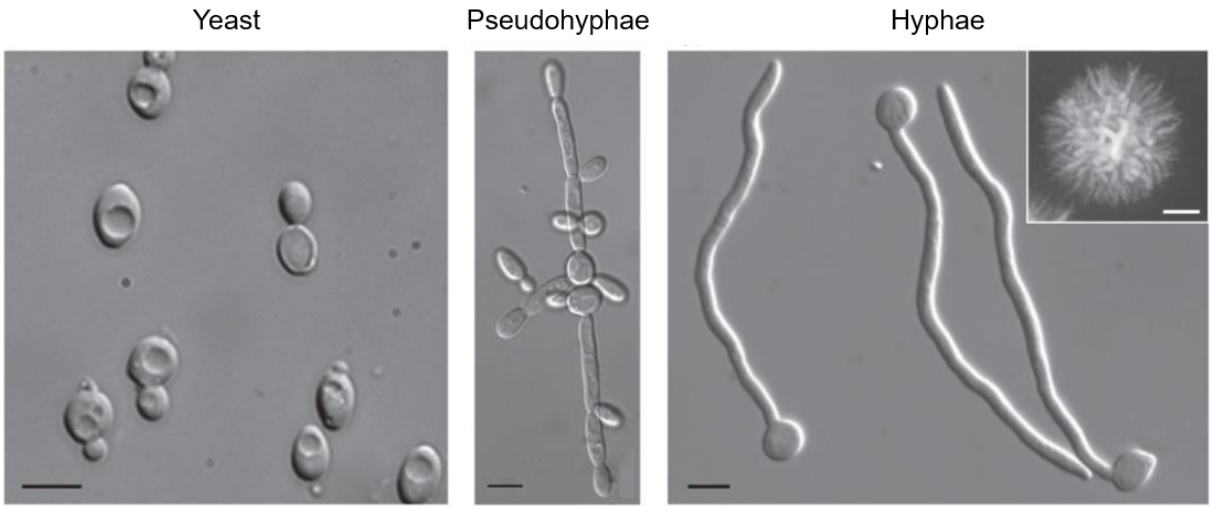

Figure 1.2: Morphology of yeast cells, pseudohyphae and hyphae. The inset shows colony morphology of a colony growing on hyphae inducing medium (Spider medium) for five days. Scale bar represents 5 µm in main panels and 1 mm in inset. Adapted from Sudbery (2011).

The induction of morphogenesis and concomitant expression of hyphae-associated genes is controlled by different pathways dependent on the environmental trigger (summarized in figure 1.3).

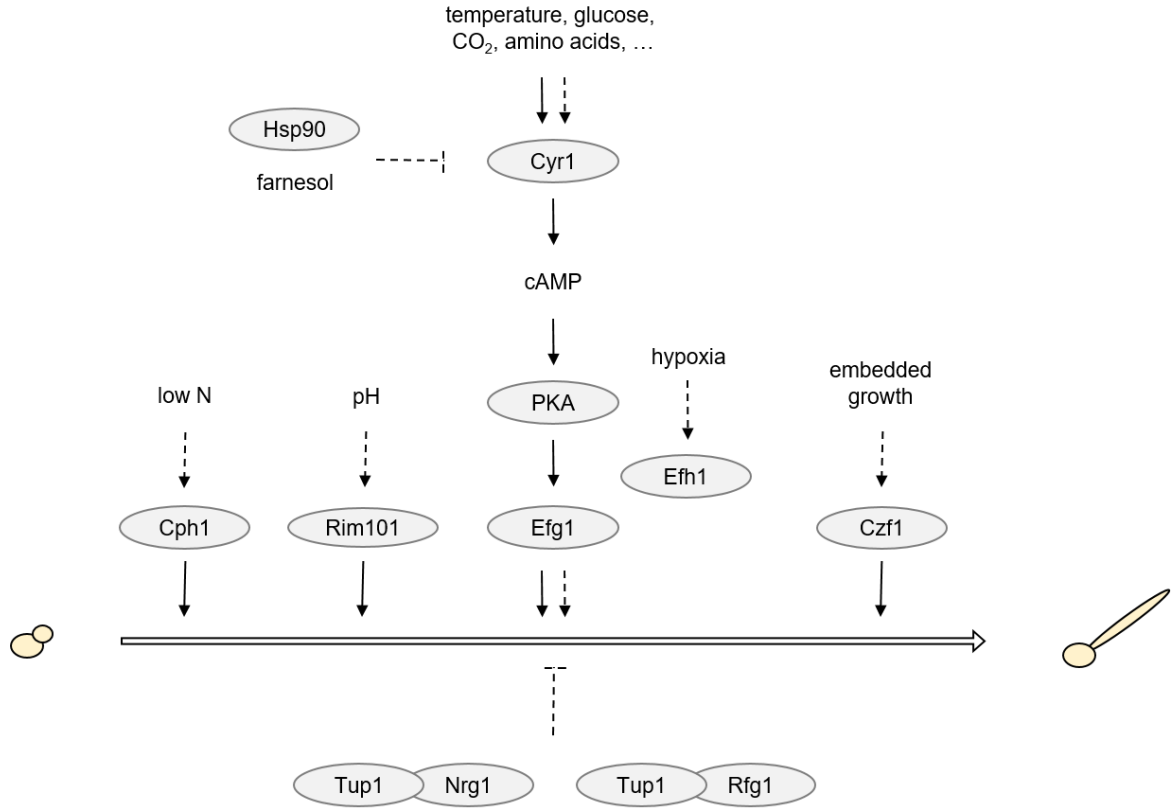

Figure 1.3: Summarized representation of the regulation of yeast-to-hyphae switching in *Candida albicans*. Dotted lines represent indirect regulation, solid lines represent direct regulation.

A multitude of stimuli such as CO_2[64] and specific nutrients[65,66] signal via the cyclic adenosine monophosphate (cAMP)-protein kinase A (PKA) pathway, in which signals are primarily coordinated by the adenylyl cyclase Cyr1[67]. Cyr1 is activated either directly[64] or indirectly[66,68] resulting in increased cAMP levels that activate PKA. In turn, PKA will phosphorylate and thereby activate the transcription factor Efg1 which is crucial for hyphae formation and transcription of hyphae specific genes[67,69-71]. Inhibitors of the cAMP-PKA pathway include the quorum sensing molecule farnesol[72] which causes inhibition of hyphae formation at cell densities surpassing 10^7 cells/mL[73] and heat shock protein 90 (Hsp90). Hsp90 acts on Cyr1 via the GTPase Ras1 and inhibition is halted when temperatures increase[74].

Other signaling pathways involved in morphogenesis are the mitogen-activated protein kinase (MAPK) pathway which activates the transcription factor Cph1[75,76], the pH sensing Rim101 pathway[77,78], the Czf1 mediated pathway sensing embedded growth[59] and the pathway sensing hypoxia working via transcription factors Efg1 and Efh1[79,80]. Lu and colleagues (2013)

showed the redundancy of some of these pathways and hypothesized that this redundancy might be responsible for the successful pathogenicity of *C. albicans*[81,82]. Further, it was shown that genotoxic stressors such as hydroxyurea and ultraviolet light cause cell cycle arrest which results in hyphae formation[83]. This was corroborated by a genome-wide analysis of regulators of filamentation which showed that most filamentation repressors are linked to cell cycle progression[84]. Negative regulation of hyphae formation is constituted by Tup1[85], which was shown to be involved in farnesol-mediated hyphal inhibition[86], working together with Nrg1[87] and/or Rfg1[88,89]. Mutants defective in either of these proteins are stuck in the pseudohyphal growth mode[85,87-89].

The role of hyphae formation within a host is most likely surface invasion. This is demonstrated in experimental models and in patient samples by the presence of most hyphae at invasive sites[56]. By showing polarized growth characterized by tip extension[58,63,90] hyphae respond thigmotropically to the presence of surface-related characteristics such as grooves and pores, which probably allows them to localize weak places in the epithelia of the host[91,92]. Moreover, hyphal cells can readily invade host cells, either via induced endocytosis[93], which is mostly important in the first stages of invasion[94], or via active hyphae-driven penetration[92], which gets more important as the infection progresses[94]. The exact mechanisms behind active penetration are unclear but it is probably mediated by both physical forces and the secretion of hydrolytic enzymes[54,92,95]. Induced endocytosis is driven only by the host cell after recognition of the hyphae-associated proteins Als3 and Ssa1[96,97]. Interestingly, it was recently discovered that host cell damage in the presence of hyphae is not caused by actual host cell invasion. Rather, a small protein secreted by *C. albicans* hyphae and named Candidalysin, is responsible for host cell damage[98,99]. On the other hand, the morphology of yeast cells is thought to make them better adapted for dissemination within a host[92] (figure 1.4). It has been proposed that sensing the morphological switch between yeast cells and hyphae at mucosal surfaces is employed by host cells to discriminate between colonizing and invading *C. albicans* cells. In the case of invading hyphae, immunity is induced[27,100] (discussed in section 1.4.3, p. 32).

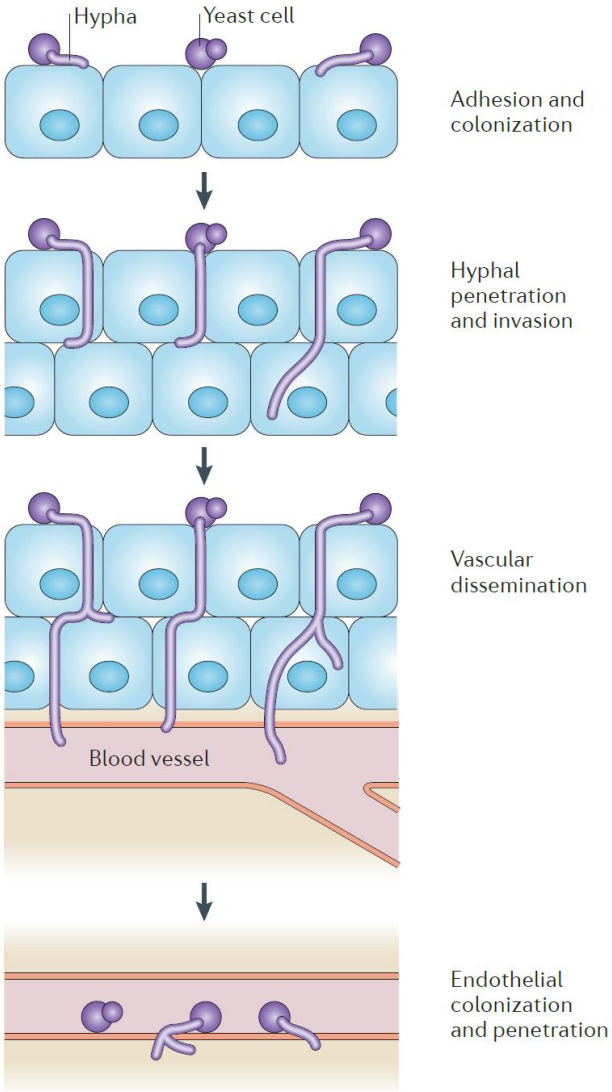

Figure 1.4: Schematic of the steps in *Candida albicans* tissue invasion. (i) Adhesion to the epithelium, (ii) epithelial penetration and invasion by hyphal cells, (iii) yeast-cell mediated vascular dissemination after hyphal penetration of the blood vessel and (iv) endothelial colonization and penetration. From Gow *et al* (2011).

The necessity of morphogenesis for *C. albicans* virulence has been studied extensively. Initial research focused on the need of filamentation for virulence by using an *efg1Δ/efg1Δ cph1Δ/cph1Δ* mutant that is locked in the yeast form[101]. This mutant with defects in both the cAMP-PKA and MAPK pathways showed severely attenuated virulence in different animal models, including a mouse model for systemic candidiasis[101-104]. Also *tup1Δ/tup1Δ* and *nrg1Δ/nrg1Δ* mutants which are locked in the pseudohyphal form showed severely reduced virulence. Together, these observations led to the assumption that the ability to switch between both morphological states rather than the morphological states themselves is necessary for virulence[87,105,106]. This was confirmed using a strain in which one copy of *NRG1* was placed

under the control of a tetracyclin-regulatable promoter resulting in the yeast cell morphology in the absence of doxycyclin and the onset of hyphae formation upon the addition of doxycyclin[107]. On the other hand, it was recently shown using this same mutant that true hyphal cells locked in this growth mode, and injected intravenously as such, did not show reduced virulence in this systemic mouse model[108]. Several other studies, including a screening of approximately 3 000 homozygous *C. albicans* deletion mutants, revealed that mutants unable to switch between the yeast and hyphal morphology still show virulence in a systemic infection model in mice[109-111]. Moreover, it is known that *C. glabrata*, which only shows the yeast morphology, can also cause severe systemic infections[112]. The tight co-regulation of gene expression regulating morphogenesis and gene expression regulating other virulence traits, makes it difficult to undisputable contribute (absence of) virulence to cell shape[58,63,92,113]. An integrative view is thus necessary, which acknowledges that both growth forms play their part in *C. albicans* infections with different steps in infection and different host niches possibly favoring one or the other[54,114].

1.2.2. Adhesion to surfaces

A first step in all *Candida* infections is the adhesion of *Candida* cells to abiotic or biotic surfaces within a human body. Initial adhesion is mediated by non-specific factors such as hydrophobicity and electrostatic forces, while adhesins present on the fungal cell wall take over during later stages of the interaction[94,115,116]. Most adhesins are linked to the cell wall with a glycosylphosphatidylinositol (GPI)-anchor and contain a structure with three characteristic domains: a substrate-binding N-terminal domain, a central domain consisting of several 36-amino acid tandem repeat sequences and a C-terminal domain containing a GPI anchor signal[73].

While it is thought that initial adhesion is primarily mediated by *C. albicans* yeast cells, hyphae also play a crucial role in adhesion[117]. It was shown that a ***ras1Δ/ras1Δ*** mutant unable to form hyphae was virtually non-adherent to epithelial cells[118]. Some hyphae-specific proteins, with primarily Als3 and Hwp1 well characterized, are major adhesins present on the cell's surface[73], and mutants lacking either *ALS3* or *HWP1* show a 70% reduction in adherence[54,118]. Since these genes are hyphae-specific, regulation of adhesin expression shares similarities with regulation of morphogenesis. For example, expression of *ALS3* is induced by Efg1 and Cph1 and repressed by Tup1, Nrg1 and Rfg1[119]. *ALS3* belongs to the *ALS* gene family which consists of eight *ALS* genes: *ALS1-7* and *ALS9*, with the proteins Als1-4 being only present on hyphae while proteins Als5-7 and Als9 are yeast-cell specific[73,120-122]. However, not all adhesins are

linked to one particular cell type, *e.g.* the adhesin Eap1 whose expression is cell-type independent[116]. Research has shown that different ALS genes play a role in different host niches, with a strain isolated from oral or vaginal candidiasis showing different expression patterns[123-125].

In *C. glabrata*, adhesins belong to the extended *EPA* gene family and are located at subtelomeric regions[126]. The number of *EPA* genes is estimated to be between 17 and 23 with the exact number depending on the genetic background of the strain[127,128]. Epa1 is the main adhesin during *in vitro* interactions with epithelial cells and deletion of the gene *EPA1* results in severely reduced adherence[128,129]. In contrast to genetic regulation of adhesion in *C. albicans*, which is primarily regulated at the transcriptional level[119], expression of *EPA* genes is regulated epigenetically by subtelomeric silencing[126]. Different levels of subtelomeric silencing have been observed between *C. glabrata* strains, resulting in great variation in adhesion although the consequences of this for strain virulence are yet unclear[126]. The presence of other adhesins has been proposed in *C. glabrata*, of which seven belong to the less well studies *PWP* gene family, while others do not seem to show homology to the *EPA* or *PWP* genes[130].

1.2.3. Biofilm formation

Biofilms are defined as structured microbial communities that are attached to a surface and surrounded by a self-produced extracellular matrix (ECM; figure 1.5)[131].

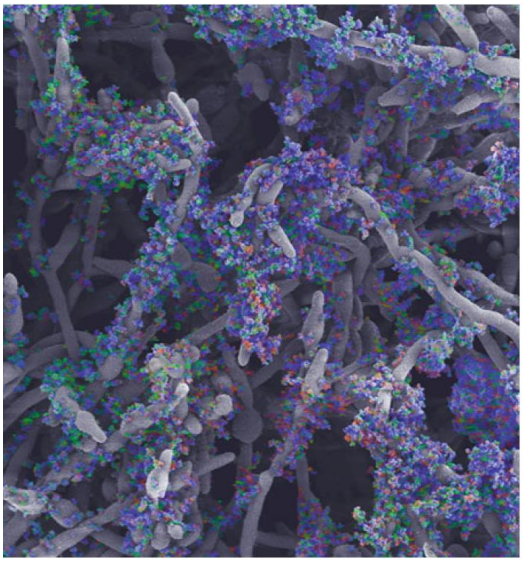

Figure 1.5: Scanning electron microscopy picture of *Candida albicans* biofilm with false-colored matrix. Matrix is colored blue, green and red. From Mitchell *et al* (2016).

In the beginning, focus was on bacterial biofilms, with a first model to study *C. albicans* biofilm development *in vitro* emerging in 1994[132]. Since then, ample model systems for the study of fungal biofilms have been developed and optimized[133,134] and *C. albicans* biofilm formation has been characterized both *in vitro* and *in vivo*[135-138]. In general, *C. albicans* biofilm formation comprises four stages (figure 1.6):(i) cell wall protein mediated adherence of yeast cells to a surface, (ii) growth of the attached yeast cells into a thin layer, (iii) maturation of the biofilm through development of pseudohyphae and hyphae and assembly of the ECM, and (iv) dispersal of yeast cells from the biofilm possibly leading to colonization of distant places[138-141]. Although the kinetics of biofilm formation and biofilm structure may differ depending on the growth conditions[142,143] mature *C. albicans* biofilms are mostly present after 24 to 48 hours of biofilm formation[135,136,141]. They consist of a thin layer of yeast cells responsible for attachment of the thicker layer, comprising both yeast and hyphal cells, to the surface[144]. Structurally, several microcolonies can be distinguished which are separated by water channels allowing circulation of nutrients[145,146]. Biofilms formed by *C. glabrata* are composed of layers of yeast cells, encapsulated in an ECM[112,147-149].

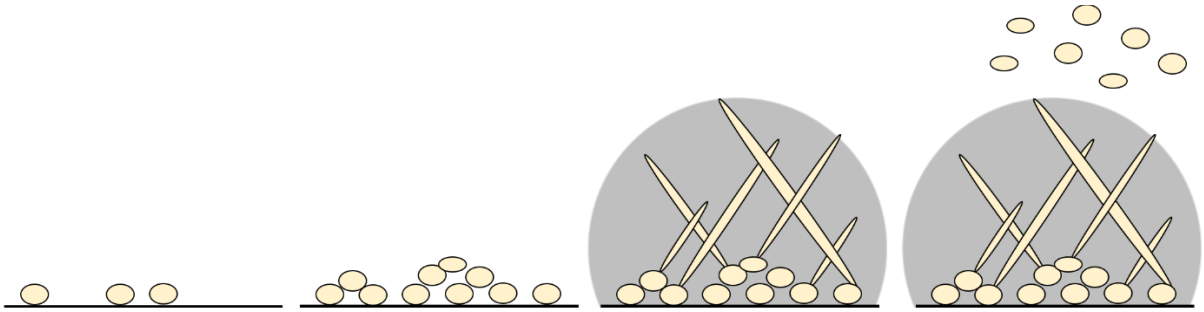

Figure 1.6: Schematic of the steps in *Candida albicans* biofilm formation. (i) adherence of yeast cells to a surface, (ii) growth of the attached yeast cells into a thin layer, (iii) maturation of the biofilm through development of hyphae and assembly of the ECM and (iv) dispersal of yeast cells from the biofilm.

The amount of ECM present depends on the growth conditions to which the biofilm is subjected, with more matrix material being produced when the cells are confronted with a liquid flow as compared to static conditions[150]. While it is known that planktonic cells also secrete an extracellular polymer, considerate differences were observed between the composition of the polymers produced by planktonic cells and biofilm-associated cells[143,150,151]. An initial study identified carbohydrates (41%) and proteins (5%) as the major constituents of biofilm ECM[143] together with phosphorus, uronic acid, hexosamine and extracellular DNA (eDNA)[151,152]. More recently, an extensive analysis of matrix material showed that 55% of the matrix dry weight is composed of proteins, 25% is carbohydrate, followed by lipids (15%) and nucleic acid (5%)[153]. These differences in the reported proportions are likely caused by less delicate matrix separation methods in earlier studies that also affected the *C. albicans* cell wall thereby analyzing both matrix and cell wall components at the same time[153]. Even though the carbohydrates β-glucan and mannan are present in both the cell wall and the biofilm matrix, the analyses performed by Mitchell and colleagues (2016) suggest that cell wall and matrix carbohydrates are assembled in a different manner[154]. First, they identified a unique mannan-glucan complex in the biofilm matrix, composed of β-1,6-glucan and α-1,2 branched α-1,6-mannan that is unidentified in the *C. albicans* cell wall. Moreover, they showed that the proportions and structure of the carbohydrates differ[153,154]. A study with mutants defective in either matrix mannan or β-1,6-glucan production showed that deletion of any of these genes resulted in a severe reduction in matrix material in *in vitro* biofilms by causing defects in the mannan-glucan complex. Strikingly, when growing mixed biofilms in which a mutant defective in mannan production was grown with a mutant defective in β-1,6-glucan production, the matrix was restored to wild-type levels[155]. This indicates that biofilm matrix assembly is an extracellular process[154,155]. The proteome of biofilm-associated cells has been shown to be different from the proteome of either yeast or hyphal cells with differentially expressed proteins

being primarily involved in several metabolic processes[156]. A group of 14 host derived proteins was found to be present in the ECM of biofilms grown in three different host niches. This group contained proteins involved in immune response and leukocyte function, that probably originated from host cells incorporated in the growing biofilm matrix[157].

The genetic network controlling biofilm formation has been investigated both *in vitro* and *in vivo*[158-165]. With the use of RNA-sequencing, a complex regulatory network was discovered containing nine master regulators (amongst which Bcr1 and Efg1) whose expression is necessary for *in vitro* and *in vivo* biofilm formation[161,164]. These master regulators interact with over 1 000 genes out of a total of approximately 6 000 genes present in *C. albicans*. The interacting genes were enriched for genes that evolved relatively recently and were depleted for genes conserved amongst the Ascomycota. This indicates that the biofilm regulatory network in *C. albicans* evolved recently[161,164]. Next to these master regulators, nearly 50 additional regulators whose deletion affects an aspect of biofilm formation have been identified[166].

It has been estimated that up to 80% of human infections are biofilm associated[167,168]. In *Candida* infections, biofilms can be formed either on a mucosal surface or on a medical implant device[169]. The risk of biofilm formation on such a medical implant device is dependent on the site of implantation. For a vascular catheter for example, the risk ranges between three and eight percent[47]. The current guidelines for management of catheter-related candidiasis entail the removal of the catheter[50,170]. NAC species are also capable of forming biofilms[132,149,171,172], but mortality seems to be higher in patients infected with *C. albicans* biofilms[173]. Patient cohort studies show that the presence of a high biofilm forming isolate (HBF) increases the mortality rate of patients significantly in comparison to infection by an isolate incapable of forming biofilms or by a low biofilm forming isolate (LBF)[173-176]. There seems to be no consensus on the proportion of HBFs versus LBFs in different *Candida* species[174,175,177]. Comparison of the transcriptional profiles between LBFs and HBFs of *C. albicans* demonstrated a differential regulation of metabolic pathways such as amino acid metabolism and fatty acid biosynthesis giving cues about potential novel antifungal diagnostics or therapeutics[178].

Next to single species bloodstream infections associated with biofilms on medical implant devices, multi-species candidemia is also encountered, making up four to eight percent of all *Candida*-associated bloodstream infections[38,179,180]. Seemingly more prevalent with seven to 27% of all candidemias are polymicrobial bloodstream infections, in which *Candida* species are present together with bacteria such as *Enterococcus* species, *Streptococcus* species, *Staphylococcus aureus* and *Pseudomonas aeruginosa*[179,181,182]. Such polymicrobial infections are often more lethal than monospecies infections, since one species can increase the

virulence of the other[183]. Examples are the attachment of *C. glabrata* and *Staphylococcus* species to *C. albicans* hyphae, with some interactions leading to increased morbidity in mouse models[184-186], and mutual protection of both *C. albicans* and bacteria by components of each other's biofilm ECM[187,188]. On the other hand, inhibitory effects of different bacteria naturally occurring together with *C. albicans* on the latter have also been described[183,189].

It has been repeatedly shown that cells associated with biofilms are less susceptible to antimicrobial agents compared to planktonic cells. Therefore, biofilms are often regarded as survival mechanisms of microorganisms. This increased resistance was first shown for bacterial species, with an increase in dosage ranging from 10- to 100-fold necessary for clearance of biofilm-associated bacteria[190]. Later, a similar trend was observed for fungal biofilms. Drug concentrations needed for a 50% reduction of metabolic activity were shown to be five to eight times higher in biofilms compared to planktonic cells and minimal inhibitory concentrations (MICs) increased 30- to 20 000-fold[191]. These findings were confirmed for biofilms on different substrates and for biofilms formed by different *Candida* species[138,144,192,193]. Interestingly, Yi *et al* (2011) discovered that *C. albicans* biofilms formed by *MTL*-heterozygous cells differed significantly in permeability and drug resistance from their *MTL*-homozygous counterparts. The viability of cells within **a**/α biofilms was found to be nine-fold higher than that of cells in **a**/**a** and α/α biofilms after challenge of mature biofilms with an antifungal. The researchers suggested that the *MTL*-heterozygous biofilms form the traditional, protective biofilm environment mostly found in nature and causing disease in patients. This seems reasonable, since 90% of the free-living *C. albicans* cells are heterozygous at their mating type locus. On the other hand, *MTL*-homozygous biofilms might form a more penetrable environment to facilitate mating[194].

Since the discovery of high drug resistance conferred by *C. albicans* biofilms, several mechanisms underlying this high resistance have been proposed. In the next chapter we will first introduce the commonly used antifungals after which we will discuss the major resistance mechanisms exhibited by planktonic cells and biofilms.

1.3. Resistance to antifungals

Current anti-*Candida* therapies fall into five classes and are summarized in table 1.1. Antifungals can either inhibit the cells from growing and reproducing (fungistatic) or can kill the cells (fungicidal)[195]. In practice, the azole fluconazole is most often used as treatment of a *Candida* bloodstream infection[11,174], followed by the echinocandins according to a recent report[11] or the polyene amphotericin B (AmB) according to an earlier report[174].

Table 1.1: Current anti-*Candida* therapy classes and their working mechanism.

Antifungal class	Example	Working mechanism (Sanglard, 2016)[196]
Polyenes	Amphotericin B	Destabilize the cell membrane by acting as an ergosterol sponge and cause electrolyte leakage by forming pores in the cell membrane.
Azoles	Fluconazole	Target ergosterol biosynthesis by blocking lanosterol 14α-demethylase.
Echinocandins	Caspofungin	Inhibit cell wall biosynthesis by blocking β-1,3-glucan synthase.
Pyrimidine analogs	5-Flucytosine	Are metabolized by fungal cells and incorporated into growing DNA and RNA strands resulting in growth arrest.
Allylamines	Terbinafine	Target ergosterol biosynthesis through blocking of the enzyme squalene epoxidase.

A variety of tests are available for *in vitro* antimicrobial activity screening of compounds on planktonic cells. The method most often used is the broth microdilution assay using 96-well plates for which a standard operating procedure is provided by the Clinical Laboratory Standards Institute (CLSI)[197] to allow for comparison between obtained results[198]. In the broth microdilution assay, the MIC of a specific strain is determined using a two-fold dilution series of the antifungal. The MIC is defined as the lowest concentration of an antifungal that can inhibit the growth of the species up to a desired level which is often specified as a subscript[199]. Both CLSI and The European Committee on Antimicrobial Susceptibility Testing (EUCAST) have determined breakpoints defining when a species is considered susceptible or resistant to the commonly used antifungals[197,200]. After incubation, the MIC endpoint can be determined either visually or via spectrophotometry[198].

In vitro susceptibility of biofilms to antifungals is generally assessed using the 96-well microtiter plate-based method first described by Ramage and colleagues (2001)[192]. This method uses a colorimetric signal based on the conversion of XTT to a colored formazan by metabolically active cells for the determination of the MIC endpoint[192]. However, due to metabolic variability between strains, species and isolates, caution should be taken in comparing results obtained

in this way and it can be useful to include additional read-outs such as the crystal violet staining of biomass[201]. Susceptibility testing under *in vivo* conditions is mostly performed using catheter lock therapies[202] or by intraperitoneal or intravenous injection of drugs into animals with catheter-associated biofilm infections[203,204].

Clinical isolates of *Candida* species primarily show resistance to the azoles and to a lesser extent to the echinocandins[11,13,38,174,205]. Reported resistance rates are highly dependent on geographical strain origin, number of isolates tested, host population and resistance breakpoints adopted[11,43,196,205]. In recent reviews, the resistance of *C. albicans* in general is considered rather low, with resistance to echinocandins occurring in two to three percent of cases and resistance to azoles occurring in three to four percent of cases[43,196,206]. However, antifungal resistance in *C. glabrata* is on the rise. In this species, resistance to echinocandins is observed in one to 13% of cases and is often associated with an increased resistance to azoles, which is generally present in eight percent of the strains[196,206-208]. Since resistance to echinocandins results in a fitness cost due to a less robust cell wall, resistance is always acquired after previous exposure to the drug. The increasing use of echinocandins in prophylaxis thus enables *Candida* strains to develop resistance[207]. On the other hand, resistance to azoles can be inherent, especially in *C. glabrata*[43]. It mostly results from mutations that are selected by drug pressure as a consequence of frequent use of azoles[195]. In general, resistance will be genetically inherited when the fitness of a resistant strain is higher than that of a susceptible strain[209]. Reports of resistance to AmB are rare and this is explained by the observation that mutations in ergosterol biosynthesis conferring resistance to AmB abrogate virulence in *C. albicans*[210,211]. Also the less toxic variants of AmB evade resistance[210,212]. For the treatment of biofilms, efficacy of echinocandins and AmB lipid formulations has been shown both *in vitro*[213-216] and *in vivo*[203,204,217]. The azole antifungal drugs, the pyrimidine analogues, allylamines and classic formulations of polyenes are not active against biofilms[138,191,192].

Over the course of time a vast amount of research groups has tried to elucidate the mechanisms underlying the increased resistance exhibited by biofilm-associated *Candida* cells. Some mechanisms are shared between planktonic and biofilm-associated cells while others are specific. In what follows, the major resistance mechanisms proposed for planktonic and biofilm cells are highlighted and they are summarized in table 1.2.

Table 1.2: Resistance mechanisms in *Candida albicans*

Resistance mechanism	Effect	Which growth form?
Reduced growth rate	Lower presence of antifungal targets which reduces the antifungal efficacy.	Planktonic cells[150]
Cell density	Quorum sensing?	Common[218,219]
Mutations altering drug targets and metabolic pathways	Reduced affinity of the drug for its target or circumvention of the pathway targeted by the drug.	Planktonic cells (effect on biofilm unknown)[220-222]
Active drug efflux by upregulation of drug efflux pumps	Antifungal is pumped out of cell and can thereby not perform its intracellular function.	Common (primarily in planktonic cells)[214,223-225]
Changes in drug target levels	Changes in target levels (often associated with changes in target structure) resulting in too much target present for the amount of drug administered.	Common[220,226-228]
Persister cells	Antifungal targets are inactive due to the dormant state of persisters.	Biofilm[229]
Drug sequestration	Specific binding of antifungals by β-1,3-glucans in biofilm matrix or capturing of drugs in cytosolic vesicles, which prevents antifungals from reaching their targets.	Common (primarily in biofilms)[147,151]
Stress response	Possibly only indirect effects via regulation of other resistance mechanisms.	Common[230,231]

1.3.1 Reduced growth rate

As many antifungal drugs target active growth and metabolic pathways, it is generally accepted that cells showing slow growth are more resistant. It was therefore proposed that biofilm cells are more resistant because they grow slower due to limited nutrient availability at different sites within the biofilm[142]. Baillie and Douglas (1998) compared the AmB susceptibility of biofilm-associated and planktonic *C. albicans* cells under different growth rates. They found that the biofilm-associated cells were resistant at all growth rates, whereas planktonic cells were only resistant when showing very slow growth[142]. This renounces the involvement of a reduced growth rate in a biofilm's resistance to antifungal drugs.

1.3.2 Cell density

Since the resistance of biofilms changes with (extreme) inoculum size, Perumal and colleagues (2007) tested the efficacy of different azoles, AmB and caspofungin on planktonic cells at densities similar to those found in biofilms (up to 1 x 10^8 cells/mL). They showed that at high cell densities planktonic cells had markedly reduced susceptibilities to all drugs. These results seemed to be independent of drug efflux or farnesol quorum sensing as strains deficient in these mechanisms showed the same trend. Moreover, the susceptibility of dissociated biofilm cells diluted to 1 x 10^3 cells/mL was similar to that of planktonic cells at the same cell density[218]. Similar conclusions were obtained by Seneviratne *et al* (2008) for the azole ketoconazole and the pyrimidine analogue 5-flucytosine. However, they did not see a density-dependent susceptibility of planktonic or biofilm-associated cells to both caspofungin and AmB, but they account the modified experimental procedures responsible for these discrepancies[219]. Therefore, cell density does seem to influence *C. albicans* resistance to several drugs, both in planktonic and biofilm-associated cells. It is reasonable to believe that quorum sensing is involved in this process.

1.3.3 Mutations altering drug targets and metabolic pathways

Mutations in drug targets play a role in resistance against the azoles and the echinocandins[196]. Non-synonymous amino acid substitutions resulting from mutations in the gene *ERG11*, which encodes the target of fluconazole 14α-demethylase, have been shown to reduce the affinity of fluconazole for 14α-demethylase[220,232-234]. Such mutations most often affect resistance to fluconazole, while susceptibility to the other azoles is affected to a lesser extent or not at all[235]. This is probably reflective of differences in the structural features of the drugs[196]. Further, resistance to azoles can be constituted via loss-of-function mutations in other genes encoding enzymes involved in the ergosterol-biosynthesis pathways, rather than the azole target itself[196,221,236]. Similar resistance mechanisms have been observed to confer resistance to 5-flucytosine in both *C. albicans* and *C. glabrata*, with loss-of-function mutations leading to the absence of metabolizing of the drug thereby rendering it ineffective[222,237].

The target of the echinocandin drugs is the enzyme glucan synthase of which the catalytic subunits are encoded by the *FKS* genes[207]. Mutations in these genes confer resistance to echinocandins and are restricted to two highly-conserved hot-spot regions in *FKS1* in

C. albicans, while they also occur in *FKS2* in *C. glabrata*[207,238-240]. So far it is not known whether such drug target mutations play a role in biofilm drug resistance[241].

1.3.4 Active drug efflux by upregulation of drug efflux pumps

Upregulation of drug efflux pumps has been described as a resistance mechanism in planktonic cells[223,224,242] and in biofilm-associated cells for several biofilm-forming microorganisms[243]. In *C. albicans*, genes belonging to two groups of efflux pumps have been shown to contribute to drug resistance: *CDR1* and *CDR2* belonging to the Pleiotropic Drug Resistance class within the ATP Binding Cassette (ABC) transporters and *MDR1* and *FLU1* belonging to the Major Facilitator Superfamily[242,244-247].

An increased expression of *CDR1* and *MDR1* was first documented in *C. albicans* clinical isolates showing high azole resistance induced by prolonged treatment[223]. Moreover, mutants lacking *CDR1* and *MDR1* lost their azole resistance together with resistance to other antifungals and metabolic inhibitors[248]. This was confirmed by White and colleagues (1997) who additionally showed that members of other families within the ABC transporters were not involved in resistance[220]. Later, the roles of *CDR2* and *FLU1* in drug resistance were uncovered, when it was shown that integration of *CDR2* and *FLU1* in a highly susceptible *S. cerevisiae pdr5Δ* mutant could increase the its resistance[224,242]. Upregulation of *CDR1*, *CDR2* and *MDR1* has been shown in clinical isolates from diverse host niches[249-251] while the role of *FLU1* in resistance of clinical isolates is unknown[196]. In *C. glabrata,* upregulation of the ABC Transporters *CgCDR1*, *CgCDR2* and *SNQ2* has been shown to increase resistance to azoles[196]. The inherent high expression of these drug transporters is probably caused by mutations leading to hyperactive transcriptional regulators (*PDR1* in *C. glabrata* and *TAC1* in *C. albicans*) that induce the expression of these transporters[252-254]. Even more, almost all azole resistant clinical isolates have been found to have mutations in *PDR1*[206]. Efflux pump upregulation seems to primarily play a role in azole resistance[214,248,255,256] and is reported not to be involved in echinocandin resistance[257].

Increased expression of *CDR1*, *CDR2*, *MDR1* and *FLU1* in biofilm-associated *C. albicans* cells compared to planktonic cells has been shown both *in vitro*[214,255,256] and *in vivo*[135,162]. Increased expression of the *CDR*-genes was mainly observed after 24 hours and to a lesser extent after 48 hours, while *MDR1* was solely overexpressed after 24 hours[214,255]. A similar trend was observed in *C. glabrata* biofilms, with *CgCDR1* and *CgCDR2* upregulation up until 15 hours of biofilms formation while this upregulation was absent at 48 hours[258]. As biofilm resistance usually increases with time, these observations indicate that upregulation of drug efflux pumps

does not play a major role in drug resistance in mature biofilms. Furthermore, studies have shown that challenging the biofilm with antifungals was not necessary for drug efflux pump upregulation since adherence to a surface was enough to trigger this gene overexpression[256,259]. Lastly, several studies have shown that *CDR1*, *CDR2* and *MDR1* single and double mutants are susceptible to azoles when grown planktonically while they retain their resistance when grown in a biofilm structure, thereby implying that the presence of these genes is not necessary for biofilm drug resistance[214,218,255].

1.3.5 Changes in drug target levels

Changes in drug target levels can result from changes in gene copy numbers or from altered expression of the gene. Isochromosome formation can cause increased gene copy numbers and thus increased expression of the genes located on the isochromosome[43]. An example is isochromosome formation on the left arm of chromosome 5 which leads to an increase in copy numbers of *ERG11* and *TAC1* which are both involved in azole drug resistance[43]. This isochromosome formation was shown to be seven-times more likely to be present in fluconazole resistant *C. albicans* isolates compared to susceptible isolates[226]. Loss of heterozygosity, which can be induced by different stressors[260], has been linked with azole resistance in strains with hyperactive alleles of *e.g. ERG11* and *TAC1*[253,261]. Loss of one complete copy of chromosome 5 has been shown to lead to increased echinocandin tolerance in laboratory mutants but it is unclear whether such chromosome loss also plays a role in echinocandin resistance in clinical practice[262,263]. The genome of *C. glabrata* also shows a high degree of plasticity which has been associated with drug resistance[264].

Upregulation of *ERG11* independent of increases in copy numbers, was shown to be present in a clinical *C. albicans* azole resistant isolate and was caused by mutations in *UPC2*, the transcriptional regulator of *ERG11*[265]. Altered expression of *CgERG11* does not seem to be very important in *C. glabrata* azole resistance, as this mechanism has only been observed in a handful of clinical isolates[206].

The role of changes in drug target levels in biofilm resistance has been researched mainly via transcriptome analyses. Changes in *ERG*-gene expression upon addition of the azole fluconazole were investigated by Borecká-Melkusová and colleagues (2009) in *C. albicans* isolates[227]. They found upregulation of *ERG9* regardless of the strain's susceptibility and downregulation of *ERG11* in fluconazole-susceptible strains. A study by Nailis *et al* (2010) showed a drug specific transcription response upon challenge of biofilms by high concentrations of antifungals. They noticed significant increases in *ERG1, ERG3, ERG11* and

ERG25 expression in mature biofilms upon addition of fluconazole and significant increases in *SKN1, KRE1* (involved in the production of β-1,6-glucan) and *ERG1* in mature biofilms upon challenge with AmB[228]. Combined, these results show that differential regulation of gene expression within biofilm-associated cells is highly dependent on the experimental set-up. Yu *et al* (2012) found that mature biofilms grown in the presence of farnesol, which is the precursor of ergosterol, showed a significant increase in fluconazole susceptibility compared to a farnesol-untreated biofilm. Using RT-PCR, they demonstrated that transcription levels of *ERG1*, *ERG3*, *ERG6*, *ERG11* and *ERG25* decreased significantly in the farnesol-treated group, indicating that the ergosterol biosynthesis pathway may contribute to the increased fluconazole susceptibility caused by farnesol[266] and further arguing that increased transcription of the *ERG*-genes does increase biofilm resistance. A whole transcriptome approach was applied by Vediyappan and colleagues (2010), who challenged mature biofilms during two hours with fluconazole, AmB or caspofungin in concentrations that were lethal for planktonic cells but not for biofilm-associated cells[267]. Upon addition of fluconazole, only five genes were differentially expressed, causing the researchers to put forth that biofilm-associated cells might be blind to fluconazole, thereby explaining its inefficacy. Upon addition of AmB, they saw a differential expression of 160 genes, whereas upon challenge with caspofungin the amount of differentially expressed genes increased up to a couple of hundred genes. Interestingly, this shows a correlation between antifungal susceptibility and the amount of differentially expressed genes, which is a trend opposite to what would be expected if genetic changes are the main reason for antifungal resistance in biofilms.

Some contrasting results arise from the studies cited above, which might reflect a highly model-dependent mechanism since the *in vitro* model systems for biofilm formation utilized in the cited studies differed. It is for example known that the presence of medium flow during the formation of biofilms significantly alters the biofilm structure[143,150,151] and that the antifungal susceptibility of biofilms grown under flow conditions differs significantly from statically grown biofilms[268,269]. It is therefore possible that the experimental set-up used for biofilm formation also influences gene expression upon challenge with antifungals, which would mean that the role of changes in drug target levels as a resistance mechanism is highly model-dependent. For these reasons, we do not expect this mechanism to be the major resistance mechanism in biofilm-associated cells.

1.3.6 Persister cells

Persister cells are phenotypic variants rather than mutants[229,270] that are able to survive antibiotic concentrations well above MICs[229]. It is thought that the inability of an antibiotic to affect persister cells is a consequence of the dormant state of persister cells, since antibiotics need an active target to perform their function[271,272].

Since the discovery of persister cells in 1944[273], their presence has been shown in biofilms formed by different bacterial species such as *Pseudomonas aeruginosa* and *Escherichia coli*[274,275] in which persisters make up 0.1 to 1% of all cells[270]. The presence of persister cells in *Candida* biofilms was first shown in 2006 when LaFleur and colleagues observed a biphasic killing of *C. albicans* biofilms. Most of the population was killed at relatively low AmB concentrations, while a very small fraction of cells remained resistant even at high concentrations of the drug. One percent of the population was completely unharmed by antifungal agents, and these cells were appointed 'persisters'. Further, the group showed that the presence of persisters was not dependent on the formation of a complex biofilm structure, but rather on the ability to attach to a surface[229]. Transcriptomics and proteomics on *C. albicans* persisters has shown downregulation of enzymes involved in glycolysis, the tricarboxylic acid cycle, and protein synthesis, and upregulation of glyoxylate shunt enzymes, compared to normal cells. This altered expression resulted in lower production of reactive oxygen species (ROS) and thereby avoided ROS-induced cell damage[276,277]. Moreover, proteins involved in stress response were upregulated[276] which is consistent with the current assumption that exposure to stress can trigger the formation of persisters[278]. Also genes involved in the ergosterol and β-1,6-glucan synthesis pathways were shown to be upregulated. This points to the contribution of changes in cell membrane and cell wall composition in the increased resistance of persisters[279]. However, as it was shown that the formation of persisters is strain- and species-specific, with much lower percentages of persisters present in *e.g. C. glabrata* biofilms, persisters cannot be the sole responsible for high biofilm resistance[280-282].

1.3.7 Drug sequestration

Drug sequestration in planktonic *C. albicans* cells was first demonstrated in a report in which fluconazole was shown to be retained in vesicular vacuoles which were only present in one resistant clinical isolate[283]. A process reminiscent of this was recently implicated in the high antifungal drug resistance of *C. albicans* in gall bladder and bile duct infections. Bile salts were

shown to form micelles encapsulating amphiphilic and lipophilic antifungals such as caspofungin and AmB[284]. However, due to the limited amount of reports available, the actual contribution of such a mechanism in the drug resistance of planktonic cells remains to be seen and might depend on the host niche.

To determine whether the biofilm ECM can sequester antifungals and as such increase the resistance of biofilms, Al-Fattani and Douglas (2006) grew *C. albicans* biofilms under static conditions, resulting in a small amount of matrix material, and under conditions of continuous flow using a modified robbins device (MRD), resulting in a thick ECM. By this means, they could show that biofilm resistance was correlated with the amount of matrix material present[151]. In contrast, two earlier publications that compared drug susceptibility of statically grown biofilms with biofilms grown under gentle shaking did not report any differences associated with the extent of matrix formation[143,150]. This might be caused by the difference in flow regimen[151]. The MRD causes a continuous unidirectional flow over the surface, thereby providing a continuous supply of nutrients, possibly mimicking natural conditions more than does gentle shaking.

One potential mechanism by which matrix material increases biofilm resistance is via restricting penetration of the drug through the biofilm. This was, however, quickly confuted when Al-Fattani and Douglas (2004) showed that after three to six hours of drug exposure, distal places in the biofilm showed drug concentrations that were several times the MIC. Even with this drug permeability into the biofilm complete killing of biofilm-associated cells could not be accomplished[285]. A new light was shed on the matter when Nett and colleagues (2007) discovered that cell walls of biofilm-associated cells were up to two times thicker and contained more carbohydrates, *e.g.* β-1,3-glucans, than stationary or log-phase planktonic cells. This was true both *in vitro*, with supernatant of biofilms containing two- to 10-fold more β-1,3-glucans than supernatant of planktonic cells, and *in vivo*, with serum of rats with a biofilm-associated infection on a central venous catheter containing nearly 10-fold more β-1,3-glucans than serum of rats with disseminated candidiasis. After isolation of matrix material, they could also show the presence of β-1,3-glucans in the biofilm matrix[147], and this amount increased over the course of biofilm maturation[225]. Moreover, they found that biofilm-associated cells could bind four- to five-fold more fluconazole per cell wall weight compared to planktonic cells. Combining these two observations indicates that β-1,3-glucans bind fluconazole in biofilm structures, thereby decreasing the drug's potential to affect biofilm-associated cells. To further corroborate this hypothesis, a combination of 1000 µg/mL fluconazole with 1.25 units/mL zymolyase (a glucanase) could decrease biofilm viability both *in vitro* and *in vivo*, whereas either one separately was not able to do so[147]. Addition of fluconazole to biofilms at 100x the MIC of fluconazole against planktonic cells only marginally affected the metabolic activity of

the biofilm-associated cells and did not alter exopolysaccharide material and biofilm architecture[286]. This gives an indication that binding of fluconazole to β-1,3-glucans does not affect matrix material or biofilm structure. Specific binding of antifungals by β-1,3-glucans was also observed for AmB[267]. Later, Mitchell *et al* (2013) found that also in NAC species, β-1,3-glucans contribute to azole resistance by specific binding[287]. The role of matrix-associated eDNA in drug resistance was indicated by demonstrating the synergistic effect of DNAse with AmB and caspofungin on *C. albicans* cells in mature biofilms. Such a synergy was not observed with fluconazole[288]. More recently, it was shown that also the matrix components mannan and β-1,6-glucan, which form the matrix mannan-glucan-complex, are necessary for sequestration of and resistance to fluconazole[155].

Since these discoveries, the involvement of different genes in drug sequestration by the biofilm matrix has been elucidated. Firstly, the gene *FKS1* was shown to be necessary for resistance. The viability of cells in a biofilm produced by a heterozygous *FKS1* deletion mutant, which showed a 30% reduction in β-1,3-glucans content, was reduced with 80% after 48 hours of treatment with 250 µg/mL fluconazole. A similar effect was not observed in planktonic cells[289]. Furthermore, genes involved in the protein kinase C cell wall integrity pathway, which controls cell wall glucan content in response to stress, were proven to be essential for maintaining the β-1,3-glucan content of the *C. albicans* cell wall and biofilm ECM[290]. Moreover, Taff and co-workers (2012) found that two predicted glucan transferases, encoded by *BGL2* and *PHR1*, and the exoglucanase Xog1, which are all predicted to be present in the extracellular matrix, are crucial for β-1,3-glucans delivery to the matrix and accumulation of β-1,3-glucan in matrix material. Biofilms formed by mutants lacking these genes showed an increased susceptibility to fluconazole. Similar phenotypes were not observed for planktonic cells[291]. The necessity for genes involved in matrix mannan and β-1,6-glucans production was shown recently by Mitchell *et al* (2015) as biofilms formed by different mutants defective in genes in the mannan and β-1,6-glucans pathways were sensitive to fluconazole[155]. Lastly, Yi and colleagues (2011) found that biofilm regulation, including matrix deposition, depends on the *MTL*-locus configuration of the strain. The more resistant *MTL*-heterozygous biofilms are regulated by the Ras1/cAMP-PKA pathway and require the subsequent action of transcription factors Efg1, Tec1 and Bcr1. On the other hand, the structurally similar but thinner and more permeable *MTL*-homozygous biofilms are regulated by the MAPK-pathway and are so far only shown to require the action of transcription factor Tec1[194]. Most interestingly, these observations might indicate the importance of regulation of matrix deposition over general biofilm architecture in conferring antifungal resistance, but further research is needed to validate this proposition.

1.3.8 Stress responses

During colonization of its host, *C. albicans* is confronted with a wide variety of stresses to which it responds via different conserved signal transduction pathways. Upregulation of such pathways is not sufficient for the onset of drug resistance, but is necessary for stabilization of the cells in the presence of drugs to allow for resistance to develop[43]. A crucial signal transduction pathway is the MAPK network[292,293] with a major role for the protein kinase C cell wall integrity pathway that signals via the MAPK Mkc1[293-295]. The importance of the cell wall integrity pathway for virulence in a murine *Candida* model for systemic infection was already published in 1997[230], However, its importance in biofilm formation and resistance was not known until 2005. Then, it was demonstrated that a *mkc1*-null mutant formed an abnormal biofilm with reduced filamentation after 48 hours of development and that biofilms formed by the *mkc1*-null mutant were susceptible to MICs 100-fold lower than wild-type and reintegrant strains[231].

Another key player in stress responses, the serine/threonine protein phosphatase calcineurin, was already known to be essential for survival in serum and therefore for disseminated infection by *C. albicans*[296]. Later, Uppuluri and colleagues (2008) showed that *Candida* strains mutated in calcineurin B (*CNB1*), which encodes the regulatory subunit of the protein, or its downstream target the transcription factor *CRZ1,* could be restricted by much lower concentrations of fluconazole than their wild-type counterparts[297]. Heat shock protein 90 (Hsp90) interacts with the catalytic subunit of calcineurin to stabilize it and prepare it for activation[298]. Hsp90 is known to be important for *C. albicans* resistance against azoles and echinocandins[298] and was shown to be necessary for biofilm dispersal and resistance to azoles *in vitro* and *in vivo*[299]. The latter might be caused by the fact that Hsp90 is a regulator of matrix glucan levels, with deletion of Hsp90 resulting in matrix material with reduced β-1,3-glucan-levels, and thus a reduced potential to capture antifungals[299]. These results indicate that a combination therapy of an Hsp90 inhibitor or calcineurin inhibitor, together with fluconazole would be an interesting therapeutic option. The potential and likelihood of *C. albicans* to develop resistance against such a combination therapy was investigated by Hill and colleagues (2013). They started from strains that were resistant to azoles in a manner dependent on Hsp90 and calcineurin. Of the 290 *C. albicans* strains they started with, seven developed resistance to fluconazole and either geldanamycin (Hsp90 inhibitor) or FK506 (calcineurin inhibitor). The identified resistance mechanisms included: drug target mutations that conferred resistance to geldanamycin and FK506, mutations in *PDR1*, mutations that transformed azole resistance from dependent on calcineurin to independent on this regulator, and mutations in the catalytic subunit of calcineurin. Moreover, they showed extensive aneuploidy in four of the

C. albicans lineages[300]. A second heat shock protein, Hsp104, was also shown to be important for *in vitro* biofilm formation and virulence in a *Caenorhabditis elegans* infection model, but a role for Hsp104 in biofilm drug resistance was not addressed in this study[301].

To conclude, resistance is clearly a complex phenomenon that results from different processes. The biofilm structure greatly enhances *Candida*'s resistance to antifungals. In a human host, *Candida* also needs to be able to withstand actions of the host's immune system. Therefore, the immune interaction of *C. albicans* with its host will be discussed next. As the work in this thesis on the immune system was performed with *C. albicans*, we will focus on this organism.

1.4. The immune response to *Candida albicans* infections

Immunity is a complex and often highly specific process involving different cell types and effector mechanisms. The knowledge available on the immune response to *C. albicans* infections will be summarized here. We will first introduce the primary cell types of the innate and adaptive immune system that are involved in anti-*Candida* immunity followed by a discussion on the recognition of *C. albicans* by our immune system. Next, we will summarize the role of the different immune cell types in specific *C. albicans* infections after which we will finish by discussing the mechanisms that *C. albicans* employs to escape the host immune system.

1.4.1. Immune cell types involved in defense against Candida albicans

The innate immune system is considered the first line of defense against pathogens and comprises different cell types. Protection against *Candida* infections is mainly conferred by epithelial cells and by the monocytes/macrophages, neutrophils, and dendritic cells, or so-called professional phagocytes[302]. Clearance of *Candida* by phagocytes is a step-wise process, requiring (i) recognition of the pathogen, (ii) recruitment of additional phagocytes to the site of infection, (iii) engulfment of the pathogen, and (iv) processing of the phagocytosed cells[303]. Recognition of the pathogen is mediated by pattern recognition receptors (PRRs) that are present on, in or are secreted by different cells of the immune system. They specifically recognize conserved moieties present on or secreted by the pathogen, called pathogen-associated molecular patterns (PAMPs)[100,304]. The PRRs and PAMPs involved in the *Candida*-host interaction will be discussed in the next section. After recognition of the pathogen, it is

bound by the phagocyte cell membrane and engulfed into the cell, forming an intracellular vesicle called the phagosome[303,305]. Killing of the phagocytosed cells happens through maturation of the phagosome transforming it into the phagolysosome. This maturation is correlated with an acidification in macrophages which enhances the activity of hydrolytic enzymes[302,306]. In neutrophils, phagosome maturation is associated with the fusion of preformed, cytosolic secretory vesicles and granules, containing antimicrobial proteins without a significant decrease in pH[302,307]. Moreover, high amounts of ROS and reactive nitrogen species (RNS) are formed inside the phagosome further enhancing its capacity to kill *Candida*[302,308]. Neutrophils can also kill pathogens extracellularly, either by degranulation, thereby releasing antimicrobial peptides in the environment[309], or by the formation of neutrophil extracellular traps (NETs) after activation of neutrophils by microorganisms that are too big to phagocytose, such as long *C. albicans* hyphae[310,311]. NETs are large, extracellular structures that are composed of chromatin decorated with histones, proteases and antimicrobial peptides[311-313]. These NETs immobilize and possibly kill the pathogen, although the latter is still under debate[309,313].

Dendritic cells (DCs) are less efficient at killing *Candida*[314] and are mainly important as antigen presenting cells that activate adaptive immune responses[100,315]. In *Candida* infections, it is known that helper T-cell (Th) subsets Th1, Th2 and Th17 and regulatory T-cells (Treg) are the most important adaptive immune cells[316]. Antigen presentation by DCs leads to T-cell differentiation dependent on the cytokine milieu. The presence of interleukin 12 (IL-12) and interferon γ (IFNγ) leads to Th1 differentiation, IL-4 and IL-10 to Th2 cells, IL-1, IL-6 and IL-23 to Th17 cells and IL-2 and tumor growth factor β to Treg cells[315]. By secretion of specific cytokines, such as IFNγ for Th1 cells and IL-17 for Th17 cells, these T-cells will recruit additional innate immune cells to the site of infection.

1.4.2. Interactions between PAMPs and PRRs

Successful binding of a ligand by PRRs causes receptor-specific signaling through a downstream cascade. This results in pathogen phagocytosis, the onset of pro-inflammatory responses by production of cytokines and chemokines, and the secretion of microbicidal compounds[317]. The major PAMPs presented by *C. albicans* are components of its cell wall[100,305,315]. In the *Candida* cell wall, two layers can be distinguished (figure 1.7).

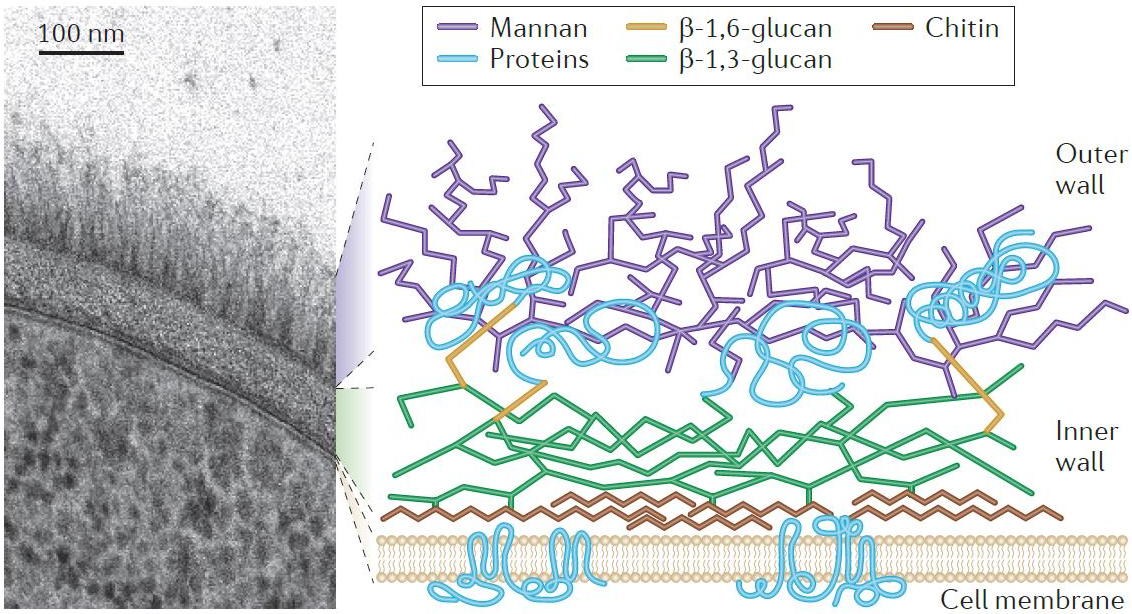

Figure 1.7: Transmission electron microscopy picture and schematic representation of the *Candida albicans* cell wall. From Gow *et al* (2011).

The inner layer is composed of chitin and β-1,3-glucan, which are skeletal polysaccharides conferring strength and rigidity to the cell. The outer layer is composed of highly mannosylated proteins forming long fibrils, that are linked to the inner wall via β-1,6-glucans[27,67,304]. Mannosylation of cell wall proteins occurs during protein synthesis in the endoplasmic reticulum and during protein transport trough the Golgi apparatus[318]. The α- and β-linked mannoses can be incorporated into linear O-linked mannan, which is attached to proteins via a Serine or Threonine residue, into highly branched N-linked mannan, which is attached to proteins via an Asparagine residue, and into phospholipomannan[318]. The exact structure of mannans depends on environmental conditions and cell morphology[319], with the latter also affecting β-glucan structure[320]. In general, glucans make up most of the cell wall polysaccharides (± 60%), followed by mannans (± 28%), and chitin (± 2%)[319,321-323]. Inter-species differences have been observed, with the amount of mannans in the *C. glabrata* cell wall being higher (± 45%) associated with reductions in glucans (± 54%) and chitin (± 1%)[322].

The *C. albicans* cell wall is highly variable. It was for example shown that environmental carbon sources greatly affect cell wall composition[324]. Growth on the non-fermentable sugar lactate for example, results in a thinner cell wall (50% decrease in cell wall dry mass) caused by a significant reduction in chitin and glucans compared to cells grown on glucose[325]. This thinner cell wall was associated with a phenotype of increased resistance to AmB, caspofungin and different cell wall stressors, altered cytokine production in human macrophages, diminished phagocyte recruitment and overall increased virulence in mouse models of systemic

candidiasis and VVC[325,326]. Cell wall plasticity has been shown to also be a result of stress as a study using supra-MICs of echinocandins failed to completely kill *C. albicans* in 10 to 50% of clinical isolates tested, depending on the caspofungin concentration used[327]. Later it was shown that this 'paradoxical effect' was caused by large decreases in cell wall glucan content and concomitant large increases in cell wall chitin content upon exposure to caspofungin[328], again indicating the ability of *Candida* to adapt to stressful environments. Increases in the amount of cell wall chitin have more frequently been shown to protect against caspofungin[329]. Studies with cell wall mutants lacking either glucans or mannans have indicated the importance of these polysaccharides for the resistance of cells to antifungals and to cell wall stressors, and for virulence in different mouse models[321,330-332].

PRRs responsible for the detection of *C. albicans* are primarily present on cells of the innate immune system and to a lesser extent on cells of the adaptive immune system[304]. Important PRRs for the detection of *C. albicans* (figure 1.8) belong to the families of the C-type lectin receptors (CLRs), the Toll-like receptors (TLRs) and the NOD-like receptors (NLRs)[100,305,315,316].

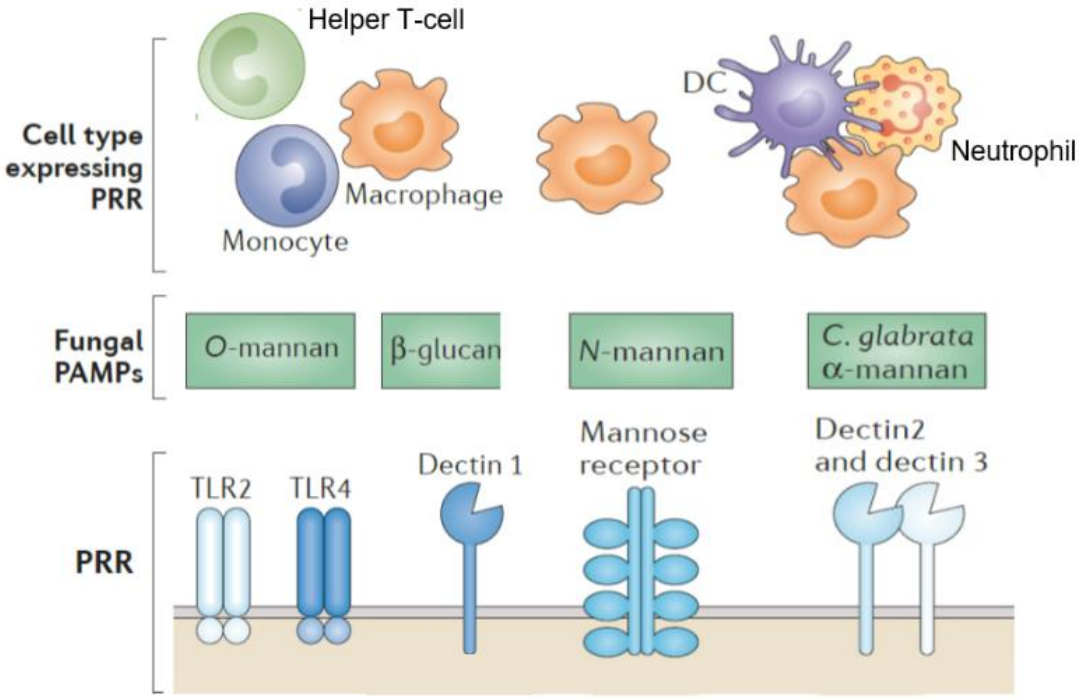

Figure 1.8: Simplified representation of recognition of *Candida albicans* by cell membrane resident PRRs. DC = dendritic cell. Adapted from Netea *et al* (2015).

The major pro-inflammatory PAMP in the fungal cell wall is β-glucan[67] and it is recognized by the CLR Dectin-1[333]. Dectin-1 is mainly present on monocytes and macrophages and signaling leads to the production of cytokines such as pro-IL-1β, tumor necrosis factor (TNF) and IL-10[100,334]. Signaling through Dectin-1 thus mainly promotes Th17 and Th1 cell differentiation in both humans and mice[335]. Other effector mechanisms induced by Dectin-1 signaling are phagocytosis of the fungus[27,334], production of ROS[336] and the prevention of uncontrolled NET release, thereby reducing extensive tissue damage[100,311]. Some of these effector mechanisms require collaboration of Dectin-1 with other PRRs[334,336]. In the cell wall, β-glucans are mostly covered by mannans and are only exposed at sites of bud scars in yeast cells[337]. While these bud scars are absent in hyphae, mannans in hyphal cells are structurally different, and possibly more accessible compared to yeast cell mannans[338,339]. The immunogenic importance of β-glucan was shown in a recent study in which a correlation between β-glucan exposure at the cell wall and decreased *C. albicans* virulence in a gastrointestinal tract infection model in mice was observed [340]. In line with this, macrophages were shown to migrate faster towards cells with increased cell wall β-glucan exposure[272]. In a murine model of systemic candidiasis, NET-dependent neutrophil attack was found responsible for increasing exposure of β-glucans over time. This process requires active cell wall remodeling by the fungus[341,342], indicating that the host has developed mechanisms to cope with fungal immune-evasion strategies. Furthermore, a study using the disseminated candidiasis model in mice showed that recognition depended more on Dectin-1 for a strain with low levels of chitin and β-glucan compared to a strain with high levels of both cell wall components[343]. This indicates that although the role of β-glucans in recognition of *Candida* by Dectin-1 is well established, other PAMP-PRR interactions are at play.

Mannans and mannoproteins are recognized by a multitude of CLRs amongst which mannose receptor, Dectin-2 and mannose-binding lectin (MBL), and some TLRs such as TLR2 and TLR4[100]. Mannose receptor is primarily present on macrophages and detects N-linked mannan[100]. Mannose receptor dependent signaling leads to the production of pro-inflammatory cytokines, such as IL-17, which has been shown to be important for neutrophil-mediated inflammatory responses[100,344]. Dectin-2 primarily recognizes α-mannans and is mainly expressed on macrophages, neutrophils and dendritic cells[100,345]. Dectin-2 signaling results in production of *e.g.* TNF, IL-1β and IL-6, the latter two important for Th17 cell differentiation[346]. When Dectin-2 dimerizes with Dectin-3, cytokine production increases[347]. The circulating CLR MBL binds to mannose-rich structures in *C. albicans* and is important for the recruitment of phagocytes, and for modulation of pro-inflammatory responses[27,100].

TLR2 and TLR4 are the major TLRs involved in recognition of *Candida* mannans, and are present on a range of immune cells, including T-cells[304]. TLR4 recognizes O-mannans and this

leads to the production of pro-inflammatory cytokines such as TNFα and IFNγ[304,348,349]. Cell wall phospholipomannans are sensed through TLR2 and induce the production of IL-10 and TNFα, albeit to a lesser extent than signaling through TLR4[348,350]. Strikingly, it has been shown that TLR4 only senses yeast cells, whereas TLR2 senses both morphologies. This indicates that the switch from yeast cells to hyphae leads to differential cytokine production with a loss of IFNγ production and an increase in IL-10 production, amongst others[348]. The intracellular TLR9 is involved in chitin recognition, and results in the production of anti-inflammatory cytokines, *e.g.* IL-10, hence playing a role in maintenance of a balanced immune response[100,351].

One important role of NLRs is their involvement in the inflammasome, which is a multi-protein complex that can be present in myeloid cells after activation by inflammatory stimuli[352]. The NOD-, LRR- and pyrin domain-containing 3 (NLRP3) inflammasome induces the enzyme caspase 1 which processes pro-IL-1*β* and pro-IL-18 into their active forms that are involved in Th17 cell differentiation[100,353]. In a *C. albicans* infection, the unmasking of β-glucan in hyphal cells, due to altered mannan structure, leads to Dectin-1-dependent activation of the inflammasome, while yeast cells are incapable of such induction[100,339,354,355]. This hyphae-specific activation of the NLRP3 inflammasome plays a role in the proposed mechanism employed by host cells to distinguish between *Candida* colonization and invasion[27], which will be discussed in the next section.

1.4.3. Primary immune effectors in Candida albicans infections

The wide variety of diseases caused by *C. albicans* is associated with compartmentalized immune responses. This will be illustrated in this section which will discuss the major immune cell types that play a role in different *C. albicans* infections.

Oropharyngeal and dermal candidiasis. Because *C. albicans* is a human commensal, epithelial cells have evolved a sensitive signaling cascade that allows them to distinguish between *Candida*'s commensal, harmless state and its pathogenic, invasive state[27]. When a small amount of yeast cells, characteristic of colonization, is present, epithelial cells will recognize these in a TLR4 dependent manner leading to activation of transcription factors NF-κB and c-Jun. However, this activation is too weak for the onset of epithelial immune responses, resulting in tolerance[30,356,357]. However, when the invasive state of *C. albicans*, characterized by hyphae, is sensed by a yet uncharacterized epithelial receptor, the transcription factor c-Fos will be activated via the MAPK pathway. This results in the production of pro-inflammatory cytokines such as IL-1β, IL-6, IL-8, and antimicrobial peptides such as β-

defensin[30,356] (figure 1.9). A study in mice deficient in β-defensin 1 showed elevated oral fungal burden and reduced production of cytokines IL-1β, IL-6, IL-17, and CXCL1 (a.k.a. KC – considered the murine analogue of human IL-8), the latter being an important attractor of neutrophils[358]. This clearly shows the importance of β-defensin 1 in protection against OPC. Further, hyphae-specific activation of the NLRP3 inflammasome leads to increased neutrophil recruitment in the infected tissue and enhanced fungal killing[27].

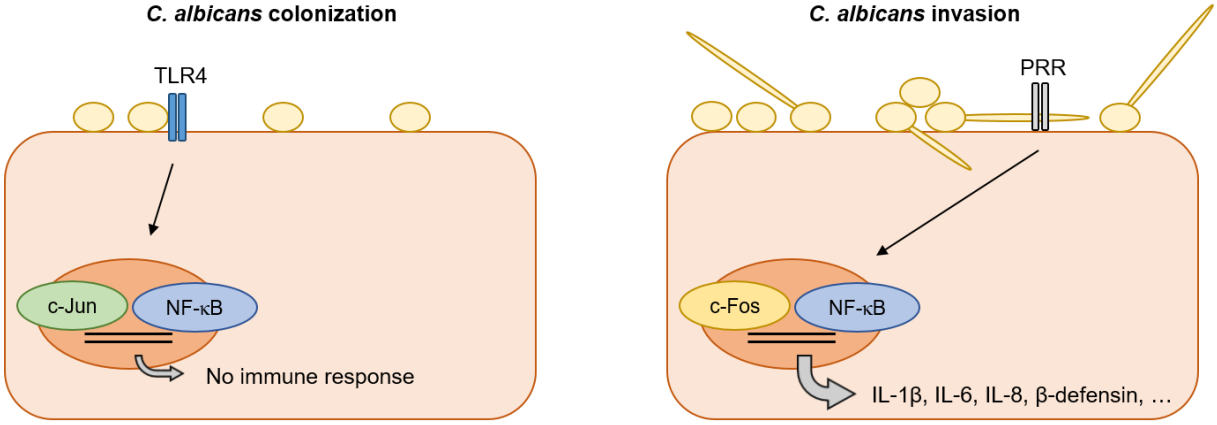

Figure 1.9: Simplified schematic representation of epithelial cell signaling induced by *Candida albicans* colonization and invasion. *C. albicans* colonization will lead to TLR4 dependent activation of transcription factors NF-κB and c-Jun but signaling is too weak and the immune response activation threshold will not be reached. *C. albicans* invasion is sensed by a yet uncharacterized epithelial receptor and will lead to the activation of transcription factor c-Fos resulting in the production of pro-inflammatory cytokines such as IL-1β, IL-6, IL-8, and antimicrobial peptides such as β-defensin. Based on Naglik (2015).

The importance of Th17 immunity in OPC and dermal candidiasis is well established[359,360]. Mice deficient in IL-17 signaling were found to be more susceptible to such infections[361]. Moreover, patients suffering from chronic mucocutaneous candidiasis (CMC), either as an isolated disease or as part of a primary immunodeficiency disorder, were shown to have a deficiency in IL-17 production or signaling or to produce IL-17 neutralizing autoantibodies[362-368]. In response to *C. albicans*, Th17 cells produce IL-17, which is important for neutrophil recruitment and defensin production, and IFNγ[369,370]. Strong neutrophil infiltration was observed in a mouse model of OPC[361] and later it was shown that this IL-17 dependent infiltration was crucial for host protection[371]. One study even found that IL-17 knockout mice are at risk of evolving disseminated *Candida* infections from OPC[372]. Tregs were found to induce Th17 cell differentiation in a murine OPC model, which was associated with a protective phenotype[373]. With regards to the role of macrophages in OPC, one study in mice showed that CX_3CR1-dependent macrophage accumulation was not crucial for host defense against OPC.

Furthermore, patients with polymorphisms in the same receptor were not found to be more susceptible to OPC[374]. In summary, protection against oropharyngeal and cutaneous candidiasis is primarily dependent on IL-17 immunity with an important role for neutrophils in *Candida* killing[359,375].

Vulvovaginal candidiasis. Vaginal epithelial responses to *C. albicans* colonization and invasion were found to be similar to the responses described above for oropharyngeal mucosa[376], while the dispensable nature of macrophage accumulation in infected tissue was also shown in VVC[374]. Lots of studies have been performed using animal models and data from women with RVVC, but no clear connection between Th1, Th2, and Th17 immunity and susceptibility to VVC has been found[377]. However, when looking at the innate immune system, massive influx of polymorphonuclear leukocytes (PMNs; includes neutrophils, eosinophils, basophils and mast cells) has been shown in infected vaginal tissue even though the presence of these PMNs did not affect fungal burden[377]. Even more, a study of VVC in neutropenic mice showed reduced vaginal inflammation[378] suggesting that neutrophil infiltration contributes to inflammation[377]. Interestingly, not the "classical" chemokines (*e.g.* CXCL1/IL-8) were found to be responsible for neutrophil recruitment, but rather a class of S100 alarmins secreted by vaginal epithelial cells, probably together with yet uncharacterized mediators[377,379]. Therefore, neither systemic nor local cell-mediated immunity is considered important in VVC and protection seems to rely more on extrinsic factors such as pH, microbial flora, hormonal balance and possibly genetic factors[34,35,359,380]. The lack of cell-mediated immunity has been proposed to be a host adaptation to avoid chronic inflammation in response to a commensal present in the reproductive tract[377].

Disseminated candidiasis. Protective immunity against disseminated candidiasis involves both innate and adaptive immune responses. Because neutropenia is one of the major risk factors for developing disseminated candidiasis, neutrophils are considered crucial protectors against systemic infections[100]. This was corroborated by several experiments using the mouse model of systemic candidiasis[48,381-383]. Two hours after infection of mice, lots of *C. albicans* hyphae were found to be present in kidneys, which are known to be the organ that is mostly infected in the mouse model of systemic candidiasis[384,385]. Infiltration of neutrophils was higher in spleen and liver than in kidney during the first 24 hours of infection, when the presence of neutrophils is crucial for pathogen control[386]. At later time points in the infection, only kidneys accumulated more neutrophils which was at these time points associated with immunopathology. This indicates the delicate balance between effective host responses and immunopathology[386]. Associated with this, it was shown that the level of CXCL1 in kidneys at 24 to 48 hours post-infection was associated with kidney pathology. Higher levels of CXCL1 were linked with higher kidney fungal burden, higher immune cell infiltrates and a higher

amount of lesions in the kidneys[387]. Together, these data might explain why kidneys show the highest fugal burden in this mouse model. The necessity of macrophages in protection against systemic infections was first assessed using a model of disseminated candidiasis in macrophage-depleted mice, which showed increased susceptibility[100,388]. This was supported by the observation that mice deficient in receptors necessary for macrophage accumulation in infected tissue showed increased mortality, and patients with polymorphisms in one receptor necessary for macrophage accumulation were more prone to disseminated candidiasis[385,389]. In a systemic challenge in mice, 90% of the *C. albicans* cells present in kidneys two hours after infection were either ingested or encircled by macrophages. This illustrates the role of macrophage-mediated immunity early in the infection[384,385].

In the adaptive branch of the immune system, mostly Th cells are involved in disseminated *C. albicans* immunity[316]. However, one recent study showed that B-cells could induce Th17 antifungal responses in naïve Th cells, and that patients deficient in B-cells showed reduced antifungal Th responses[390]. This implies a costimulatory antibody-independent role for B-cells in anti-*C. albicans* immunity, but more research is needed. The role of Th cells in anti-*Candida* immunity has been studied more extensively. The signature cytokine for Th1 responses is IFNγ, which confers fungicidal activities via activation of neutrophils and macrophages, and mice deficient in IFNγ production were shown to be more susceptible to disseminated candidiasis[100,316]. Both IL-18 and IL-12 are strong inducers of IFNγ, but only mice deficient in the former showed increased susceptibility to disseminated candidiasis, which was associated with decreased recruitment of phagocytes to infected organs[391]. Treatment of mice and humans with IFNγ or IL-18 was found to protect against systemic candidiasis, as evidenced by decreased kidney colonization[100,392] or (partially) restored immune function[393] respectively. This indicates the potential of adjunctive immunotherapy in clinical use (see also section 1.5.1, p. 41). Mice deficient in Th17 signaling were more susceptible to disseminated candidiasis[346,361,394,395], and *C. albicans* expressing mammalian IL-17A was shown to be less virulent in a mouse model for systemic candidiasis[371]. However, the CMC immunodeficiencies associated with IL-17 immunity in humans discussed before are not linked with a higher risk for disseminated candidiasis[100]. This indicates that Th17 immunity plays a less important role than Th1 and neutrophil immunity[375]. Further, Forkhead box P3 (Foxp3+) expressing Tregs were found to induce Th17 cell numbers in a mouse model for disseminated candidiasis. These Th17 cells worsened disease outcome, suggesting that the role of Th17 cells in disseminated candidiasis is dependent on the levels of IL-17 produced[396]. The role of Th2 immunity is not completely clear yet, with possible time- and *C. albicans* dose-dependent effects[100,397]. On the one hand, therapeutic ablation of IL-4 and IL-10 in mice resulted in increased resistance to

systemic candidiasis[398-400]. On the other hand, IL-4 and IL-10 were shown to induce protective Th1 responses, although this only seemed to be the case early in the infection[100,401,402].

Biofilms *ex vivo*. Analysis of the interaction between biofilm-associated *C. albicans* cells and our immune system started only recently and seems to be very distinct from interactions with planktonic *C. albicans* cells. Two research groups showed that peripheral blood mononuclear cells (PBMCs; includes lymphocytes and monocytes) and phagocytes did not phagocytose biofilm-associated cells, as opposed to planktonic cells and resuspended biofilm cells[403,404]. In contrast, the presence of PBMCs during biofilm development enhanced the process with significantly thicker biofilms being formed as a consequence of unknown factors secreted by the immune cells[403]. Moreover, priming PMNs with the pro-inflammatory cytokines IFNγ and granulocyte colony-stimulating factor (G-CSF; a cytokine that stimulates the production and proliferation of granulocytes/PMNs) increased damage to planktonic cells, but not to biofilm-associated cells[404]. Exposing the biofilms to sub-inhibitory concentrations of anidulafungin (0.12 µg/L), which has been shown to induce exposure of β-1,3-glucan[341], led to a significant increase in phagocyte induced damage and altered the cytokine profile secreted by phagocytes into a more pro-inflammatory response. This points to a role for β-1,3-glucan detection in phagocyte recognition[405]. By a mechanism that is still unknown, biofilm-associated *C. albicans* cells seemed to change the profile of cytokines secreted by PBMCs[403] and phagocytes[405]. Combining these observations might suggest that masking β-glucans in the biofilm ECM is involved in the mechanism of defective immune response induction in the biofilm[406].

The hypothesis that cells are primarily protected in mature biofilms was established by Xie and colleagues (2012). When three-hours old biofilms were exposed to HL-60 (a human neutrophil-like cell line) cells, their metabolic activity fell back to 20% of untreated biofilms, whereas the metabolic activity of 24- and 48-hour biofilms was only reduced up to 70% of untreated biofilms. Consistent with this, mature biofilms did not elicit a robust oxidative response in sharp contrast with three-hour old biofilms. Moreover, dispersed 24-hour biofilm cells failed to prevent a ROS response, leading the group to suspect a role for the biofilm matrix. This role was confirmed when biofilm matrix alone did not trigger a ROS response, and glucanase treatment of the matrix completely abrogated the matrix ROS-attenuating effect[407]. Infiltration of immune cells into the biofilm structure has been observed repeatedly. In *in vitro* studies, PBMCs and PMNs were shown only to be present in the top and middle layers of most biofilms[194,403], whereas the less frequently encountered, more penetrable *MTL*-homozygous biofilms possessed PMNs distributed over their whole volume[194]. Recently, a study showed that even though neutrophils were recruited to biofilms, they failed to trigger NET release in response to the biofilm-associated cells (figure 1.10), while they were able to do so in the presence of dispersed

biofilm-associated cells. This implies that the inhibition was associated with the biofilm structure[408].

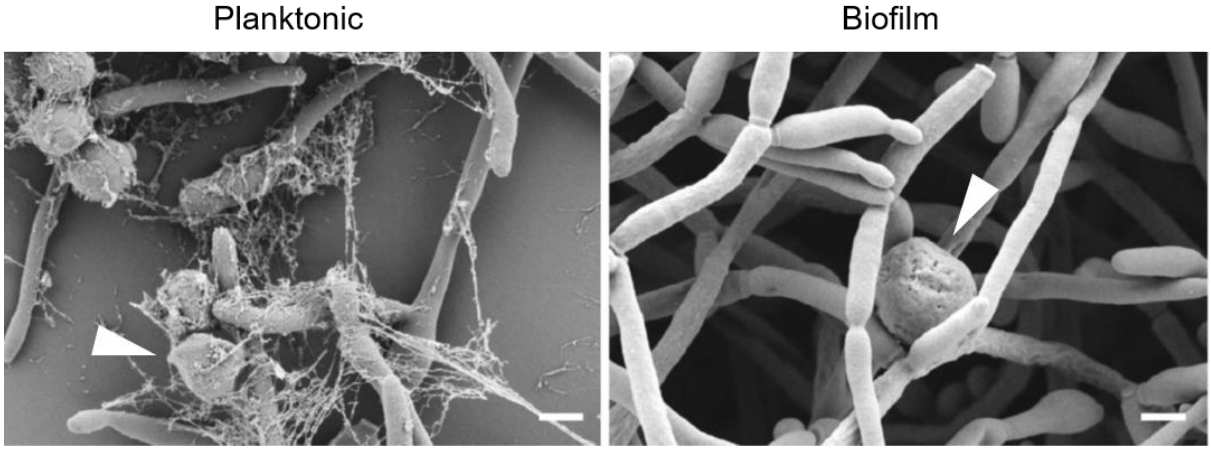

Figure 1.10: Microscopic comparison of interaction between neutrophils (arrowhead) and *Candida albicans* planktonic and biofilm-associated cells. Neutrophils were co-cultured with planktonic and biofilm *Candida albicans* cells at a 1:1 ratio during 4 hours. Thread-like NETs can be observed when neutrophils were co-cultured with planktonic cells, but not when co-cultured with biofilms. Scale bar represents 2 µm. Adapted from Johnson *et al* (2016).

More specifically, inhibition seemed to depend on the presence of ECM mannans, because neutrophils in the presence of a biofilm formed by a *pmr1Δ/pmr1Δ* mutant, impaired in mannan production but still capable of forming a mature biofilm, showed increased NETosis. At the same time, no differences in NET production were observed between the wild-type and *pmr1Δ/pmr1Δ* mutant in planktonic form[408]. This again points at the hypothesis stating that β-glucan masking in the biofilm ECM is involved in biofilm resistance. Together, these *ex vivo* studies suggest that phagocytes are recruited to *C. albicans* biofilms, but that their effector functions are abrogated due to structural features of the biofilm. Further research into this process, including the role of adaptive immunity is however needed.

Biofilms on biotic surfaces. *C. albicans* was found to form biofilms *in vivo* on both oral[409,410] and vaginal mucosa[181], indicating that OPC, VVC and CMC are often biofilm-associated diseases[406]. Oral mucosal biofilms were found to contain commensal bacteria and host cells, in addition to *Candida* cells[409,410]. Neutrophils clustered in and around the oral biofilm, but did not succeed in clearing the biofilm[409]. This was shown to be partly mediated by the hyphae specific cell wall protein Hyr1, because mutants lacking the gene *HYR1* were much less virulent in the murine OPC model[410]. The induction of NETosis was not addressed in these studies, but it is possible that this process was affected as was shown for *in vitro* biofilms[408]. No additional studies were found addressing biofilms on oral and vaginal mucosa specifically.

However, the discussion of immune effectors in OPC and VVC elaborated above possibly applies here. This would indicate that variable immune responses are at play in the immunological interaction with mucosal biofilms in different host niches, possibly related to *e.g.* differences in nutrient availability, host proteins present in the environment, and the commensal flora[406].

Biofilms on abiotic surfaces. Considering that mucosal biofilms occur more often in immunocompromised patients, while this is not the case for device-associated infections, we expect different immune effector mechanisms to be involved here[100,406]. Up till now however, few studies are available that research the immunological interaction between the host and *in vivo* biofilms on medical implant devices. The study by Johnson and colleagues (2016) which was introduced before, showed that NETosis was also inhibited in a biofilm formed in a central venous catheter in rats[408]. Implantation of small catheter pieces, infected with *Candida* cells, under the skin of the back in mice allows for the study of subcutaneous biofilm formation[136,411]. In this model, immunosuppression is used to decrease the variation in biofilm formation on different catheter pieces which is expected to result from an immune response to the catheters implanted[136]. In a variant on this model, a biofilm-specific infiltrate of PMNs was observed in tissue surrounding boxes used for *in vivo* biofilm formation. This infiltrate was not observed in uninfected control mice[412], suggesting that it was biofilm-specific.

Together, the literature reviewed here demonstrates compartmentalized immune responses that comprise fungicidal mechanisms that contribute to pathogen eradication. Usually they are well-balanced with tolerogenic mechanisms to prevent unnecessary damage. The mechanisms employed by *C. albicans* to escape immune recognition and killing will be discussed in the next section.

1.4.4. Candida's tools for host immune evasion

Reducing detection. The normal cell wall structure of *C. albicans* imposes the shielding of β-glucan, which is considered the major pro-inflammatory PAMP exhibited by *C. albicans*, by a layer of mannans[67]. This decreases the ease with which an immune response can be mounted and is therefore considered a host immune evasion mechanism[100].

Inhibiting phagocyte effector mechanisms. *C. albicans* employs several mechanisms to escape from macrophages. *In vitro* studies have shown that when macrophages phagocytose *C. albicans* cells, a rise in CO_2 concentration within the macrophages leads to cAMP-PKA

dependent switching to the hyphal morphology[413,414]. These hyphae can eventually puncture and kill the macrophage, thereby ensuring *Candida*'s escape[305,415] (figure 1.11).

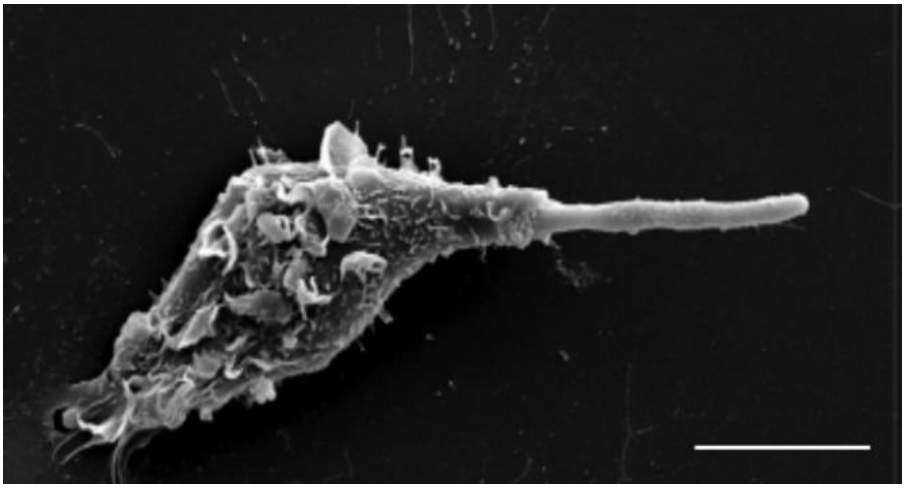

Figure 1.11: Scanning electron microscopy picture of a *Candida albicans* hyphae protruding from a J774 macrophage. Scale bar represents 10 µm. Adapted from McKenzie *et al* (2010).

However, this piercing of macrophages was not observed *in vivo* in a zebrafish larvae model of disseminated candidiasis. Here, *C. albicans* was ingested by macrophages with subsequent survival and cell division inside the macrophage, without filamentation[103]. Later, it was discovered that this filamentation-associated macrophage killing employs pyroptosis, rather than simple piercing of the macrophage, at least early in the infection[305,416-418]. Pyroptosis is a NLRP3 inflammasome- and caspase 1-mediated programmed cell death that is usually used by macrophages to contain intracellular pathogens[416]. A recent study using *C. albicans* mutants defective in filamentation argued that cell wall changes that occur during the yeast-to-hyphae transition, rather than filamentation itself, are causing this pyroptosis[84,419]. Another mechanism of *C. albicans* macrophage escape is non-lytic expulsion/exocytosis, which results in complete expulsion of *C. albicans* from the macrophage leaving both *Candida* and the macrophage viable and able to reproduce[420]. This process was, however, found to be limited to less than one percent of all *C. albicans*-macrophage interactions. *C. albicans* has also been shown to delay phagosome maturation and inhibit the formation of phagolysosomes. Both processes require live *C. albicans* cells and are enhanced by filamentous strains[414,421]. Further, *C. albicans* has developed several mechanisms to block or counteract ROS and RNS production, employing its own enzymes, such as catalase or superoxide dismutase[422,423], by secreting inhibitory factors[424], or even by employing host enzymes[425]. Filamentation and rupture was also observed when *C. albicans* was phagocytosed by murine neutrophils, but not

when phagocytosed by human neutrophils. This difference was attributed to lower enzyme activity and the lack of defensins in murine neutrophils[426]. Lastly, *C. albicans* was found to secrete DNase, allowing its escape from NETs[427].

Modulating cytokine production and immune cell differentiation. As shown before, IL-17 plays a major role in immunological resistance to *C. albicans* infections, especially at the oral and dermal mucosa[359]. However, *C. albicans* is able to cause a shift in tryptophan metabolism in human PBMCs leading to the inhibition of IL-17 production via a secreted factor[428]. Moreover, when *C. albicans* was bound by IL-17, it showed a more virulent phenotype associated with an increase in adhesion, filamentous growth, and biofilm formation[429]. Next to inhibiting the production of specific cytokines, *C. albicans* can also change the cytokine profile secreted by immune cells. For example, secretion of a yet unidentified glycoprotein by *C. albicans* inhibited IL-12 and IFNγ production by human PBMCs[430]. Another group found that an unknown secreted factor could amplify IL-6 and IL-8 production, upregulate IL-10 production, and downregulate IFNγ production in human PBMCs[414,431]. As mentioned before, switching between the yeast and hyphal morphology inhibits *C. albicans* recognition by TLR4, which is associated with a more anti-inflammatory cytokine profile[348]. This process is also often considered an escape mechanism. Further, signaling through TLR2, which can be triggered by hyphal cells, leads to expansion of the Treg population[432] and of a subset of DCs with a more tolerogenic phenotype[433], further indicating that the immunological profile is influenced by the yeast-to-hyphae switch. Moreover, *C. albicans* cell wall chitin was shown to induce a shift from an M1 to a more tolerogenic M2 phenotype in macrophages[425,434]. Altogether, these studies show that *C. albicans* has evolved elaborate mechanisms to steer the immune response into a more tolerogenic one.

The elaborate mechanisms that *C. albicans* employs for decreasing a drugs' potency and for escaping actions of the host's immune system introduced above illustrate why so many research groups are searching for ways to overcome this resistance.

1.5. Overcoming *Candida*'s resistance

Several strategies are being employed to overcome resistance against commonly used antifungals. On the one hand, combination therapies of an antifungal with an adjuvant have been gaining attention[435]. These adjuvants can be very diverse and go from immunotherapies[100,304] over known drugs[436] to molecules that by themselves do not show an antifungal activity[435]. Combination therapies are especially interesting when the adjuvant can directly block resistance mechanisms thereby decreasing the likelihood of resistance

development[437]. On the other hand, efforts are being made to find new antifungals. This however proves to be a very long and difficult process, evidenced by the 30-year span needed to get from discovery to approval of the newest class of antifungals, the echinocandins[438]. Recently, the new echinocandin CD101 is showing promising results in clinical trials with low potential for resistance development[439-442]. Natural products are considered important sources of new therapeutic agents[443] as they show an unmatched chemical diversity[444]. The commonly used antifungal classes of the polyenes and the echinocandins are natural product based[445]. Given the importance of biofilm infections in human disease, the biofilm phenotype should be taken into account when developing novel antifungal therapies[446-448]. Prophylactic therapies to prevent biofilm formation such as catheter lock solution are also highly sought after[202]. Discussing all these would take us too far. Therefore we will focus on immunotherapies and essential oils as they are (indirectly) linked with this work.

1.5.1. Immunotherapies

Combining standard antifungal treatment with adjunctive immunotherapy has been proposed as a means of ameliorating the outcome of *Candida* infections[100,304,449,450]. The rationale behind this is that *e.g.* systemic *C. albicans* infections and OPC occur more frequently in immunocompromised patients. Hence, correcting immune functions by using immunotherapies might be useful as an additional therapy working synergistically with current antifungals[451,452]. Despite their use in *e.g.* aspergillosis[453], no immunotherapies are being used in the treatment of *Candida* infections to date. However, several research groups are focusing on the development of such therapies. Immunotherapies under study range from vaccination over antibodies and recombinant cytokines, to adoptive transfer of primed immune cells[449] and will be shortly discussed below. Obviously, these immunotherapies need to be controlled appropriately to prevent chronic inflammation[453].

Vaccination. The aim of a vaccine is to produce a long-term immune memory response that prevents *C. albicans* infection when effective pre-existing immunity has been lost or modified. The vaccine should not have severe side-effects on the host[454,455]. In the case of *C. albicans* infections, it has been proposed that these vaccines do not need to eliminate the fungus, but may just force it into its commensal state by eliminating major virulence factors[455]. Several studies using mouse models of disseminated candidiasis have shown the protective effect of live attenuated *C. albicans* strains, low doses of virulent *C. albicans* strain, and heat-killed *S. cerevisiae* on a subsequent infection with a high dose of a virulent *C. albicans* strain[456-460]. However, it is expected that attenuated vaccines will not be readily approved by the Food and

Drug Administration (FDA), due to intrinsic risks especially in immunocompromised patients[460]. Therefore, vaccines containing protein antigens are considered safer alternatives[460,461]. Adjuvants added to the vaccine, such as β-glucan, can significantly enhance the antigenicity of an immunogen and trigger different cytokine profiles[449,461]. Moreover, adding an adjuvant to a vaccine can broaden the spectrum of protection and as such decrease the risk of the fungus developing resistance[460]. The choice of adjuvant in a vaccine is thus crucial in steering the immune response towards an effective Th1 response for disseminated candidasis, and β-glucan is often considered a good choice as it stimulates both Th1 and Th17 immunity[449].

A vaccine's success depends on the ability of the host's immune system to effectively respond and provide protection. This possibly hampers the usability of vaccines in immunocompromised patients which are often most vulnerable[449,454]. It has however been proposed that vaccination can be useful in such patients when the timing is right, *e.g.* in transplant patients prior to transplant, and in cancer patients at the time of diagnosis[459]. On the other hand, given the commensal status of *C. albicans*, completely eradicating the fungus prophylactically may have implications on human health that need to be taken into account[454]. Considering these challenges, passive immunization (*e.g.* antibodies and cytokine therapy) is often considered a better alternative in immunocompromised patients. A group of patients that might be ideal candidates for vaccination are women suffering from RVVC who have a fully competent immune system[454,462]. Ideally, such a vaccine would target virulence factors associated with pathogenicity such as morphogenesis, without altering the delicate balance between tolerance and inflammation discussed before[377,462].

So far, two vaccines targeted at patients with RVVC have successfully completed Phase I clinical trials[455]. The first one, NDV-3, contains the N-terminal portion of *C. albicans* Als3 and an aluminum hydroxide adjuvant[463]. A phase I clinical trial showed promising results involving the production of specific anti-Als3 antibodies and a Th1/Th17 associated response, which was confirmed in studies in mice[463-465]. The second vaccine, PEV7, contains truncated, recombinant Sap2 embedded in a virosomal formulation acting as adjuvant[455]. A study using the rat model of VVC showed that production of antibodies in response to the vaccine is probably responsible for the vaccine's protective effect[466]. So far, no further clinical trials have been reported with these vaccines. The fact that the observed responses are different from the natural immune responses observed in patients with RVVC is considered a bonus as effective vaccines against commensals or chronic infections ideally improve the natural situation by eliciting a response that is different from the natural one[455]. A possible problem reported for these vaccines is that they are univalent, which may make it rather easy for *C. albicans* to circumvent the vaccine's activity[455].

Antibodies. Administration of anti-*Candida* antibodies is a means of passive immunization which can be used to directly target virulence traits. An example is Efungumab (Mycograb), which is a human recombinant antibody directed against fungal Hsp90[449]. Combination therapy of this antibody together with lipid formulations of AmB showed a significantly better outcome for patients with invasive candidiasis compared to a combination of AmB with a placebo[467]. A comparable synergy was observed between caspofungin and Efungumab using a mouse model of systemic candidiasis[468]. However, study issues were later pointed out in the former study[469]. So far, no further studies using this antibody have been reported. One study reported that a polyclonal anti-*C. albicans* antibody produced in chicken egg yolk could efficiently prevent adherence and biofilm formation of several *Candida* species *in vitro*[470]. Other approaches include the use of monoclonal antibodies and immune serum from mice[449], but no reports of such approaches being tested in patients were found.

Cytokine therapy. Given that systemic candidiasis and OPC often result from defects in neutrophil and IL-17 immunity, enhancing the immune response using cytokine therapy might be a good option[450,453]. Such therapies are already used and experience regarding efficacy and safety in patients is thus available[449]. Considering the importance of neutrophils and monocytes/macrophages in protection against disseminated candidiasis, the use of hematopoietic cytokines that induce proliferation, differentiation, and maturation of these cell types has been researched[453]. Granulocyte-macrophage colony-stimulating factor (GM-CSF) stimulates the production of monocytes and neutrophils, it enhances the release of ROS by PMNs, prolongs the survival of neutrophils, and upregulates Dectin-1 expression on macrophages[449]. In a study in neutropenic rats with disseminated candidiasis, GM-CSF has been shown to reduce mortality[471]. In patients, a handful of studies are available in which treatment of the patient with GM-CSF, in combination with IFNγ or with antifungals, led to favorable responses in both patients with mucosal infections[472] and with disseminated candidiasis[473,474]. G-CSF promotes the proliferation and differentiation of neutrophils and enhances the antifungal activity of PMNs[450,475]. Treatment of mice with G-CSF enhanced the outcome of a disseminated infection and lowered fungal growth[476]. Administration of G-CSF in combination with fluconazole in nonneutropenic patients with disseminated candidiasis was shown to be safe and trended towards faster clearance of the infection compared to fluconazole alone in a first placebo-controlled trial[450]. Recombinant IFNγ is already being used in practice for several decades[477], for example as treatment for resistant aspergillosis infections[453]. Mice with disseminated candidiasis showed decreased kidney colonization after treatment with recombinant IFNγ[392] and patients with invasive candidiasis showed increased production of IL-1β and restored Th17 responses after treatment with recombinant IFNγ in addition to standard antifungal therapy[393]. Other pro-inflammatory cytokines, such as TNF,

cannot be administered as they elicit strong systemic effects possibly leading to sepsis symptoms[477]. In general, recombinant cytokine therapy seems to be a promising avenue in treating *Candida* infections, but further research and clinical trials are necessary[450,453].

Adoptive transfer of primed immune cells. Infusion of DCs or T-cells in patients with disseminated candidiasis after priming these cells with *C. albicans* or *C. albicans* derived products to generate the desired immunological profile has been proposed[478,479]. However, research is very limited and highly needed to further explore this option.

1.5.2. Discovering new antifungals: essential oils and their components

Essential oils (EOs) are produced by plants as secondary metabolites and have potent antifungal, antibacterial, antiviral, and immunomodulatory activities, among others[480-483]. In plants, they are important for protection and internal messaging. EOs are synthesized by all plant organs *e.g.* flowers, buds, leaves, bark, root, and EOs produced by different organs of the same plant can exhibit different biological and medical properties[481]. They are obtained by steam, water or dry distillation or by pressing the peel of fruits of *Citrus* species. Plant products derived in other ways *e.g.* solvent extraction, are not considered EOs[484]. EOs are complex mixtures of volatile, hydrophobic compounds and one EO typically contains many individual EO components (EOCs) of which a few are usually present at high concentrations and the others in trace amounts[480,484,485]. Often, the components present at high concentrations are causative for the biological effects exhibited by EOs although sometimes minor components, or synergies between different (minor) EOCs are responsible[481,486]. Most EOCs belong to the chemical groups of the phenylpropanoids, which arise from the shikimate pathway, and of the terpenoids, which are formed via the mevalonate and methylerythritol phosphate pathways[487,488] (figure 1.12).

The shikimate pathway is unique to plants and microorganisms and gives rise to aromatic amino acids such as phenylalanine and tyrosine. These can then be further metabolized into phenylpropanoids such as cinnamaldehyde, estragole and eugenol[488]. Mevalonic acid and methylerythritol phosphate are produced from intermediates of the glycolysis pathway. They both form isopentenyl diphosphate, which can convert into dimethylallyl diphosphate. A combination of isopentenyl diphosphate and dimethylallyl diphosphate results in geranyl diphosphate which forms the basis for monoterpenes and monoterpenoids. Addition of one more molecule of isopentenyl diphosphate onto geranyl diphosphate gives rise to farnesyl diphosphate, which is the basis for sesquiterpenes and sesquiterpenoids[488].

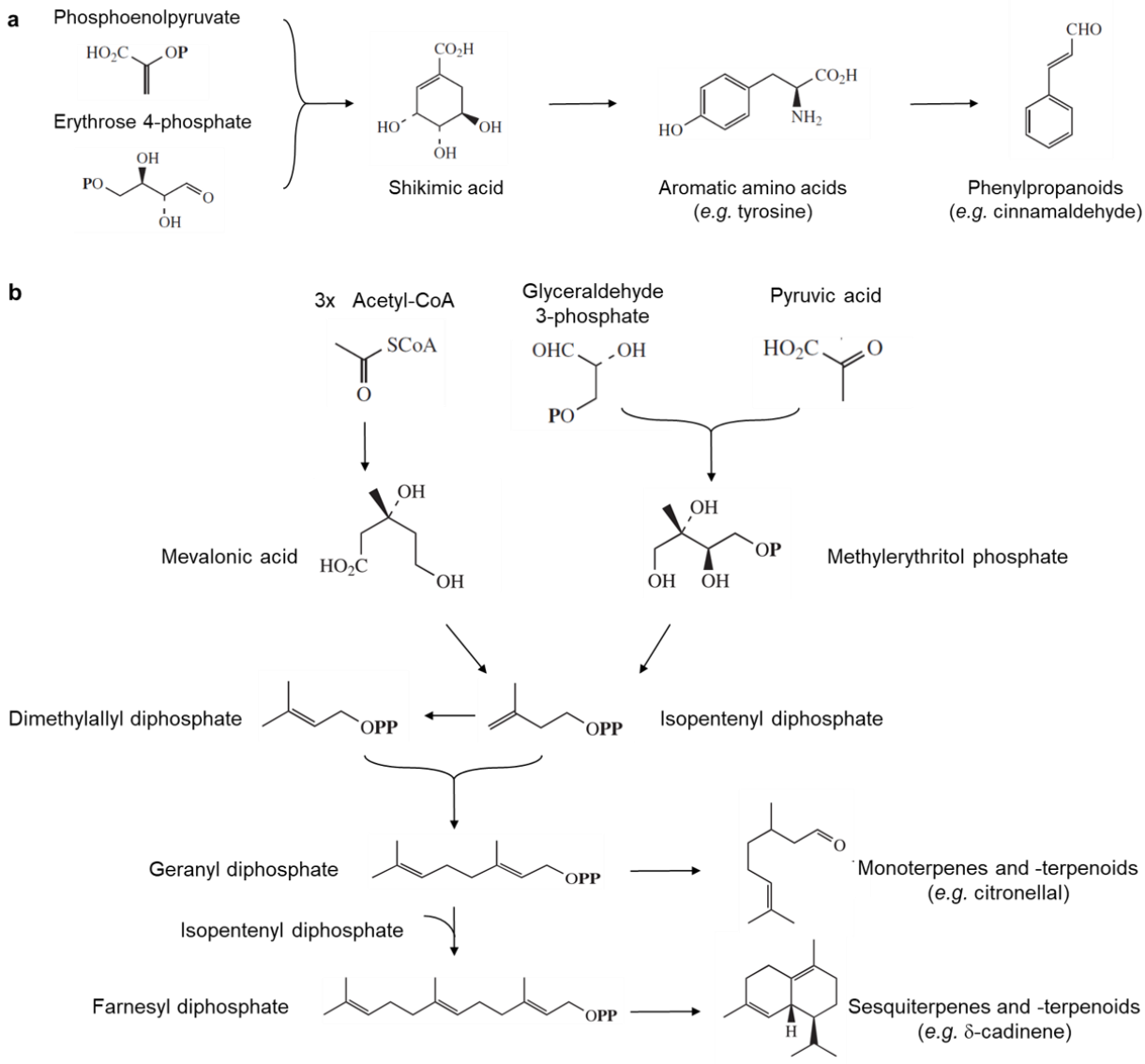

Figure 1.12: Summary of metabolic plant pathways leading to the production of EOCs. a: Production of phenylpropanoids via the shikimate pathway. Phosphoenolpyruvate (glycolysis) will combine with erythrose 4-phosphate (pentose phosphate pathway) to give rise to shikimic acid. This will be used to produce aromatic amino acids that can be further metabolized into phenylpropanoids. **P** = phosphate group. **b:** Production of terpenoids in plants via the mevalonate and methylerythritol phosphate pathways. Three molecules of acetyl-coenzyme A (glycolysis) give rise to mevalonic acid and the combination of glyceraldehyde 3-phophate and pyruvic acid (glycolysis) give rise to methylerythritol phosphate. This combines with mevalonic acid to form isopentenyl diphosphate which forms geranyl diphosphate, the basis for monoterpenes and monoterpenoids, through combination with dimethylallyl diphosphate. Addition of another molecule of isopentenyl diphosphate leads to farnesyl diphosphate, which forms the basis for sesquiterpenes and sesquiterpenoids. **P** = phosphate group. Based on Dewick (1997).

Several EO(C)s show strong antimicrobial activities in general, including anti-*Candida* activities and activity against *Candida* biofilms[115,486,489,490]. To be able to compare the antimicrobial activities of different EO(C)s, the MIC is often determined using for example the broth microdilution assay[491] (see also section 1.3, p. 16). Examples of EOs with anti-*Candida* activity are *Melaleuca alternifolia* (tea tree oil)[492], *Ocimum basilicum* (basil)[493], *Lavandula* species (lavender)[494], and *Mentha* species (mint)[493,495]. The anti-*Candida* activities shown by these EO(C)s can be fungistatic or fungicidal *e.g.* nerol which exhibits apoptosis-like effects[496], or can directly affect virulence traits of *Candida e.g.* citronellal which can inhibit the yeast-to-hyphae transition in *C. albicans*[497]. Given that many EO(C)s are hydrophobic, a commonly observed mode of action is interference with the fungal membrane[481,490,497,498]. Some EOCs have been shown to increase the activity of commonly used antifungals. An example is carvacrol which sensitized *C. albicans* biofilms to fluconazole[499].

An interesting property of EO(C)s is their volatility, and the vapor-phase of EO(C)s has been shown to have antimicrobial properties that can be different from the antimicrobial properties of the EO(C) in liquid form. The vapor-phase can show a higher antimicrobial activity in some cases[498,500]. One possible explanation would be that, due to the hydrophobic nature of EO(C)s combined with their poor solubility in an aqueous environment, there is poor interaction between the organism in culture and the EOC, while the vapor-phase allows direct interaction[500]. The antimicrobial activity of the vapor-phase of specific EO(C)s has been shown against multiresistant *Staphylococcus aureus*[501], bacterial biofilms[502], and *Candida* planktonic cells and biofilms[498,503,504]. The prime method to determine the vapor-phase activity of essential oils is the vapor diffusion method in which the microorganism of interest is grown in a petri dish. This is then incubated upside down on top of a container containing an EO(C) after which a zone of inhibition in is measured[500]. Moreover, methods have been developed to determine the minimal inhibitory dose, which is calculated by dividing the dose of EO(C) by the volume of air in the petri dish[500]. Next to this vapor-phase activity, EO(C)s can also exhibit antimicrobial activities in solution but over a distance *i.e.* vapor-phase-mediated antimicrobial activities (VMAA). This activity resembles the antimicrobial activity quantified by the MIC, but incorporates the volatility of the EO(C). Quantifying this activity allows for different applications of EO(C)s that benefit from the activity over a distance. However, up to date no straightforward assays are available for the detection of such vapor-phase-mediated antimicrobial activities.

Even though EO(C)s have been used for centuries in alternative medicine, scientific research into the antimicrobial activities of EO(C)s only started recently[484]. Double-blinded clinical trials are however complicated due to the odorous nature of EO(C)s which makes the choice of a proper placebo troublesome[484]. Several advantages are associated with the use of EO(C)s as antimicrobials such as low production cost (for most EO(C)s) and the ability of EOs to act on

multiple targets due to their complex nature[481]. The latter, however, is also potentially associated with increased toxicity towards host cells, pointing at the importance of proper toxicity studies[484]. Nowadays, several EO(C)s are already used in food and have obtained the 'Generally recognized as safe' status from the FDA[481]. To further explore the potential of EO(C)s in both the liquid and vapor-phase, standardized assays[201], and screenings of EO collections are necessary[481].

1.6. Aim of this study

1.6.1 The immune response to subcutaneous Candida albicans biofilms

Immunotherapies seem promising as adjunctive therapies against *Candida* infections. Because lots of *Candida* infections are biofilm related it would be interesting to explore the potential of immunotherapies against biofilm-related infections. Unfortunately, our knowledge on the interaction between the host-immune system and *Candida* biofilms is limited, which makes that the necessary knowledge for developing immunotherapies is missing. In this work, we aim to shed light on the mechanisms underlying the resistance of a *C. albicans* biofilm to the host immune system. Three hypotheses are plausible to explain why *C. albicans* biofilms are not spontaneously cleared, and these are explained in detail in the introduction of part I – Immune response (p. 51). Estimating the contribution of these hypotheses in the resistance of biofilms to the host immune system would provide crucial information for the development of immunotherapies.

In a subcutaneous catheter model system[136] in C57BL/6 mice, we will first use a *pmr1Δ/pmr1Δ* mutant with reduced mannan and increased glucan content in cell wall and biofilm ECM[155,321]. Given the important role for biofilm matrix in antifungal resistance (see section 1.3.7, p. 23) we hypothesize that the reduced matrix and increased exposure of β-1,3-glucan in the cell wall and matrix in biofilms formed by the mutant strain will result in biofilms that are more susceptible to the immune system. We therefore expect that these biofilms will be cleared more easily. After the infection, we aim at distinguishing between the hypotheses by measuring the systemic immune response towards the infection. However, this approach is highly dependent on our capacity to detect a systemic immune response and is therefore risky. For this reason, we will adopt a second approach with a more straightforward readout.

In the second approach we will research the influence of a 14 day immunization with subcutaneous biofilms on the outcome of a subsequent systemic infection. It has previously

been shown that a low dose *C. albicans* injected intravenously (i.v.) in mice protects them from a subsequent lethal dose (= immunization)[457]. Here, we want to research if subcutaneous biofilms can confer the same protection. To this purpose, we will again use the subcutaneous catheter model system, together with the systemic infection model, and immunize mice during 14 days with either a low dose of *C. albicans* injected intravenously or with subcutaneous biofilms on catheters. As a control, naïve mice will be included. By following survival and determining the infectious load in kidneys we will aim to distinguish between the three hypotheses.

Eventually we want to uncover the contribution of each of the three hypotheses in the lack of clearance of a biofilm *in vivo* by the host immune system. This will give us crucial information for the development of immunotherapies against biofilms. Moreover, by including a cell wall and biofilm ECM mutant with increased β-1,3-glucan exposure, we will gain insight in the role of the biofilm ECM in the process.

1.6.2 The vapor-phase-mediated anti-Candida activity of essential oils and their components

In the second part of this work we will try and overcome antifungal drug resistance by finding new antifungals to which no resistance is present. We will specifically focus on the vapor-phase-mediated anti-*Candida* activity of essential oils and their components. As no straightforward quantitative assays are available up to date for the detection of such vapor-phase-mediated activities, we will first develop a novel assay. The assay is based on the protocol for the broth microdilution assay used for the determination of the MIC of antimicrobials[197,198,505]. To exhaustively characterize the activity of volatiles in the assay, we will test a collection of over 200 EO(C)s and as such map the vapor-phase-mediated activity of commonly used essential oils against *C. albicans* and *C. glabrata*.

Part I: The immune response to subcutaneous *Candida albicans* biofilms

The data presented here were part of a collaboration with the Translational Immunology Lab of Prof. Adrian Liston where Josselyn Garcia-Perez worked on the project. Part of this work has been submitted to Frontiers in immunology (first page of manuscript below) and the following text may contain text based on this manuscript.

Candida biofilms trigger, but resist, effective anti-*Candida* immunity

Authors: Josselyn E. Garcia-Perez[1,2¶], Lotte Mathé[3,4¶], Stephanie Humblet-Baron[1,2], Annabel Braem[5], Katrien Lagrou[2,6#], Patrick Van Dijck[3,4&*] and Adrian Liston[1,2&*].

Running title: Candida biofilm immune evasion

Affiliations:

[1] VIB Center for Brain & Disease Research, Leuven, Belgium

[2] Department of Microbiology and Immunology, University of Leuven, Leuven, Belgium

[3] VIB – KU Leuven Center for Microbiology, Heverlee, Belgium

[4] Laboratory of Molecular Cell Biology, KU Leuven, Heverlee, Belgium

[5] Department of Materials Engineering (MTM), KU Leuven, Heverlee, Belgium

[6] Department of Laboratory Medicine and National Reference Center for Medical Mycology, University Hospitals Leuven, Leuven, Belgium

*Corresponding Authors: Patrick Van Dijck (patrick.vandijck@kuleuven.vib.be), Adrian Liston (adrian.liston@vib.be) **Lead contact for editorial purposes only:** Adrian Liston

[¶] Equal contribution first authors

# Equal contribution last-authors

2. Part I - Immune response: Introduction

An indwelling catheter in a central vein is a major risk factor for the development of systemic candidiasis[11] and the presence of a biofilm on such a catheter significantly worsens the outcome of a systemic infection[173]. While it is known that our immune system is incapable of clearing a biofilm infection, we lack knowledge on the interaction of our immune system with a *C. albicans* biofilm on a medical implant device[406,506]. Three hypotheses are plausible to explain why *C. albicans* biofilms are not spontaneously cleared (figure 2.1).

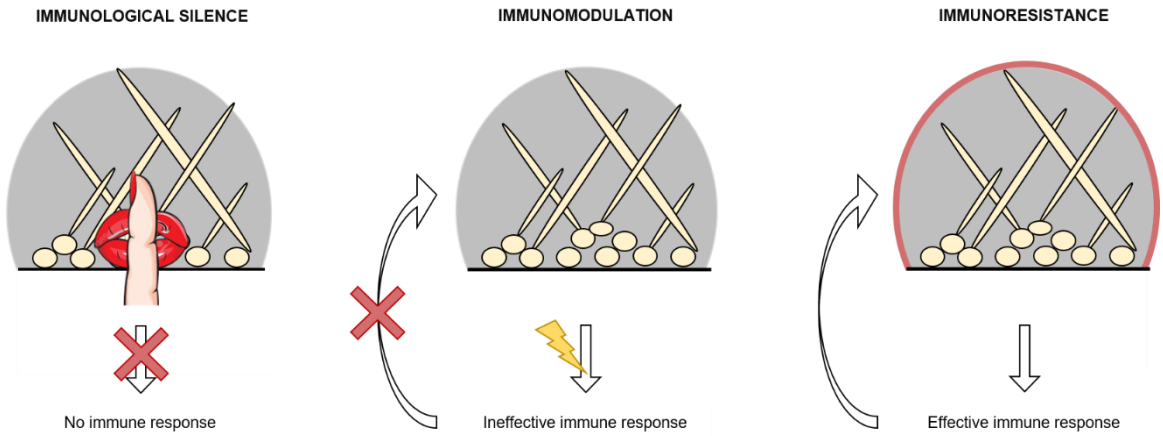

Figure 2.1: Three possible hypotheses might explain why biofilms are not affected by the immune response. The hypothesis of immunological silence assumes that the immune system remains unaware of biofilm presence. The hypothesis of immunomodulation assumes that the biofilm induces an ineffective immune response, which per definition cannot affect the biofilm. The hypothesis of immunoresistance assumes that the biofilm does induce an effective immune response, but that the structure of the biofilm protects it from this immune response.

First, the biofilm may be immunologically silent for example by preventing the release of PAMPs and microbial antigens through the matrix serving as a shield, thereby ensuring that the host immune system remains ignorant of biofilm presence[408]. Second, the biofilm may induce the expression of immunomodulatory factors capable of reducing effective immune responses. This process would resemble the immunomodulation by planktonic *Candida* cells through the downregulation of IL-17 and IFNγ production and upregulation of IL-10 production shown before[428,430,431]. Third, effective anti-*Candida* immunity may be induced in the host, but the structural features of the biofilm may render the biofilm-associated *Candida* resistant to immune clearance. This is reminiscent of the role of the extracellular matrix in resistance to antifungal drugs[155,225]. Formally proving the contribution of any of these hypotheses in biofilm resistance to host defense mechanisms would provide us with essential tools for creating anti-

Candida adjunctive immunotherapies by showing whether an appropriate strategy would aim at overcoming local resistance or at rerouting immunity to an effective response.

To discriminate between these hypotheses, we first adapted the subcutaneous biofilm model system[136,411] for use in C57BL/6 mice. In this model, *C. albicans* is let to adhere *in vitro* to catheter pieces, which are later implanted subcutaneously under the skin on the back of mice (figure 2.2). This is an ideal model as it does not induce severe illness in the mouse, while still mimicking *in vivo* biofilm formation.

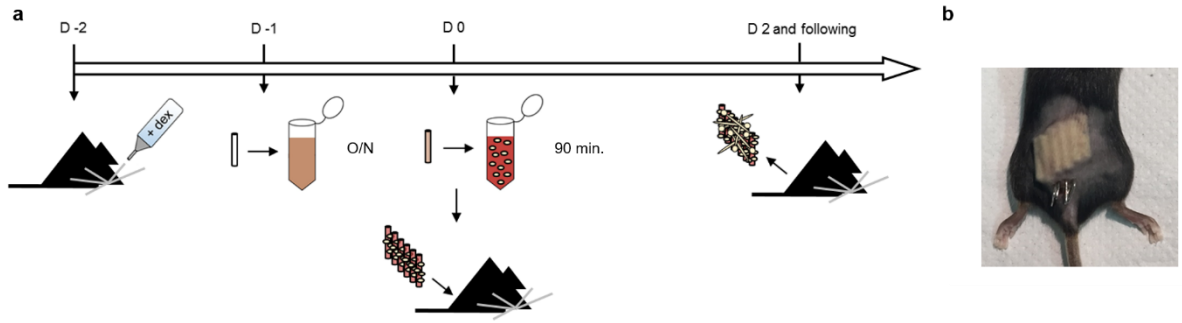

Figure 2.2: The subcutaneous biofilm model system in mice. a: Immunosuppression is started two days prior to catheter implant by adding 1 mg/L of dexamethasone to drinking water (D -2). Catheter pieces are incubated overnight (O/N) in fetal bovine serum (D -1), incubated for 90 minutes in a *C. albicans* cell suspension and implanted subcutaneously (D 0). Colony forming units are determined at day 2 and following. **b:** Image of catheter pieces implanted subcutaneously in a C57BL/6 mouse.

To establish whether subcutaneous biofilms are immunologically silent, we determined immune cell populations in the secondary lymphoid organs spleen and lymph nodes in which induction of adaptive immunity takes place[507]. In case of immunological silence, we would expect not to see an immune response being induced in response to the biofilm infection. To further discriminate between hypotheses, we included a glycosylation mutant lacking the Golgi P-type ATPase Pmr1 which transports divalent cations, that act as essential cofactors for mannosyltransferases, into the Golgi[321]. Deletion of both copies of *PMR1* results in an 80% reduction in total mannans in the cell wall[321] and biofilm matrix[155]. This is associated with increased exposure of the major pro-inflammatory PAMP β-glucan[421]. It has been shown that β-glucan exposed as a consequence of caspofungin treatment is bound by the PRR Dectin-1[341]. β-glucan signaling via Dectin-1 promotes Th1/Th17 immunity in both humans and mice[100,335,508]. A differential interaction of the murine and human immune system with this *pmr1Δ/pmr1Δ* mutant has been shown *in vitro* and *in vivo*[408,509-513]. Moreover, the biofilm formed by *pmr1Δ/pmr1Δ* was shown to be 40% more susceptible to fluconazole[155], and more host cells, *e.g.* immune cells, were present within an *in* vivo biofilm formed by the *pmr1Δ/pmr1Δ*

mutant compared to the background strain[408]. Based on these data, and the role of the biofilm matrix in resistance to antifungal drugs (see section 1.3.7, p. 23), we hypothesized a role for biofilm matrix in protection of the biofilm from the immune system. Due to the increased exposure of β-glucan in the biofilm ECM and cell wall of the mutant, including the mutant in our experiment will allow us to distinguish between the hypotheses of immunomodulation and immunoresistance (figure 2.3).

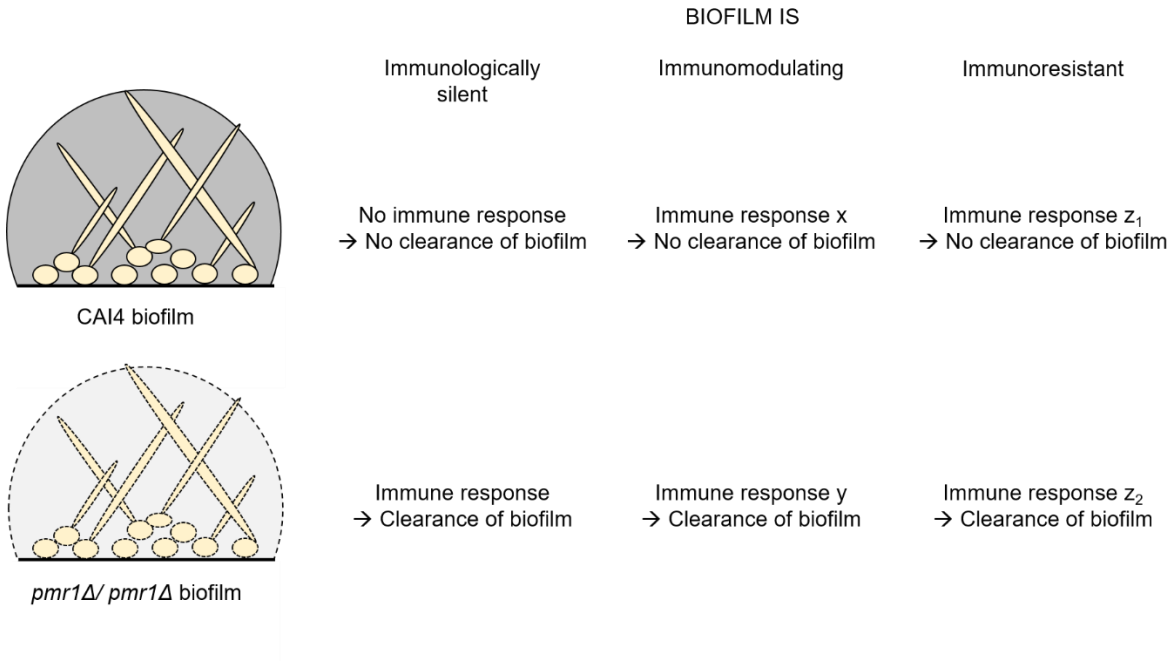

Figure 2.3: Rationale behind the matrix-mutant biofilm approach used to distinguish between hypotheses. CAI4 biofilm = biofilm formed by the background strain (CAI4-CIp10), in which both copies of *PMR1* were deleted resulting in the *pmr1Δ/pmr1Δ* strain.

On the one hand, a shift in immunity when comparing the response to biofilms formed by wild-type and mutant strains, associated with increased clearance of the mutant biofilm, would indicate that the biofilm-associated *C. albicans* actively immunomodulates. Alternatively, a comparable immune response against wild-type and mutant biofilms, associated with increased clearance of the mutant biofilm would show that the biofilm ECM renders the biofilm resistant. Since this approach relies heavily on the detection of an immune response in the chosen experimental set-up, it is risky. Therefore, we also adopted a different approach with an easier read-out.

It has been shown that a low concentration of *C. albicans* cells injected i.v. via the tail vein can confer protective immunity in mice and as such protect them from a subsequent lethal *C. albicans* challenge[457]. This study was the first one showing the immunological memory of innate immune cells in mammals, as the process was mediated by monocytes, and was termed 'trained immunity'[457,514]. Here, we wanted to see whether a biofilm on subcutaneous catheter pieces could confer the same protective immunization as a low dose of cells injected i.v. Moreover, we believed that the outcome of this experiment could further elucidate the contribution of the three different hypotheses in biofilm resistance to the immune system. In an ideal situation, the possible outcomes would be (figure 2.4): If the biofilm was immunologically silent, a subcutaneous biofilm would fail to protect against a lethal systemic challenge, reflected by an experimental outcome indistinguishable from that in naïve mice. If immunization with a subcutaneous biofilm would decrease survival rate and result in an increased infectious load in kidneys, the main infected organ in a systemic infection, compared to naïve mice, it would be indicative of biofilm immunomodulation. Lastly, a protective immunity reflected in increased survival rate and associated with decreased kidney counts would indicate biofilm resistance to the immune response. These are however ideal situations, and it is possible that more processes play a role and/or that over the course of the infection the interaction between biofilm and immune system changes.

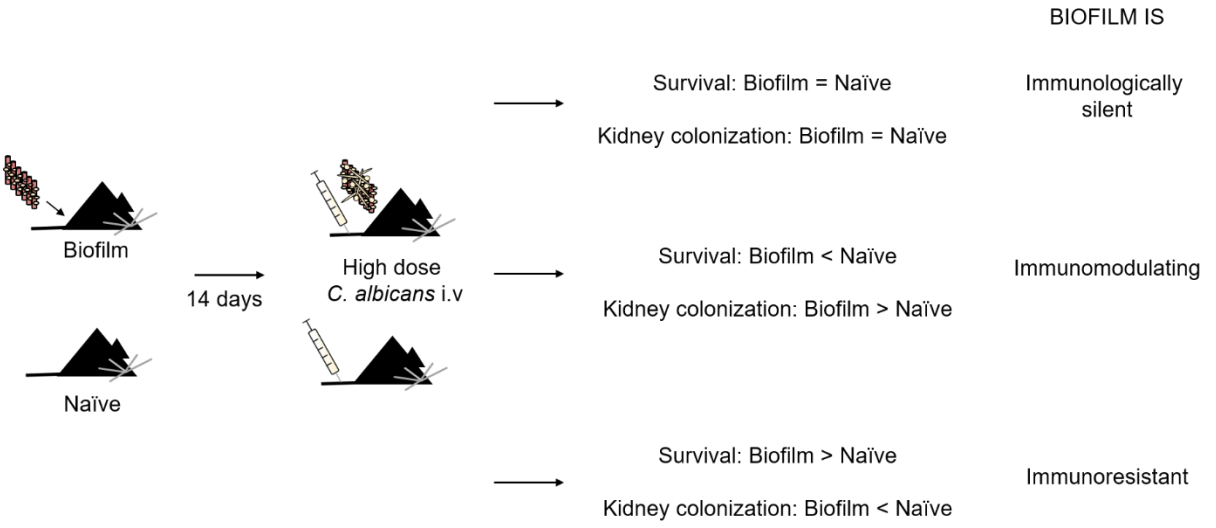

Figure 2.4: Rationale behind the immunization approach used to distinguish between hypotheses. *C. albicans* biofilms formed subcutaneously in the back of mice for 14 days after which mice were challenged with a high, lethal dose of *C. albicans* injected i.v. Different experimental outcomes would allow to distinguish between different hypotheses as demonstrated.

3. Part I - Immune response: Results and discussion

3.1. *Candida albicans* biofilms are robustly maintained in the subcutaneous biofilm model system in immunocompetent C57BL/6 mice

In the original subcutaneous biofilm model system, Sprague Dawley rats or Balb/c mice were immunocompromised to reduce inflammation in response to catheter implantation and thereby decrease variation in biofilm biomass[136,411]. However, for the study of the immune response to subcutaneous biofilms, an intact immune system is indispensable. Therefore, we tested whether biofilms are maintained robustly in immunocompetent C57BL/6 mice. To this purpose, catheter pieces with approximately 1 000 *C. albicans* SC5314 cells adhered were implanted subcutaneously in immunocompetent (IC) and immunosuppressed (IS) mice. Immunosuppression was carried out by the synthetic glucocorticoid dexamethasone, which is often used as an anti-inflammatory drug, and results in a generally decreased immune response[515].

We did not observe significant differences in the mean or variance of biofilm formation between the groups of mice at day two or day six (figure 3.1a) or in the standard deviation (SD) of technical repeats (= catheter pieces) within one mouse (figure 3.1b). In fact, the SD of technical repeats seems to be higher in immunosuppressed mice, but this is probably due to the limited number of mice included in the study. This indicates that C57BL/6 mice do not need to be immunosuppressed for robust biofilm maintenance in contrast to what was found before for Sprague Dawley rats[136]. Differences between species are probably causing these results. Also in the original model, catheter pieces are incubated overnight in fetal bovine serum to ensure *C. albicans* adherence to the catheter pieces. To decrease the chance of a murine immune response to the material itself, we incubated the catheter pieces in mouse serum instead of fetal bovine serum, which did not significantly alter the ability of *C. albicans* to adhere to the catheter pieces (data not shown). Assessment of the kinetics of biofilm biomass in the implanted catheters demonstrated that most of the biofilm growth occurred in the first four days following implantation, with stable biomass maintenance up to 15 days post-implantation (figure 3.1c). Scanning electron microscopy and confocal laser scanning microscopy on catheter pieces implanted in immunocompetent mice revealed a mature biofilm containing an extensive network of hyphae present two days post-implantation, which is covered by a thick matrix at 15 days post-implantation (figure 3.1d). Together these results indicate that immunosuppression is not necessary for robust biofilm maintenance. Moreover, they reflect the limited capacity of the murine immune system to clear *C. albicans* biofilms on subcutaneous catheter pieces in the 15 day study period.

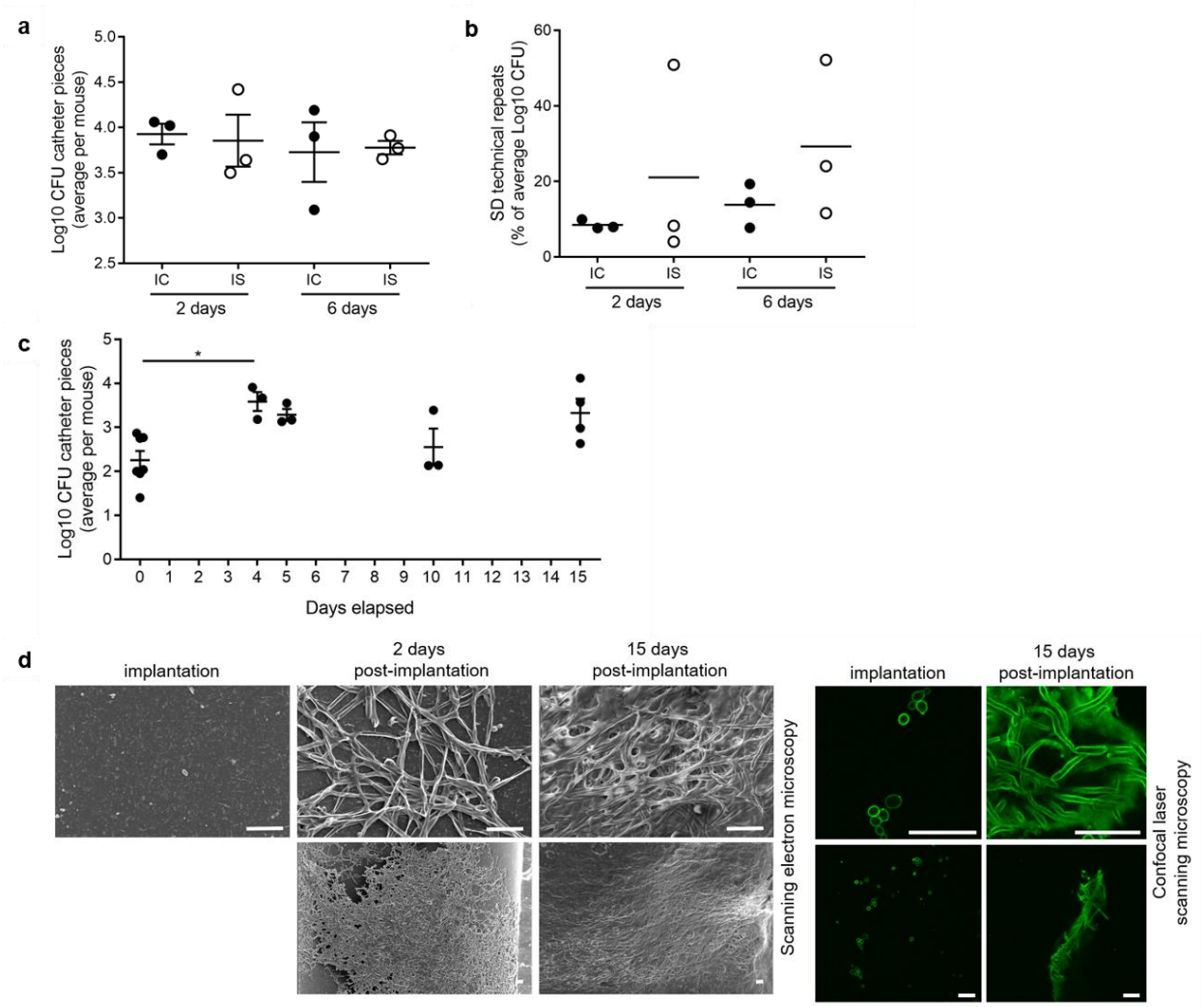

Figure 3.1: *Candida albicans* biofilms are robustly maintained in immunocompetent C57BL/6 mice. **a:** Log_{10} of biofilm CFU compared between immunocompetent (IC) and immunosuppressed (IS) mice (n=3) at two and six days post-implantation. Each data point is the mean CFU on all catheter pieces in one mouse. Mean and standard error of the mean (SEM) is shown. Unpaired t-test was performed between groups within time points. **b:** SD of 6 catheter pieces within each mouse (technical repeats; n=3) compared between IC and IS mice at two and six days post-implantation. Unpaired t-test was performed between groups within time points. **c:** Log_{10} of biofilm CFU followed over time (n=3-6). Day 0 = before implantation of catheter pieces. Each data point is the mean CFU of all catheter pieces in one mouse. Mean and SEM are shown. ANOVA with Tukey's test for multiple comparisons was performed. *$p<0.05$. **d:** Representative scanning electron microscopy and confocal laser scanning microscopy images of catheter pieces prior to implantation, and two and 15 days post-implantation. Scale bar represents 20 µm.

3.2. *In vitro* biofilm formation is not affected in the *Candida albicans* glycosylation mutant *pmr1Δ/pmr1Δ*

All experiments involving the *pmr1Δ/pmr1Δ* strain were performed with the wild-type background strain CAI4-CIp10 (further referred to as CAI4), the *pmr1Δ/pmr1Δ* mutant and a heterozygous reintegrant strain in which one copy of *PMR1* was supposedly reintegrated ectopically in the deletion background[321]. All strains have *URA3* reintegrated on a CIp10 plasmid. However, a PCR on *PMR1* in the original locus revealed that the gene was still present there in the reintegrant strain. Moreover, RT-PCR showed that gene expression was higher in the reintegrant compared to the wild-type background strain (data not shown). This shows that the reintegrant strain that we received does not have the correct genotype and results obtained with this strain are therefore excluded in this work. The genotype for the *pmr1Δ/pmr1Δ* mutant was confirmed using PCR and RT-PCR.

It is known that *in vitro* growth of the *pmr1Δ/pmr1Δ* strain is not markedly affected compared to CAI4, as witnessed by similar growth rates in YPD and SD medium[321]. However, before using the *pmr1Δ/pmr1Δ* strain in the *in vivo* biofilm model, we verified whether the gene deletion influenced growth in RPMI and hyphae formation in response to serum, which are both important for *in vitro* biofilm formation. Furthermore, we tested *in vitro* biofilm formation on catheter pieces, as this is a prerequisite before using the strain in the subcutaneous biofilm model system. The growth of the wild-type background strain CAI4 and the mutant strain *pmr1Δ/pmr1Δ* was compared by growing the strains during 24 hours in RPMI at 30°C and 37°C. No differences in growth were observed between the CAI4 and *pmr1Δ/pmr1Δ* strains, and a representative example (RPMI 37°C) is shown in figure 3.2a. After 15 hours of growth, big fluctuations in growth between technical repeats and subsequent time points were observed for all strains, probably due to hyphae formation influencing the measurements. As these later time points were thus not informative, we only show the first 15 hours of growth in figure 3.2a. To test whether hyphae formation was affected by the homozygous deletion of gene *PMR1*, we grew the CAI4 and *pmr1Δ/pmr1Δ* strains in the presence of fetal bovine serum at 37°C, both being hyphae-inducing conditions[58]. After 90 minutes of growth we see the initiation of filamentation in both strains, with short hyphae being present after 170 minutes (figure 3.2b). Assessment of the *in vitro* biofilm formation of both strains revealed no significant differences in biofilm formation between both strains after 48 hours at which point mature biofilms are expected to be present[136] (figure 3.2c). Hence, from these experiments we can conclude that *in vitro* biofilm formation, measured in terms of CFUs, is not affected by homozygous deletion of the gene *PMR1*.

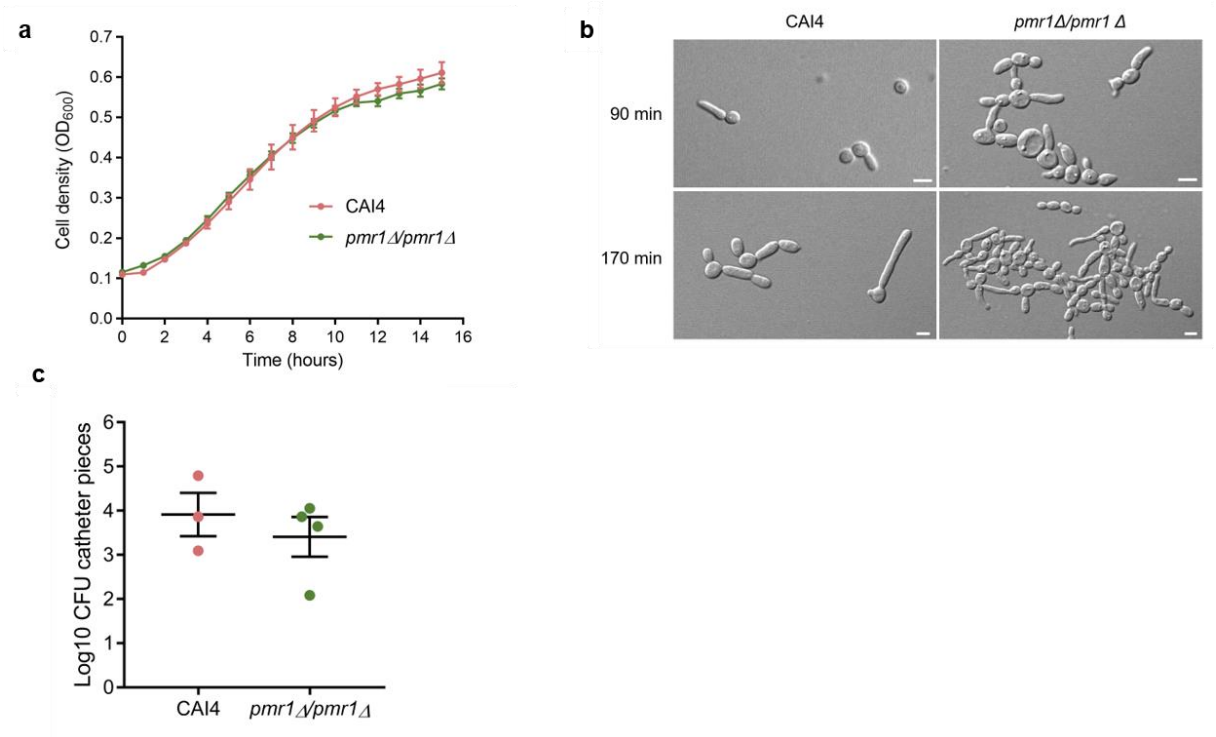

Figure 3.2: *In vitro* biofilm formation is not affected in strain *pmr1Δ/pmr1Δ*. a: Growth of the background strain CAI4 and the deletion mutant *pmr1Δ/pmr1Δ* in RPMI medium at 37°C. Each time point represents the mean and SD of three technical repeats. **b**: Yeast-to-hyphae switching of CAI4 and *pmr1Δ/pmr1Δ* in response to serum. Scale bar represents 5 µm. **c**: Log_{10} of biofilm CFU compared between CAI4 and *pmr1Δ/pmr1Δ* (n=3-4). Each data point is the mean CFU of three to four technical repeats. Mean and SEM are shown. Unpaired t-test was performed.

3.3. *In vivo pmr1Δ/pmr1Δ* biofilm CFUs are decreased and this is associated with expansion of the murine CD4+IL-17+ population

To test whether an immune response towards *C. albicans* biofilms on subcutaneous catheter pieces can be detected, we implanted catheter pieces infected with the wild-type background strain CAI4 under the skin of the back of a group of C57/BL6 mice. The effect of an altered biofilm ECM on the immune response was assessed in a second group of mice by implanting catheter pieces infected with the deletion strain *pmr1Δ/pmr1Δ*. To control for surgery, we implanted clean catheters in a third group of mice. We determined biofilm CFUs and immune cell populations in lymph nodes, spleen, (and blood) after five days, which represented the onset of adaptive immunity, and after 15 days, to mimic a chronic infection. The experiment was performed twice in this set-up, and we show pooled data. However, at the 15 days time point in the second run of the experiment we encountered bacterial contamination on the catheter pieces and these data had to be excluded.

Using this experimental set-up, we could show a significant reduction in the mean CFUs of biofilms formed by the *pmr1Δ/pmr1Δ* strain (mean $\log_{10}$ biofilm CFU=2.5; mean biofilm CFU=316) compared to the wild-type strain (mean $\log_{10}$ biofilm CFU=3.2; mean biofilm CFU=1585) at five days post-implantation (figure 3.3a). Moreover, variation increased as reflected by a significantly increased SD between technical repeats (catheters within one mouse) in *pmr1Δ/pmr1Δ* samples compared to CAI4 samples (figure 3.3b). After 15 days, these significant differences were not present anymore although similar trends could be observed (figure 3.3a, b). Scanning electron microscopy did not reveal differences in structure between biofilms formed by the two different strains at the 15 days time point (figure 3.3c).

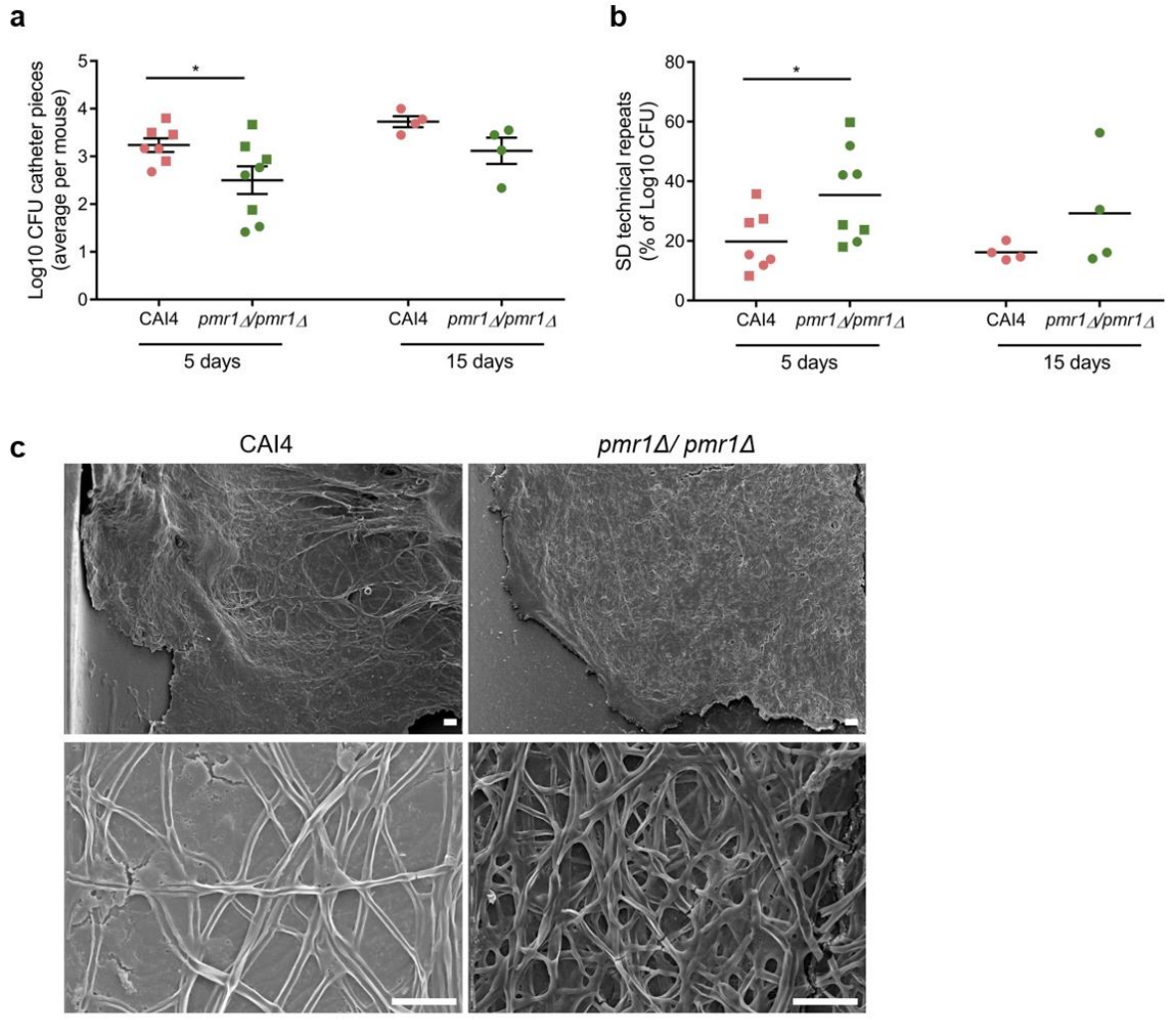

Figure 3.3: Biofilm formation by the *C. albicans* glycosylation mutant *pmr1Δ/pmr1Δ* is decreased at five days post-implantation. a: Log_{10} biofilm CFU compared between biofilms formed by the wild-type background strain CAI4 and the deletion mutant *pmr1Δ/pmr1Δ* (KO) after five days (n=7-8) and 15 days (n=4) of biofilm formation. Each data point is the mean CFU of all catheter pieces in one mouse. Mean and SEM are shown. ● = first experiment; ■ = second experiment. Unpaired t-test was performed to compare between groups within time points. *p<0.05. **b**: SD of six catheter pieces within each mouse (technical repeats) compared between CAI4 and *pmr1Δ/pmr1Δ* at five days (n=7-8) and 15 days (n=4) post-implantation. ● = first experiment; ■ = second experiment. Mean is shown. Unpaired t-test was performed to compare between groups within time points. *p<0.05. **c**: Representative scanning electron microscope images of biofilms formed by CAI4 and *pmr1Δ/pmr1Δ* at 15 days post-implantation. Scale bars represent 20 µm.

Together, these results indicated that *in vivo* biofilm formation by the *pmr1Δ/pmr1Δ* strain in the subcutaneous catheter model system was affected at five days. This was reflected by an 80% decrease in mean biofilm CFU, a trend towards increased variation between mice and an increase in variation between catheter pieces within one mouse. After 15 days, these significant differences were not present anymore. This could indicate that biofilm formation by the deletion strain is restored after 15 days. It is known that the virulence of the *pmr1Δ/pmr1Δ* strain is reduced in a mouse model for systemic candidiasis[321,512]. The recent study by Johnson *et al* (2016), using a catheter implanted in the jugular vein of rats as a surface for biofilm formation also showed a 70% reduction in fungal burden in biofilms formed by *pmr1Δ/pmr1Δ* compared to CAI4 biofilms. No differences between the biofilms could be observed microscopically[408]. Therefore, the results obtained here are in line with what is known in literature.

The immune cell populations formed in response to the subcutaneous biofilms were determined in the secondary lymphoid organs spleen and pooled lymph nodes (figure 3.4) in which adaptive immune cells are activated[507]. Our focus was on cells known to be involved in anti-*Candida* immunity[100,316,370] (see section 1.4, p. 27), namely T-helper (Th) cell subsets expressing CD4 (figure 3.5a-b), while the expansion/activation marker for Th cells, IL-2, was included (figure 3.5c-d). The following CD4+ subsets were analyzed: Th1 (CD4+IFNγ+; figure 3.5e-f), Th2 (CD4+IL-4+; figure 3.5g-h) and Th17 (CD4+IL-17+; figure 3.5i-j). Regulatory T-cells (Tregs) were analyzed based on the expression of the transcription factor Foxp3 which is responsible for Treg development and function (figure 3.5k-l)[516-519]. As such, this set-up allowed us to distinguish between the major types of adaptive immune cells involved in anti-*Candida* immunity. Because neutrophils are one of the primary cell types to respond to a fungal infection, neutrophil (CD11b+ Gr1+) cell populations were determined as well (figure 3.6). Next to looking at the neutrophil response in lymph nodes and spleen, we also analyzed neutrophil populations in blood because that is where they are mainly present[309]. We also studied other immune cell types (see part I: Materials and methods p. 75 and appendix I p. 151 for a complete overview). However, we decided not to show these data, because their role in anti-*Candida* immunity is minor or has never been shown and/or we did not observe relevant differences.

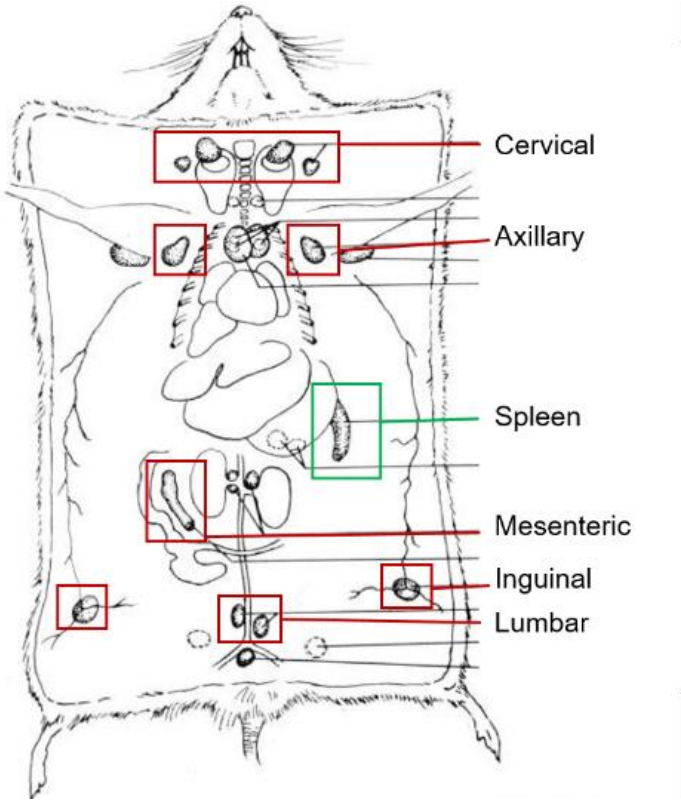

Figure 3.4: Location of pooled lymph nodes (red) and spleen in the murine body. Adapted from Dunn (1954)[520].

To be able to exclude the hypothesis of immunological silence and thus find evidence of an immune response being mounted towards *C. albicans* biofilms on subcutaneous catheter pieces, we first compared immune cell populations between mice infected with biofilms formed by the wild-type strain CAI4 (CA) and mice that had clean catheters implanted (CC). At the five day time point we did not observe any significant differences in either lymph nodes or spleen (figure 3.5). Fifteen days post-implantation, we observed a significant expansion of the CD4+IL-4+ population in spleen (figure 3.5h). This expansion is an unexpected result, given that Th2 cells are primarily involved in responses to parasitic infections and show effector mechanisms that are reminiscent of responses to allergies[521]. The role of Th2 cells in anti-*Candida* immunity seems to be unknown. Cytokines associated with a Th2 cell-type, *e.g.* IL-4 and IL-10, have been shown to have protective effects early in a disseminated infection[401], while ablation of IL-4 and IL-10 resulted in increased survival after systemic challenge of mice[398-400]. However, the expansion of the CD4+IL-4+ population observed here was not associated with a decreased biofilm biomass (figure 3.3a). Moreover, no correlation between number of CD4+IL4+ cells and biofilm biomass was observed (data not shown). It is thus not clear what the biological significance of this expansion is. Because the results obtained here are based on limited numbers, it is necessary to confirm this Th2 cell expansion in follow-up

experiments. Overall, this lack of detection of an immune response towards *C. albicans* biofilms on subcutaneous catheter pieces seems to point at the hypothesis of immunological silence.

When comparing the immune response to biofilms formed by the mutant strain *pmr1Δ/pmr1Δ* (KO) with the response in control (CC) mice, we observed a decrease in total CD4+ cells from 30% to 26% of total lymphocytes in lymph nodes at five days(figure 3.5a). This was associated with a significant expansion of the CD4+IL-17+ population, from 0.07% to 0.22% of CD4+ cells (figure 3.5i). The latter increase was also observed when comparing CD4+IL-17+ cells in response to mutant biofilms with the response to wild-type biofilms (CA), with a significant expansion of this population from 0.09% to 0.22% of total CD4+ cells (figure 3.5i). This could be expected since the biofilms formed by the *pmr1Δ/pmr1Δ* mutant lack most matrix mannan and thus have an increased exposure of β-glucans in the cell wall[421] and probably also in the matrix. Furthermore, sensing of β-glucans is known to be associated with Th17 cell expansion[100,335,508]. However, while the role of Th17 cells in protection against *Candida* infections is recruitment of neutrophils, amongst others, this Th17 cell expansion was not associated with an expansion of the neutrophil population in lymph nodes, spleen or blood (figure 3.6a). Further, we observed a significantly decreased CD4+Foxp3+ population in response to biofilms formed by the *pmr1Δ/pmr1Δ* mutant (KO; 14% of CD4+ cells) compared to biofilms formed by the wild-type strain in spleen (CA; 19% of CD4+ cells) at 15 days post-implantation (figure 3.5l). The role of Tregs in anti-*Candida* immunity is known to be highly niche-dependent. In disseminated candidiasis, expansion of the Treg population is associated with increased pathogenicity, while a protective function for Tregs has been shown in OPC[522]. However, here we did not see a significant change in biofilm CFU associated with this decreased CD4+Foxp3+ population (figure 3.3a), nor did we see a correlation between the number of CD4+Foxp3+ and biofilm CFU (data not shown). Therefore, we cannot draw conclusions on the role of CD4+Foxp3+ cells in an immune response to subcutaneous biofilms at this point.

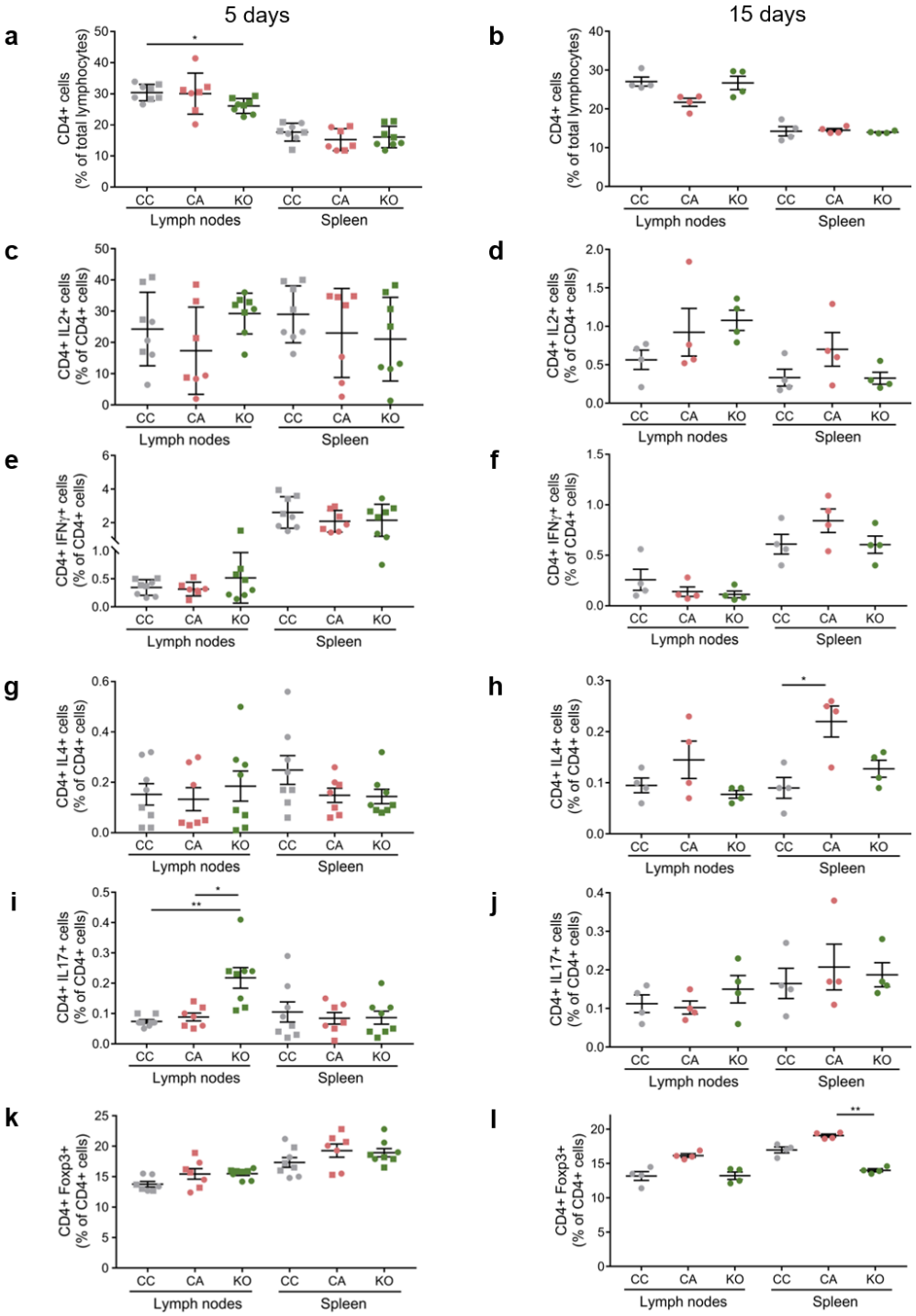

Figure 3.5: Significant expansion of the CD4+IL-17+ population in mice infected with *pmr1Δ/pmr1Δ* biofilms. Percentages of CD4+ cells at five days (n=7-8) (**a**) and 15 days (n=4) (**b**), CD4+IL2+ cells at five days (**c**) and 15 days (**d**), CD4+IFNγ+ cells at five days (**e**) and 15 days (**f**), CD4+IL4+ cells at five days (**g**) and 15 days (**h**), CD4+IL17+ cells at five days (**i**) and 15 days (**j**), and CD4+Foxp3+ cells at five days (**k**) and 15 days (**l**) in pooled lymph nodes and spleen of mice with clean catheters (CC) and mice with catheters infected with CAI4 (CA) or *pmr1Δ/pmr1Δ* (KO). Each data point represents one mouse. ● = first experiment; ■ = second experiment. Mean and SEM are shown. Kruskal-Wallis test with Dunn's multiple comparisons test was performed. *p<0.05. **p<0.01.

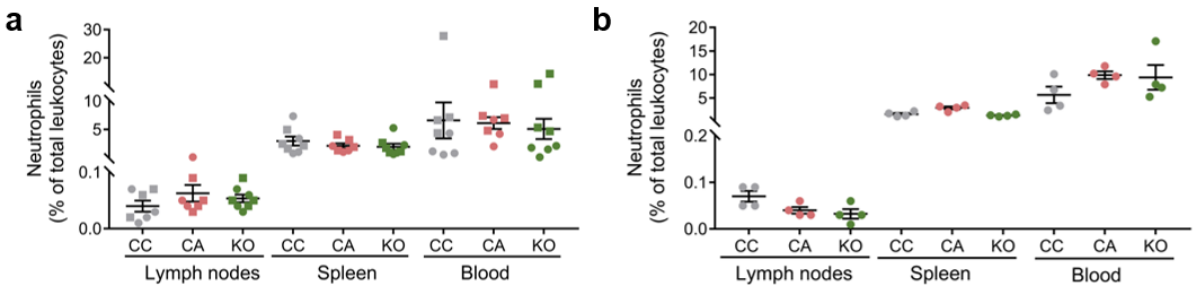

Figure 3.6: The neutrophil population does not change in response to a *C. albicans* biofilm infection. Percentages of neutrophils at five days (n=7-8) (**a**) and 15 days (n=4) (**b**) in combined lymph nodes, spleen and blood of mice with clean catheters (CC) and mice with catheters infected with CAI4 (CA) or *pmr1Δ/pmr1Δ* (KO). Each data point represents one mouse. ● = first experiment; ■ = second experiment. Mean and SEM are shown. Kruskal-Wallis test with Dunn's multiple comparisons test was performed.

To verify whether the significant expansion of the CD4+IL-17+ population in lymph nodes in response to *pmr1Δ/pmr1Δ* biofilms is linked with the decrease in biofilm biomass shown in figure 3.3a, we analyzed the correlation between Log_{10} CFU biofilm and the CD4+ parent population (figure 3.7a) or the CD4+IL-17+ population (figure 3.7b). While no correlation could be observed in the former (Spearman rank correlation coefficient ρ=0.22, p=0.43), indicating that CD4+ cells and biofilm biomass do not vary together, a negative correlation was observed between the percentage of CD4+IL-17+ cells and Log_{10} biofilm CFU (ρ=-0.59, p=0.023). This correlation shows that when the number of CD4+ IL-17+ cells increases, the biofilm biomass decreases. Therefore, at least part of the reduced biofilm formation in the *pmr1Δ/pmr1Δ* strain might be explained by the expansion of CD4+IL-17+ cells.

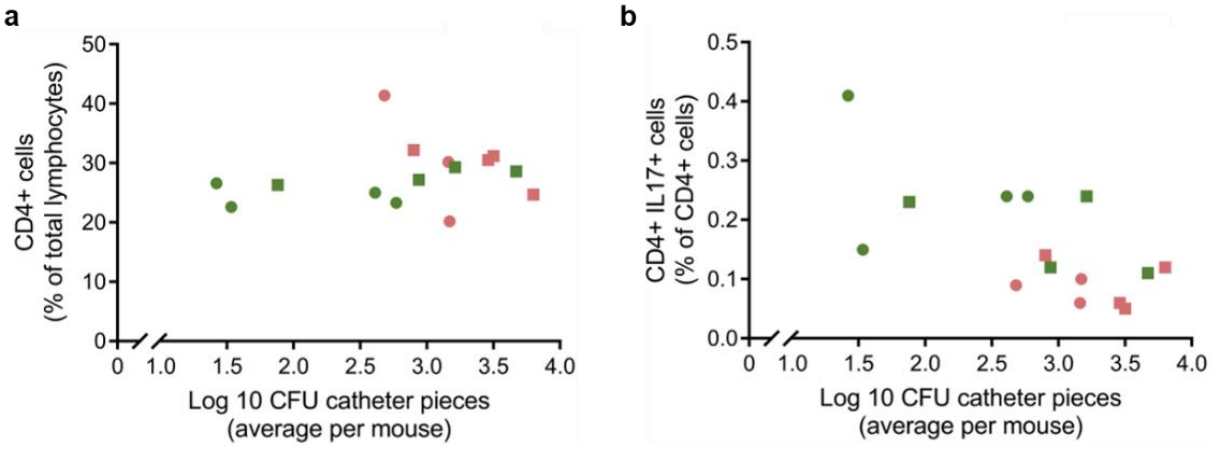

Figure 3.7: CD4+IL-17+ cell expansion is correlated with decreased biofilm CFU. Correlation between CD4+ cells (**a**; ρ=0.22, p=0.43) or CD4+IL-17+ cells (**b**; ρ =-0.59, p=0.023) and Log_{10} CFU biofilm biomass. n=15. Each data point is the mean CFU on all catheter pieces in one mouse and the percentage of CD4+ or CD4+IL17+ cells in that mouse. Red = CAI4 biofilms; Green = *pmr1Δ/pmr1Δ* biofilms. ● = first experiment; ■ = second experiment. Spearman rank correlation was performed. ρ = Spearman rank correlation coefficient.

Together, these data fail to show an immune response to subcutaneous biofilms formed by the wild-type strain CAI4. However, we cannot be sure that the lack of observed immune response to CAI4 biofilms is reflective of real immunological silence, since our experimental set-up, which was focused on detecting a systemic immune response, might have failed at detecting the immune response. An alternative methodology, aimed at detecting a local immune response in the infected tissue[523,524], might be more suitable. Moreover, we lack statistical power at the 15 days time point as a result of data that needed to be excluded due to contamination. This illustrates the necessity of a clean room with individually ventilated cages for mouse housing in this type of studies. Experiments up till now were performed in normal type II cages in a room in which different experiments took place at the same time. From here on, the experiments were moved to a clean room with individually ventilated cages, after which we did not observe contamination on the catheter pieces anymore.

Rather than repeating these experiments in an alternative set-up, we opted for a completely different experiment with an easier read-out. In this set-up, we wanted to study whether the protection from a lethal systemic challenge obtained by injecting a low dose of *C. albicans* i.v.[457], could be mimicked by a subcutaneous biofilm on catheter pieces (see also part I: Introduction p. 5'). As controls we also included i.v. immunized mice in the study. We first determined an appropriate low concentration of *Candida* for immunization, and a high lethal

Candida dose, in a dose-response experiment. Next, we performed two runs of the immunization experiment.

3.4. Dose response curve for determination of immunization dose and lethal systemic dose

In the systemic infection model, a *C. albicans* cell suspension of the desired dose in 200 µl of saline is injected in a lateral tail vein[525]. In order to determine a suitable *C. albicans* dose that immunizes but is not lethal, and a dose that is lethal, we injected groups of five to 10 mice with increasing doses of *C. albicans* SC5314. The mice were monitored closely during two weeks and mice showing severe signs of morbidity were euthanized after which kidney CFUs were determined.

As expected, increasing doses of *C. albicans* inoculum were associated with an increased mortality rate (figure 3.8a) and increased Log_{10} kidney CFU (figure 3.8b). All mice infected with 5 x 10^3 CFU and 5 x 10^4 CFU survived over the 14 day window of observation, while all mice infected with the highest dose, 5 x 10^7 CFU, died within seven days post-challenge. Of the mice infected with intermediate doses 75-90% survived until the end of the experiment. The significance of this trend was confirmed by the Logrank test for trend ($p<0.0001$). Mice that died before the end of the experiment mostly had kidney counts of five to six Log_{10} CFU, while mice surviving until day 14 mostly had kidney counts below four Log_{10} CFU. This possibly indicates that *C. albicans* cell counts in the kidneys need to reach a treshold before triggering significant disease in mice.

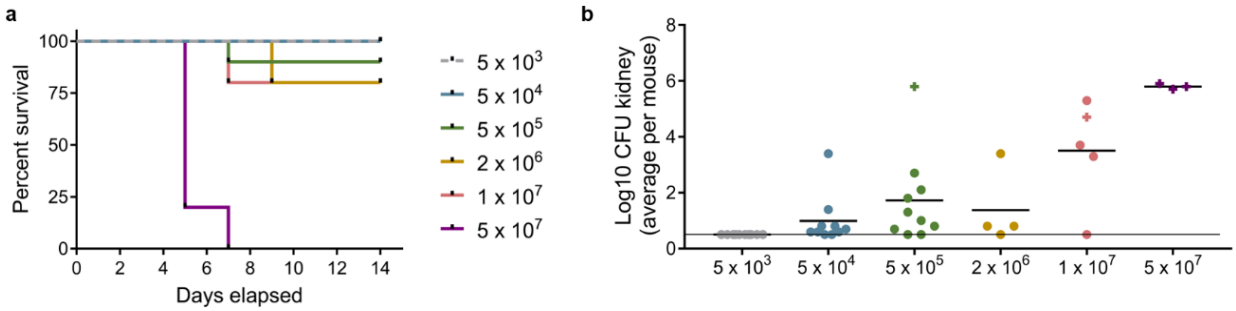

Figure 3.8: Determination of immunization and lethal *Candida albicans* SC5314 dose. a: Surival rate of all groups following i.v. injection (n=5-10). **b**: Log_{10} CFU kidneys of all groups at time of takedown during the 14 day time frame (**+**) or at day 14 (●). Each point represents average CFU of both kidneys within one mouse. Mean is shown. Horizontal line at 0.5 Log_{10} indicates half of detection limit, which was the Log10 CFU assigned to mice for which both kidneys seemed clean.

In the immunization experiment, mice would first undergo surgery and three cheek bleeds prior to being challenged with the high dose. Since we expected that this would substantially weaken them and decrease their surival rate, we chose 1 x 10^7 cells as our lethal dose. To allow for proper immunization, we chose the highest of two doses allowing 100% survival up to 14 days post-challenge, *i.e.* 5 x 10^4 cells, as our immunization dose.

3.5. *Candida albicans* subcutaneous biofilms confer protective immunity to a high dose systemic challenge

For the immunization experiment, three groups of 23 to 24 mice each were used in two independent experiments of which pooled data is shown in figures 3.9 and 3.10. Catheter pieces were infected with 50 000 CFUs, resulting in 500 to 1 000 CFUs attached to the pieces, and implanted subcutaneously in mice immunized with a biofilm (IC). To control for surgery, naïve mice had clean catheters implanted (CC). The third group of mice (IV) was immunized by an i.v. injection of 50 000 CFUs. Fourteen days after the surgery or low dose injection, all mice were challenged with a lethal dose of 1×10^7 CFU, and morbidity was followed closely (figure 3.9a). Overall comparison of the survival curves showed that they differ significantly ($p=0.02$). Pairwise comparison of survival curves showed a significantly increased survival rate in mice immunized with a low dose i.v. compared to naïve mice, as was shown before[457] (figure 3.9b). While the increased survival rate of mice immunized with a subcutaneous biofilm was nearly significant when compared to naïve mice ($p=0.04$; p-value for significance after Bonferroni correction for multiple testing = 0.016), it did not differ significantly from the survival rate of mice immunized with a low dose i.v. ($p=0.65$). This shows the immunization potential of subcutaneous biofilms. Deaths occurring in the naïve mice were more frequent, with only 17% of mice surviving in the naïve group compared to 44% in the biofilm group and 50% in the i.v. group, and occurred sooner in the experiment.

When comparing kidney CFUs at time of death between the different groups, the biofilm group mostly seemed to have higher kidney CFUs, and this difference is statistically significant between biofilm and i.v. groups at day two post-challenge (figure 3.9c). At this time point, the average kidney CFUs in i.v. mice is 60% of that of biofilm mice (6.9×10^5 CFU versus 1.8×10^6 CFU). Even though this might not represent a biologically significant difference in kidney CFUs, it is noteworthy that the difference is seemingly present at three different time points. However, at days three and seven, statistical analysis was not performed since data was only available for one mouse in at least one group. This trend towards higher kidney CFUs in biofilm immunized mice was not present anymore at the end of the experiment. In line with this, we observed significantly reduced biofilm biomass in mice that survived until day 14 post-challenge compared to mice that died before the end of the experiment. Biofilm biomass of the former was 23% of biofilm biomass in latter (figure 3.9d). This can be interpreted as an ineffective immune response being mounted towards the biofilms alone, which gets corrected to an efficient immune response over the course of the infection in response to the high i.v. challenge. Surprisingly, this might support the hypothesis of immunomodulation by the biofilm,

which is in contrast with efficient immunization that we observed in terms of increased survival rate in the biofilm group.

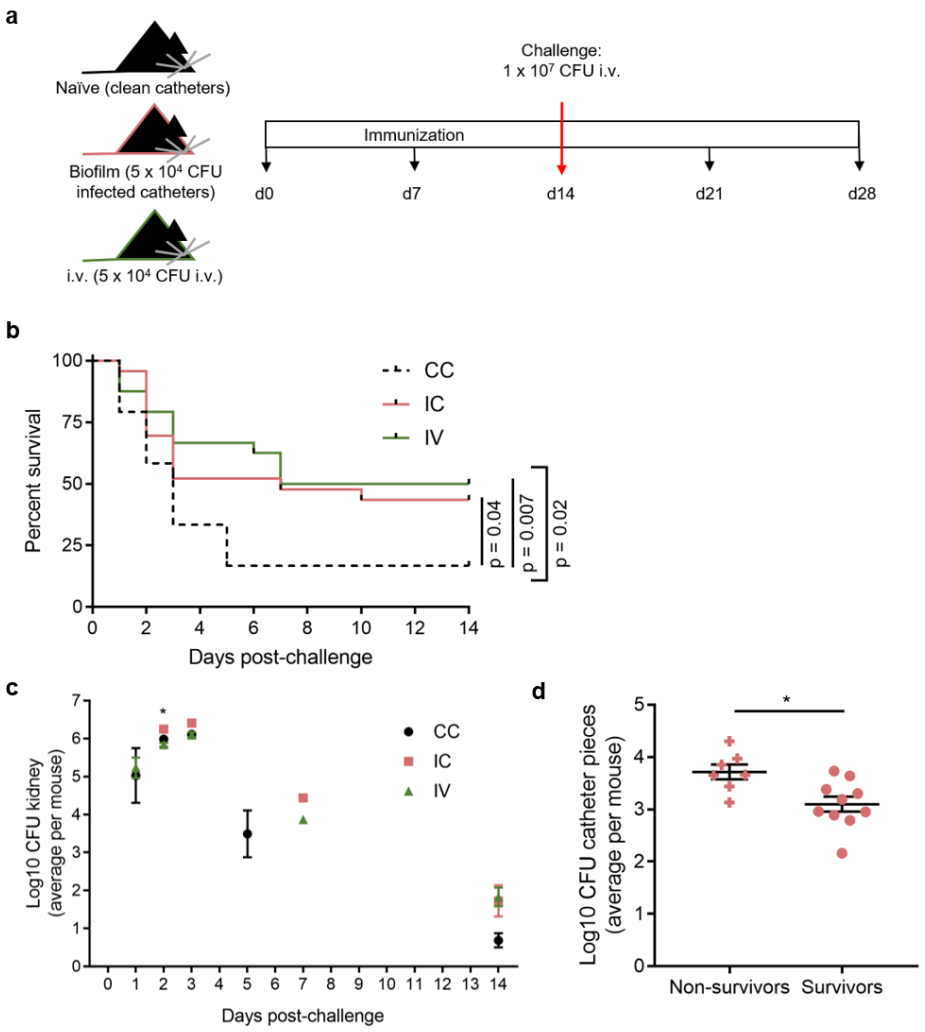

Figure 3.9: *C. albicans* subcutaneous biofilms confer protective immunity to a high dose systemic challenge. a: Naïve mice with catheter pieces, or mice immunized with biofilms on subcutaneous catheter pieces or a low dose i.v. were challenged with a high dose i.v. challenge after which survival was followed. **b:** Survival rate of all groups after high i.v. challenge (n=24). Overall comparison of survival curves was performed with Gehan-Breslow-Wilcoxon test (p=0.02); Pairwise comparisons were performed with Log-rank (Mantel-Cox) test; Bonferroni correction reduces the necessary p-value for significance in the latter case to 0.016. **c:** Log_{10} kidney CFUs of mice euthanized at indicated days post-challenge. Each data point represents the mean Log_{10} kidney CFU per mouse and per time point. Error bars represent SEM. At 2 days an ANOVA with Tukey's multiple comparisons test was used to compare differences between Log_{10} kidney CFUs in different groups. *p<0.05. **d:** Comparison of Log_{10} biofilm CFU between mice that died before the end of the experiment (Non-survivors; **+**) and mice surviving until the end of the experiment (Survivors; ●). Each data point is the mean CFUs of all catheter pieces in one mouse. Mean and standard error of the mean (SEM) are shown. Unpaired t-test was performed. *p<0.05.

Analysis of serum cytokine levels at baseline (before surgery or i.v. immunization) and at seven-days intervals was performed to track cytokine production during progression of infection (figure 3.10). The levels of IL-2, important for Th cell differentiation, and of IL-10, associated with Th2 immunity, remained at baselevel throughout the whole experiment (figure 3.10a, b). As a marker for systemic inflammation, TNFα was included. Moreover, TNFα has been shown to be crucial for anti-*Candida* immunity via the recruitment of neutrophils and stimulation of phagocytosis[314]. TNFα increased significantly between the start of the experiment and day seven in the naïve and biofilm-infected mice. At day 14, TNFα production differed significantly between the groups, with levels seemingly highest in the biofilm immunized group, while they were lowest in the i.v. immunized group. This seems to indicate that the presence of a biofilm results in higher systemic inflammation than does a low dose i.v. injection. As expected, levels rose further after the challenge at day 14 but no differences could be observed between groups at day 21 or day 28 (figure 3.10c). Levels of IFNγ, which is the key cytokine associated with the Th1 cell type, increased in all groups following the high dose challenge (day 14) and this increase was significant in the naïve and biofilm immunized mice. No differences were observed between groups, possibly due to rather high variations between measurements (figure 3.10d). In the Th17 branch of the immune system we measured IL-17, the key cytokine produced by Th17 cells, which was under detection limit at all time points, as well as IL-6, critical for Th17 induction, and CXCL1, an attractor of neutrophils. Between days zero and seven, IL-6 levels increased significantly in all groups of mice, and at day seven and 14 levels were significantly different between the groups of mice. In all groups levels increased significantly after the high dose challenge and were again significantly different between all groups at day 28. From the high dose injection onwards (day 14), IL-6 levels seemed lowest in naïve mice (figure 3.10e). Levels of CXCL1 decreased in mice immunized with either a biofilm or a low i.v. injection from day zero to day seven and between day 14 and day 21 in IV mice. At days seven, 14, 21 and 28, levels differed significantly between all groups. CXCL1 levels seemed lowest at all time points in mice immunized i.v. (figure 3.10f).

Before, it has been shown that immunization of mice with a low dose i.v. resulted in a higher induction of IL-6 and TNFα in blood compared to naïve mice, after a 90 minute challenge with bacterial lipopolysaccharides[457]. Here, IL-6 and TNFα levels increased in all groups of mice after the high dose challenge, although we do see a trend towards higher levels of TNFα and IL-6 induced in mice immunized with either a biofilm or i.v. injection at seven days post-challenge (day 21) (figure 3.10c, e). Overall, the levels of IL-6 are lowest in naïve mice, possibly pointing at a protective role for Th17 cells in increased survival. However, their involvement in protection in systemic infections is said to be inferior to Th1 cells[316] and possibly dose dependent[396]. Here, we see a trend towards higher levels of IFNγ produced in naïve mice,

while no significant increase in this cytokine could be detected in i.v. immunized mice after the high dose challenge (figure 3.10d). The chemokine CXCL1 is lowest overall in mice immunized i.v. and levels are comparable between i.v. and biofilm immunized mice up until the time of challenge. From then on, CXCL1 levels in biofilm immunized mice increase (figure 3.10f).

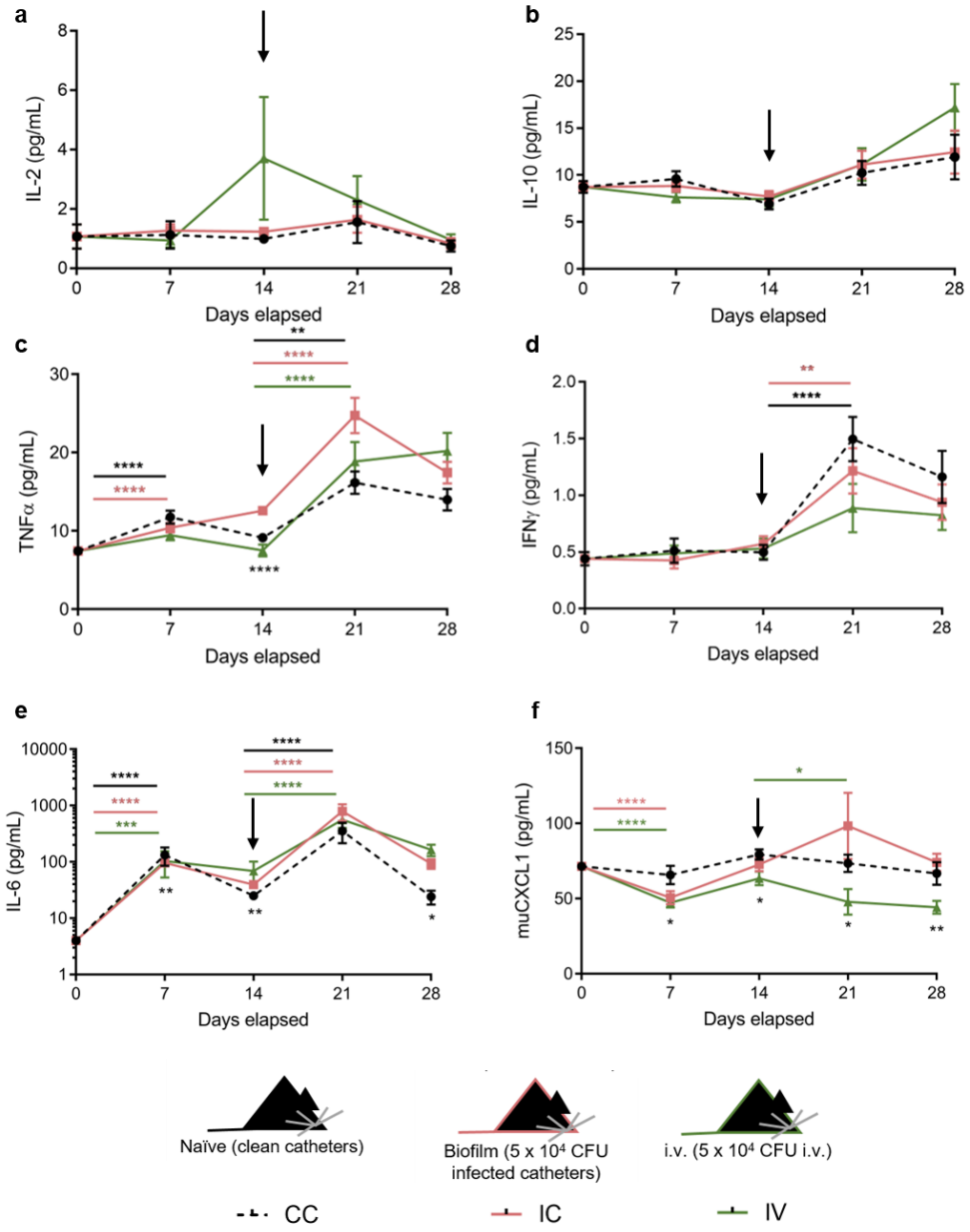

Figure 3.10: Immune system shows inflammation during subcutaneous biofilm infection. Serum samples for all time points and all groups of mice were analyzed for IL-2 (**a**), IL-10 (**b**), TNFα (**c**), IFNγ (**d**), IL-6 (**e**) and CXCL1 (**f**). Mean and SEM are shown. Arrow indicates high i.v. challenge. Kruskal-Wallis test with Dunn's multiple comparisons test was performed for comparisons between groups within one time point. Mann-Whitney-U test was performed for comparison within groups between time points. *p<0.05, **p<0.01, ***p<0.001, ****p<0.0001.

Overall, while our results obtained by the first approach, using the *pmr1Δ/pmr1Δ* matrix and cell wall mutant, seemed to point at the hypothesis of immunological silence, we clearly observed an increased survival rate in mice immunized with subcutaneous biofilms compared to naïve mice in the immunization experiment. Moreover, no difference in survival rate was present between mice immunized with subcutaneous biofilms and mice immunized i.v. These results dispute the possibility of immunological silence in the biofilm. We expect that the absence of an immune response as observed in the first part of this research is reflective of our looking for an immune response in the wrong place, rather than the real absence of an immune response. The increased survival of mice immunized with a biofilm, compared to naïve mice, would support the hypothesis of biofilm immunoresistance. A role for biofilm matrix could be hypothesized based on literature and the decrease in biofilm CFU associated with an expansion of the CD4+IL-17+ population that we observed in (response to) biofilms formed by the matrix mutant *pmr1Δ/pmr1Δ*. However, kidney cell counts seemed higher over the course of the immunization experiment in mice immunized with a biofilm compared to the other two groups and this was confirmed statistically at one out of three time points. This would support the hypothesis of biofilm immunomodulation. When following serum cytokine progression, we observed a peak in CXCL1 at day 21 (seven days post-challenge) in mice immunized with a biofilm. Considering that recruitment of neutrophils to the kidneys at time points past 12 hours has been associated with pathology, including increased kidney CFUs, this might be causative for the higher number of CFUs in kidneys[385,387]. However, this did not seem to be associated with a decreased survival rate, and might thus not be biologically significant. Despite differences in cytokine levels between time points and groups, overall trends are mostly similar. Thus, we cannot point at clear immunomodulation involving a specific cell type based on these data. Combining all observations, we believe that both immunomodulation and immunoresistance are at play in the incapability of our immune system to clear a biofilm infection. More experiments are necessary to further appreciate the contribution of each of these hypotheses.

4. Part I – Immune response: Materials and methods

4.1. Materials

4.1.1. Strains

Table 4.1: Strains used in this study

Name	Genotype | Description | Use	Source
SC5314	*URA3/URA3; PMR1/PMR1* | Wild-type *C. albicans* lab strain isolated from hemoculture | Strain used in immunization experiment (second approach)	526
CAI4-CIp10 (NGY152)	*ura3Δ-iro1Δ*::*imm434/ura3Δ-iro1Δ*::*imm434, RPS1*/*rps1*Δ::CIp10 | Wild-type *C. albicans* lab strain derived from SC5314 by deletion of both copies of *URA3* and part of both copies of *IRO1*. One copy of *URA3* is reintegrated in the RPS1 locus on a CIp10 plasmid. | Background strain for homozygous *PMR1* deletion and used as control strain in experiments using this mutant.	527
pmr1Δ/pmr1Δ (NGY98)	*ura3Δ-iro1Δ*::*imm434/ura3Δ-iro1Δ*::*imm434, RPS1*/*rps1*Δ::CIp10, *pmr1*Δ::*hisG*/*pmr1*Δ::*hisG* | Mutant *C. albicans* strain in which both copies of gene *PMR1* are deleted in de CAI4-CIp10 background. | Mutant strain.	321

4.1.2. Media and buffers

Table 4.2: Composition of YPD medium and derived media

YPD medium and derived media* (1 L)		
Yeast extract	10 g	
Peptone	20 g	
Glucose	2%	
Agar	15 g	For plates
Uridine	50 µg	For strains CAI4-CIp10 and *pmr1Δ/pmr1Δ*
Glycerol	33%	For stock medium

Table 4.3: Composition of 10x PBS

10x PBS* (1 L)	
NaCl	80 g
KCl	2 g
Na_2HPO_4	14.4 g
KH_2PO_4	2.4 g

Table 4.4: Composition of RPMI-MOPS, complete RPMI (CRPMI) and stimulation medium

RPMI-MOPS and derived media (1 L)**		
RPMI-1640	10.4 g	
MOPS	34.53 g	
Adjust pH to 7.0 (NaOH tablets)		
Heat inactivated fetal bovine serum	10%	For CRPMI & stimulation medium
L-Glutamine	20 mM	For CRPMI & stimulation medium
Penicillin	2000 U	For CRPMI & stimulation medium
Streptomycin	2 mg	For CRPMI & stimulation medium
β-Mercaptoethanol	0.05 mM	For CRPMI & stimulation medium
PMA	50 ng/mL	For stimulation medium
Ionomycin	0.5 µg/mL	For stimulation medium
GolgiStop	1/1000	For stimulation medium

Table 4.5: Composition of 10x Lysis buffer

10x Lysis buffer (1 L)**	
NH_4Cl	82.6 g
$NaHCO_3$	11.9 g
EDTA (0,5 M, pH 8)	2 mL

* YPD medium and derived media and 10x PBS are sterilized by autoclavation during 20 minutes at 121°C and 120 kPa.

** RPMI-MOPS and derived media and lysis buffer are filter-sterilized over 0.20 µm non-pyrogenic Nalgene filters.

4.2. Methods

4.2.1. Candida albicans

All strains used in this study were stored in stock medium at -80°C. *C. albicans* strain SC5314 was maintained on YPD agar plates. Strains CAI4-CIp10 and *pmr1Δ/ pmr1Δ*, which are expressing the *URA3* gene from a CIp10 plasmid, were maintained on YPD agar plates supplemented with uridine. Plates for strain maintenance were stored at room temperature and refreshed weekly.

4.2.2. Animals

All animal experiments were carried out in accordance with European regulations regarding the protection and well-being of laboratory animals and were approved by the KU Leuven animal ethical committee (project numbers P018/2013 and P122/2013). The animals used for all experiments were 8 to 10 weeks old female C57Bl/6J mice bred in-house or purchased from Janvier Labs. Food and water were supplied *ad libitum*. Immunosuppression was carried out by dexamethasone in drinking water at 1 mg/L. Animals were monitored at least daily for signs of distress or disease. When humane endpoints were reached or at the end of the experimental procedure, animals were euthanized by cervical dislocation.

4.2.3. In vitro biofilm assay

The *in vitro* biofilm assay was carried out as described before[136] with few adaptations. In short, polyurethane catheters were cut in pieces of 1 cm and incubated overnight in fetal bovine serum or mouse serum at 37°C. A *C. albicans* pre-culture was inoculated in 3 mL liquid YPD medium and grown overnight at 30°C shaking at 200 rpm. Cell density was estimated using a Bürker chamber and an inoculum of 5 x 10^4 cells/mL was prepared in RPMI-MOPS. Catheter pieces were incubated individually in 1 mL inoculum at 37°C for 90 minutes (adhesion period). Catheter pieces were washed twice with 1 mL of 1x PBS to remove non-adherent cells and then incubated in fresh RPMI-MOPS for 2 days. After the incubation period, catheter pieces were washed twice with 1 mL of 1x PBS and placed in Eppendorf tubes containing 1 mL of 1x PBS. To loosen biofilm-associated cells, catheter pieces were sonicated for 10 minutes in a water bath sonicator at 40 kHz and vortexed vigorously for 30 seconds. Serial dilutions were made and 100 µL was plated on YPD agar plates. CFUs were counted after 24 to 48 hours of incubation at 37°C.

4.2.4. Subcutaneous catheter model system

Preparation of catheter pieces, cell inoculum and adhesion of cells to catheter pieces was performed as described in section 4.2.3. After adhesion, catheter pieces were washed twice with 1x PBS and placed individually in empty Eppendorf tubes on ice. Surgery and explant of the catheter pieces was performed as described before[136,411] with few adaptations. In short, animals were anesthetized by an intraperitoneal injection of a cocktail of 45-60 mg/kg ketamine

(Anesketin) and 0.6-0.8 mg/kg medetomidine (Domitor) in sterile saline. The lower back of the mouse was shaved and disinfected before an incision of approximately 1 cm was made. Using blunt end scissors, the skin was loosened from underlying muscular tissue, after which up to six catheter pieces were inserted subcutaneously. Wounds were closed using surgical staples, disinfected and lidocaïne hydrochloride 2% (Linisol) was applied as analgesic. Anesthesia was reversed by intraperitoneal injection of 0.5 mg/kg atipamezole (Antisedan) in sterile saline. For explant, mice were euthanized by cervical dislocation after which the skin in the lower back was disinfected. Catheter pieces were removed aseptically, washed twice with 1 mL of 1x PBS and placed individually in Eppendorf tubes containing 1 mL of 1x PBS. Quantification of biomass on catheter pieces was performed via CFU counting as described in paragraph 4.2.3.

When immunological staining was performed (see section 4.2.8), blood was obtained by cheek bleed. Spleen and selected lymph nodes were removed and homogenized in complete RPMI (CRPMI). When quantification of biomass in kidneys was performed (see sections 4.2.9 and 4.2.10), kidneys were removed and homogenized in 1 mL of 1x PBS. Serial dilutions were made and plated on YPD agar plates supplemented with 50 mg/L chloramphenicol to reduce the risk of bacterial contamination. CFUs were counted after 24 to 48 hours of incubation at 37°C.

4.2.5. Microscopy

For scanning electron microscopy, catheter pieces were cut longitudinally and allowed to air dry overnight. Mounted samples were sputter-coated with Au-Pd and examined on a XL30-FEG, FEI at 10kV. For confocal laser scanning microscopy catheter pieces were cut longitudinally. Staining was performed for one to two hours using a 1/1 000 dilution of the fluorochrome Alexa488 conjugated to the sugar binding lectin Concanavalin A in 1x PBS. As such, the *Candida* cell wall would be stained. Samples were examined using an Olympus Fluoview FV1000 IX81.

4.2.6. Growth curve

A *C. albicans* pre-culture was grown overnight in 3 mL of YPD at 30°C shaking at 200 rpm. The OD_{600} of this pre-culture was measured and an inoculum with OD_{600} 0.1 was prepared in RPMI-MOPS. Samples were loaded in triplicate on 100-well honeycomb plates, together with blanks, after which the OD_{600} was measured at 15 minute intervals during 24 hours.

4.2.7. Yeast to hyphae switching

A *C. albicans* pre-culture was grown overnight in 3 mL of YPD at 30°C shaking at 200 rpm. The OD_{600} of this pre-culture was measured and an inoculum with OD_{600} 0.2 was prepared in YP medium + 10% fetal bovine serum. Cultures were incubated at 37°C and morphology was assessed using microscopy after 90 and 170 minutes.

4.2.8. Immunological staining

Some of the work for the immunological staining was performed by Josselyn Garcia-Perez from the Translational Immunology lab of Prof. Adrian Liston. We performed all the preparative steps before flow cytometry (*i.e.* sample preparation, surface staining and intracellular staining) together. Josselyn Garcia-Perez performed the flow cytometry alone because this needed to happen at the same time as the quantification of biomass on catheter pieces as described in paragraph 4.2.3, which I performed. Analysis and interpretation of the data obtained by flow cytometry was performed together. To be able to detect the cell types of interest, antibody staining cocktails (summarized in table 4.6) were prepared and added to the appropriate samples. Each staining cocktail contains antibodies conjugated to a fluorochrome (summarized in table 4.7) directed against a specific surface or intracellular marker.

Sample preparation. Homogenized spleen and lymph nodes were pelleted (5 min., 400 g, 2 °C; this program was used throughout the whole protocol unless stated otherwise) and erythrocytes present in spleen samples were lysed by adding 3 mL of a 1:2 dilution of 1x lysis buffer in complete RPMI (CRPMI). Pellets were resuspended in 3 mL of CRPMI and filtered to remove unwanted tissue. The immune cells present in the samples were counted with an automated cell counter after diluting the samples 1:1 with 10x Trypan Blue dye. Counted spleen and lymph node samples were centrifuged and resuspended in 1 mL or 400 µL CRPMI respectively. Erythrocytes present in blood samples were lysed by adding 100 µL of a 1:2 dilution of 1x lysis buffer in CRPMI, samples were centrifuged (2 min., 5000 rpm) and resuspended in 100 µL CRPMI. To reach measurable cytokine levels, 5×10^5 cells per sample were plated in duplicate in 96-well plates, centrifuged and incubated for four hours at 37°C in 100 µL of stimulation medium.

Surface staining. All samples (stimulated and unstimulated) were plated at 1×10^6 of cells per sample to stain surface markers for the detection of selected immune cells (table 4.6). Samples in all plates were pelleted and washed three times with 150 µL of cold FACS wash

(1x PBS + 3% fetal bovine serum). Fifty microliters of the appropriate surface antibody staining cocktail (T cell - excluding Foxp3 - or myeloid and B cell; summarized in table 4.6) was added to the samples and unstained and single color controls were included on each plate. Plates were incubated for 20 minutes at 4°C, and washed three times with 150 µL of FACS wash.

Intracellular staining. For intracellular staining, cells were fixed for 20 minutes at 4°C in BD Cytofix/Cytoperm for cytokines and in eBio-Fix for Foxp3 staining, after which the samples were washed three times with 150 µL of 1x Perm/Wash. Samples were incubated for 30 minutes at 4°C in 50 µL of the cytokine intracellular antibody staining cocktail for cytokine staining or of Foxp3-APC for the T-cell staining (see table 4.6), after which samples were washed three times 150 µL of FACS wash. Samples were resuspended in 200 µL of FACS wash and transferred to FACS tubes.

Flow cytometry. Flow cytometry was performed using the FACS Canto II by BD. First, signals from the sideward scatter channel (SSC) and the forward scatter channel (FSC) were plotted. Further analyses were performed using 3 x 10^5 cells acquired per organ, either based on the lymphocyte gate for T-cells or on the leukocyte (total cells) gate for neutrophils. These were analyzed in subsequent steps, by plotting different markers on axes after which gating was adapted to distinguish between cell types. An example of the different steps in gating used for each staining set is shown in appendix I (p. 151).

Table 4.6: Antibody staining cocktails used to detect cell types in flow cytometry. The indicated fluorochrome is conjugated to an antibody directed towards the indicated marker. Detection of that fluorochrome indicates that the marker and thus the associated cell type is present. NA = not applicable. * Added during intracellular staining step; others are added during surface staining step.

Staining set name	Used on samples from	Kit from	Marker	Fluorochrome	Used for detection of	Dilution of stock in cocktail(1/x)
T-cell	Lymph nodes Spleen	Ebio	CD4	FITC	Helper and regulatory T-cells	100
			CD25	PE	Regulatory T-cells	250
			CD44	PerCP-Cy5.5	Memory T-cells	500
			CD62L	PE-Cy7	Central memory T-cells	1 000
			FoxP3*	APC	Regulatory T-cells	100
			CD8	APC-Cy7	Cytotoxic T-cells	100
Myeloid and B-cell	Lymph nodes Spleen Blood	BD	Gr1	FITC	Neutrophils	250
			Siglec F	PE	Eosinophils	200
			Ly6C	PerCP-Cy5.5	Monocytes	3 000
			CD11b	PE-Cy7	Neutrophils	3 000
			CD19	Biotin and APC-Cy7 Biotin	B-cells	500
Cytokine*	Lymph nodes Spleen	BD	CD4	FITC	Helper and regulatory T-cells	50
			IL-2	PE	T-cell activation	100
			IFN-y	PerCP-Cy5.5	Th1 cells	400
			IL-4	PE-Cy7	Th2 cells	400
			IL-17	APC	Th17 cells	150
			CD8	APC-Cy7	Cytotoxic T-cells	100
			NA	BV510	Dead cells	500

Table 4.7: Fluorochromes used in this study. BV510 is excited by the violet 405 nm laser of the flow cytometer, the next five fluorochromes are excited by the blue 488 nm laser, while the latter two are excited by the red 633 nm laser. The excitation and emission peak wavelengths were obtained from the website of BD Biosciences[528], and might differ slightly from values reported in other sources.

Fluorochrome	Full name	Peak wavelength excitation | emission (nm)	
BV510	Brilliant Violet 510	405	510
FITC	Fluorescein isothiocyanate	494	520
PE	R-phycoerythrin	496	578
PerCP-Cy5.5	Peridinin-chlorophyll proteins-Cyanine 5.5	482	676
PE-Cy7	R-phycoerythrin-Cyanine 7	496	785
AmCyan	*Anemonia majano* cyan	457	491
APC	Allophycocyanin	650	660
APC-Cy7	Allophycocyanin-Cyanine 7	650	785

4.2.9. Systemic infection model

For systemic infection, a single *C. albicans* colony from a YPD agar plate, incubated at 30°C for 24 h, was restreaked on a fresh YPD agar plate and incubated at 30°C for 24 h. A single colony from the latter was incubated in 50 mL YPD medium and grown for 12 to 14 hours at 30°C and 200 rpm. Cells were counted using the Bürker chamber, the desired inocula were prepared in a sterile saline solution and confirmed by plating. Mice were infected or mock infected (1x PBS) by injection in the lateral tail vein. In the dose response experiment (section 3.4 p. 68) inocula ranging from 5 x 10^3 CFUs until 5 x 10^7 CFUs per mouse were injected. *C. albicans* biomass in kidneys was quantified as described in paragraph 4.2.4.

4.2.10. Immunization experiment

For immunization experiments, C57BL/6J mice were subcutaneously implanted with 5 clean catheter pieces, 5 catheter pieces colonized with *C. albicans*, or injected intravenously with 5 x 10^4 *Candida* CFU. The same *Candida* pre-culture was used in the latter two cases and cultured as described before (paragraph 4.2.9). Day 14 after treatment, all mice received 10^7 *Candida* CFUs i.v. Takedown of surviving mice and catheter and kidney manipulation was performed at day 28 as described before (paragraph 4.2.4).

4.2.11. Serum cytokine analysis

Blood was obtained via cheek bleed and serum was isolated after centrifugation in microtainer tubes with serum separator for 5 minutes at 2 000 g. Cytokine serum levels were quantified by an electrochemiluminescence immunoassay format using the Meso Scale Discovery murine V-plex Pro-inflammatory panel 1. Serum cytokine analysis was performed by Josselyn Garcia-Perez in the Translational Immunology lab of Prof. Adrian Liston.

4.2.12. Statistics

Statistical analyses were performed using GraphPad Prism version 7.01. For biofilm CFUs, separate catheter pieces within one experimental run or within one mouse were considered technical repeats. The average of all catheter pieces within one experimental run or one mouse was considered one biological repeat. Normal distribution of data was analyzed using a Shapiro-Wilk normality test. To compare means between groups, a t-test or ANOVA with Tukey's multiple comparisons test was performed in case data followed a normal distribution. A Mann-Whitney-U test or Kruskal-Wallis test with Dunn's multiple comparisons test was used in case data did not follow a normal distribution. For analysis of survival curves, a Log-rank (Mantel-Cox) test was used for pairwise comparisons of survival curves whereas a Log-rank test for trend was used to test for significance of trends.

Part II: The vapor-phase-mediated anti-*Candida* activity of essential oils and their components

The second part of this thesis is composed of two manuscripts. The first manuscript entitled "Assay and recommendations for the detection of vapor-phase-mediated antimicrobial activities" has been published in Flavour and Fragrance Journal. The second manuscript entitled "Essential oils and their components are a class of antifungals with potent vapor-phase-mediated anti-*Candida* activity" will be submitted to PNAS. I am shared first author for both as I helped with the optimization of the assays introduced, performed experiments and helped in writing the manuscript. Both manuscripts are slightly adapted to match the format and lay-out of this thesis.

5. Assay and recommendations for the detection of vapor-phase-mediated antimicrobial activities

Adam F. Feyaerts[1,2,#], Lotte Mathé[1,2,#], Walter Luyten[3], Hélène Tournu[1,2], Katrien Van Dyck[1,2], Lize Broekx[1,2], and Patrick Van Dijck[1,2,*]

[1]VIB-KU Leuven Center for Microbiology, KU Leuven, 3001, Leuven, BELGIUM

[2]Laboratory of Molecular Cell Biology, KU Leuven, 3001, Leuven, BELGIUM
[3]Department of Biology, KU Leuven, 3000, Leuven, BELGIUM

[#]These authors contributed equally to this work

**Corresponding author:*

Patrick Van Dijck

Laboratory of Molecular Cell Biology, KU Leuven

VIB-KU Leuven Center for Microbiology

Kasteelpark Arenberg 31 bus 2438

3001 Heverlee, Belgium

Tel.: (0032) 16 321512

Fax: (0032) 16 321979

E-mail: Patrick.vandijck@mmbio.vib-kuleuven.be

Keywords: vapor-phase-mediated antimicrobial activity, essential oil, essential oil component, bioassay, *Candida* species

Antimicrobial activity assays can be carried out in aqueous solutions using multi-well plates. However, some bioactive compounds are volatile and can cause effects at a distance. To detect such vapor-phase-mediated antimicrobial activity, we introduce the vapor-phase-mediated patch assay, a simple bioassay that uses standard microtiter plates. As a proof-of-principle, we use the vapor-phase-mediated patch assay to test a small but chemically diverse set of selected essential oils with known antifungal activities *i.e. Origanum compactum*, *Artemisia dracunculus*, *Cinnamomum camphora ct linalool*, *Cinnamomum cassia,* and *Melissa officinalis*, as well as their corresponding major components carvacrol, estragole, linalool, trans-cinnamaldehyde, and citral, against two pathogenic *Candida* species. As all but one of the tested essential oils *i.e. Artemisia dracunculus* and its corresponding component estragole showed vapor-phase-mediated antimicrobial activity, we conclude that it is a rather common characteristic of essential oils and their components that should always be taken into consideration. Additionally, we provide suggestions to prevent false positive results due to possible vapor-phase-mediated antimicrobial activities in bioactivity tests.

5.1. Introduction

The treatment of multi-resistant microorganisms is increasingly difficult, making the discovery of new antimicrobials urgent and imperative. To this purpose, large compound libraries that aim to cover a wide range of the chemical space are typically screened[437,438,529,530]. A wide variety of methods are available for testing antimicrobial activities *in vitro,* recently reviewed by Balouiri *et al* (2016).

The potency of a molecule against a microorganism is typically expressed as its minimal inhibitory concentration (MIC) *i.e.* the lowest concentration necessary to cause a specified reduction in (visible) growth[197]. Although different set-ups are possible, the MIC is mostly determined in multi-well plates because this format yields reliable results with limited resources. In addition, standardized protocols are preferred to increase reproducibility and permit comparison between experiments[198]. However, determining the MIC for molecules with a relatively high vapor pressure can be challenging as these volatiles tend to evaporate over the course of the assay. This may lead to underestimation of the activity in the well containing the compound, and spurious activity in adjacent wells. To limit loss due to evaporation and to limit interference, the microtiter plates could be sealed, although this is not always possible or effective, nor desirable. Furthermore, standard screening protocols and MIC assays do not

take vapor-phase-mediated effects of volatiles into account, which therefore mostly remain unnoticed.

Volatiles are typically enriched in essential oils (EOs), several of which are known for their antimicrobial activity against a wide variety of microorganisms including multi-resistant strains[489,501,504,531,532]. Different assays are available to test the antimicrobial activity of the vapor-phase of volatiles[198,500,501,533,534]. However, they mostly focus on the direct activity of the vapor-phase, and do not account for the vapor-phase-mediated effect, which is defined as the effect of a compound in solution at a distance.

In this study, we introduce the vapor-phase-mediated patch (VMP) assay which is a simple assay for detecting the vapor-phase-mediated antimicrobial activity (VMAA) of EOs and their components (EOCs) and other volatiles. It uses standard 96-well plates where a patch is defined as the set of wells in a (square) area surrounding one or more test wells. Moreover, we introduce an alternative microtiter plate set-up that can be used in accordance with standard broth microdilution protocols to easily unmask false-positive results caused by the volatility of EO(C)s. As a proof-of-principle, we studied the VMAA of selected EO(C)s against two pathogenic yeast species, *Candida albicans* and *C. glabrata,* and compared this to their MIC and corresponding minimal fungicidal concentrations (MFC). These *Candida* species are dominant members of the human mycobiome[3], and the most common pathogenic fungi in humans[115]. Even though they belong to the same genus, they are genetically and phenotypically very different[128,535]. In a healthy host, they reside on mucosal surfaces as commensals. However, under predisposing conditions they can become pathogenic, causing diseases ranging in severity from local superficial infections to life-threatening systemic candidiasis[28].

5.2. Results and discussion

In an antimicrobial screening (data not shown) of more than one hundred EOs against different bacteria and yeasts using standard 96-well microtiter plates and 100-well honeycomb titer plates with lids, three phenomena were frequently observed. Firstly, in some microtiter plates there were patches of wells with reduced or no growth, even if some of those wells contained EO(C)s that were known to be inactive at the tested concentrations. Secondly, there was reduced or no cell growth in some negative controls adjacent to the wells containing EO(C)s. The EO(C)s in the center of the affected patches or next to the affected negative controls were often known for their strong antimicrobial activity. Thirdly, the cell growth in the negative control wells was inversely related to the overall quantity of EO(C)s in a microtiter plate. These phenomena occurred when the microtiter plates were covered with a lid with or without condensation rings, although they were more pronounced in the latter case. We hypothesized that the observed phenomena were caused by the VMAA of some of the EO(C)s under study.

Based on these antimicrobial screening results, we selected one EO with (EO of *Origanum compactum*) and one EO without (EO of *Pimenta racemosa*) VMAA, and tested the hypothesis using the VMP assay. Briefly, four times 20 µL of each EO was added to the center four wells of a 36-well patch after which half of the patch was sealed, rendering these wells atmospherically inaccessible, before covering the plate with a lid. After 24 hours of incubation, cell growth was clearly affected in non-sealed wells in the patch adjacent to wells containing *Origanum compactum* EO (which has VMAA), but not in those adjacent to the wells containing the EO of *Pimenta racemosa* (which is devoid of VMAA). Growth was unaffected in all sealed wells, independent of the EO added and the position of the wells with respect to the EO added (figure 5.1a). Cell growth in the sealed wells was indistinguishable from growth in internal negative control wells that were not sealed and that were located far enough from the center wells not to be affected by the EOs, indicating that growth was not substantially affected by sealing of the plate (figure 5.1b). Together, these results provided a direct link between the presence of an EO with VMAA and the inhibition of cell growth in adjacent wells that were not sealed.

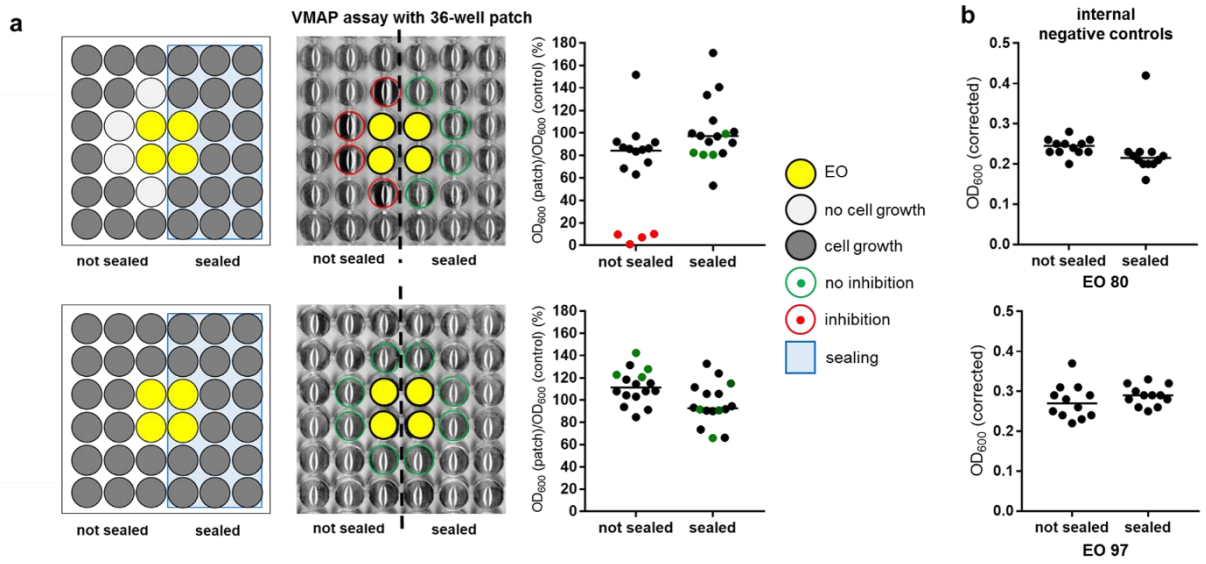

Figure 5.1: The vapor-phase-mediated antimicrobial activity of EOs affects *Candida albicans* cell growth (24h) in adjacent wells that were not sealed. a: Schematic illustration (left column), optical scan of microtiter plate (second column) and OD measurements (right columns) of the vapor-phase-mediated patch assay showing the effect of the EO of *Origanum compactum* with vapor-phase-mediated antimicrobial activity (upper panels) and the EO of *Pimenta racemosa* without vapor-phase-mediated antimicrobial activity (lower panels) on growth of *C. albicans* cells in the wells of the patch. **b**: Comparison of cell growth (OD measurements) in negative control wells (not sealed and sealed).

However, the absence of VMAA on the growth in nearby wells does not exclude possible effects of the tested EO on cells in surrounding wells. For instance: (i) the tested quantity of the EO may be sub-inhibitory, meaning that higher quantities might still affect cell growth in surrounding wells, (ii) an endpoint measurement may not be sufficient to detect an effect on cell growth such as a lag phase extension, which could be solved by measurements during the incubation, or (iii) the effects on the cells in nearby wells may not be growth-related but linked to for example the phenotype *e.g.* induction or repression of hyphal growth, which could be revealed by microscopy.

As a proof-of-principle, we selected five commercially available and chemically diverse EOs, each rich in one specific EOC and known for its antimicrobial potential, as well as their corresponding commercially available EOCs. Their MIC and MFC against a strain of both *C. albicans* and *C. glabrata* were determined (table 5.1), yielding values ≤ 0.13% (v/v) for most EO(C)s. For *Cinnamomum camphora ct linalool* EO, *Melissa officinalis* EO and linalool EOC the MIC could not be determined as 0,13% (v/v) was the highest concentration that could be tested in this experimental set-up due to cytotoxicity of the solvent DMSO. However, the anti-*Candida* activity of these EOs has been described before[489,536,537].

Table 5.1: Minimal inhibitory concentration and minimal fungicidal concentration of the EO(C)s under study against *Candida albicans* and *Candida glabrata* (24h). EO(C): essential oil (component). #a mixture of the isomers geranial and neral.

EO(C)	Rich in EOC	*C. albicans*		*C. glabrata*	
		MIC (% v/v)	MFC (% v/v)	MIC (% v/v)	MFC (% v/v)
estragole	estragole	0.063	0.063	0.0078	0.016
Artemisia dracunculus		0.063	0.063	0.016	0.016
carvacrol	carvacrol	0.13	0.13	0.13	0.13
Origanum compactum		0.13	0.13	0.13	0.13
linalool	linalool	≥ 0.13	≥ 0.13	≥ 0.13	≥ 0.13
Cinnamomum camphora ct linalool		≥ 0.13	≥ 0.13	≥ 0.13	≥ 0.13
citral	citral#	0.13	0.13	0.13	≥ 0.13
Melissa officinalis		≥ 0.13	≥ 0.13	≥ 0.13	≥ 0.13
trans-cinnamaldehyde	trans-cinnamaldehyde	0.016	0.016	0.016	0.016
Cinnamomum cassia		0.0078	0.0078	0.0078	0.0078

We then tested if these EO(C)s had VMAA against either *Candida* species. Moreover, we included the commonly used antifungals fluconazole, caspofungin, AmB, 5-flucytosine and terbinafine. To determine whether each of the observed VMAA was also fungicidal, in addition to inhibiting cell growth, spot tests were performed. We did not observe inhibitory or cidal VMAA for any of the above-mentioned antifungals when added at a concentration five to ten times their MIC (data not shown). On the other hand, several of the tested EO(C)s showed VMAA, often both inhibitory and fungicidal. A representative selection of results is shown as an illustration (figure 5.2), along with negative controls in which no EO(C) was added to the center of the patches. Some EO(C)s were cidal when tested at volumes as small as 0.25 µL (carvacrol and trans-cinnamaldehyde-rich EO of *Cinnamomum cassia*), while others had no effect on cell growth in adjacent wells even at volumes as high as 64 µL (estragole and estragole-rich EO of *Artemisia dracunculus*) (figure 5.2).

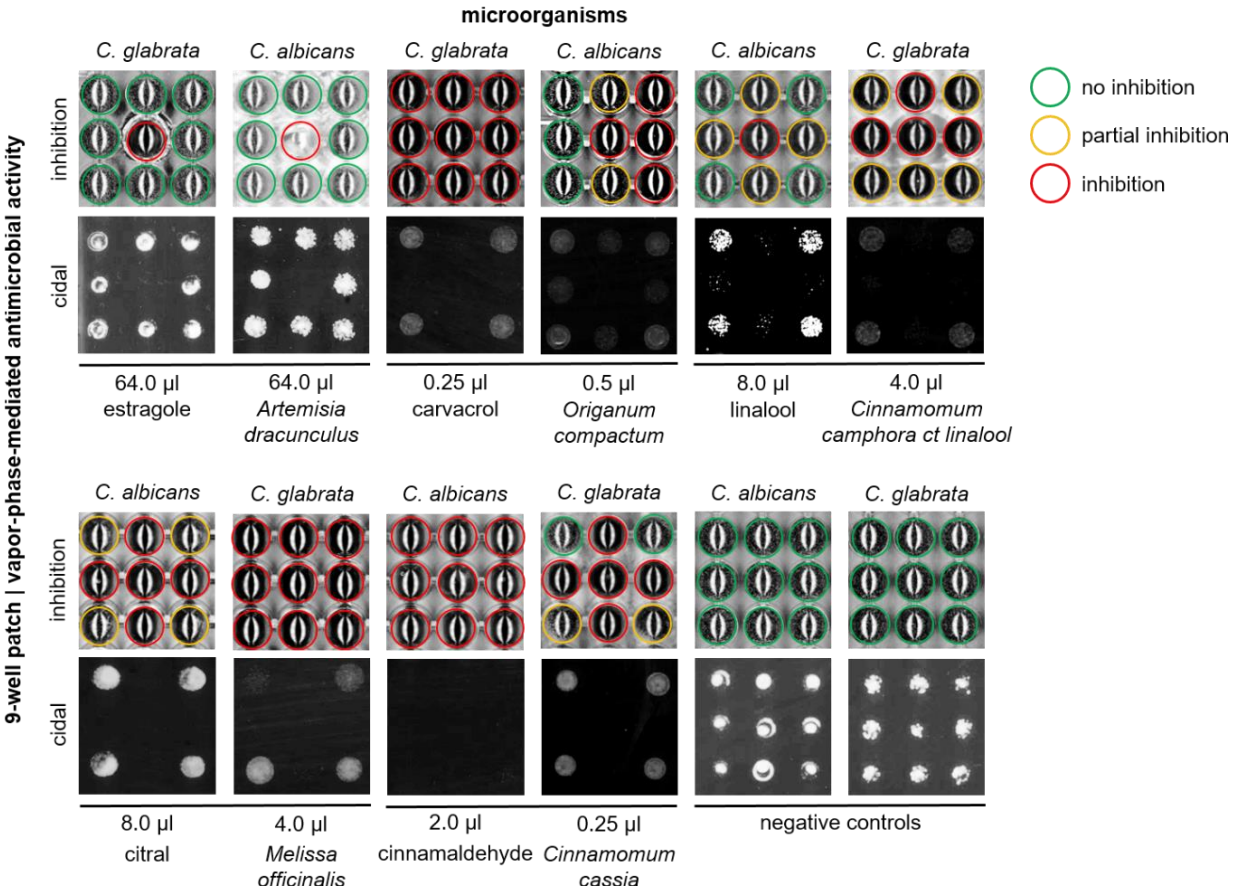

Figure 5.2: Different EO(C)s show inhibitory and fungicidal vapor-phase-mediated antimicrobial activity against two *Candida* species. Optical scans of 9-well patches of microtiter plates (top rows) and YPD agar plates with spot tests (bottom rows) showing growth inhibition and cidal activity, respectively, caused by the vapor-phase-mediated antimicrobial activity of selected EO(C)s on *C. albicans* and *C. glabrata*. Volume below YPD agar plates with spot tests indicates quantity of pure EO(C) added to the center well.

Moreover, these results show concordance between the VMAA exhibited by a component and an EO rich in this component, even though the VMAA was often tested against different species. Even when tested on the same species, the results between the EO and its corresponding major EOC may not match exactly for instance because of differing percentages of the compound present in the EO versus EOC and/or the effect of other compounds with VMAA present in the EO. We demonstrated that the chemically diverse EOCs carvacrol, citral, trans-cinnamaldehyde and linalool, and EOs rich in these EOCs, exhibit VMAA against both *Candida* species tested, even at µL volumes. Direct vapor-phase antimicrobial activities were shown before for citral-, carvacrol- and linalool-rich EOs and their corresponding EOCs using different assays[498,536,538]. Taking the variability of EO composition[484,539] into account, this demonstrates that there is a degree of overlap between the direct vapor-phase antimicrobial activity and the VMAA measured here. Moreover, it indicates that reliable results can be

obtained using the assay that we introduced here. All EO(C)s with VMAA have in common that they have a relatively low MIC. However, a low MIC does not automatically imply VMAA. The MIC of both *Artemisia dracunculus* EO and its main component estragole was relatively low while no VMAA was observed even at volumes as high as 64 µL.

Since EO(C)s are frequently dissolved in DMSO before testing, we explored whether this affected their VMAA. Although DMSO itself had no VMAA, the VMAA of most of the tested EO(C)s that were dissolved in DMSO was still present, albeit attenuated (figure 5.3).

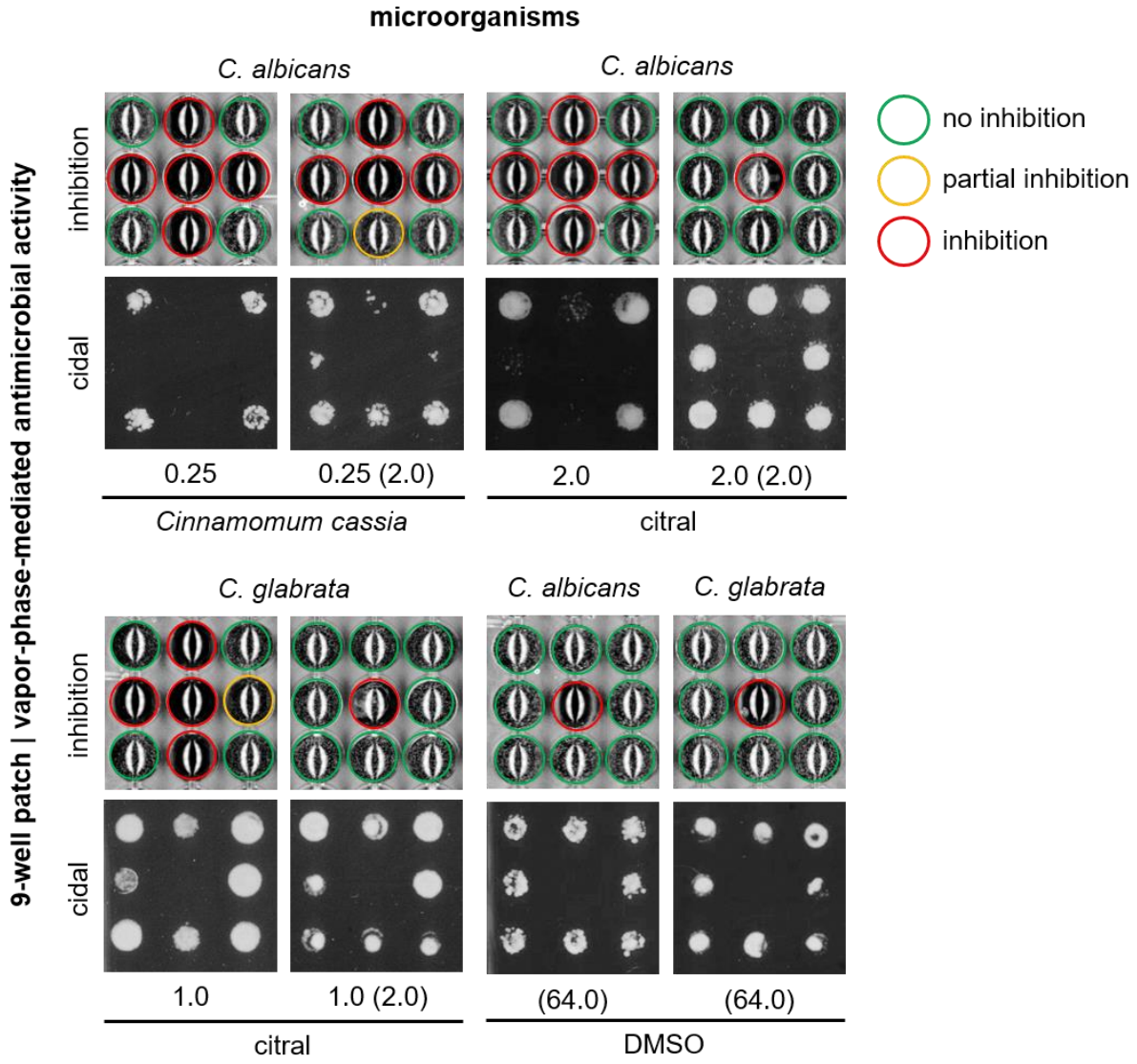

Figure 5.3: Dissolving EO(C)s in DMSO seems to attenuate vapor-phase-mediated antimicrobial activity. Optical scans of 9-well patches of microtiter plates (top rows) and YPD agar plates with spot tests (bottom rows) showing possible growth inhibition and cidal activity respectively, caused by vapor-phase-mediated antimicrobial activity of selected EO(C)s dissolved in DMSO on *C. albicans* and *C glabrata*. Volumes below YPD agar plates with spot tests indicate the quantity (µL) of EO(C) added to the center well, pure in the left panel of each set, and dissolved in DMSO in the right panel of each set. Volumes between brackets indicate the quantity (µL) of DMSO used to dissolve the EO(C) before addition to the center well (upper left, upper right, bottom left), or indicates the volume of pure DMSO added as a control (bottom right).

A comparable effect was shown in a study on the antimicrobial activity of the EO of *Cinnamomum zeylanicum* on the yeast *Saccharomyces cerevisiae* using the broth microdilution assay. The antimicrobial activity was shown to be diminished after dissolving the EO in DMSO compared to using the EO pure. The researchers suggested that this was caused

by the partitioning of the EO between the aqueous phase and DMSO, thus occluding the EO from the cells[540]. It is conceivable that EO(C)s are contained by DMSO in the aqueous environment which would limit their evaporation[541] hence resulting in an attenuated VMAA. However, since it seems difficult to predict whether DMSO will affect VMAA, we recommend to avoid using DMSO as a solvent in the VMP assay.

Together, these results demonstrate that EOs with a diverse chemical composition, and their main EOCs, showed VMAA at µL volumes both when added pure or dissolved in DMSO (figure 5.2 and 5.3). Therefore, when performing antimicrobial screenings with EO(C)s, the VMAA must be taken into account as typically one or more EO(C)s are tested in the same microtiter plate. Moreover, if EO(C)s can affect the growth in adjacent wells, it is plausible that testing several EO(C)s in the same microtiter plate can affect multiple or even all wells.

MIC measurements of EO(C)s typically follow procedures described in reference methods (*e.g.* by CLSI), although adaptations are often applied. A commonly used adaptation to contain the EO(C)s in the wells is sealing off the microtiter plates, which could also be a valid strategy to prevent EO(C) cross-contamination. However, at the same time it eliminates air circulation thereby reducing available oxygen and creating a different microenvironment in the sealed wells. The acetate Corning® Cap Mats used in this study were impermeable to EO(C)s and closed off the wells tightly, impeding the evaporation of EO(C)s. In contrast, adhesive seals proved insufficient in several of our tests (data not shown), either because the wells were not sealed tightly enough from the start of the experiment or because of the glue loosening over the course of the experiment, resulting in cross-contamination. Thus, even seemingly minor adaptations of a reference methods, such as sealing off the microtiter plate, can modify the outcome of an experiment.

We therefore adopted an alternative approach that proved successful in practice. Multiple reasons justify this strategy *e.g.* (i) several types of microtiter plates (*e.g.* honeycomb plates) do not permit tight closing of the wells, thereby allowing cross-contamination of EO(C)s and (ii) EO(C)s may interfere with adhesive seals. Our approach does not intrinsically change the CLSI protocol, while at the same time assuring that the experiment is controlled for false positive results caused by possible VMAA of EO(C). It implies adding rows and/or columns of negative controls between the wells containing the EO(C)s to be tested. In this way, EO(C)s with VMAA will be detected as growth in adjacent negative control wells will be affected. In most cases, it will be clear from the spatial pattern which EO(C) is responsible for the VMAA. However, if different EO(C)s with VMAA would be in close proximity, identifying the causative one(s) might not be straightforward. Therefore, all the EO(C)s near a VMAA disturbance should be retested using a different plate lay-out.

In conclusion, we have demonstrated that EOCs of diverse chemical classes *i.e.* phenols (EOC carvacrol), aldehydes (EOCs cinnamaldehyde and citral) and alcohols (EOC linalool), as well as EOs rich in these components show VMAA. Since many of the EO(C)s tested showed this effect, it may be a common characteristic of EO(C)s. Hence, it is not a negligible phenomenon and has to be taken into account when planning and designing an experiment with EO(C)s. Our proof-of-principle study was not intended to exhaustively document this phenomenon for EO(C)s. Rather, we aim at providing new tools: (i) an assay to study the VMAA of EO(C)s or volatiles in general, and (ii) a microtiter plate set-up allowing researchers to unmask false positive results in a standard MIC screening.

5.3. Materials and methods

5.3.1. Essential oils and essential oil components.

All EOs (n=7) were purchased from Pranarôm International S.A. (Ghislenghien, Belgium) (table 5.2) and all EOCs (n=5) from Sigma-Aldrich (Steinheim, Germany) (table 5.3). Quality, origin and composition of the EO(C)s were certified by both companies. Chemical analysis of the EOs was performed by GC-FID using the NF ISO 11024-1/2 standard, and is available in table A-II (p. 155). The EO(C)s were aliquoted in sterile glass vials (Screening Devices, Amersfoort, Netherlands) and coded to blind the experiments. Dimethyl sulfoxide (stock solution of 99%; DMSO; Sigma-Aldrich) was used as a solvent if the EO(C)s were dissolved prior to testing, and as a corresponding control. In case EO(C)s were dissolved in DMSO prior to testing, the eventual concentration of DMSO never exceeded 1%, *i.e.* the concentration of DMSO used was not toxic for the cells. In case DMSO was used alone as a control, the concentration used did exceed 1%. However, such high concentration were only used to illustrate that even at high volumes DMSO did not exhibit vapor-phase-mediated antimicrobial activity.

Table 5.2: List of chemically defined essential oils with components (≥ 10%). AP: aerial parts; F: fruit; FT: flowering top; T: twigs; W: wood. *Batches of the same essential oil. #a mixture of the isomers geranial and neral.

Plant	Part of plant	Place of origin	Lot number	Component(s) ≥ 10% (v/v)	% (v/v)
*Origanum compactum**	FT	Morocco	OCH13 (figure 5.1)	carvacrol	39.95
				thymol	19.51
				γ-terpinene	16.23
				p-cymene	10.86
			OF10299 (figure 5.2)	carvacrol	43.67
				thymol	19.52
				γ-terpinene	16.16
Pimenta racemosa	F	Antilles	PRS4	eugenol	45.23
				β-myrcene	25.92
				chavicol	10.6
Artemisia dracunculus	FT	France	OF10105	estragole	79.36
				β-ocimene	15.05
Cinnamomum camphora ct linalool	W	China	OF10369	linalool	98.35
Cinnamomum cassia	T	China	OF10584	trans-cinnamaldehyde	78.45
				2-methoxycinnamaldehyde	10.75
Melissa officinalis	AP	Bulgaria	OF10300	citral#	36.76
				β-caryophyllene	23.46
				germacrene D	11.52

Table 5.3: List of highly enriched essential oil components. #a mixture of the isomers geranial and neral.

Highly enriched EOCs	Purity (%)	Product number	Lot number
estragole	≥ 98	A29208	MKBR0582V
carvacrol	≥ 99	W224511	MKBR8607V
linalool	≥ 97	L2602	STBF6800V
citral#	≥ 95	C83007	STBC5273V
trans-cinnamaldehyde	≥ 99	C80687	MKBV8774V

5.3.2. Candida albicans and Candida glabrata.

C. albicans strain SC5314 and *C. glabrata* strain ATCC 2001 were maintained on yeast extract peptone dextrose (YPD) agar plates composed of 10 g/L yeast extract (Merck, Darmstadt, Germany), 20 g/L bactopeptone (Oxoid, Basingstone, Hampshire, England), 20 g/L glucose (Sigma-Aldrich) and 15 g/L Difco™ agar (Becton, Dickinson & Co., MD, USA). Prior to experiments, the strains were grown overnight at 35°C on Sabouraud agar plates containing 47 g/L Sabouraud agar (Sigma-Aldrich).

5.3.3. Preparation of the cell inoculum

A small loop of overnight propagated cells was suspended in 1x Phosphate-Buffered Saline (PBS) containing 8 g/L sodium chloride (Sigma-Aldrich), 0.2 g/L potassium chloride (VWR International, Leuven, Belgium), 1.44 g/L disodium hydrogen phosphate (Merck), and 0.24 g/L potassium dihydrogen phosphate (Merck). The cell density was estimated by measuring the Optical Density at 600 nm (OD_{600}) with a biophotometer (Eppendorf, Hamburg, Germany) and the desired cell suspension was made in Roswell Park Memorial Institute-1640 (RPMI) medium (Sigma-Aldrich). This medium was buffered with 3-(N-morpholino) propanesulfonic acid (MOPS; Sigma-Aldrich) and filter-sterilized over a 0.20 µm non-pyrogenic Nalgene™ filter (Fisher Scientific, Merelbeke, Belgium) in accordance with Clinical and Laboratory Standards Institute (CLSI) guidelines[197].

5.3.4. Vapor-phase-mediated patch assay

To all wells of a 96-well microtiter plate with U-shaped wells (Greiner Bio-One, Vilvoorde, Belgium) 200 µL of a 5 x 10^3 cells/mL inoculum was added, except for the corner wells to which 200 µL RPMI-MOPS was added and which served as blanks. In the middle of a square patch containing 9 or 36 wells, the desired volume of an EO(C) to be tested was added either on top of the cell suspension, or into the suspension if the EO(C)s were dissolved in DMSO. Wells located outside the patch, and distant enough not to be affected by the EO(C)s, served as internal negative controls. Optionally, half of the patch and corresponding control wells were sealed with an acetate Corning® Cap Mat (Sigma-Aldrich). Multiple EO(C)s were tested in different microtiter plates in one experimental run. For each run, a microtiter plate without EO(C)s was included as external negative control. The microtiter plates were covered with a lid and then statically incubated (Heraterm, ThermoFisher Scientific, Aalst, Belgium) for 24 hours at 35°C, while limiting air draughts. Optical scans (Epson Perfection V600, Seiko Epson Corp, Nagano, Japan) of the microtiter plates were made, and the OD_{600} was measured with a multi-well plate reader (Synergy H1, BioTek Germany, Bad Friedrichshall, Germany) after resuspending the cells. Optionally, cells from each well were spotted onto YPD agar plates using a plate replicator (V&P Scientific, San Diego, CA, USA). These YPD plates were incubated overnight, after which optical scans were made.

5.3.5. Broth microdilution assay followed by spot test

The broth microdilution assays were performed in accordance with the CLSI protocol[197] with few adaptations. Briefly, to all wells of a 96-well microtiter plate 100 µL of a 1 x 10^4 cells/mL inoculum was added, except for wells serving as blanks, to which 200 µL RPMI-MOPS was added. For each EO(C) to be tested, a test solution was prepared by dissolving one part EO(C) in eight parts (v/v) DMSO. A two-fold serial dilution ranging from 0.25% (v/v) EO(C) to 0.0078% (v/v) EO(C) was prepared in RPMI-MOPS, and 100 µL of each dilution was added to the wells with cell suspension resulting in a final cell concentration of 5 x 10^3 cells/mL and final EO(C) concentrations ranging from 0.125% (v/v) to 0.0039% (v/v). To wells serving as negative controls, 100 µl of RPMI-MOPS was added resulting in a final cell concentration of 5 x 10^3 cells/mL. Plates were sealed with an acetate Corning® Cap Mat and incubated for 24 hours at 35°C. The MIC was determined as the lowest concentration required for visible growth inhibition or was based on OD_{600} measurements with a multi-well plate reader after resuspending the cells. Optical scans of the microtiter plates were made and a spot test was performed as described above.

6. Essential oils and their components are a class of antifungals with potent vapor-phase-mediated anti-*Candida* activity

Adam F. Feyaerts[1,2,#], Lotte Mathé[1,2,#], Walter Luyten[3], Stijn De Graeve[1,2], Katrien Van Dyck[1,2], Lize Broekx[1,2] and Patrick Van Dijck[1,2,*]

[1]VIB Center of Microbiology, KU Leuven, 3001, Leuven, BELGIUM

[2]Laboratory of Molecular Cell Biology, KU Leuven, 3001, Leuven, BELGIUM
[3]Department of Biology, KU Leuven, 3000, Leuven, BELGIUM

[#]These authors contributed equally to this work

*Corresponding author:

Patrick Van Dijck

Laboratory of Molecular Cell Biology, KU Leuven

VIB-KU Leuven Center for Microbiology

Kasteelpark Arenberg 31 bus 2438

3001 Heverlee, Belgium

Tel.: (0032) 16 321512

Fax: (0032) 16 321979

patrick.vandijck@kuleuven.vib.be

Keywords: vapor-phase-mediated antimicrobial activity, essential oil, essential oil component, *Candida* species

Multi-resistant microorganisms continue to challenge medicine and fuel the search for new antimicrobials. Here we show that essential oils and their components are a promising class of antifungals that can have specific anti-*Candida* activity via their vapor-phase. We quantify the vapor-phase-mediated antimicrobial activity (VMAA) of 175 essential oils and 37 essential oil components against *C. albicans* and *C. glabrata* in a novel vapor-phase-mediated susceptibility assay. Approximately half of the essential oils and components tested show growth-inhibitory VMAA. Moreover, an average greater activity was observed against the intrinsically more resistant *C. glabrata*, with essential oil component citronellal showing the most significant difference. In contrast, representatives of each class of antifungals currently used in clinical practice showed no VMAA. The vapor-phase-mediated susceptibility assay introduced here thus allows for the simple detection of VMAA and can advance the search for novel (applications of existing) antimicrobials. This study represents the first comprehensive characterization of essential oils and their components as a unique class of antifungals with antimicrobial properties that differentiate them from existing antifungal classes.

6.1. Introduction

The worldwide incidence of infectious diseases continues to mount and causative microorganisms are increasingly showing (multi-)drug resistance. Therefore, the discovery of new antimicrobials and the repurposing of old ones is critical[438,530,542,543]. Fungal infections in humans are mostly caused by *C. albicans* and *C. glabrata,* which are both dominant members of the human mycobiome that are genetically and phenotypically very different[3,128]. While *C. albicans* is most frequently identified as the causative species, the incidence of infections caused by *C. glabrata* is rising. Moreover, this species shows an overall lower susceptibility to common antifungals[544,545].

Many antimicrobials, such as the polyenes, macrolides, echinocandins, penicillins and essential oils (EOs), are natural products or derivatives thereof[482,546-549]. EOs are complex mixtures of secondary plant metabolites that have a relatively high vapor pressure, are poorly water-soluble and known for exerting a multitude of biological effects, including anti-*Candida* activity[484,550]. EOs contain many components (EOCs), which are mostly derived from intermediates of the mevalonate, methylerythritol phosphate and shikimic acid metabolic pathways[484,488]. The composition of EOs can be determined accurately by using analytical methods such as ^{1}H-Nuclear Magnetic Resonance spectroscopy with a certified internal

standard or gas chromatography combined with flame ionization detection and/or mass spectrometry[551,552]. Typically, within one EO, a few EOCs are present at high concentrations while the others are present in small or trace amounts[550].

To quantify the antimicrobial activity of a molecule against a specific microorganism, the minimal inhibitory concentration (MIC) is typically determined, preferably using standardized protocols such as the broth microdilution assay[198,553-555]. However, standardized protocols are not always suitable for testing antimicrobials with a high vapor-pressure. These molecules may exhibit an antimicrobial activity at a distance that is mediated by their vapor-phase, which permits easy administration by inhalation, treatment of *e.g.* porous substances, and rapid removal by airing. Despite this, the vapor-phase-mediated antimicrobial activity (VMAA) is often overlooked, undervalued or neglected. Therefore, we introduce the vapor-phase-mediated susceptibility (VMS) assay which allows a semi-quantitative study of the VMAA. The procedure is based on the Clinical and Laboratory Standards Institute (CLSI) protocol for the broth microdilution assay using standard 96-well plates[197]. As such, the VMS assay resembles the previously introduced vapor-phase-mediated patch assay which can be used for the detection of VMAA[556].

Here, we quantify the VMAA of a large collection of commercially available EO(C)s against two pathogenic *Candida* species. This allowed us to (i) identify EO(C)s with a strong VMAA against pathogenic *Candida* species, (ii) compare the average susceptibility of both yeasts to our EO(C) collection, and (iii) identify EO(C)s showing a differential activity against both *Candida* species. As such, this proof-of-principle study demonstrates that gauging the VMAA of bioactives using the VMS assay can lead to the discovery of novel (applications of) antimicrobials.

6.2. Results

6.2.1. The VMAA of a volatile spreads symmetrically across a microtiter plate

To quantify the vapor-phase-mediated activity in a straightforward manner, we developed the VMS assay and characterized the behavior of volatiles in this assay using 96-well plates. We hypothesized that, under ideal conditions, a volatile added to the center four wells would spread symmetrically in a spherical manner, thus establishing a concentration gradient across the microtiter plate. A circle enclosing the four wells to which the volatile is added, was designated the volatility-center (figure 6.1a upper left). Around this center, concentric circles can be drawn that successively touch the nearest equidistant wells, with each set of wells making up a new distance category. These categories were defined to correct for the different number of wells in different categories and were ranked ordinally, with category one located closest to the volatility-center (figure 6.1a-b). The distance between the circles and the volatility-center is the minimal distance that a volatile needs to travel to possibly exert effects in the corresponding wells. Therefore, the content of all wells belonging to one category would be affected equally, due to radial symmetry.

This was illustrated by the growth inhibitory VMAA of the EO of *Litsea citrata*, rich in citral (71.80%; table A-III-1, p. 163), on *C. albicans* in a VMS assay (figure 6.1c). As predicted, growth inhibition clearly increased the closer wells were located to the volatility-center and this visual impression was confirmed spectrophotometrically (figure A-III-1, p. 176). Headspace solid-phase micro-extraction gas chromatography mass spectrometry (HS-SPME-GC-MS) on the content of the wells of the microtiter plates confirmed the presence of α-citral and β-citral in all wells, as quickly as one hour after addition of the EOC citral (≥ 95%) and this amount increased over the next hours (figure 6.1d). Comparison with figure 6.1c clearly shows a correlation between the EOC concentration and the observed growth inhibitory effect. The concentration gradient established by both enantiomers can explain the observed graded effect of citral on *C. albicans* cells in wells of different distance categories. The largest effects were observed in wells located close to the volatility-center, and they were associated with the highest concentration of citral measured (figure 6.1c-d).

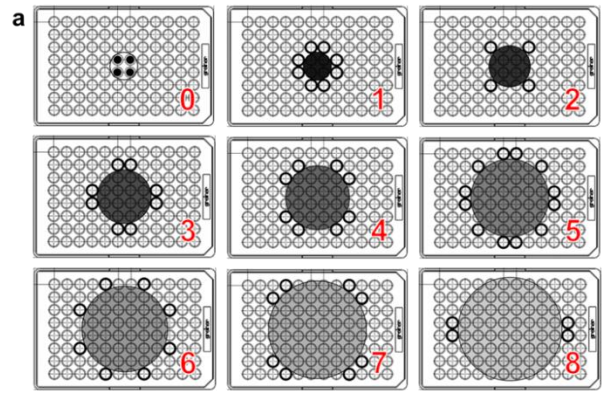

b

category (ordinal)	number of wells per category | cumulative number of wells	distance from volatility-center (mm)
0	0 | 0	0.0
1	8 | 8	0.9
2	4 | 12	5.8
3	8 | 20	9.7
4	8 | 28	13.0
5	12 | 40	18.6
6	8 | 48	21.0
7	8 | 56	25.5
8	4 | 60	27.5
9	4 | 64	29.5
10	4 | 68	31.1
11	4 | 72	33.1
12	4 | 76	36.5
13	8 | 84	38.1
14	4 | 88	41.2
15	4 | 92	45.5

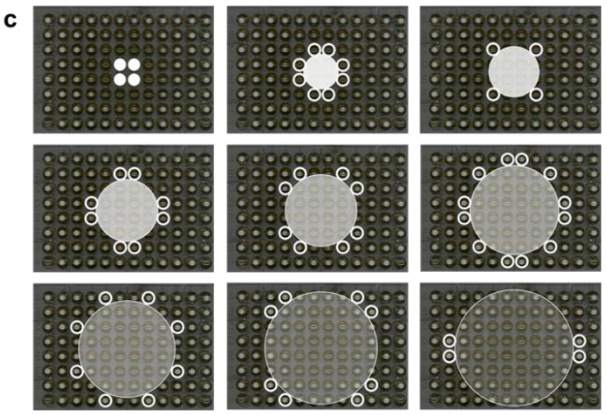

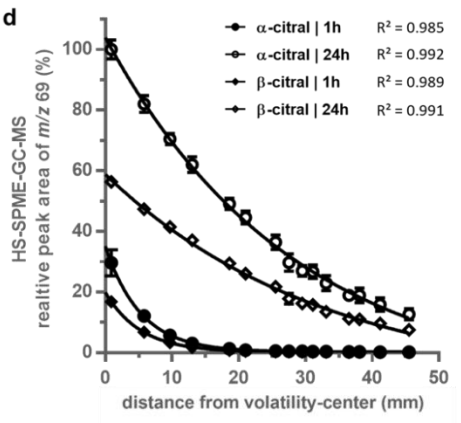

Figure 6.1: The VMAA of a volatile spreads symmetrically across a microtiter plate. a: Illustrations of the spreading of a volatile in the VMS assay under ideal circumstances starting from the center four wells (= volatility-center which corresponds to category 0: upper-left); upper-middle to bottom-right: The first eight categories in which equidistant wells are affected. **b**: The number of equidistant wells and cumulative number of wells in successive categories with their distance to the volatility-center. **c**: Optical scans of the bottom of a 96-well microtiter plate illustrating the VMAA of *Litsea citrata* against *C. albicans* after 24 hours of incubation. Panels correspond to categories shown in figure 6.1a. **d**: Graph illustrating the negative exponential distribution of both enantiomers of EOC citral over the microtiter plate in the VMS assay after one and 24 hours of incubation. Adjusted R^2 values represent goodness of fit. Each dot represents the relative peak area in HS-SPME-GC-MS analysis representing the concentration of pooled equidistant wells belonging to the same distance category as a function of their distance to the volatility-center. Data from three independent experiments are shown and error bars represent standard deviation.

We defined the inhibitory VMAA (iVMAA) as the categorized cumulative number of wells (figure 6.1a-b), determined by visual assessment and excluding the volatility-center, in which growth was completely inhibited. When growth was only inhibited in some wells of one category, due to asymmetrical iVMAA patterns resulting from *e.g.* uncontrolled airflows, we assigned the intermediate value of 0.5. Only one intermediate categorical value was introduced between every two categories because the different categories can contain a different number of

equidistant wells. Therefore, proportionally assigning the fraction of wells affected would result in an unequal number of intermediate values between every two categories.

A spectrophotometric determination of iVMAA, termed $iVMAA_{90}$ and defined as the inhibitory VMAA resulting in a 90% reduction of growth as compared to control growth, showed a very high correlation (ρ=0.991, p<0.0001; figure A-III-2, p. 177) with iVMAA. This reflects a very high similarity between visual and spectrophotometric assessment and shows that both read-outs are equally valid.

6.2.2. The MIC of EO(C)s cannot be used to predict their iVMAA and vice versa

To characterize the vapor-phase-mediated growth inhibitory activity of EO(C)s, we determined the iVMAA of 175 chemically defined EOs (table A-III-1, p. 163), and 37 of the most common EOCs (table A-III-2, p. 178) against *C. albicans* and *C. glabrata* (figure 6.2a). As the VMS assay set-up is based on CLSI guidelines for the broth microdilution assay[197], we also determined the MIC of our EO(C) collection against both *Candida* species (figure 6.2a). Despite the highly comparable experimental procedures used to determine the iVMAA and MIC, a correlation between these values for both species showed that the iVMAA of an EO(C) cannot be predicted from its MIC value and vice versa (figure 6.2b).

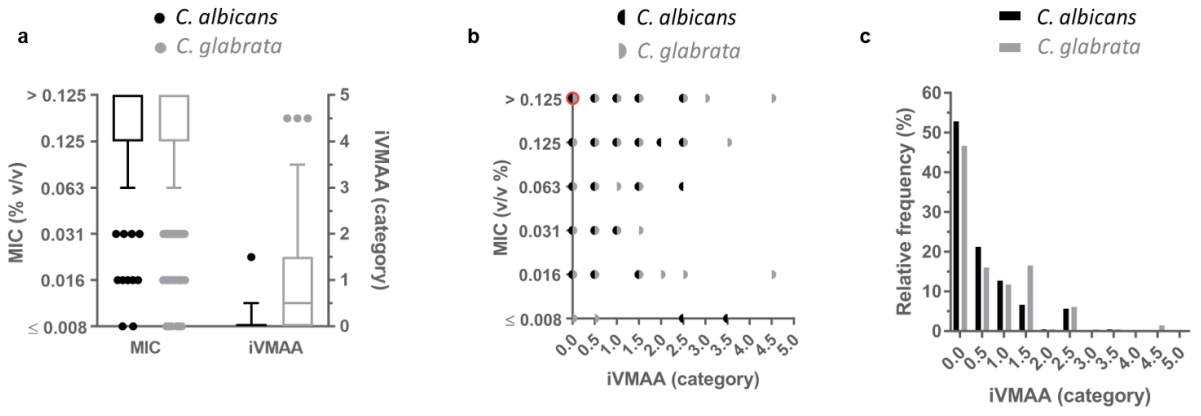

Figure 6.2: MIC of EO(C)s cannot be used to predict their iVMAA and vice versa. **a**: Tukey boxplots showing MIC and iVMAA of EO(C) (n=212) against *C. albicans* and *C. glabrata*. **b**: Scatterplot of the correlations between MIC and iVMAA of EO(C)s (n=212) against *C. albicans* (ρ=-0.0376, p=0.59) and *C. glabrata* (ρ=-0.0555, p=0.42). **c**: Histogram with the relative frequency distribution of iVMAA of EO(C)s (n=212) against *C. albicans* and *C. glabrata*.; MIC = minimal inhibitory concentration; iVMAA = inhibitory vapor-phase-mediated antimicrobial activity

Nine of the EOCs tested (24.3%) showed an iVMAA larger than 0.5 against both *Candida* species. The greatest activity was observed for EOC citronellal, followed by EOCs citral, thymol, trans-cinnamaldehyde, linalool, α-pinene, carvacrol, (-)-terpinen-4-ol, and allo-ocimene. A comparable proportion of the EOs tested (25.7%; n=45) showed an activity larger than 0.5 against both *Candida* species (figure 6.2c). Of these, 30 were rich in at least one of the previously mentioned EOCs, while seven of the 15 remaining EOs primarily contained components that were not included in our collection. By contrast, the iVMAA was zero for representatives of all antifungal classes commonly used in clinical practice *i.e.* AmB, caspofungin, fluconazole, terbinafine and 5-flucytosine when tested at five to ten times their MIC (data not shown). This lack of iVMAA was to be expected, considering the relatively high molecular weight and concomitant low vapor pressure at room temperature and/or high solubility in water of the tested molecules. Surprisingly, ethanol also failed to inhibit growth when tested in the VMS assay using the standard set-up (= 4 x 20 µl), despite its known antimicrobial activity and relatively high vapor pressure at room temperature. However, since it is known that relatively high concentrations of ethanol are needed to inhibit microbial growth[557,558], we theorized that higher volumes were needed to observe iVMAA. Indeed, when testing ethanol at ten times the standard volume, *i.e.* 4 x 200 µL, an iVMAA of 3.5 to 4 was obtained (data not shown).

6.2.3. The major components present in an EO largely determine the presence or absence of iVMAA

To study the effect of the major individual EOCs in the EOs on their iVMAA, we categorized all EOs in 10 chemical classes. These classes were defined based on the number of carbon atoms and the presence of specific functional groups in the dominant EOCs (figure 6.3a and table A-III-1, p. 163). Categorization occurred by the chemical class present at the highest concentration after combining all EOCs (>10% v/v) belonging to the same chemical class. This revealed that EO(C)s rich in aldehydes *e.g.* citronellal, citral, and trans-cinnamaldehyde showed the highest iVMAA, followed by EO(C)s rich in phenols, *e.g.* carvacrol and thymol, monoterpenols, *e.g.* linalool and terpinen-4-ol, ethers, *e.g.* 1,8-cineol, and ketones such as carvone.

While monoterpenol-rich EO(C)s were among the most active classes, EO(C)s rich in sesquiterpenols, *e.g.* farnesol, did not show iVMAA. Furthermore, absence of iVMAA was shown in EOs that were mainly rich in sesquiterpenes such as β-caryophyllene, and iVMAA was very limited in EOs that were rich in phenol methyl ethers, *e.g.* methyleugenol. The high iVMAA observed for aldehyde-rich EOs was not only a result of the presence of aldehyde(s), but was also strongly correlated with the quantity of aldehyde(s) present in the EO (figure 6.3b). In contrast, for monoterpenol-rich EOs and the corresponding EOCs the correlation between iVMAA and monoterpenol concentration was weak for *C. albicans*, while no correlation could be demonstrated for *C. glabrata* (figure 6.3c). While there was a moderate to strong correlation between the concentration of the tertiary monoterpenol linalool in an EO(C) and its iVMAA (figure 6.3d), we did not observe a correlation between the concentration of geraniol, a primary monoterpenol, in an EO and its iVMAA (figure A-III-3, p. 179). Together this shows that while major components in EOs often determine the presence or absence of iVMAA, they are not always responsible for the observed biological effects. It is thus advisable to also be attentive to the contributions of minor components when performing this kind of analysis.

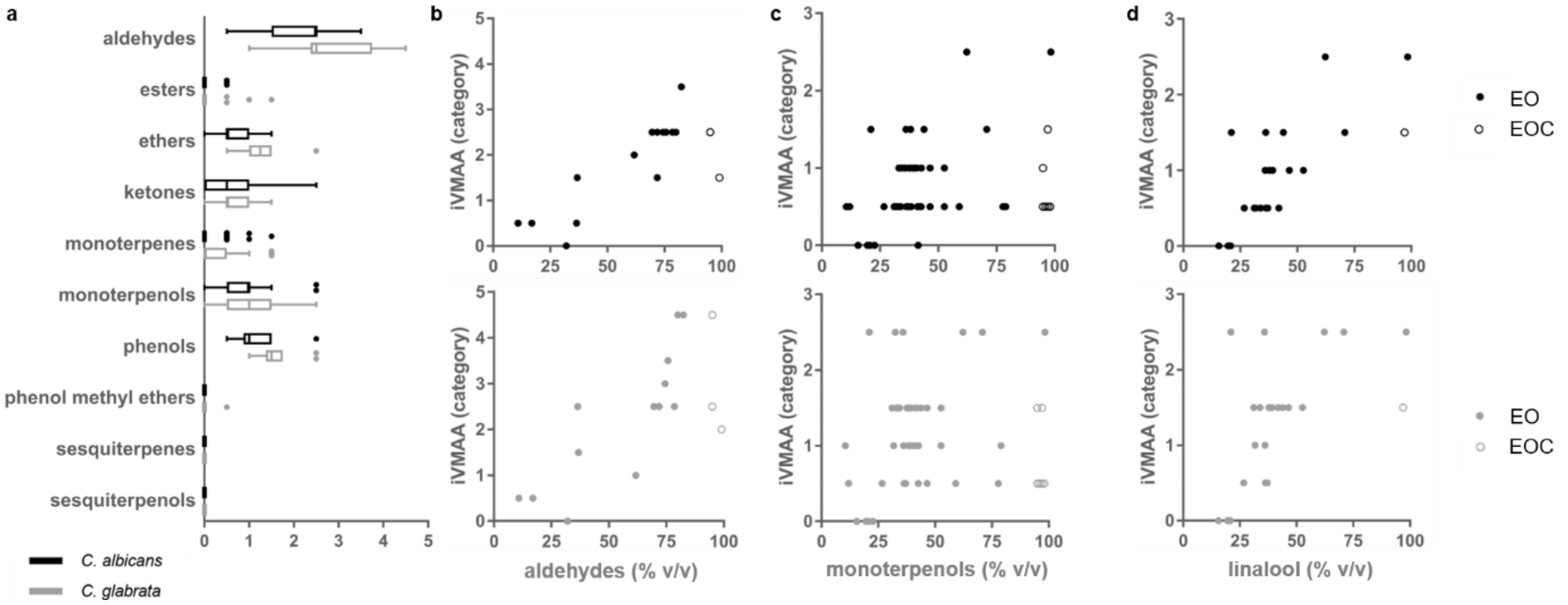

Figure 6.3: The major components present in an EO largely determine the presence or absence of iVMAA. **a**: Tukey boxplots showing the iVMAA of EO(C)s (n=209) categorized by the chemical class present at the highest concentration after combining all EOCs (>10%) belonging to the same chemical class. EOs for which one single major component could not be determined or for which this major component belonged to other chemical classes than defined in this paper were excluded (n=3). **b**: Correlations between the iVMAA of an EO(C) and its aldehyde concentration (>10%, n=17) for *C. albicans* (top; ρ=0.709, p=0.0020) and for *C. glabrata* (bottom; ρ=0.694, p=0.0025). **c**: Correlations between the iVMAA of an EO(C) and its monoterpenol concentration (>10%, n=48) for *C. albicans* (top; ρ=0.341, p=0.018) and *C. glabrata* (bottom; ρ=0.176, p=0.23). **d**: Correlations between the iVMAA of an EO(C) and its linalool concentration (>10%, n=22) for *C. albicans* (top; ρ=0.736, p<0.0001) and *C. glabrata* (bottom; ρ=0.6065, p=0.0028)

6.2.4. Candida glabrata shows an average higher susceptibility to the iVMAA of EO(C)s than Candida albicans

Determining the iVMAA of our EO(C) collection against two different *Candida* species allows to estimate the possibility of species-specific iVMAA exhibited by EO(C)s. While the iVMAAs of the EO(C)s against the two *Candida* species tested correlated strongly (figure 6.4a), their population wide-susceptibility to both the EOs and EOCs differed significantly ($p<0.0001$). Despite the lower susceptibility of *C. glabrata* to antifungals in general[43,197,545], it showed a higher average susceptibility to EO(C)s in the VMS assay compared to *C. albicans*. This higher susceptibility was evidenced by (i) more EO(C)s showing an iVMAA against *C. glabrata* (n=113) than against *C. albicans* (n=100) and (ii) on average a higher iVMAA of the EO(C)s (iVMAA>0; n=113) against *C. glabrata* ($\bar{x}$=1.28; 95% CI=1.13-1.44) than against *C. albicans* ($\bar{x}$=0.916; 95% CI=0.783-1.05). This resulted in more data points above the diagonal in the correlation analysis (figure 6.4a) and a clear contrast between the iVMAA of the two species visualized with a heat map (figure 6.4b). This indicates that EOs, and most likely specific EOCs within these EOs, can show a specific activity. To find those EO(C)s that showed the largest differential iVMAA against both species, the false discovery rate method was applied using a Q-value of 1%, *i.e.* accepting that 1% of the declared discoveries were false positives[559]. This resulted in four discovered EO(C)s *i.e.* organic EO *Eucalyptus citriodora* ct citronellal, EOC citronellal, EO *Cymbopogon winterianus*, and organic EO *Cinnamomum cassia* (figure 6.4b). Alternatively, when performing t-tests corrected for multiple comparisons (α=0.05), the same EO(C)s were shown to have a differential iVMAA against both species. All EO(C)s found were aldehyde-rich *i.e.* the EOC citronellal, two EOs rich in citronellal and one EO rich in trans-cinnamaldehyde (figure 6.4b).

When a Q-value of 2% was applied, two additional EOs were shown to be differentially active including *Leptospermum petersonii*, thereby finding all EO(C)s present in our collection that contain citronellal at more than 10% (table A-III-1, p. 163). Together, this gives a very strong indication that the aldehyde citronellal is responsible for the observed stronger iVMAA of these EOs against *C. glabrata*. Although organic EO *Cinnamomum cassia* was also differentially active, its main component trans-cinnamaldehyde itself was not, and no other EOs rich in this EOC were found to be differentially active at the tested statistical cut-offs. Therefore, another component or a combination of components is most likely causing this differential activity. The other EO found with at a Q-value of 2% was *Ammi visnage* EO, which contains linalool and two esters at more than 10% (table A-III-1, p. 163).

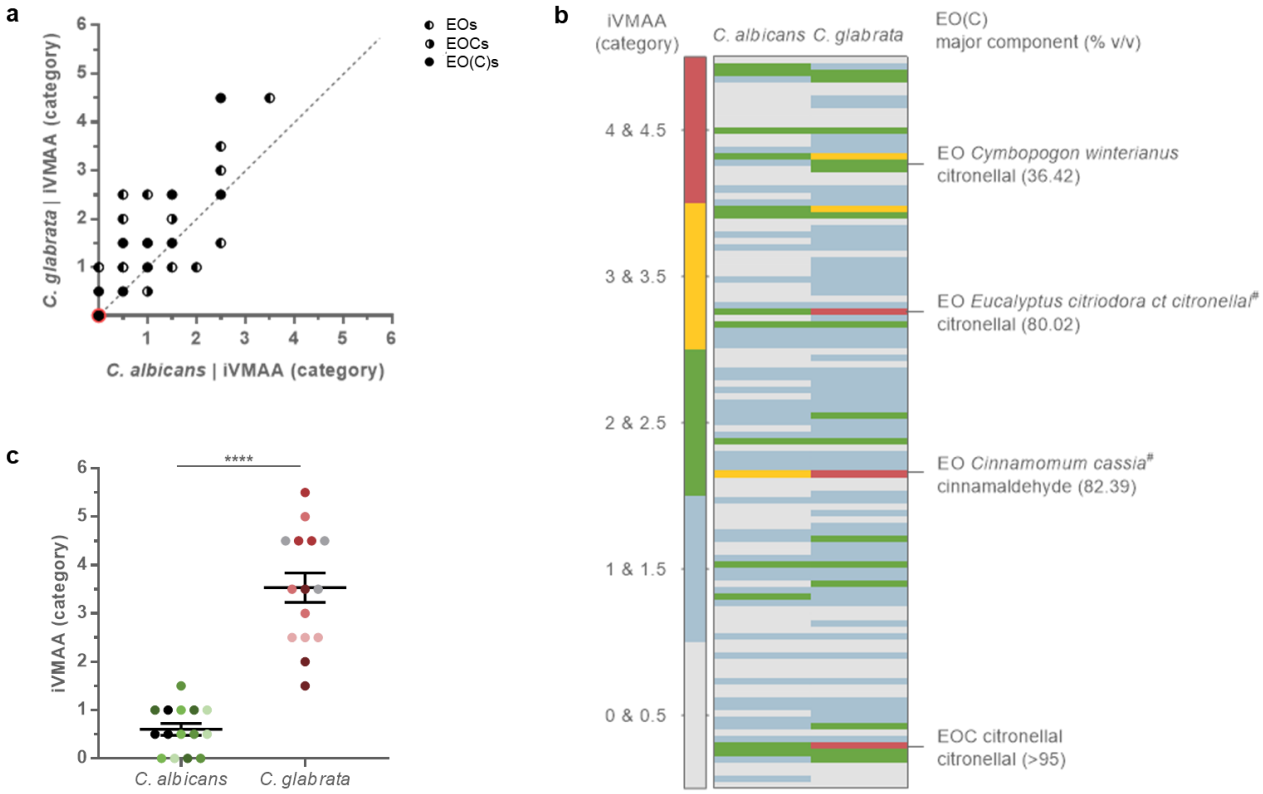

Figure 6.4: *Candida glabrata* is on average more susceptible to the iVMAA of EO(C)s than *Candida albicans*. **a**: Scatterplot of the correlation (ρ=0.930, p<0.0001) between iVMAAs of EO(C)s (n=212) against *C. albicans* and *C. glabrata*. **b**: Heat map of iVMAAs (>0 against at least one species) indicating the most differentially active of the EO(C)s (n=113) against *C. albicans* and *C. glabrata*. # indicates that EO originates from an organic cultivar. **c**: Graph showing iVMAA of citronellal in the VMS assay against five *C. albicans* strains (SC5314 in black, and four clinical isolates) and five *C. glabrata* strains (ATCC2001 in grey, and four clinical isolates). Three independent experiments per strain are shown in the same color and error bars represent standard error of the mean. iVMAA = inhibitory vapor-phase-mediated antimicrobial activity. ****p<0.0001

To exclude that the higher susceptibility to citronellal of *C. glabrata* compared to *C. albicans* was strain-dependent, the iVMAA of EOC citronellal was additionally determined against four clinical isolates of each species (fig. 6.4c). An unpaired t test with Welch's correction corroborated that *C. glabrata* as a species is more susceptible to EOC citronellal than *C. albicans*.

6.3. Discussion

Over the past decade there has been a renewed interest in investigating the biological activities and application potential of EO(C)s. Although data on the anti-*Candida* activity of EO(C)s have been summarized[490,560], it is often impossible to make reliable comparisons between results obtained in different studies because of different methodologies used[561]. Moreover, often only a few EO(C)s are included in each study. Together, this results in poor documentation of the antifungal activity of EO(C)s.

To obtain and compare results in a reliable way, standardized assays are required[198,561]. While the broth microdilution assay is considered the gold standard for the detection of antimicrobial activity in solution[562,563], it fails to detect VMAA of volatiles. Moreover, unless it has been taken into account in the design of an experiment, VMAA may lead to false positive results[556]. Therefore, we developed the VMS assay which quantifies the activity of a volatile on microorganisms in a liquid culture, whereas other vapor-phase assays quantify the antimicrobial activity of the vapor-phase itself[198,534,564]. By determining the *in vitro* growth-inhibitory activity of a large EO(C) collection against well-characterized strains of two pathogenic *Candida* species using the VMS and broth microdilution assay, we generated reliable and directly comparable data on the antimicrobial activity of EO(C)s (figure 6.2a). We found no correlation between iVMAA and MIC (figure 6.2b) which demonstrates that the iVMAA is a valuable additional measure to obtain a more complete picture of the antimicrobial potential of molecules by incorporating volatility and antimicrobial activity. The dissimilarity between MIC and iVMAA was further illustrated by the very low iVMAA shown by EOs rich in phenol methyl ethers and phenol methyl ether EOCs (figure 6.3a), whereas some phenol methyl ethers tested here show potent anti-*Candida* activity in the broth microdilution assay[556]. While most of the EO(C)s that we studied showed VMAA, none of the representatives of each class of antifungals currently used in clinical practice[196] did so, indicating that this characteristic differentiates EO(C)s from currently used classes of antifungals. Furthermore, the high correlation between the iVMAA of EO(C)s against the two *Candida* species tested (figure 6.4a), shows that both microorganisms are generally equally susceptible to EO(C)s. This might reflect a non-specific mode of action, such as membrane destabilization, often ascribed to EO(C)s[490,550]. However, *C. glabrata* showed on average a higher susceptibility to EO(C)s compared to *C. albicans*. While multiple EO(C)s were shown to differentially affect both *Candida* species (figure 6.4b), the EOC citronellal showed the strongest differential activity (figure 6.4b-c). In case the molecular target of citronellal is the same in both *Candida* species, it would thus be more sensitive in *C. glabrata*. The activity of citronellal against *Candida* species has been shown before, and the proposed mode of action is an alteration of membrane homeostasis associated

with decreased ergosterol content[497]. On the other hand, the higher susceptibility of *C. glabrata* might indicate a more specific mode of action. The fact that we could not show differential activity for the related aldehyde citral, which structurally only differs from citronellal by one additional double bond between positions 2 and 3 and is known for its strong antimicrobial activity[531,538], points in the direction of such a specific mode of action.

The VMS assay is very versatile and is only limited by the architecture of standard 96-well microtiter plates. Obvious assay modifications would be (i) altering the size of the volatility-center, which would only imply redefining the categories (*e.g.* for a volatility-center of one well in figure A-III-4a, p. 180), and (ii) testing multiple volatiles in the same microtiter plate (*e.g*. with two volatility-centers of four wells). The latter would for instance allow for the detection of synergies between different antimicrobials acting via their vapor-phase (figure A-III-4b, p. 180). Most of our experiments were performed with two EO(C)s on the same plate and the maximum possible iVMAA that could be measured thus corresponded to category 5.5. The highest iVMAA observed in our experimental set-up was category 4.5, exhibited by the organic EO of *Cinnamomum cassia* of which the anti-*Candida activity* in liquid cultures is well-documented[565-567]. Moreover, (iii) multiple volumes of the same volatile could be tested in parallel to determine the minimal volume necessary to inhibit cell growth in all the wells of category one (*e.g.* with four one well volatility-centers distributed over the microtiter plate in figure A-III-4c, p. 180). By (iv) using standard multi-well plates with a higher number of wells, the resolution could be increased allowing the detection of more subtle differences, and thus a more detailed characterization of the VMAA. The VMS assay was tested extensively using pathogenic fungi. However, it can be used (v) to assess the influence of any volatile on anything that fits into the wells of a microtiter plate and that can be assayed in such a format[197,568-570].

A basic classification of the EO(C)s in our collection revealed that the presence/absence of iVMAA can often be predicted from the chemical class that predominates in the EOs, with aldehyde-, phenol-, monoterpenol-, ether- and ketone-rich EOs showing the highest iVMAA. This was substantiated by a high correlation between the aldehyde content or the monoterpenol linalool content of EOs and iVMAA exhibited by these EOs. Conversely, iVMAA was absent in EOs rich in sesquiterpenols and sesquiterpenes (figure 6.3a). This can partially be explained by the weak anti-*Candida* activity of terpenes in general. However, iVMAA not only reflects antimicrobial activity, but depends greatly on volatility and the aqueous solubility of the bioactive compound(s), which is highly influenced by *e.g.* temperature and duration of the experiment. For example, it is known that phenol methyl ethers, sesquiterpenes and -terpenols show a much lower evaporation than monoterpenes and -terpenoids at 35°C[571].

In conclusion, this study illustrates the potent anti-*Candida* activity of EO(C)s by testing an extended collection of common EOs and EOCs. We demonstrate anti-*Candida* activity of EO(C)s both in liquid cultures and via their vapor-phase, as assessed in the VMS assay. Thanks to the procedural similarities between the VMS and the broth microdilution assays, the former can become a standard assay for the detection of VMA and can complement the latter. Thus, the detection of VMA allows a more complete description of the antimicrobial activity of molecules, thereby boosting the search for new antimicrobials and expanding the application potential of existing ones.

6.4. Materials and methods

6.4.1. Essential oils (EOs), essential oil components (EOCs), antifungals and ethanol.

All EOs (n=175; table A-III-1, p. 163) and all highly enriched EOCs (n=37; table A-III-2, p. 178) were purchased from and certified by Pranarôm International S.A. and Sigma-Aldrich, respectively. Chemical analysis of the EOs was performed by GC-FID using the NF ISO 11024-1/2 standard (list of components present at >10% per EO in table A-III-1, p. 163). All EOs under study are dissimilar *i.e.* originating from different plant parts and/or from (non-)organic cultivation. EOs were considered rich in a component if that component was present at more than 10%. The only EOC that was solid at room temperature (thymol) was dissolved in dimethyl sulfoxide (DMSO; proportion thymol:DMSO 5:1; Sigma-Aldrich) (see table A-III-2, p. 178). Pure DMSO was used as a negative control. All EO(C)s were aliquoted in brown sterile glass vials (Screening Devices), coded to blind the experiments and stored at 4°C. The antifungals caspofungin, fluconazole, terbinafine and 5-flucytosine purchased from and certified by Sigma-Aldrich were dissolved (5 mg/mL) in DMSO, DMSO, methanol (Acros Organics) and Milli-Q® water (Merck Millepore), respectively, and stored at -20°C. The antifungal AmB (Gibco Life Technologies) was dissolved in fungizone (Gibco Life Technologies) at a concentration of 250 µg/mL prior to storage at -20°C. The antiseptic ethanol (Fisher chemical grade) was stored according to the supplier's instructions.

6.4.2. Candida albicans and Candida glabrata.

C. albicans strain SC5314[526], *C. glabrata* strain ATCC 2001™ and four randomly selected clinical isolates from hemocultures of each species were used in this study. All strains were maintained on YPD agar plates (10 g/L yeast extract, 20 g/L bactopeptone, 20 g/L glucose, 15 g/L Difco™ agar) and refreshed weekly. Prior to experiments, the strains were grown overnight at 35°C on 47 g/L Sabouraud agar plates.

6.4.3. Preparation of the cell inocula.

The cell density of a small loop of overnight propagated cells, suspended in 1x phosphate-buffered saline (PBS; 8 g/L sodium chloride, 0.2 g/L potassium chloride, 1.44 g/L disodium hydrogen phosphate, 0.24 g/L potassium dihydrogen phosphate) was estimated by measuring the optical density at 600 nm (OD_{600}). For the illustration of the growth inhibitory VMAA of EO *Litsea citrata* (figure 6.1c), YPD medium (10 g/L yeast extract, 20 g/L bactopeptone, 20 g/L glucose) was used. For all other experiments, the cell suspension was made in Roswell Park Memorial Institute-1640 (RPMI) medium (Sigma-Aldrich), prepared in accordance with CLSI guidelines[197]. Briefly, the medium was buffered with 3-(N-morpholino) propanesulfonic acid (MOPS; Sigma-Aldrich) and filter-sterilized over a 0.20 µm non-pyrogenic Nalgene™ filter (Fisher Scientific).

6.4.4. Vapor-phase-mediated susceptibility assay (VMS assay).

The VMS assay was based on the protocol for the vapor-phase-mediated patch assay described before[556]. In the standard VMS set-up, 200 µL of a 5 x 10^3 cells/mL inoculum was added to all wells of a polystyrene 96-well microtiter plate with U-shaped wells (Greiner Bio-One), except for wells H1 and H12 which served as blanks and contained 200 µL medium. Next, 20 µL of the EO(C) under study was added on top of the cell suspension in wells D/E6-7. Alternatively, when testing the complete EO(C) collection, two EO(C)s were tested per microtiter plate by adding the first one on top of the cell suspension in wells D/E3-4 and the second one on top of the cell suspension in wells D/E9-10. For each run, one microtiter plate without EO(C)s was included as external negative control and one microtiter plate with 2 µL of EOC trans-cinnamaldehyde was added to wells D/E3-4 as a positive control. The microtiter

plates were covered with a lid and statically incubated for 24 hours at 35°C while limiting air draughts. The OD_{600} was measured with a multi-well plate reader (Synergy H1, BioTek Germany) after resuspending the cells. Wells in which growth was visually absent ($OD_{600} \leq 0.07$) or wells with OD_{600} <10% of the OD_{600} of the external control plate (after correcting for the blank) were counted, excluding wells to which the EO(C) was added and blanks, to determine iVMAA and $iVMAA_{90}$, respectively. The resulting number of wells was categorized according to the categories defined in figure 6.1b. To exclude possible interactions between two EO(C)s tested in the same plate, only wells located in columns 1-3 and in columns 10-12 were included, and multiplied by two before categorization. All EO(C)s with an iVMAA larger than zero against at least one of the two *Candida* species were tested three times.

6.4.5. Headspace solid-phase micro-extraction gas chromatography mass spectrometry (HS-SPME-GC-MS).

For the sample preparation, the VMS assay was run for one and 24 hours with 200 µL double-distilled water instead of medium in the wells of the microtiter plate. The content of wells belonging to the same category was pooled and mixed, after which 700 µL was transferred to 10 mL headspace crimp vials (Restek). For SPME sample extraction, a PDMS-coated fiber (100 µm, Supelco Inc.) was used, mounted in a TriPlus RSH autosampler (Thermo Fischer Scientific). The fiber was placed in the headspace of each sample for 10 min, positioned in the agitator and heated to 70°C. Sample desorption occurred in the SSL injection port of the GC at 250°C for 3 min. Before and after sampling, the fiber was inserted in an SPME fiber conditioning station for 5 min for thermal desorption at 250°C. GC-MS analysis was performed using a Trace 1300 Gas Chromatograph (Thermo Fischer Scientific) with a Stabilwax capillary column, 60 m x 0.25 mm i.d. x 0.25 µm f.t. (Restek), coupled to an ISQ QD Single Quadrupole Mass Spectrometer (Thermo Fischer Scientific). Carrier gas: helium 2 mL/min; split ratio: 15; temperature: 35°C for 2 min, then raised from 35 to 215°C at 10°C/min and a 2 min hold at 215°C; transfer line temperature: 250°C; detector temperature: 175°C; mass range: m/z 40−300. For both enantiomers alpha- and beta-citral, response signals were obtained by integration of the peaks in the Total Ion Current channel at 16.98 min and 16.40 min, respectively. The identity of the components was confirmed by comparison of the apex MS spectra to the NIST Mass Spectral Search Program, version 2.0f. As the quantity of analyte extracted by the SPME-fiber is proportional to its concentration in the sample when equilibrium is reached, relative concentrations can be compared to each other.

6.4.6. Broth microdilution assay.

The broth microdilution assay was performed in accordance with the CLSI protocol[197] with few adaptations. Briefly, 100 µL of a 1 x 10^4 cells/mL inoculum was added to all wells of a polystyrene 96-well microtiter plate with U-shaped wells, with the exception of wells serving as blanks to which 200 µL RPMI-MOPS was added. One part of each EO(C) was dissolved in eight parts (v/v) DMSO, after which a two-fold dilution series ranging from 0.25% (v/v) EO(C) to 0.0078% (v/v) EO(C) was prepared in RPMI-MOPS. One hundred µL of each dilution was added to the respective wells with cell suspension, resulting in a final cell concentration of 5 x 10^3 cells/mL and final EO(C) concentrations ranging from 0.125% (v/v) to 0.0039% (v/v). Plates were sealed with an acetate Corning® Cap Mat, and incubated for 24 hours at 35°C. The MIC was determined as the lowest EO(C) concentration required for visually assessed complete growth inhibition.

6.4.7. Statistical analyses.

Statistical analyses were performed using GraphPad Prism version 7.03 and they included all biological repeats. Figures show category-corrected averages (in accordance with figure 6.1a-b) of the biological repeats. A mono-exponential equation (one-phase decay equation), which resulted in the best goodness of fit (adjusted R^2), was used to describe the distribution of EOC citral across the microtiter plate. For correlation analyses the Spearman rank correlation coefficient (ρ) was calculated. The population-wide susceptibility of both *Candida* species to EO(C)s was compared using the Wilcoxon matched-pairs signed rank test. Differentially active EO(C)s were identified using multiple t-tests performed on all EO(C)s with an iVMAA larger than zero against at least one of the species, followed by two methods for post-hoc testing *i.e.* the false discovery rate (FDR) and the statistical significance approach[559,572]. The citronellal susceptibility of five *C. albicans* and five *C. glabrata* strains was compared using the unpaired t-test with Welch's correction.

Acknowledgements

We thank Katrien Lagrou for providing the clinical isolates of the *Candida* species and thank Jean-François Baudoux for his logistical support. This work was supported by grants from the Fund for Scientific Research Flanders (FWO projects WO.009.16 N and G0D4813N).

Author contribution

A.F.F. and L.M. designed the experiments. A.F.F., L.M., K.V.D., L.B. and S.D.G. performed the experiments. A.F.F., L.M., W.L., S.D.G. and P.V.D. contributed to manuscript preparation. P.V.D. supervised the project.

7. General conclusion

7.1. Part I: The murine immune response to subcutaneous *Candida albicans* biofilms

In the first part of this thesis we aimed at elucidating why *C. albicans* biofilms on medical implant devices are not readily cleared by the host immune system. This lack of clearance was demonstrated in the first experiment which showed no difference in *in vivo* biofilm maintenance in the subcutaneous catheter model system between immunocompetent C57BL/6 mice, and mice that received the general immunosuppressant dexamethasone (figure 3.1a-b, p. 57). By using two different experimental approaches, we tried to estimate the contribution of three possible hypotheses in this lack of biofilm clearance (figure 2.1, p. 51): the biofilms are immunologically silent, the biofilms immunomodulate, and/or the biofilms are immunoresistant.

7.1.1. Biofilms on medical implant devices are not immunologically silent

By using the first approach (explained on p. 52-53), we did not observe a biofilm-specific immune response when comparing the immune response in mice with clean catheters implanted (CC) to that in mice with catheters infected by the wild-type *C. albicans* strain CAI4 implanted (CA) (figure 3.5, p. 65 and figure 3.6, p. 66). This result supported our hypothesis of immunological silence, which has also been proposed by Johnson *et al* (2016). They observed reduced NETosis in response to *C. albicans* biofilms compared to planktonic cells, despite the migration of neutrophils into the biofilm surroundings[408]. However, in our experiments, the absence of an immune response observed might be the consequence of our inability to detect an immune response because we were looking in the wrong place rather than being reflective of the complete absence of an immune response. We focused on detecting a systemic immune response, by looking in lymph nodes, spleen and blood, while it is possible that only a local immune response *e.g.* in the tissue surrounding the infected catheter pieces, was present. Such a strategy, in which the immune response in infected tissue is determined, is often applied when working with *C. albicans* infections[387,523,524]. To do so, leukocytes can be isolated from mouse skin by enzymatic digestion and gradient centrifugation. Flow cytometry following this cell-isolation would allow us to interpret a local immune response to the biofilms. The same scenarios as discussed in figure 2.3 (p. 53) would apply to allow discrimination between the different hypotheses. Additionally, tissue surrounding the catheters could be staining to

visualize immune cell infiltration. For the detection of neutrophils, for example, a hematoxylin and eosin (H&E) staining is frequently employed[412,573]. Such a staining would allow us to distinguish a lack of immune response from a lack of immune cell recruitment/infiltration, similar to what was observed by Johnson *et al* (2016).

The subcutaneous model system used (figure 2.2, p. 52) was chosen because it does not cause great discomfort in the mice. Therefore, it can be used to study *in vivo* biofilm formation for a longer period that allows the proper induction of an immune response. However, exactly this limited discomfort afflicted on the mice might also be why we failed to detect a systemic immune response. An alternative model would have been *e.g.* the central venous catheter model system in which a catheter is implanted in the jugular vein of the mice[574]. However, due to its invasive nature, the model is not suitable for long-term experiments. Moreover, a biofilm present in a central venous catheter can seed planktonic *C. albicans* cells via the bloodstream to different organs[574]. This would make it impossible to distinguish between the immune response to the biofilm infection and to the systemic infection. Therefore, the subcutaneous biofilm model system was considered most suitable.

To confirm the hypothesis of immunological silence suggested by the results of the experiments in the first approach, we adopted a second approach with an easier read-out (explained on p. 54). As such, we could confirm the immunization potential of a low i.v. injection and show that also biofilms on subcutaneous catheter pieces could confer such protective immunity (figure 3.9b, p. 71). This clearly demonstrated that biofilms are not immunologically silent.

7.1.2. Biofilms on medical implant devices might be immunoresistant and/or immunomodulating

This leaves the hypotheses of immunoresistance and of immunomodulation, which are possibly not mutually exclusive. In the first approach, we included a *pmr1Δ/pmr1Δ* mutant with an altered ECM and cell wall due to abrogated mannan production, which leads to an increased exposure of β-glucan[155,331]. In concordance with this, we could observe a significant expansion of the CD4+IL-17+ population in lymph nodes in response to biofilms produced by the mutant strain as compared to biofilms produced by the wild-type strain (figure 3.5i, p. 65). Moreover, the size of the CD4+IL-17+ population was negatively correlated with biofilm CFU (figure 3.7b, p. 67). It has been shown before that in a murine systemic infection, cell wall β-glucan gets exposed in kidney-resident *C. albicans* cells in a NET-dependent manner as the infection

progresses[341,342]. Whether such a process is also at play in biofilms is unknown. Our results do not allow us to draw clear conclusion with regards to this phenomenon in biofilms since we only see a limited expansion of the CD4+IL-17+ population in spleen, but not in lymph nodes, between five and 15 days in response to wild-type biofilms (figure 3.5i-j, p. 65). To unequivocally prove such an *in vivo* exposure of β-glucan in biofilms, a more direct approach would be more suitable. For example, β-glucan in biofilms could be stained using a fluorochrome attached to anti-β-glucan antibodies at different time points post-implantation. A similar experimental set-up was employed by Wheeler *et al* (2008).

It is possible that the shielding of β-glucan by mannan in the wild-type biofilm ECM leads to an inefficient immune response, since wild-type biofilms seem to fail at inducing a Th17 expansion, while mutant biofilms do induce such an expansion. This would be similar to the shielding of cell wall β-glucan by mannans which is considered an immune evasion mechanism[100]. While we did find a correlation between the amount of CD4+IL-17+ cells and biofilm CFUs we cannot prove that the expansion of CD4+IL-17+ cells is responsible for the reduced biofilm CFUs because also the ECM and cell wall of the mutant (biofilm) changed drastically. These changes might have made the biofilm-associated cells in mutant biofilms more accessible to host immune cells. Only by assessing the effect of the same amount of CD4+IL-17+ cells on a wild-type biofilm, we would be able to draw conclusions with regards to a possible causative relation. However, experimentally inducing Th17 cell expansion, which could theoretically be done by administrating IL-6 or IL-17, is not applied in practice because unrestrained IL-17 signaling can promote immunopathology[575]. Alternatively, Th17 cells could be ablated by administrating anti-IL-23 antibodies[576] or by using Th17 knockout mice. Using other cell wall or biofilm ECM mutants would be a possibility, but would most likely result in similar issues concerning the interpretation of the data. In case the *in vivo* exposure of β-glucan observed in a systemic infection and discussed above could also be proven for biofilms, this process could be employed to research the role of β-glucan shielding by mannans in biofilms as a means of escaping host immunity. For example, Th17 cell populations could be followed over time, and thus possibly with increasing degrees of β-glucan exposure, in tissue surrounding the biofilms. However, given that we do not see a complete clearance of the biofilm in mice infected by the mutant, the observed expansion of the CD4+IL-17+ population is not enough to completely clear the biofilm, and other mechanisms are likely at play.

Next to the expansion of CD4+IL-17+ cells in response to mutant biofilms (KO), we observed a significantly reduced population of CD4+ cells in response to mutant biofilms, compared to mice that had clean catheters implanted (CC) (figure 3.5a, p. 65). This would indicate that biofilms produced by the mutant strain elicit a lower immune response than surgery, arguing that the mutant biofilm downregulates the immune response. However, a correlation analysis

revealed that the amount of CD4+ cells did not co-vary with biofilm CFU (figure 3.7a, p. 67), and the biological significance of this decrease is thus not clear. Lastly, we observed a significantly reduced splenic population of Foxp3+ Tregs in mice with *pmr1Δ/pmr1Δ* biofilms, compared to mice with wild-type biofilms (figure 3.5l, p. 65). The role of Tregs in *C. albicans* infections is highly niche dependent, with Treg expansion found to be associated with a worse disease outcome in disseminated candidiasis, while it showed to be protective in OPC. In both cases, Treg expansion was associated with expansion of Th17 cells[373,396,522]. However, here we did not observe a correlation between the number of Foxp3+ Tregs and biofilm CFU (data not shown). Together, these changes in immune cell populations in lymph nodes/spleen of mice infected with *pmr1Δ/pmr1Δ* biofilms compared to wild-type biofilms might be considered support for the hypothesis of immunomodulation, with a role for biofilm ECM in the process.

The increased survival (rate) in mice immunized with biofilms is supporting the hypothesis of immunoresistance (figure 3.9b, p. 71). On the other hand, we also observed an overall trend to higher kidney CFUs in mice immunized with a biofilm after the lethal challenge compared to the other two groups. This difference was only confirmed statistically at one time point (figure 3.9c, p. 71). However, given the prolonged survival, these higher kidney CFUs do not seem to be biologically significant. At the end of the experiment, 14 days after the high i.v. challenge, this difference in kidney CFUs was not present anymore. Moreover, we observed significantly lower catheter CFUs in mice immunized with a biofilm that survived until the end of the experiment compared to mice immunized with a biofilm that died over the course of the experiment (figure 3.9d, p. 71). Together these results could be interpreted as support for the hypothesis of immunomodulation, which gets overruled by an immune response to the high i.v. challenge. This “corrected” immune response may then lead to a decreased overall infection burden. The fact that this ‘corrected’ immune response also affects the biofilms, would argue against the hypothesis of immunoresistance.

While protection from the high-dose infection is the key read-out in this experiment, we also took blood at seven-day intervals, to look for signs of immunomodulation in the cytokines in circulation (figure 3.10, p. 73). However, while we do see some differences in cytokine levels between groups overall, none of them clearly point at immunomodulation involving a specific cell type.

Based on all these findings, we cannot rule out the hypothesis of immunoresistance nor the hypothesis of immunomodulation. This possibly indicates that they are both involved. Future experiments could be aimed at further elucidating the role of immune cell populations involved in the process of immunization by subcutaneous biofilms. It has already been shown that Rag1KO mice, which lack cells of the adaptive immune system, can also be immunized with a

low dose i.v. This means that adaptive immunity plays a minor role in the process. Mice lacking monocytes (CCR2KO) could not be immunized, showing the importance of this cell type[457]. Here, we again demonstrated the importance of a mature matrix in biofilm protection from the host immune system and found indications that expansion of the Th17 population might increase host protection against biofilms on medical implant devices. Together, these results provide a general basis for future research, primarily in the role of the biofilm ECM and possibly a downregulation of Th17 cells in the failed clearance of *in vivo* biofilms on medical implant devices. In conclusion, we have shown here for the first time that subcutaneous biofilms can confer protective immunity to a subsequent lethal systemic challenge thereby formally disproving that biofilms are immunologically silent. We do not have enough information to rule out any of the other two hypotheses and consider it possible that both are involved.

7.2. Part II: The vapor-phase-mediated anti-*Candida* activity of essential oils and their components

In the second part of the thesis, we developed a method for the assessment of the vapor-phase-mediated activity (VMA) of bioactive compounds. To this aim, we first introduced the vapor-phase-mediated patch (VMP) assay which allows for the detection of VMA (chapter 5, p. 87). Later, we developed the vapor-phase-mediated susceptibility (VMS) assay, which is a variation of the VMP assay that allows quantification of the VMA (chapter 6, p. 101). To standardize the VMP/VMS assay, its protocol follows the CLSI guidelines for the broth microdilution method for assessment of the MIC as much as possible. Moreover, we used standard 96-well plates and lids to make sure that the distance categories introduced (figure 6.1a-b, p. 105) are widely applicable. The vapor-phase-mediated antimicrobial activity (VMAA) assessed here, is different from the antimicrobial activity in solution commonly quantified by the MIC and often assessed via the broth microdilution method[197], and from the vapor-phase antimicrobial activity that can be detected via *e.g.* the vapor diffusion method[500]. The former was demonstrated by the absence of correlation between MIC and iVMAA as determined in our study (figure 6.2b, p. 106). This is to be expected, considering that iVMAA is defined as the inhibitory activity of a compound in solution at a distance, and integrates the volatility and antimicrobial activity of a compound. We demonstrated in the experiment shown in figure 5.1a (p. 91) that the observed effects are indeed mediated by the vapor-phase, even though the vapor-phase is not directly responsible for the observed effects because they are assessed in solution. The latter implies that the bioactives that travel via their vapor-phase also need to be able to dissolve again in the medium in distant wells. Bioactive compounds that have an antimicrobial activity but are not volatile might show an antimicrobial activity in the broth

microdilution assay at a given concentration, but will not show iVMAA. This was observed for commonly used antifungals.

To characterize the behavior of volatiles in the VMP/VMS assay, we tested the effect of different incubation temperatures and durations, media with a different pH, different plate and lid types, and different means of limiting atmospheric disturbances (data not shown). While we did observe changes in iVMAA values obtained when changing these parameters, changes were mostly limited to one category. Other parameters such as ambient temperature and humidity, and CO_2 concentration during incubation might affect the outcome of the experiment and future experiments could research this influence.

The EO(C)s tested in the VMP/VMS assay were added to the wells of the volatility-center on top of the cell suspension. As such, the contact-surface between EO(C) and the plastic polystyrene of the microtiter plate was reduced, to minimize possible interactions between the plastic and the EO(C)s that were observed in some cases. However, this also implied that the EO(C)s were in contact with an aqueous solution, which is known to reduce the volatility of compounds with hydroxyl groups[577]. Therefore, it might be interesting to test the EO(C)s when added directly to the well. Despite this interaction between EO(C)s and polystyrene, we know that possible reaction-products are not responsible for the observed effects, as we could detect the EOC citral added to the volatility-center in all wells of the multi-well plate using SPME-GC-MS (figure 6.1d, p. 105) and we see similar effects in glass-coated multi-well plates (data not shown).

When testing the complete collection of EO(C)s in the VMS assay, we see absence of iVMAA in EO(C)s that primarily contain phenol methyl ethers, sesquiterpenols and sesquiterpenes (% v/v) (figure 6.3a, p. 109). Possibly, compounds belonging to these classes do not readily evaporate at the experimental temperature[571], inhibit EOCs belonging to other chemical classes from evaporating, and/or cannot dissolve properly in surrounding wells. In the future, it would be interesting to link the physicochemical properties (*e.g.* boiling point and solubility) of the components with the iVMAA observed, and look for parameters that correlate with iVMAA. Given that we do see a link between the chemical classes primarily present and iVMAA, it does seem like this would allow us to make predictions about the iVMAA of EOs of which the chemical composition is known.

Surprisingly, we found that *C. glabrata* was overall more susceptible to the EO(C)s than *C. albicans*. Statistical analyses of the results demonstrated that this differential activity was primarily present for EOs rich in the aldehyde citronellal and the EOC citronellal itself. The physiological relevance of these findings needs to be confirmed using *in vivo* models. An interesting first step would be to use one of the so-called mini-hosts *e.g.* larvae of the waxmoth

Galleria mellonella. In this model, the species to be researched can be injected directly into the haemocoel of the larvae, after which survival of the larvae is followed closely[578]. The model is often considered comparable to the murine systemic infection model[579]. By using different groups of larvae, infected with pathogenicity-controlled doses of either *C. albicans* or *C. glabrata*, a potential therapeutic effect of the EOC citronellal could be assessed. Therefore, the EOC citronellal would have to be injected into the haemocoel of the larvae after infection. Preliminary results obtained by a colleague in the lab show that *G. mellonella* can be used as a model to test the therapeutic effect of EO(C)s. In case the VMAA of citronellal should be tested, the EOC could be dropped onto a cotton swab or into a container present in the petri dishes used to maintain *G. mellonella* and as such evaporate into the surrounding space. It is however not known whether the intra-larval dose of citronellal would get high enough to affect *Candida* survival. The murine model of disseminated candidasis does not seem to work well with *C. glabrata* as mice do not succumb to the infection, even if high amounts of *C. glabrata* CFUs are present in kidneys[580,581]. Of the mouse models for biofilm development on medical implant devices mentioned before for *C. albicans*, the subcutaneous catheter model system[112] and the central venous catheter model system[147] have also been shown to work with *C. glabrata*. Citronellal could then be administered by oral gavage or could possibly be injected subcutaneously after dissolving it in a vegetal oil such as sesame oil. In case the VMAA of citronellal should be tested, the model of OPC could be used after which citronellal could be administered by evaporation using for example a nose cone for the mice. However, it has been shown that *C. glabrata* can only be maintained in the oral niche together with *C. albicans*[186] which might make it difficult to distinguish direct differential activity against *C. glabrata* from indirect effects via *C. albicans*. Of course, in these *in vivo* models, the use of a proper control for citronellal (*e.g.* an EOC that does not show anti-*Candida* activity) should be included.

While we use *Candida* species as a read-out, other biotic and abiotic read-outs are possible. Preliminary experiments with different yeast species, bacteria, *Candida* biofilms and the nematode *Caenorhabditis elegans* were performed in the VMS assay. All tested organisms showed to be susceptible to the VMA of specific EO(C)s (data not shown). A common concern when using EO(C)s in practice, is their toxicity. We do however believe that the VMP/VMS assays introduced here can be adapted to accommodate human cell lines in the multi-well plates, allowing to research toxicity of the tested EO(C)s for example by employing a lactate dehydrogenase assay[582].

In conclusion, we introduce the new VMP/VMS assays to assess the vapor-phase-mediated effects of volatiles. This effect over a distance allows for extended applications as it implies that the volatile bioactives can exert their function in places where they were not directly added.

References

1 Oever, J. T. & Netea, M. G. The bacteriome-mycobiome interaction and antifungal host defense. *Eur J Immunol* **44**, 3182-3191 (2014).

2 Human Microbiome Project, C. Structure, function and diversity of the healthy human microbiome. *Nature* **486**, 207-214 (2012).

3 Underhill, D. M. & Iliev, I. D. The mycobiota: interactions between commensal fungi and the host immune system. *Nat Rev Immunol* **14**, 405-416 (2014).

4 Sung, O. S. B., M.; Kurtzman, C.P.; Lachance, M.-A. Phylogenetics of Saccharomycetales, the ascomycete yeasts. *Mycologia* **98**, 1006-1017 (2006).

5 Butler, G. *et al.* Evolution of pathogenicity and sexual reproduction in eight *Candida* genomes. *Nature* **459**, 657-662 (2009).

6 Kohler, J. R., Casadevall, A. & Perfect, J. The spectrum of fungi that infects humans. *Cold Spring Harb Perspect Med* **5**, a019273 (2014).

7 Pfaller, M. A. & Diekema, D. J. Epidemiology of invasive candidiasis: a persistent public health problem. *Clin Microbiol Rev* **20**, 133-163 (2007).

8 Guinea, J. Global trends in the distribution of *Candida* species causing candidemia. *Clin Microbiol Infect* **20** 5-10 (2014).

9 Kim, G. Y., Jeon, J. S. & Kim, J. K. Isolation Frequency Characteristics of *Candida* Species from Clinical Specimens. *Mycobiology* **44**, 99-104 (2016).

10 Khatib, R., Johnson, L. B., Fakih, M. G., Riederer, K. & Briski, L. Current trends in candidemia and species distribution among adults: *Candida glabrata* surpasses *C. albicans* in diabetic patients and abdominal sources. *Mycoses* **59**(12), 781-786 (2016).

11 Rajendran, R. *et al.* A Prospective Surveillance Study of Candidaemia: Epidemiology, Risk Factors, Antifungal Treatment and Outcome in Hospitalized Patients. *Front Microbiol* **7**, 915 (2016).

12 Quindos, G. Epidemiology of candidaemia and invasive candidiasis. A changing face. *Rev Iberoam Micol* **31**, 42-48 (2014).

13 Trouve, C. *et al.* Epidemiology and reporting of candidaemia in Belgium: a multi-centre study. *Eur J Clin Microbiol Infect Dis* (2016).

14 Hickman, M. A. *et al.* The 'obligate diploid' *Candida albicans* forms mating-competent haploids. *Nature* **494**, 55-59 (2013).

15 Gabaldon, T. & Carrete, L. The birth of a deadly yeast: tracing the evolutionary emergence of virulence traits in *Candida glabrata*. *FEMS Yeast Res* **16**, fov110 (2016).

16 Hull, C. M. & Johnson, A. D. Identification of a mating type-like locus in the asexual pathogenic yeast *Candida albicans*. *Science* **285**, 1271-1275 (1999).

17 Hull, C. M., Raisner, R. M. & Johnson, A. D. Evidence for mating of the "asexual" yeast *Candida albicans* in a mammalian host. *Science* **289**, 307-310 (2000).

18 Magee, B. B. & Magee, P. T. Induction of mating in *Candida albicans* by construction of MTLa and MTLalpha strains. *Science* **289**, 310-313 (2000).

19 Miller, M. G. & Johnson, A. D. White-opaque switching in *Candida albicans* is controlled by mating-type locus homeodomain proteins and allows efficient mating. *Cell* **110**, 293-302 (2002).

20 Schmid, J. *et al.* Last hope for the doomed? Thoughts on the importance of a parasexual cycle for the yeast *Candida albicans*. *Curr Genet* **62**, 81-85 (2016).

21 Ene, I. V. & Bennett, R. J. The cryptic sexual strategies of human fungal pathogens. *Nat Rev Microbiol* **12**, 239-251 (2014).

22 Srikantha, T., Lachke, S. A. & Soll, D. R. Three Mating Type-Like Loci in *Candida glabrata*. *Eukaryotic Cell* **2**, 328-340 (2003).

23 Ghannoum, M. A. *et al.* Characterization of the oral fungal microbiome (mycobiome) in healthy individuals. *PLoS Pathog* **6**, e1000713 (2010).

24 Hoffmann, C. *et al.* Archaea and fungi of the human gut microbiome: correlations with diet and bacterial residents. *PLoS One* **8**, e66019 (2013).

25 Gajer, P. *et al.* Temporal Dynamics of the Human Vaginal Microbiota. *Sci Transl Med* **4** (2012).

26 Koh, A. Y. Gastrointestinal Colonization of Fungi. *Current Fungal Infection Reports* **7**, 144-151 (2013).

27 Gow, N. A., van de Veerdonk, F. L., Brown, A. J. & Netea, M. G. *Candida albicans* morphogenesis and host defence: discriminating invasion from colonization. *Nat Rev Microbiol* **10**, 112-122 (2011).
28 Kim, J. & Sudbery, P. *Candida albicans*, a major human fungal pathogen. *J Microbiol* **49**, 171-177 (2011).
29 Brown, G. D. *et al.* Hidden killers: human fungal infections. *Sci Transl Med* **4**, 165rv113 (2012).
30 Naglik, J. R. R., J. P.; Moyes, D. L. *Candida albicans* pathogenicity and epithelial immunity. *PLoS Pathog* **10** (2014).
31 Jabra-Rizk, M. A. *et al. Candida albicans* Pathogenesis: Fitting within the Host-Microbe Damage Response Framework. *Infect Immun* **84**, 2724-2739 (2016).
32 Fidel, P. L., Jr. *Candida*-host interactions in HIV disease: implications for oropharyngeal candidiasis. *Adv Dent Res* **23**, 45-49 (2011).
33 Fidel, P. L., Jr. Immunity to *Candida*. *Oral disease* **8**(Suppl 2), 69-75 (2002).
34 Peters, B. M., Yano, J., Noverr, M. C. & Fidel, P. L., Jr. *Candida* vaginitis: when opportunism knocks, the host responds. *PLoS Pathog* **10**, e1003965 (2014).
35 Cauchie, M., Desmet, S. & Lagrou, K. *Candida* and its dual lifestyle as a commensal and a pathogen. *Res Microbiol* (2017).
36 Fidel, P. L. *et al.* An Intravaginal Live *Candida* Challenge in Humans Leads to New Hypotheses for the Immunopathogenesis of Vulvovaginal Candidiasis. *Infection and Immunity* **72**, 2939-2946 (2004).
37 Salerno, C. *et al. Candida*-associated denture stomatitis. *Medicina Oral Patología Oral y Cirugia Bucal*, **16**(2), e139-e143 (2011).
38 Lagrou, K. *et al.* Fungemia at a tertiary care hospital: incidence, therapy, and distribution and antifungal susceptibility of causative species. *Eur J Clin Microbiol Infect Dis* **26**, 541-547 (2007).
39 Swinne, D. *et al.* A one-year survey of candidemia in Belgium in 2002. *Epidemiology and Infection* **132**, 1175-1180 (2004).
40 Arendrup, M. C. *et al.* Epidemiological changes with potential implication for antifungal prescription recommendations for fungaemia: data from a nationwide fungaemia surveillance programme. *Clin Microbiol Infect* **19**, E343-353 (2013).
41 Cleveland, A. A. *et al.* Declining incidence of candidemia and the shifting epidemiology of *Candida* resistance in two US metropolitan areas, 2008-2013: results from population-based surveillance. *PLoS One* **10**, e0120452 (2015).
42 Gamaletsou, M. N. *et al.* A prospective, cohort, multicentre study of candidaemia in hospitalized adult patients with haematological malignancies. *Clin Microbiol Infect* **20**, O50-57 (2014).
43 Perlin, D. S., Shor, E. & Zhao, Y. Update on Antifungal Drug Resistance. *Curr Clin Microbiol Rep* **2**, 84-95 (2015).
44 Lehrnbecher, T. *et al.* Trends in the postmortem epidemiology of invasive fungal infections at a university hospital. *J Infect* **61**, 259-265 (2010).
45 Spellberg, B., Ibrahim, A. S., Edwards, J. E., Jr. & Filler, S. G. Mice with disseminated candidiasis die of progressive sepsis. *J Infect Dis* **192**, 336-343 (2005).
46 Duggan, S., Leonhardt, I., Hunniger, K. & Kurzai, O. Host response to *Candida albicans* bloodstream infection and sepsis. *Virulence* **6**, 316-326 (2015).
47 Ramage, G., Martinez, J. P. & Lopez-Ribot, J. L. *Candida* biofilms on implanted biomaterials: a clinically significant problem. *FEMS Yeast Res* **6**, 979-986 (2006).
48 Koh, A. Y., Kohler, J. R., Coggshall, K. T., Van Rooijen, N. & Pier, G. B. Mucosal damage and neutropenia are required for *Candida albicans* dissemination. *PLoS Pathog* **4**, e35 (2008).
49 Andes, D. R. *et al.* Impact of treatment strategy on outcomes in patients with candidemia and other forms of invasive candidiasis: a patient-level quantitative review of randomized trials. *Clin Infect Dis* **54**, 1110-1122 (2012).
50 Cornely, O. A. *et al.* ESCMID* guideline for the diagnosis and management of *Candida* diseases 2012: non-neutropenic adult patients. *Clin Microbiol Infect* **18 Suppl 7**, 19-37 (2012).
51 Cuenca-Estrella, M. *et al.* ESCMID* guideline for the diagnosis and management of *Candida* diseases 2012: diagnostic procedures. *Clin Microbiol Infect* **18 Suppl 7**, 9-18 (2012).
52 Avni, T., Leibovici, L. & Paul, M. PCR diagnosis of invasive candidiasis: systematic review and meta-analysis. *J Clin Microbiol* **49**, 665-670 (2011).
53 Yaman, G., Akyar, I. & Can, S. Evaluation of the MALDI TOF-MS method for identification of *Candida* strains isolated from blood cultures. *Diagn Microbiol Infect Dis* **73**, 65-67 (2012).

54 Polke, M., Hube, B. & Jacobsen, I. D. *Candida* survival strategies. *Adv Appl Microbiol* **91**, 139-235 (2015).

55 Romani, L., Bistoni, F. & Puccetti, P. Adaptation of *Candida albicans* to the host environment: the role of morphogenesis in virulence and survival in mammalian hosts. *Current Opinion in Microbiology* **6**, 338-343 (2003).

56 Berman, J. & Sudbery, P. E. *Candida albicans*: a molecular revolution built on lessons from budding yeast. *Nat Rev Genet* **3**, 918-930 (2002).

57 Sudbery, P., Gow, N. & Berman, J. The distinct morphogenic states of *Candida albicans*. *Trends Microbiol* **12**, 317-324 (2004).

58 Berman, J. Morphogenesis and cell cycle progression in *Candida albicans*. *Curr Opin Microbiol* **9**, 595-601 (2006).

59 Brown, D. H., Jr., Giusani, A. D., Chen, X. & Kumamoto, C. A. Filamentous growth of *Candida albicans* in response to physical environmental cues and its regulation by the unique *CZF1* gene. *Mol Microbiol* **34**, 651-662 (1999).

60 Buffo, J., Herman, M. A. & Soll, D. R. A characterization of pH-regulated dimorphism in *Candida albicans*. *Mycopathologia* **85**, 21-30 (1984).

61 Simonetti, N., Strippoli, V. & Cassone, A. Yeast-mycelial conversion induced by N-acetyl-D-glucosamine in *Candida albicans*. *Nature* **250**, 344-346 (1974).

62 Mardon, D., Balish, E. & Phillips, A. W. Control of dimorphism in a biochemical variant of *Candida albicans*. *J Bacteriol* **100**, 701-707 (1969).

63 Sudbery, P. E. Growth of *Candida albicans* hyphae. *Nat Rev Microbiol* **9**, 737-748 (2011).

64 Hall, R. A. *et al.* CO(2) acts as a signalling molecule in populations of the fungal pathogen *Candida albicans*. *PLoS Pathog* **6**, e1001193 (2010).

65 Hudson, D. A. *et al.* Identification of the dialysable serum inducer of germ-tube formation in *Candida albicans*. *Microbiology* **150**, 3041-3049 (2004).

66 Maidan, M. M. *et al.* The G protein-coupled receptor Gpr1 and the Galpha protein Gpa2 act through the cAMP-protein kinase A pathway to induce morphogenesis in *Candida albicans*. *Mol Biol Cell* **16**, 1971-1986 (2005).

67 Gow, N. A. & Hube, B. Importance of the *Candida albicans* cell wall during commensalism and infection. *Curr Opin Microbiol* **15**, 406-412 (2012).

68 Feng, Q., Summers, E., Guo, B. & Fink, G. Ras signaling is required for serum-induced hyphal differentiation in *Candida albicans*. *J Bacteriol* **181**, 6339-6346 (1999).

69 Stoldt, V. R., Sonneborn, A., Leuker, C. E. & Ernst, J. F. Efg1p, an essential regulator of morphogenesis of the human pathogen *Candida albicans*, is a member of a conserved class of bHLH proteins regulating morphogenetic processes in fungi. *EMBO J* **16**, 1982-1991 (1997).

70 Bockmuhl, D. P. & Ernst, J. F. A potential phosphorylation site for an A-type kinase in the Efg1 regulator protein contributes to hyphal morphogenesis of *Candida albicans*. *Genetics* **157**, 1523-1530 (2001).

71 Sohn, K., Urban, C., Brunner, H. & Rupp, S. *EFG1* is a major regulator of cell wall dynamics in *Candida albicans* as revealed by DNA microarrays. *Mol Microbiol* **47**, 89-102 (2003).

72 Deveau, A., Piispanen, A. E., Jackson, A. A. & Hogan, D. A. Farnesol induces hydrogen peroxide resistance in *Candida albicans* yeast by inhibiting the Ras-cyclic AMP signaling pathway. *Eukaryot Cell* **9**, 569-577 (2010).

73 Hofs, S., Mogavero, S. & Hube, B. Interaction of *Candida albicans* with host cells: virulence factors, host defense, escape strategies, and the microbiota. *J Microbiol* **54**, 149-169 (2016).

74 Shapiro, R. S. *et al.* Hsp90 orchestrates temperature-dependent *Candida albicans* morphogenesis via Ras1-PKA signaling. *Curr Biol* **19**, 621-629 (2009).

75 Liu, H., Kohler, J. & Fink, G. R. Suppression of hyphal formation in *Candida albicans* by mutation of a STE12 homolog. *Science* **266**, 1723-1726 (1994).

76 Eisman, B. *et al.* The Cek1 and Hog1 mitogen-activated protein kinases play complementary roles in cell wall biogenesis and chlamydospore formation in the fungal pathogen *Candida albicans*. *Eukaryot Cell* **5**, 347-358 (2006).

77 Lotz, H., Sohn, K., Brunner, H., Muhlschlegel, F. A. & Rupp, S. *RBR1*, a novel pH-regulated cell wall gene of C*andida albicans*, is repressed by *RIM101* and activated by *NRG1*. *Eukaryot Cell* **3**, 776-784 (2004).

78 Baek, Y. U., Martin, S. J. & Davis, D. A. Evidence for novel pH-dependent regulation of *Candida albicans* Rim101, a direct transcriptional repressor of the cell wall beta-glycosidase Phr2. *Eukaryot Cell* **5**, 1550-1559 (2006).

79 Stichternoth, C. & Ernst, J. F. Hypoxic adaptation by Efg1 regulates biofilm formation by *Candida albicans*. *Appl Environ Microbiol* **75**, 3663-3672 (2009).
80 Stichternoth, C. *et al.* Sch9 kinase integrates hypoxia and CO2 sensing to suppress hyphal morphogenesis in *Candida albicans*. *Eukaryot Cell* **10**, 502-511 (2011).
81 Lu, Y., Su, C., Solis, N. V., Filler, S. G. & Liu, H. Synergistic regulation of hyphal elongation by hypoxia, CO(2), and nutrient conditions controls the virulence of *Candida albicans*. *Cell Host Microbe* **14**, 499-509 (2013).
82 Kadosh, D. & Lopez-Ribot, J. L. *Candida albicans*: adapting to succeed. *Cell Host Microbe* **14**, 483-485 (2013).
83 Shi, Q. M., Wang, Y. M., Zheng, X. D., Lee, R. T. & Wang, Y. Critical role of DNA checkpoints in mediating genotoxic-stress-induced filamentous growth in *Candida albicans*. *Mol Biol Cell* **18**, 815-826 (2007).
84 O'Meara, T. R. *et al.* Global analysis of fungal morphology exposes mechanisms of host cell escape. *Nat Commun* **6**, 6741 (2015).
85 Braun, B. R. & Johnson, A. D. Control of filament formation in *Candida albicans* by the transcriptional repressor *TUP1*. *Science* **277**, 105-109 (1997).
86 Kebaara, B. W. *et al. Candida albicans* Tup1 is involved in farnesol-mediated inhibition of filamentous-growth induction. *Eukaryot Cell* **7**, 980-987 (2008).
87 Braun, B. R., Kadosh, D. & Johnson, A. D. *NRG1*, a repressor of filamentous growth in *C. albicans*, is down-regulated during filament induction. *EMBO J* **20**, 4753-4761 (2001).
88 Khalaf, R. A. & Zitomer, R. S. The DNA binding protein Rfg1 is a repressor of filamentation in *Candida albicans*. *Genetics* **157**, 1503-1512 (2001).
89 Kadosh, D. & Johnson, A. D. Rfg1, a protein related to the *Saccharomyces cerevisiae* hypoxic regulator Rox1, controls filamentous growth and virulence in *Candida albicans*. *Mol Cell Biol* **21**, 2496-2505 (2001).
90 Gow, N. A. Germ tube growth of *Candida albicans*. *Curr Top Med Mycol* **8**, 43-55 (1997).
91 Gow, N. A. *et al.* Investigation of touch-sensitive responses by hyphae of the human pathogenic fungus *Candida albicans*. *Scanning Microsc* **8**, 705-710 (1994).
92 Gow, N. A., Brown, A. J. & Odds, F. C. Fungal morphogenesis and host invasion. *Curr Opin Microbiol* **5**, 366-371 (2002).
93 Park, H. *et al.* Role of the fungal Ras-protein kinase A pathway in governing epithelial cell interactions during oropharyngeal candidiasis. *Cell Microbiol* **7**, 499-510 (2005).
94 da Silva Dantas, A. *et al.* Cell biology of *Candida albicans*-host interactions. *Curr Opin Microbiol* **34**, 111-118 (2016).
95 Hube, B. & Naglik, J. *Candida albicans* proteinases: resolving the mystery of a gene family. *Microbiology* **147**, 1997-2005 (2001).
96 Phan, Q. T. *et al.* Als3 is a *Candida albicans* invasin that binds to cadherins and induces endocytosis by host cells. *PLoS Biol* **5**, e64 (2007).
97 Sun, J. N. *et al.* Host cell invasion and virulence mediated by *Candida albicans* Ssa1. *PLoS Pathog* **6**, e1001181 (2010).
98 Moyes, D. L. *et al.* Candidalysin is a fungal peptide toxin critical for mucosal infection. *Nature* **532**, 64-68 (2016).
99 Wilson, D., Naglik, J. R. & Hube, B. The Missing Link between *Candida albicans* Hyphal Morphogenesis and Host Cell Damage. *PLoS Pathog* **12**, e1005867 (2016).
100 Netea, M. G., Joosten, L. A., van der Meer, J. W., Kullberg, B. J. & van de Veerdonk, F. L. Immune defence against *Candida* fungal infections. *Nat Rev Immunol* **15**, 630-642 (2015).
101 Lo, H. J. *et al.* Nonfilamentous *C. albicans* mutants are avirulent. *Cell* **90**, 939-949 (1997).
102 Davis, M. M. *et al.* Wild-type *Drosophila melanogaster* as a model host to analyze nitrogen source dependent virulence of *Candida albicans*. *PLoS One* **6**, e27434 (2011).
103 Brothers, K. M., Newman, Z. R. & Wheeler, R. T. Live imaging of disseminated candidiasis in zebrafish reveals role of phagocyte oxidase in limiting filamentous growth. *Eukaryot Cell* **10**, 932-944 (2011).
104 Pukkila-Worley, R., Peleg, A. Y., Tampakakis, E. & Mylonakis, E. *Candida albicans* hyphal formation and virulence assessed using a *Caenorhabditis elegans* infection model. *Eukaryot Cell* **8**, 1750-1758 (2009).
105 Braun, B. R., Head, W. S., Wang, M. X. & Johnson, A. D. Identification and characterization of *TUP1*-regulated genes in *Candida albicans*. *Genetics* **156**, 31-44 (2000).
106 Murad, A. M. *et al. NRG1* represses yeast-hypha morphogenesis and hypha-specific gene expression in *Candida albicans*. *EMBO J* **20**, 4742-4752 (2001).

107 Saville, S. P., Lazzell, A. L., Monteagudo, C. & Lopez-Ribot, J. L. Engineered Control of Cell Morphology *In Vivo* Reveals Distinct Roles for Yeast and Filamentous Forms of *Candida albicans* during Infection. *Eukaryotic Cell* **2**, 1053-1060 (2003).

108 Cleary, I. A. *et al.* Examination of the pathogenic potential of *C. albicans* filamentous cells in an animal model of haematogenously disseminated candidiasis. *FEMS Yeast Research* **16**, fow011 (2016).

109 Banerjee, M. *et al. UME6*, a novel filament-specific regulator of *Candida albicans* hyphal extension and virulence. *Mol Biol Cell* **19**, 1354-1365 (2008).

110 Noble, S. M., French, S., Kohn, L. A., Chen, V. & Johnson, A. D. Systematic screens of a *Candida albicans* homozygous deletion library decouple morphogenetic switching and pathogenicity. *Nat Genet* **42**, 590-598 (2010).

111 Spiering, M. J. *et al.* Comparative transcript profiling of *Candida albicans* and *Candida dubliniensis* identifies *SFL2*, a *C. albicans* gene required for virulence in a reconstituted epithelial infection model. *Eukaryot Cell* **9**, 251-265 (2010).

112 Kucharikova, S. *et al. In vivo Candida glabrata* biofilm development on foreign bodies in a rat subcutaneous model. *J Antimicrob Chemother* **70**, 846-856 (2015).

113 Kumamoto, C. A. & Vinces, M. D. Contributions of hyphae and hypha-co-regulated genes to *Candida albicans* virulence. *Cell Microbiol* **7**, 1546-1554 (2005).

114 Jacobsen, I. D. *et al. Candida albicans* dimorphism as a therapeutic target. *Expert Rev Anti Infect Ther* **10**, 85-93 (2012).

115 Sardi, J. C., Scorzoni, L., Bernardi, T., Fusco-Almeida, A. M. & Mendes Giannini, M. J. *Candida* species: current epidemiology, pathogenicity, biofilm formation, natural antifungal products and new therapeutic options. *J Med Microbiol* **62**, 10-24 (2013).

116 Naglik, J. R., Moyes, D. L., Wachtler, B. & Hube, B. *Candida albicans* interactions with epithelial cells and mucosal immunity. *Microbes Infect* **13**, 963-976 (2011).

117 Moyes, D. L., Richardson, J. P. & Naglik, J. R. *Candida albicans*-epithelial interactions and pathogenicity mechanisms: scratching the surface. *Virulence* **6**, 338-346 (2015).

118 Wachtler, B., Wilson, D., Haedicke, K., Dalle, F. & Hube, B. From attachment to damage: defined genes of *Candida albicans* mediate adhesion, invasion and damage during interaction with oral epithelial cells. *PLoS One* **6**, e17046 (2011).

119 Liu, Y. & Filler, S. G. *Candida albicans* Als3, a multifunctional adhesin and invasin. *Eukaryot Cell* **10**, 168-173 (2011).

120 Gaur, N. K. & Klotz, S. A. Expression, cloning, and characterization of a *Candida albicans* gene, *ALA1*, that confers adherence properties upon *Saccharomyces cerevisiae* for extracellular matrix proteins. *Infect Immun* **65**, 5289-5294 (1997).

121 Sheppard, D. C. *et al.* Functional and structural diversity in the Als protein family of *Candida albicans*. *J Biol Chem* **279**, 30480-30489 (2004).

122 Hoyer, L. L. & Cota, E. *Candida albicans* Agglutinin-Like Sequence (Als) Family Vignettes: A Review of Als Protein Structure and Function. *Front Microbiol* **7**, 280 (2016).

123 Cheng, G. *et al.* Comparison between *Candida albicans* agglutinin-like sequence gene expression patterns in human clinical specimens and models of vaginal candidiasis. *Infect Immun* **73**, 1656-1663 (2005).

124 Green, C. B. *et al.* RT-PCR detection of *Candida albicans ALS* gene expression in the reconstituted human epithelium (RHE) model of oral candidiasis and in model biofilms. *Microbiology* **150**, 267-275 (2004).

125 Verstrepen, K. J. & Klis, F. M. Flocculation, adhesion and biofilm formation in yeasts. *Mol Microbiol* **60**, 5-15 (2006).

126 De Las Penas, A. *et al.* Local and regional chromatin silencing in *Candida glabrata*: consequences for adhesion and the response to stress. *FEMS Yeast Res* **15** (2015).

127 Kaur, R., Domergue, R., Zupancic, M. L. & Cormack, B. P. A yeast by any other name: *Candida glabrata* and its interaction with the host. *Curr Opin Microbiol* **8**, 378-384 (2005).

128 Brunke, S. & Hube, B. Two unlike cousins: *Candida albicans* and *C. glabrata* infection strategies. *Cell Microbiol* **15**, 701-708 (2013).

129 Cormack, B. P., Ghori, N. & Falkow, S. An adhesin of the yeast pathogen *Candida glabrata* mediating adherence to human epithelial cells. *Science* **285**, 578-582 (1999).

130 de Groot, P. W., Bader, O., de Boer, A. D., Weig, M. & Chauhan, N. Adhesins in human fungal pathogens: glue with plenty of stick. *Eukaryot Cell* **12**, 470-481 (2013).

131 Costerton, J. W. Overview of microbial biofilms. *J Ind Microbiol* **15**, 137-140 (1995).

132 Hawser, S. P. & Douglas, L. J. Biofilm formation by *Candida* species on the surface of catheter materials *in vitro*. *Infect Immun* **62**, 915-921 (1994).

133 Lohse, M. B. *et al.* Assessment and optimizations of *Candida albicans in vitro* biofilm assays. *Antimicrob Agents Chemother*, Epub ahead of print (2017).
134 Tournu, H. & Van Dijck, P. *Candida* biofilms and the host: models and new concepts for eradication. *Int J Microbiol* **2012** (2012).
135 Andes, D. *et al.* Development and characterization of an *in vivo* central venous catheter *Candida albicans* biofilm model. *Infect Immun* **72**, 6023-6031 (2004).
136 Ricicova, M. *et al. Candida albicans* biofilm formation in a new *in vivo* rat model. *Microbiology* **156**, 909-919 (2010).
137 Chandra, J., Long, L., Ghannoum, M. A. & Mukherjee, P. K. A rabbit model for evaluation of catheter-associated fungal biofilms. *Virulence* **2**, 466-474 (2011).
138 Chandra, J. *et al.* Biofilm formation by the fungal pathogen *Candida albicans*: development, architecture, and drug resistance. *J Bacteriol* **183**, 5385-5394 (2001).
139 Blankenship, J. R. & Mitchell, A. P. How to build a biofilm: a fungal perspective. *Curr Opin Microbiol* **9**, 588-594 (2006).
140 Uppuluri, P. *et al.* Dispersion as an important step in the *Candida albicans* biofilm developmental cycle. *PLoS Pathog* **6**, e1000828 (2010).
141 Kaneko, Y. *et al.* Real-Time Microscopic Observation of *Candida* Biofilm Development and Effects Due to Micafungin and Fluconazole. *Antimicrobial Agents and Chemotherapy* **57**, 2226-2230 (2013).
142 Baillie, G. S. & Douglas, L. J. Effect of growth rate on resistance of *Candida albicans* biofilms to antifungal agents. *Antimicrob Agents Chemother* **42**, 1900-1905 (1998).
143 Baillie, G. S. & Douglas, L. J. Matrix polymers of *Candida* biofilms and their possible role in biofilm resistance to antifungal agents. *J Antimicrob Chemother* **46**, 397-403 (2000).
144 Baillie, G. S. & Douglas, L. J. *Candida* biofilms and their susceptibility to antifungal agents. *Methods in enzymology* **310**, 644-656 (1999).
145 Watnick, P. & Kolter, R. Biofilm, city of microbes. *J Bacteriol* **182**, 2675-2679 (2000).
146 Douglas, L. J. *Candida* biofilms and their role in infection. *Trends in Microbiology* **11**, 30-36 (2003).
147 Nett, J., Lincoln, L., Marchillo, K. & Andes, D. Beta -1,3 glucan as a test for central venous catheter biofilm infection. *J Infect Dis* **195**, 1705-1712 (2007).
148 Paulitsch, A. H. *et al. In vivo Candida* biofilms in scanning electron microscopy. *Med Mycol* **47**, 690-696 (2009).
149 Silva, S. *et al.* Biofilms of non-*Candida albicans Candida* species: quantification, structure and matrix composition. *Med Mycol* **47**, 681-689 (2009).
150 Hawser, S. P., Baillie, G. S. & Douglas, L. J. Production of extracellular matrix by *Candida albicans* biofilms. *J Med Microbiol* **47**, 253-256 (1998).
151 Al-Fattani, M. A. & Douglas, L. J. Biofilm matrix of *Candida albicans* and *Candida tropicalis*: chemical composition and role in drug resistance. *J Med Microbiol* **55**, 999-1008 (2006).
152 Lal, P., Sharma, D., Pruthi, P. & Pruthi, V. Exopolysaccharide analysis of biofilm-forming *Candida albicans*. *J Appl Microbiol* **109**, 128-136 (2010).
153 Zarnowski, R. *et al.* Novel entries in a fungal biofilm matrix encyclopedia. *MBio* **5**, e01333-01314 (2014).
154 Mitchell, K. F., Zarnowski, R. & Andes, D. R. The Extracellular Matrix of Fungal Biofilms. *Adv Exp Med Biol* **931**, 21-35 (2016).
155 Mitchell, K. F. *et al.* Community participation in biofilm matrix assembly and function. *Proc Natl Acad Sci U S A* **112**, 4092-4097 (2015).
156 Martinez-Gomariz, M. *et al.* Proteomic analysis of cytoplasmic and surface proteins from yeast cells, hyphae, and biofilms of *Candida albicans*. *Proteomics* **9**, 2230-2252 (2009).
157 Nett, J. E. *et al.* Host contributions to construction of three device-associated *Candida albicans* biofilms. *Infect Immun* **83**, 4630-4638 (2015).
158 Garcia-Sanchez, S. *et al. Candida albicans* Biofilms: a Developmental State Associated With Specific and Stable Gene Expression Patterns. *Eukaryotic Cell* **3**, 536-545 (2004).
159 Murillo, L. A. *et al.* Genome-wide transcription profiling of the early phase of biofilm formation by *Candida albicans*. *Eukaryot Cell* **4**, 1562-1573 (2005).
160 Bonhomme, J. *et al.* Contribution of the glycolytic flux and hypoxia adaptation to efficient biofilm formation by *Candida albicans*. *Mol Microbiol* **80**, 995-1013 (2011).
161 Nobile, C. J. *et al.* A recently evolved transcriptional network controls biofilm development in *Candida albicans*. *Cell* **148**, 126-138 (2012).
162 Nett, J. E., Lepak, A. J., Marchillo, K. & Andes, D. R. Time course global gene expression analysis of an *in vivo Candida* biofilm. *J Infect Dis* **200**, 307-313 (2009).

163 Fanning, S. *et al.* Divergent targets of *Candida albicans* biofilm regulator Bcr1 *in vitro* and *in vivo*. *Eukaryot Cell* **11**, 896-904 (2012).

164 Fox, E. P. *et al.* An expanded regulatory network temporally controls *Candida albicans* biofilm formation. *Mol Microbiol* **96**, 1226-1239 (2015).

165 Yeater, K. M. *et al.* Temporal analysis of *Candida albicans* gene expression during biofilm development. *Microbiology* **153**, 2373-2385 (2007).

166 Nobile, C. J. & Johnson, A. D. *Candida albicans* Biofilms and Human Disease. *Annu Rev Microbiol* **69**, 71-92 (2015).

167 Davies, D. Understanding biofilm resistance to antibacterial agents. *Nat Rev Drug Discov* **2**, 114-122 (2003).

168 Cos, P., Tote, K., Horemans, T. & Maes, L. Biofilms: an extra hurdle for effective antimicrobial therapy. *Curr Pharm Des* **16**, 2279-2295 (2010).

169 Gulati, M. & Nobile, C. J. *Candida albicans* biofilms: development, regulation, and molecular mechanisms. *Microbes Infect* **18**, 310-321 (2016).

170 Koehler, P., Tacke, D. & Cornely, O. A. Our 2014 approach to candidaemia. *Mycoses* **57**, 581-583 (2014).

171 Silva, S., Henriques, M., Oliveira, R., Williams, D. & Azeredo, J. *In Vitro* Biofilm Activity of Non-*Candida albicans Candida* Species. *Current Microbiology* **61**, 534-540 (2010).

172 Shin, J. H. *et al.* Biofilm Production by Isolates of *Candida* Species Recovered from Nonneutropenic Patients: Comparison of Bloodstream Isolates with Isolates from Other Sources. *Journal of Clinical Microbiology* **40**, 1244-1248 (2002).

173 Rajendran, R. *et al.* Biofilm formation is a risk factor for mortality in patients with *Candida albicans* bloodstream infection-Scotland, 2012-2013. *Clin Microbiol Infect* **22**, 87-93 (2016).

174 Tumbarello, M. *et al.* Biofilm production by *Candida* species and inadequate antifungal therapy as predictors of mortality for patients with candidemia. *J Clin Microbiol* **45**, 1843-1850 (2007).

175 Guembe, M. *et al.* Is biofilm production a predictor of catheter-related candidemia? *Med Mycol* **52**, 407-410 (2014).

176 Sherry, L. *et al.* Biofilms formed by *Candida albicans* bloodstream isolates display phenotypic and transcriptional heterogeneity that are associated with resistance and pathogenicity. *BMC Microbiol* **14**, 182 (2014).

177 Pannanusorn, S., Fernandez, V. & Romling, U. Prevalence of biofilm formation in clinical isolates of *Candida* species causing bloodstream infection. *Mycoses* **56**, 264-272 (2013).

178 Rajendran, R. *et al.* Integrating *Candida albicans* metabolism with biofilm heterogeneity by transcriptome mapping. *Sci Rep* **6**, 35436 (2016).

179 Klotz, S. A., Chasin, B. S., Powell, B., Gaur, N. K. & Lipke, P. N. Polymicrobial bloodstream infections involving *Candida* species: analysis of patients and review of the literature. *Diagnostic Microbiology and Infectious Disease* **59**, 401-406 (2007).

180 Nace, H. L., Horn, D. & Neofytos, D. Epidemiology and outcome of multiple-species candidemia at a tertiary care center between 2004 and 2007. *Diagn Microbiol Infect Dis* **64**, 289-294 (2009).

181 Harriott, M. M., Lilly, E. A., Rodriguez, T. E., Fidel, P. L., Jr. & Noverr, M. C. *Candida albicans* forms biofilms on the vaginal mucosa. *Microbiology* **156**, 3635-3644 (2010).

182 Bouza, E. *et al.* Mixed bloodstream infections involving bacteria and *Candida* spp. *J Antimicrob Chemother* **68**, 1881-1888 (2013).

183 Forster, T. M. *et al.* Enemies and brothers in arms: *Candida albicans* and gram-positive bacteria. *Cell Microbiol* (2016).

184 Shirtliff, M. E., Peters, B. M. & Jabra-Rizk, M. A. Cross-kingdom interactions: *Candida albicans* and bacteria. *FEMS Microbiol Lett* **299**, 1-8 (2009).

185 Beaussart, A. *et al.* Single-cell force spectroscopy of the medically important *Staphylococcus epidermidis-Candida albicans* interaction. *Nanoscale* **5**, 10894-10900 (2013).

186 Tati, S. *et al. Candida glabrata* Binding to *Candida albicans* Hyphae Enables Its Development in Oropharyngeal Candidiasis. *PLoS Pathog* **12**, e1005522 (2016).

187 De Brucker, K. *et al.* Fungal beta-1,3-glucan increases ofloxacin tolerance of *Escherichia coli* in a polymicrobial *E. coli*/*Candida albicans* biofilm. *Antimicrob Agents Chemother* **59**, 3052-3058 (2015).

188 Kong, E. F. *et al.* Commensal Protection of *Staphylococcus aureus* against Antimicrobials by *Candida albicans* Biofilm Matrix. *MBio* **7** (2016).

189 Barbosa, J. O. *et al. Streptococcus mutans* Can Modulate Biofilm Formation and Attenuate the Virulence of *Candida albicans*. *PLoS One* **11**, e0150457 (2016).

190 Donlan, R. M. & Costerton, J. W. Biofilms: Survival Mechanisms of Clinically Relevant Microorganisms. *Clinical Microbiology Reviews* **15**, 167-193 (2002).
191 Hawser, S. P. & Douglas, L. J. Resistance of *Candida albicans* biofilms to antifungal agents *in vitro*. *Antimicrob Agents Chemother* **39**, 2128-2131 (1995).
192 Ramage, G., Vande Walle, K., Wickes, B. L. & Lopez-Ribot, J. L. Standardized method for *in vitro* antifungal susceptibility testing of *Candida albicans* biofilms. *Antimicrob Agents Chemother* **45**, 2475-2479 (2001).
193 Lewis, R. E., Kontoyiannis, D. P., Darouiche, R. O., Raad, II & Prince, R. A. Antifungal activity of amphotericin B, fluconazole, and voriconazole in an *in vitro* model of *Candida* catheter-related bloodstream infection. *Antimicrob Agents Chemother* **46**, 3499-3505 (2002).
194 Yi, S. *et al.* Alternative mating type configurations (a/alpha versus a/a or alpha/alpha) of *Candida albicans* result in alternative biofilms regulated by different pathways. *PLoS Biol* **9**, e1001117 (2011).
195 Rodrigues, C. F., Silva, S. & Henriques, M. *Candida glabrata*: a review of its features and resistance. *Eur J Clin Microbiol Infect Dis* **33**, 673-688 (2014).
196 Sanglard, D. Emerging Threats in Antifungal-Resistant Fungal Pathogens. *Front Med (Lausanne)* **3**, 11 (2016).
197 CLSI. Reference Method for Broth Dilution Antifungal Susceptibility Testing of Yeasts; Fourth Informational Supplement. *CLSI document M27-S4. Wayne, PA: Clinical and Laboratory Standards Institute* (2012).
198 Balouiri, M., Sadiki, M. & Ibnsouda, S. K. Methods for *in vitro* evaluating antimicrobial activity: A review. *Journal of Pharmaceutical Analysis* **6**, 71-79 (2016).
199 Anderson, J. B. Evolution of antifungal-drug resistance: mechanisms and pathogen fitness. *Nat Rev Microbiol* **3**, 547-556 (2005).
200 EUCAST. Breakpoint tables for interpretation of MICs and zone diameters, version 8.1. http://www.eucast.org/fileadmin/src/media/PDFs/EUCAST_files/AFST/Clinical_breakpoints/Antifungal_breakpoints_v_8.1_March_2017.pdf (2017).
201 Ramage, G. Comparing apples and oranges: considerations for quantifying candidal biofilms with XTT [2,3-bis(2-methoxy-4-nitro-5-sulfo-phenyl)-2H-tetrazolium-5-carboxanilide] and the need for standardized testing. *J Med Microbiol* **65**, 259-260 (2016).
202 Walraven, C. J. & Lee, S. A. Antifungal lock therapy. *Antimicrob Agents Chemother* **57**, 1-8 (2013).
203 Kucharikova, S., Tournu, H., Holtappels, M., Van Dijck, P. & Lagrou, K. *In vivo* efficacy of anidulafungin against mature *Candida albicans* biofilms in a novel rat model of catheter-associated Candidiasis. *Antimicrob Agents Chemother* **54**, 4474-4475 (2010).
204 Kucharikova, S. *et al.* Activities of systemically administered echinocandins against *in vivo* mature *Candida albicans* biofilms developed in a rat subcutaneous model. *Antimicrob Agents Chemother* **57**, 2365-2368 (2013).
205 Meletiadis, J., Curfs-Breuker, I., Meis, J. F. & Mouton, J. W. *In vitro* antifungal susceptibility testing of *Candida* isolates with the EUCAST methodology. *Antimicrob Agents Chemother* (2017).
206 Whaley, S. G. *et al.* Azole Antifungal Resistance in *Candida albicans* and Emerging Non-*albicans Candida* Species. *Front Microbiol* **7**, 2173 (2016).
207 Perlin, D. S. Mechanisms of echinocandin antifungal drug resistance. *Ann N Y Acad Sci* **1354**, 1-11 (2015).
208 Alexander, B. D. *et al.* Increasing echinocandin resistance in *Candida glabrata*: clinical failure correlates with presence of *FKS* mutations and elevated minimum inhibitory concentrations. *Clin Infect Dis* **56**, 1724-1732 (2013).
209 Hill, J. A., O'Meara, T. R. & Cowen, L. E. Fitness Trade-Offs Associated with the Evolution of Resistance to Antifungal Drug Combinations. *Cell Rep* **10**(5), 809-819 (2015).
210 Davis, S. A. *et al.* Nontoxic antimicrobials that evade drug resistance. *Nat Chem Biol* **11**, 481-487 (2015).
211 Vincent, B. M., Lancaster, A. K., Scherz-Shouval, R., Whitesell, L. & Lindquist, S. Fitness trade-offs restrict the evolution of resistance to amphotericin B. *PLoS Biol* **11**, e1001692 (2013).
212 Volmer, A. A., Szpilman, A. M. & Carreira, E. M. Synthesis and biological evaluation of amphotericin B derivatives. *Nat Prod Rep* **27**, 1329-1349 (2010).
213 Bachmann, S. P. *et al. In Vitro* Activity of Caspofungin against *Candida albicans* Biofilms. *Antimicrobial Agents and Chemotherapy* **46**, 3591-3596 (2002).

214 Ramage, G., VandeWalle, K., Bachmann, S. P., Wickes, B. L. & Lopez-Ribot, J. L. *In vitro* pharmacodynamic properties of three antifungal agents against preformed *Candida albicans* biofilms determined by time-kill studies. *Antimicrob Agents Chemother* **46**, 3634-3636 (2002).
215 Kuhn, D. M., George, T., Chandra, J., Mukherjee, P. K. & Ghannoum, M. A. Antifungal Susceptibility of *Candida* Biofilms: Unique Efficacy of Amphotericin B Lipid Formulations and Echinocandins. *Antimicrobial Agents and Chemotherapy* **46**, 1773-1780 (2002).
216 Ramage, G. *et al.* Liposomal amphotericin B displays rapid dose-dependent activity against *Candida albicans* biofilms. *Antimicrob Agents Chemother* **57**, 2369-2371 (2013).
217 Mukherjee, P. K., Long, L., Kim, H. G. & Ghannoum, M. A. Amphotericin B lipid complex is efficacious in the treatment of *Candida albicans* biofilms using a model of catheter-associated *Candida* biofilms. *Int J Antimicrob Agents* **33**, 149-153 (2009).
218 Perumal, P., Mekala, S. & Chaffin, W. L. Role for cell density in antifungal drug resistance in *Candida albicans* biofilms. *Antimicrob Agents Chemother* **51**, 2454-2463 (2007).
219 Seneviratne, C. J., Jin, L. & Samaranayake, L. P. Biofilm lifestyle of *Candida*: a mini review. *Oral diseases* **14**, 582-590 (2008).
220 White, T. C. The presence of an R467K amino acid substitution and loss of allelic variation correlate with an azole-resistant lanosterol 14alpha demethylase in *Candida albicans*. *Antimicrob Agents Chemother* **41**, 1488-1494 (1997).
221 Chau, A. S. *et al.* Inactivation of sterol Delta5,6-desaturase attenuates virulence in *Candida albicans*. *Antimicrob Agents Chemother* **49**, 3646-3651 (2005).
222 Hope, W. W., Tabernero, L., Denning, D. W. & Anderson, M. J. Molecular mechanisms of primary resistance to flucytosine in *Candida albicans*. *Antimicrob Agents Chemother* **48**, 4377-4386 (2004).
223 Sanglard, D. *et al.* Mechanisms of resistance to azole antifungal agents in *Candida albicans* isolates from AIDS patients involve specific multidrug transporters. *Antimicrob Agents Chemother* **39**, 2378-2386 (1995).
224 Sanglard, D., Ischer, F., Monod, M. & Bille, J. Cloning of *Candida albicans* genes conferring resistance to azole antifungal agents: characterization of *CDR2*, a new multidrug ABC transporter gene. *Microbiology* **143 (Pt 2)**, 405-416 (1997).
225 Nett, J. E., Sanchez, H., Cain, M. T. & Andes, D. R. Genetic basis of *Candida* biofilm resistance due to drug-sequestering matrix glucan. *J Infect Dis* **202**, 171-175 (2010).
226 Selmecki, A., Forche, A. & Berman, J. Aneuploidy and isochromosome formation in drug-resistant *Candida albicans*. *Science* **313**, 367-370 (2006).
227 Borecka-Melkusova, S. *et al.* The expression of genes involved in the ergosterol biosynthesis pathway in *Candida albicans* and *Candida dubliniensis* biofilms exposed to fluconazole. *Mycoses* **52**, 118-128 (2009).
228 Nailis, H. *et al.* Real-time PCR expression profiling of genes encoding potential virulence factors in *Candida albicans* biofilms: identification of model-dependent and -independent gene expression. *BMC Microbiol* **10**, 114 (2010).
229 LaFleur, M. D., Kumamoto, C. A. & Lewis, K. *Candida albicans* biofilms produce antifungal-tolerant persister cells. *Antimicrob Agents Chemother* **50**, 3839-3846 (2006).
230 Diez-Orejas, R. *et al.* Reduced virulence of *Candida albicans MKC1* mutants: a role for mitogen-activated protein kinase in pathogenesis. *Infect Immun* **65**, 833-837 (1997).
231 Kumamoto, C. A. A contact-activated kinase signals *Candida albicans* invasive growth and biofilm development. *Proc Natl Acad Sci U S A* **102**, 5576-5581 (2005).
232 Lamb, D. C., Kelly, D. E., White, T. C. & Kelly, S. L. The R467K amino acid substitution in *Candida albicans* sterol 14alpha-demethylase causes drug resistance through reduced affinity. *Antimicrob Agents Chemother* **44**, 63-67 (2000).
233 Flowers, S. A., Colon, B., Whaley, S. G., Schuler, M. A. & Rogers, P. D. Contribution of clinically derived mutations in *ERG11* to azole resistance in *Candida albicans*. *Antimicrob Agents Chemother* **59**, 450-460 (2015).
234 Xu, Y., Chen, L. & Li, C. Susceptibility of clinical isolates of *Candida* species to fluconazole and detection of *Candida albicans ERG11* mutations. *J Antimicrob Chemother* **61**, 798-804 (2008).
235 Sanglard, D. & Coste, A. T. Activity of Isavuconazole and Other Azoles against *Candida* Clinical Isolates and Yeast Model Systems with Known Azole Resistance Mechanisms. *Antimicrob Agents Chemother* **60**, 229-238 (2015).
236 Morio, F., Pagniez, F., Lacroix, C., Miegeville, M. & Le Pape, P. Amino acid substitutions in the *Candida albicans* sterol Delta5,6-desaturase (Erg3p) confer azole resistance:

characterization of two novel mutants with impaired virulence. *J Antimicrob Chemother* **67**, 2131-2138 (2012).
237 Edlind, T. D. & Katiyar, S. K. Mutational analysis of flucytosine resistance in *Candida glabrata*. *Antimicrob Agents Chemother* **54**, 4733-4738 (2010).
238 Shields, R. K. *et al.* The presence of an *FKS* mutation rather than MIC is an independent risk factor for failure of echinocandin therapy among patients with invasive candidiasis due to *Candida glabrata*. *Antimicrob Agents Chemother* **56**, 4862-4869 (2012).
239 Katiyar, S., Pfaller, M. & Edlind, T. *Candida albicans* and *Candida glabrata* clinical isolates exhibiting reduced echinocandin susceptibility. *Antimicrob Agents Chemother* **50**, 2892-2894 (2006).
240 Lackner, M. *et al.* Positions and numbers of *FKS* mutations in *Candida albicans* selectively influence *in vitro* and *in vivo* susceptibilities to echinocandin treatment. *Antimicrob Agents Chemother* **58**, 3626-3635 (2014).
241 Tsui, C., Kong, E. F. & Jabra-Rizk, M. A. Pathogenesis of *Candida albicans* biofilm. *Pathog Dis* **74**, ftw018 (2016).
242 Calabrese, D., Bille, J. & Sanglard, D. A novel multidrug efflux transporter gene of the major facilitator superfamily from *Candida albicans* (*FLU1*) conferring resistance to fluconazole. *Microbiology* **146 (Pt 11)**, 2743-2754 (2000).
243 Soto, S. M. Role of efflux pumps in the antibiotic resistance of bacteria embedded in a biofilm. *Virulence* **4**, 223-229 (2013).
244 Fling, M. E. *et al.* Analysis of a *Candida albicans* gene that encodes a novel mechanism for resistance to benomyl and methotrexate. *Mol Gen Genet* **227**, 318-329 (1991).
245 Prasad, R., De Wergifosse, P., Goffeau, A. & Balzi, E. Molecular cloning and characterization of a novel gene of *Candida albicans*, *CDR1*, conferring multiple resistance to drugs and antifungals. *Curr Genet* **27**, 320-329 (1995).
246 Marger, M. D. & Saier, M. H., Jr. A major superfamily of transmembrane facilitators that catalyse uniport, symport and antiport. *Trends Biochem Sci* **18**, 13-20 (1993).
247 Ben-Yaacov, R., Knoller, S., Caldwell, G. A., Becker, J. M. & Koltin, Y. *Candida albicans* gene encoding resistance to benomyl and methotrexate is a multidrug resistance gene. *Antimicrob Agents Chemother* **38**, 648-652 (1994).
248 Sanglard, D., Ischer, F., Monod, M. & Bille, J. Susceptibilities of *Candida albicans* multidrug transporter mutants to various antifungal agents and other metabolic inhibitors. *Antimicrob Agents Chemother* **40**, 2300-2305 (1996).
249 Bhattacharya, S., Sobel, J. D. & White, T. C. A Combination Fluorescence Assay Demonstrates Increased Efflux Pump Activity as a Resistance Mechanism in Azole-Resistant Vaginal *Candida albicans* Isolates. *Antimicrob Agents Chemother* **60**, 5858-5866 (2016).
250 White, T. C., Holleman, S., Dy, F., Mirels, L. F. & Stevens, D. A. Resistance Mechanisms in Clinical Isolates of *Candida albicans*. *Antimicrobial Agents and Chemotherapy* **46**, 1704-1713 (2002).
251 Wirsching, S., Michel, S. & Morschhauser, J. Targeted gene disruption in *Candida albicans* wild-type strains: the role of the *MDR1* gene in fluconazole resistance of clinical *Candida albicans* isolates. *Mol Microbiol* **36**, 856-865 (2000).
252 Coste, A. T., Karababa, M., Ischer, F., Bille, J. & Sanglard, D. *TAC1*, transcriptional activator of *CDR* genes, is a new transcription factor involved in the regulation of *Candida albicans* ABC transporters *CDR1* and *CDR2*. *Eukaryot Cell* **3**, 1639-1652 (2004).
253 Coste, A. *et al.* A mutation in Tac1p, a transcription factor regulating *CDR1* and *CDR2*, is coupled with loss of heterozygosity at chromosome 5 to mediate antifungal resistance in *Candida albicans*. *Genetics* **172**, 2139-2156 (2006).
254 Ferrari, S. *et al.* Gain of function mutations in Cg*PDR1* of *Candida glabrata* not only mediate antifungal resistance but also enhance virulence. *PLoS Pathog* **5**, e1000268 (2009).
255 Mukherjee, P. K., Chandra, J., Kuhn, D. M. & Ghannoum, M. A. Mechanism of Fluconazole Resistance in *Candida albicans* Biofilms: Phase-Specific Role of Efflux Pumps and Membrane Sterols. *Infection and Immunity* **71**, 4333-4340 (2003).
256 Mateus, C., Crow, S. A., Jr. & Ahearn, D. G. Adherence of *Candida albicans* to silicone induces immediate enhanced tolerance to fluconazole. *Antimicrob Agents Chemother* **48**, 3358-3366 (2004).
257 Niimi, K. *et al.* Overexpression of *Candida albicans CDR1*, *CDR2*, or *MDR1* does not produce significant changes in echinocandin susceptibility. *Antimicrob Agents Chemother* **50**, 1148-1155 (2006).

258 Song, J. W. *et al.* Expression of *CgCDR1*, *CgCDR2*, and *CgERG11* in *Candida glabrata* biofilms formed by bloodstream isolates. *Med Mycol* **47**, 545-548 (2009).

259 Lepak, A., Nett, J., Lincoln, L., Marchillo, K. & Andes, D. Time course of microbiologic outcome and gene expression in *Candida albicans* during and following *in vitro* and *in vivo* exposure to fluconazole. *Antimicrob Agents Chemother* **50**, 1311-1319 (2006).

260 Forche, A. *et al.* Stress alters rates and types of loss of heterozygosity in *Candida albicans*. *MBio* **2** (2011).

261 Coste, A. *et al.* Genotypic evolution of azole resistance mechanisms in sequential *Candida albicans* isolates. *Eukaryot Cell* **6**, 1889-1904 (2007).

262 Suwunnakorn, S., Wakabayashi, H. & Rustchenko, E. Chromosome 5 of human pathogen *Candida albicans* carries multiple genes for negative control of caspofungin and anidulafungin susceptibility. *Antimicrob Agents Chemother* **60**(12), 7457-7467 (2016).

263 Yang, F., Kravets, A., Bethlendy, G., Welle, S. & Rustchenko, E. Chromosome 5 monosomy of *Candida albicans* controls susceptibility to various toxic agents, including major antifungals. *Antimicrob Agents Chemother* **57**, 5026-5036 (2013).

264 Polakova, S. *et al.* Formation of new chromosomes as a virulence mechanism in yeast *Candida glabrata*. *Proc Natl Acad Sci U S A* **106**, 2688-2693 (2009).

265 Dunkel, N. *et al.* A gain-of-function mutation in the transcription factor Upc2p causes upregulation of ergosterol biosynthesis genes and increased fluconazole resistance in a clinical *Candida albicans* isolate. *Eukaryot Cell* **7**, 1180-1190 (2008).

266 Yu, L. H., Wei, X., Ma, M., Chen, X. J. & Xu, S. B. Possible inhibitory molecular mechanism of farnesol on the development of fluconazole resistance in *Candida albicans* biofilm. *Antimicrob Agents Chemother* **56**, 770-775 (2012).

267 Vediyappan, G., Rossignol, T. & d'Enfert, C. Interaction of *Candida albicans* biofilms with antifungals: transcriptional response and binding of antifungals to beta-glucans. *Antimicrob Agents Chemother* **54**, 2096-2111 (2010).

268 Uppuluri, P., Srinivasan, A., Ramasubramanian, A. & Lopez-Ribot, J. L. Effects of fluconazole, amphotericin B, and caspofungin on *Candida albicans* biofilms under conditions of flow and on biofilm dispersion. *Antimicrob Agents Chemother* **55**, 3591-3593 (2011).

269 Uppuluri, P., Chaturvedi, A. K. & Lopez-Ribot, J. L. Design of a Simple Model of *Candida albicans* Biofilms Formed under Conditions of Flow: Development, Architecture, and Drug Resistance. *Mycopathologia* **168**, 101 (2009).

270 Keren, I., Shah, D., Spoering, A., Kaldalu, N. & Lewis, K. Specialized persister cells and the mechanism of multidrug tolerance in *Escherichia coli*. *J Bacteriol* **186**, 8172-8180 (2004).

271 Lewis, K. Persister cells. *Annu Rev Microbiol* **64**, 357-372 (2010).

272 Lewis, L. E. *et al.* Stage specific assessment of *Candida albicans* phagocytosis by macrophages identifies cell wall composition and morphogenesis as key determinants. *PLoS Pathog* **8**, e1002578 (2012).

273 Bigger, J. W. Treatment of staphylococcal infections with penicillin by intermittent sterilisation. *The Lancet* **244**, 497-500 (1944).

274 Spoering, A. L. & Lewis, K. Biofilms and planktonic cells of *Pseudomonas aeruginosa* have similar resistance to killing by antimicrobials. *J Bacteriol* **183**, 6746-6751 (2001).

275 Harrison, J. J. *et al.* The chromosomal toxin gene *yafQ* is a determinant of multidrug tolerance for *Escherichia coli* growing in a biofilm. *Antimicrob Agents Chemother* **53**, 2253-2258 (2009).

276 Li, P., Seneviratne, C. J., Alpi, E., Vizcaino, J. A. & Jin, L. Delicate Metabolic Control and Coordinated Stress Response Critically Determine Antifungal Tolerance of *Candida albicans* Biofilm Persisters. *Antimicrob Agents Chemother* **59**, 6101-6112 (2015).

277 Borghi, E., Borgo, F. & Morace, G. Fungal Biofilms: Update on Resistance. *Adv Exp Med Biol* **931**, 37-47 (2016).

278 Dawson, C. C., Intapa, C. & Jabra-Rizk, M. A. "Persisters": survival at the cellular level. *PLoS Pathog* **7**, e1002121 (2011).

279 Khot, P. D., Suci, P. A., Miller, R. L., Nelson, R. D. & Tyler, B. J. A small subpopulation of blastospores in *Candida albicans* biofilms exhibit resistance to amphotericin B associated with differential regulation of ergosterol and beta-1,6-glucan pathway genes. *Antimicrob Agents Chemother* **50**, 3708-3716 (2006).

280 Lafleur, M. D., Qi, Q. & Lewis, K. Patients with long-term oral carriage harbor high-persister mutants of *Candida albicans*. *Antimicrob Agents Chemother* **54**, 39-44 (2010).

281 Al-Dhaheri, R. S. & Douglas, L. J. Absence of amphotericin B-tolerant persister cells in biofilms of some *Candida* species. *Antimicrob Agents Chemother* **52**, 1884-1887 (2008).

282 Al-Dhaheri, R. S. & Douglas, L. J. Apoptosis in *Candida* biofilms exposed to amphotericin B. *J Med Microbiol* **59**, 149-157 (2010).
283 Maebashi, K. *et al.* A novel mechanism of fluconazole resistance associated with fluconazole sequestration in *Candida albicans* isolates from a myelofibrosis patient. *Microbiol Immunol* **46**, 317-326 (2002).
284 Hsieh, S. H., Brunke, S. & Brock, M. Encapsulation of Antifungals in Micelles Protects *Candida albicans* during Gall-Bladder Infection. *Front Microbiol* **8**, 117 (2017).
285 Al-Fattani, M. A. & Douglas, L. J. Penetration of *Candida* biofilms by antifungal agents. *Antimicrob Agents Chemother* **48**, 3291-3297 (2004).
286 da Silva, W. J. *et al.* Exopolysaccharide matrix of developed *Candida albicans* biofilms after exposure to antifungal agents. *Braz Dent J* **23**, 716-722 (2012).
287 Mitchell, K. F. *et al.* Role of matrix beta-1,3 glucan in antifungal resistance of non-*albicans Candida* biofilms. *Antimicrob Agents Chemother* **57**, 1918-1920 (2013).
288 Martins, M., Henriques, M., Lopez-Ribot, J. L. & Oliveira, R. Addition of DNase improves the *in vitro* activity of antifungal drugs against *Candida albicans* biofilms. *Mycoses* **55**, 80-85 (2012).
289 Nett, J. E., Crawford, K., Marchillo, K. & Andes, D. R. Role of Fks1p and matrix glucan in *Candida albicans* biofilm resistance to an echinocandin, pyrimidine, and polyene. *Antimicrob Agents Chemother* **54**, 3505-3508 (2010).
290 Nett, J. E., Sanchez, H., Cain, M. T., Ross, K. M. & Andes, D. R. Interface of *Candida albicans* biofilm matrix-associated drug resistance and cell wall integrity regulation. *Eukaryot Cell* **10**, 1660-1669 (2011).
291 Taff, H. T. *et al.* A *Candida* biofilm-induced pathway for matrix glucan delivery: implications for drug resistance. *PLoS Pathog* **8**, e1002848 (2012).
292 Monge, R. A., Roman, E., Nombela, C. & Pla, J. The MAP kinase signal transduction network in *Candida albicans*. *Microbiology* **152**, 905-912 (2006).
293 Cannon, R. D. *et al. Candida albicans* drug resistance another way to cope with stress. *Microbiology* **153**, 3211-3217 (2007).
294 Navarro-Garcia, F., Sanchez, M., Pla, J. & Nombela, C. Functional characterization of the *MKC1* gene of *Candida albicans*, which encodes a mitogen-activated protein kinase homolog related to cell integrity. *Mol Cell Biol* **15**, 2197-2206 (1995).
295 Navarro-Garcia, F. *et al.* A role for the MAP kinase gene *MKC1* in cell wall construction and morphological transitions in *Candida albicans*. *Microbiology* **144 (Pt 2)**, 411-424 (1998).
296 Blankenship, J. R. & Heitman, J. Calcineurin is required for *Candida albicans* to survive calcium stress in serum. *Infect Immun* **73**, 5767-5774 (2005).
297 Uppuluri, P., Nett, J., Heitman, J. & Andes, D. Synergistic effect of calcineurin inhibitors and fluconazole against *Candida albicans* biofilms. *Antimicrob Agents Chemother* **52**, 1127-1132 (2008).
298 Singh, S. D. *et al.* Hsp90 governs echinocandin resistance in the pathogenic yeast *Candida albicans* via calcineurin. *PLoS Pathog* **5**, e1000532 (2009).
299 Robbins, N. *et al.* Hsp90 governs dispersion and drug resistance of fungal biofilms. *PLoS Pathog* **7**, e1002257 (2011).
300 Hill, J. A., Ammar, R., Torti, D., Nislow, C. & Cowen, L. E. Genetic and genomic architecture of the evolution of resistance to antifungal drug combinations. *PLoS Genet* **9**, e1003390 (2013).
301 Fiori, A. *et al.* The heat-induced molecular disaggregase Hsp104 of *Candida albicans* plays a role in biofilm formation and pathogenicity in a worm infection model. *Eukaryot Cell* **11**, 1012-1020 (2012).
302 Miramon, P., Kasper, L. & Hube, B. Thriving within the host: *Candida* spp. interactions with phagocytic cells. *Med Microbiol Immunol* **202**, 183-195 (2013).
303 Bain, J. M., Lewis, L. E. & Erwig, L. P. Differential expression of macrophage and neutrophil phagocytic receptors recognising fungal pathogens in mouse and human. *Immunol Cell Biol* **90**, 837-838 (2012).
304 Netea, M. G., Brown, G. D., Kullberg, B. J. & Gow, N. A. An integrated model of the recognition of C*andida albicans* by the innate immune system. *Nat Rev Microbiol* **6**, 67-78 (2008).
305 Erwig, L. P. & Gow, N. A. Interactions of fungal pathogens with phagocytes. *Nat Rev Microbiol* **14**, 163-176 (2016).
306 Vieira, O. V., Botelho, R. J. & Grinstein, S. Phagosome maturation: aging gracefully. *Biochem J* **366**, 689-704 (2002).
307 Lee, W. L., Harrison, R. E. & Grinstein, S. Phagocytosis by neutrophils. *Microbes and Infection* **5**, 1299-1306 (2003).

308 Roos, D. & Winterbourn, C. C. Immunology. Lethal weapons. *Science* **296**, 669-671 (2002).
309 Kolaczkowska, E. & Kubes, P. Neutrophil recruitment and function in health and inflammation. *Nat Rev Immunol* **13**, 159-175 (2013).
310 Wheeler, M. L. & Underhill, D. M. Time to cast a larger net. *Nat Immunol* **15**, 1000-1001 (2014).
311 Branzk, N. *et al.* Neutrophils sense microbe size and selectively release neutrophil extracellular traps in response to large pathogens. *Nat Immunol* **15**, 1017-1025 (2014).
312 Urban, C. F. *et al.* Neutrophil extracellular traps contain calprotectin, a cytosolic protein complex involved in host defense against *Candida albicans*. *PLoS Pathog* **5**, e1000639 (2009).
313 Gazendam, R. P., van de Geer, A., Roos, D., van den Berg, T. K. & Kuijpers, T. W. How neutrophils kill fungi. *Immunol Rev* **273**, 299-311 (2016).
314 Netea, M. G. *et al.* Human dendritic cells are less potent at killing *Candida albicans* than both monocytes and macrophages. *Microbes Infect* **6**, 985-989 (2004).
315 Naglik, J. R. *Candida* Immunity. *New Journal of Science* **2014**, 1-27 (2014).
316 Romani, L. Immunity to fungal infections. *Nat Rev Immunol* **11**, 275-288 (2011).
317 Seider, K., Heyken, A., Luttich, A., Miramon, P. & Hube, B. Interaction of pathogenic yeasts with phagocytes: survival, persistence and escape. *Curr Opin Microbiol* **13**, 392-400 (2010).
318 Hall, R. A. & Gow, N. A. Mannosylation in *Candida albicans*: role in cell wall function and immune recognition. *Mol Microbiol* **90**, 1147-1161 (2013).
319 Hall, R. A. Dressed to impress: impact of environmental adaptation on the *Candida albicans* cell wall. *Mol Microbiol* **97**, 7-17 (2015).
320 Lowman, D. W. *et al.* Novel structural features in *Candida albicans* hyphal glucan provide a basis for differential innate immune recognition of hyphae versus yeast. *J Biol Chem* **289**, 3432-3443 (2014).
321 Bates, S. *et al. Candida albicans* Pmr1p, a secretory pathway P-type Ca2+/Mn2+-ATPase, is required for glycosylation and virulence. *J Biol Chem* **280**, 23408-23415 (2005).
322 de Groot, P. W. *et al.* The cell wall of the human pathogen *Candida glabrata*: differential incorporation of novel adhesin-like wall proteins. *Eukaryot Cell* **7**, 1951-1964 (2008).
323 Brown, A. J., Brown, G. D., Netea, M. G. & Gow, N. A. Metabolism impacts upon *Candida* immunogenicity and pathogenicity at multiple levels. *Trends Microbiol* **22**, 614-622 (2014).
324 Brown, A. J. *et al.* Stress adaptation in a pathogenic fungus. *J Exp Biol* **217**, 144-155 (2014).
325 Ene, I. V. *et al.* Host carbon sources modulate cell wall architecture, drug resistance and virulence in a fungal pathogen. *Cell Microbiol* **14**, 1319-1335 (2012).
326 Ballou, E. R. *et al.* Lactate signalling regulates fungal beta-glucan masking and immune evasion. *Nat Microbiol* **2**, 16238 (2016).
327 Stevens, D. A., Espiritu, M. & Parmar, R. Paradoxical effect of caspofungin: reduced activity against *Candida albicans* at high drug concentrations. *Antimicrob Agents Chemother* **48**, 3407-3411 (2004).
328 Stevens, D. A., Ichinomiya, M., Koshi, Y. & Horiuchi, H. Escape of *Candida* from caspofungin inhibition at concentrations above the MIC (paradoxical effect) accomplished by increased cell wall chitin; evidence for beta-1,6-glucan synthesis inhibition by caspofungin. *Antimicrob Agents Chemother* **50**, 3160-3161 (2006).
329 Walker, L. A. *et al.* Stimulation of chitin synthesis rescues *Candida albicans* from echinocandins. *PLoS Pathog* **4**, e1000040 (2008).
330 Perez-Garcia, L. A. *et al.* Role of Protein Glycosylation in *Candida parapsilosis* Cell Wall Integrity and Host Interaction. *Front Microbiol* **7**, 306 (2016).
331 Bates, S. *et al.* Outer chain N-glycans are required for cell wall integrity and virulence of *Candida albicans*. *J Biol Chem* **281**, 90-98 (2006).
332 Munro, C. A. *et al.* Mnt1p and Mnt2p of *Candida albicans* are partially redundant alpha-1,2-mannosyltransferases that participate in O-linked mannosylation and are required for adhesion and virulence. *J Biol Chem* **280**, 1051-1060 (2005).
333 Brown, G. D. & Gordon, S. Immune recognition. A new receptor for beta-glucans. *Nature* **413**, 36-37 (2001).
334 Brown, G. D. Dectin-1: a signalling non-TLR pattern-recognition receptor. *Nat Rev Immunol* **6**, 33-43 (2006).
335 Bourgeois, C., Majer, O., Frohner, I. E., Tierney, L. & Kuchler, K. Fungal attacks on mammalian hosts: pathogen elimination requires sensing and tasting. *Curr Opin Microbiol* **13**, 401-408 (2010).

336 Gantner, B. N., Simmons, R. M., Canavera, S. J., Akira, S. & Underhill, D. M. Collaborative Induction of Inflammatory Responses by Dectin-1 and Toll-like Receptor 2. *The Journal of Experimental Medicine* **197**, 1107-1117 (2003).
337 Gantner, B. N., Simmons, R. M. & Underhill, D. M. Dectin-1 mediates macrophage recognition of *Candida albicans* yeast but not filaments. *EMBO J* **24**, 1277-1286 (2005).
338 Shibata, N., Suzuki, A., Kobayashi, H. & Okawa, Y. Chemical structure of the cell-wall mannan of *Candida albicans* serotype A and its difference in yeast and hyphal forms. *Biochem J* **404**, 365-372 (2007).
339 Cheng, S.-C. *et al.* The dectin-1/inflammasome pathway is responsible for the induction of protective T-helper 17 responses that discriminate between yeasts and hyphae of *Candida albicans*. *Journal of Leukocyte Biology* **90**, 357-366 (2011).
340 Sem, X. *et al.* beta-glucan Exposure on the Fungal Cell Wall Tightly Correlates with Competitive Fitness of *Candida* Species in the Mouse Gastrointestinal Tract. *Front Cell Infect Microbiol* **6**, 186 (2016).
341 Wheeler, R. T., Kombe, D., Agarwala, S. D. & Fink, G. R. Dynamic, morphotype-specific *Candida albicans* beta-glucan exposure during infection and drug treatment. *PLoS Pathog* **4**, e1000227 (2008).
342 Hopke, A. *et al.* Neutrophil Attack Triggers Extracellular Trap-Dependent *Candida* Cell Wall Remodeling and Altered Immune Recognition. *PLoS Pathog* **12**, e1005644 (2016).
343 Marakalala, M. J. *et al.* Differential adaptation of *Candida albicans in vivo* modulates immune recognition by dectin-1. *PLoS Pathog* **9**, e1003315 (2013).
344 van de Veerdonk, F. L. *et al.* The macrophage mannose receptor induces IL-17 in response to *Candida albicans*. *Cell Host Microbe* **5**, 329-340 (2009).
345 Ifrim, D. C. *et al.* The Role of Dectin-2 for Host Defense Against Disseminated Candidiasis. *J Interferon Cytokine Res* **36**, 267-276 (2016).
346 Saijo, S. *et al.* Dectin-2 recognition of alpha-mannans and induction of Th17 cell differentiation is essential for host defense against *Candida albicans*. *Immunity* **32**, 681-691 (2010).
347 Zhu, L.-L. *et al.* C-Type Lectin Receptors Dectin-3 and Dectin-2 Form a Heterodimeric Pattern-Recognition Receptor for Host Defense against Fungal Infection. *Immunity* **39**, 324-334 (2013).
348 van der Graaf, C. A., Netea, M. G., Verschueren, I., van der Meer, J. W. & Kullberg, B. J. Differential cytokine production and Toll-like receptor signaling pathways by *Candida albicans* blastoconidia and hyphae. *Infect Immun* **73**, 7458-7464 (2005).
349 Tada, H. *et al. Saccharomyces cerevisiae*- and *Candida albicans*-derived mannan induced production of tumor necrosis factor alpha by human monocytes in a CD14- and Toll-like receptor 4-dependent manner. *Microbiol Immunol* **46**, 503-512 (2002).
350 Jouault, T. *et al. Candida albicans* Phospholipomannan Is Sensed through Toll-Like Receptors. *The Journal of Infectious Diseases* **188**, 165-172 (2003).
351 Wagener, J. *et al.* Fungal chitin dampens inflammation through IL-10 induction mediated by NOD2 and TLR9 activation. *PLoS Pathog* **10**, e1004050 (2014).
352 Shao, B. Z., Xu, Z. Q., Han, B. Z., Su, D. F. & Liu, C. NLRP3 inflammasome and its inhibitors: a review. *Front Pharmacol* **6**, 262 (2015).
353 Gross, O. *et al.* Syk kinase signalling couples to the Nlrp3 inflammasome for anti-fungal host defence. *Nature* **459**, 433-436 (2009).
354 Joly, S. *et al.* Cutting edge: *Candida albicans* hyphae formation triggers activation of the Nlrp3 inflammasome. *J Immunol* **183**, 3578-3581 (2009).
355 Kumar, H. *et al.* Involvement of the NLRP3 inflammasome in innate and humoral adaptive immune responses to fungal beta-glucan. *J Immunol* **183**, 8061-8067 (2009).
356 Moyes, D. L. *et al.* A biphasic innate immune MAPK response discriminates between the yeast and hyphal forms of *Candida albicans* in epithelial cells. *Cell Host Microbe* **8**, 225-235 (2010).
357 Weindl, G. *et al.* Human epithelial cells establish direct antifungal defense through TLR4-mediated signaling. *J Clin Invest* **117**, 3664-3672 (2007).
358 Tomalka, J. *et al.* beta-Defensin 1 plays a role in acute mucosal defense against *Candida albicans*. *J Immunol* **194**, 1788-1795 (2015).
359 Conti, H. R. & Gaffen, S. L. IL-17-Mediated Immunity to the Opportunistic Fungal Pathogen *Candida albicans*. *J Immunol* **195**, 780-788 (2015).
360 Kashem, S. W. *et al. Candida albicans* morphology and dendritic cell subsets determine T helper cell differentiation. *Immunity* **42**, 356-366 (2015).

361 Conti, H. R. *et al.* Th17 cells and IL-17 receptor signaling are essential for mucosal host defense against oral candidiasis. *The Journal of Experimental Medicine* **206**, 299 (2009).

362 Puel, A. *et al.* Chronic mucocutaneous candidiasis in humans with inborn errors of interleukin-17 immunity. *Science* **332**, 65-68 (2011).

363 Milner, J. D. *et al.* Impaired TH17 cell differentiation in subjects with autosomal dominant hyper-IgE syndrome. *Nature* **452**, 773-776 (2008).

364 van de Veerdonk , F. L. *et al.* STAT1 Mutations in Autosomal Dominant Chronic Mucocutaneous Candidiasis. *New England Journal of Medicine* **365**, 54-61 (2011).

365 Liu, L. *et al.* Gain-of-function human STAT1 mutations impair IL-17 immunity and underlie chronic mucocutaneous candidiasis. *The Journal of Experimental Medicine* **208**, 1635-1648 (2011).

366 Eyerich, K. *et al.* Patients with chronic mucocutaneous candidiasis exhibit reduced production of Th17-associated cytokines IL-17 and IL-22. *J Invest Dermatol* **128**, 2640-2645 (2008).

367 Ng, W.-F. *et al.* Impaired TH17 responses in patients with chronic mucocutaneous candidiasis with and without autoimmune polyendocrinopathy candidiasis ectodermal dystrophy. *Journal of Allergy and Clinical Immunology* **126**, 1006-1015.e1004 (2010).

368 Kisand, K. *et al.* Chronic mucocutaneous candidiasis in APECED or thymoma patients correlates with autoimmunity to Th17-associated cytokines. *J Exp Med* **207**, 299-308 (2010).

369 Zielinski, C. E. *et al.* Pathogen-induced human TH17 cells produce IFN-gamma or IL-10 and are regulated by IL-1beta. *Nature* **484**, 514-518 (2012).

370 Borghi, M. *et al.* Antifungal Th Immunity: Growing up in Family. *Front Immunol* **5**, 506 (2014).

371 Huppler, A. R. *et al.* A *Candida albicans* Strain Expressing Mammalian Interleukin-17A Results in Early Control of Fungal Growth during Disseminated Infection. *Infection and Immunity* **83**, 3684-3692 (2015).

372 Mosci, P. *et al.* Involvement of IL-17A in preventing the development of deep-seated candidiasis from oropharyngeal infection. *Microbes Infect* **16**, 678-689 (2014).

373 Pandiyan, P. *et al.* CD4(+)CD25(+)Foxp3(+) regulatory T cells promote Th17 cells *in vitro* and enhance host resistance in mouse *Candida albicans* Th17 cell infection model. *Immunity* **34**, 422-434 (2011).

374 Break, T. J. *et al.* CX3CR1 is dispensable for control of mucosal *Candida albicans* infections in mice and humans. *Infect Immun* **83**, 958-965 (2015).

375 Richardson, J. P. & Moyes, D. L. Adaptive immune responses to *Candida albicans* infection. *Virulence* **6**, 327-337 (2015).

376 Moyes, D. L. *et al. Candida albicans* yeast and hyphae are discriminated by MAPK signaling in vaginal epithelial cells. *PLoS One* **6**, e26580 (2011).

377 Yano, J., Noverr, M. C. & Fidel, P. L., Jr. Cytokines in the host response to *Candida* vaginitis: Identifying a role for non-classical immune mediators, S100 alarmins. *Cytokine* **58**, 118-128 (2012).

378 Black, C. A. *et al.* Acute neutropenia decreases inflammation associated with murine vaginal candidiasis but has no effect on the course of infection. *Infect Immun* **66**, 1273-1275 (1998).

379 Yano, J. *et al.* Vaginal epithelial cell-derived S100 alarmins induced by *Candida albicans* via pattern recognition receptor interactions are sufficient but not necessary for the acute neutrophil response during experimental vaginal candidiasis. *Infect Immun* **82**, 783-792 (2014).

380 Fidel, P. L., Jr. Distinct protective host defenses against oral and vaginal candidiasis. *Med Mycol* **40**, 359-375 (2002).

381 Kullberg, B. J., van 't Wout, J. W. & van Furth, R. Role of granulocytes in increased host resistance to *Candida albicans* induced by recombinant interleukin-1. *Infect Immun* **58**, 3319-3324 (1990).

382 Swamydas, M. *et al.* CXCR1-mediated neutrophil degranulation and fungal killing promote *Candida* clearance and host survival. *Sci Transl Med* **8**, 322ra310 (2016).

383 Fradin, C. *et al.* Granulocytes govern the transcriptional response, morphology and proliferation of *Candida albicans* in human blood. *Mol Microbiol* **56**, 397-415 (2005).

384 Leavy, O. Macrophages: Early antifungal defence in kidneys. *Nat Rev Immunol* **14**, 6-7 (2014).

385 Lionakis, M. S. *et al.* CX3CR1-dependent renal macrophage survival promotes *Candida* control and host survival. *J Clin Invest* **123**, 5035-5051 (2013).

386 Lionakis, M. S., Lim, J. K., Lee, C. C. R. & Murphy, P. M. Organ-Specific Innate Immune Responses in a Mouse Model of Invasive Candidiasis. *Journal of Innate Immunity* **3**, 180-199 (2011).

387 MacCallum, D. M., Castillo, L., Brown, A. J., Gow, N. A. & Odds, F. C. Early-expressed chemokines predict kidney immunopathology in experimental disseminated *Candida albicans* infections. *PLoS One* **4**, e6420 (2009).
388 Qian, Q., Jutila, M. A., Van Rooijen, N. & Cutler, J. E. Elimination of mouse splenic macrophages correlates with increased susceptibility to experimental disseminated candidiasis. *J Immunol* **152**, 5000-5008 (1994).
389 Ngo, L. Y. *et al.* Inflammatory monocytes mediate early and organ-specific innate defense during systemic candidiasis. *J Infect Dis* **209**, 109-119 (2014).
390 Li, R. *et al.* Antibody-Independent Function of Human B Cells Contributes to Antifungal T Cell Responses. *J Immunol* (2017).
391 Netea, M. G. *et al.* Differential role of IL-18 and IL-12 in the host defense against disseminated *Candida albicans* infection. *Eur J Immunol* **33**, 3409-3417 (2003).
392 Kullberg, B. J., van 't Wout, J. W., Hoogstraten, C. & van Furth, R. Recombinant interferon-gamma enhances resistance to acute disseminated *Candida albicans* infection in mice. *J Infect Dis* **168**, 436-443 (1993).
393 Delsing, C. E. *et al.* Interferon-gamma as adjunctive immunotherapy for invasive fungal infections: a case series. *BMC Infect Dis* **14**, 166 (2014).
394 Huang, W., Na, L., Fidel, P. L. & Schwarzenberger, P. Requirement of interleukin-17A for systemic anti-*Candida albicans* host defense in mice. *J Infect Dis* **190**, 624-631 (2004).
395 van de Veerdonk, F. L. *et al.* Differential effects of IL-17 pathway in disseminated candidiasis and zymosan-induced multiple organ failure. *Shock* **34**, 407-411 (2010).
396 Whibley, N. *et al.* Expansion of Foxp3(+) T-cell populations by *Candida albicans* enhances both Th17-cell responses and fungal dissemination after intravenous challenge. *Eur J Immunol* **44**, 1069-1083 (2014).
397 Mencacci, A. *et al.* CD4+ T-helper-cell responses in mice with low-level *Candida albicans* infection. *Infect Immun* **64**, 4907-4914 (1996).
398 Mencacci, A. *et al.* Defective antifungal T-helper 1 (TH1) immunity in a murine model of allogeneic T-cell-depleted bone marrow transplantation and its restoration by treatment with TH2 cytokine antagonists. *Blood* **97**, 1483-1490 (2001).
399 Tavares, D., Ferreira, P. & Arala-Chaves, M. Increased resistance to systemic candidiasis in athymic or interleukin-10-depleted mice. *J Infect Dis* **182**, 266-273 (2000).
400 Vazquez-Torres, A., Jones-Carson, J., Wagner, R. D., Warner, T. & Balish, E. Early resistance of interleukin-10 knockout mice to acute systemic candidiasis. *Infect Immun* **67**, 670-674 (1999).
401 Mencacci, A. *et al.* IL-10 is required for development of protective Th1 responses in IL-12-deficient mice upon *Candida albicans* infection. *J Immunol* **161**, 6228-6237 (1998).
402 Mencacci, A. *et al.* Endogenous interleukin 4 is required for development of protective CD4+ T helper type 1 cell responses to *Candida albicans*. *J Exp Med* **187**, 307-317 (1998).
403 Chandra, J., McCormick, T. S., Imamura, Y., Mukherjee, P. K. & Ghannoum, M. A. Interaction of *Candida albicans* with adherent human peripheral blood mononuclear cells increases *C. albicans* biofilm formation and results in differential expression of pro- and anti-inflammatory cytokines. *Infect Immun* **75**, 2612-2620 (2007).
404 Katragkou, A. *et al.* Effects of interferon-gamma and granulocyte colony-stimulating factor on antifungal activity of human polymorphonuclear neutrophils against *Candida albicans* grown as biofilms or planktonic cells. *Cytokine* **55**, 330-334 (2011).
405 Katragkou, A. *et al.* Interactions between human phagocytes and *Candida albicans* biofilms alone and in combination with antifungal agents. *J Infect Dis* **201**, 1941-1949 (2010).
406 Nett, J. E. The Host's Reply to *Candida* Biofilm. *Pathogens* **5** (2016).
407 Xie, Z. *et al. Candida albicans* biofilms do not trigger reactive oxygen species and evade neutrophil killing. *J Infect Dis* **206**, 1936-1945 (2012).
408 Johnson, C. J. *et al.* The Extracellular Matrix of *Candida albicans* Biofilms Impairs Formation of Neutrophil Extracellular Traps. *PLoS Pathog* **12**, e1005884 (2016).
409 Dongari-Bagtzoglou, A., Kashleva, H., Dwivedi, P., Diaz, P. & Vasilakos, J. Characterization of mucosal *Candida albicans* biofilms. *PLoS One* **4**, e7967 (2009).
410 Dwivedi, P. *et al.* Role of Bcr1-activated genes Hwp1 and Hyr1 in *Candida albicans* oral mucosal biofilms and neutrophil evasion. *PLoS One* **6**, e16218 (2011).
411 Kucharikova, S., Vande Velde, G., Himmelreich, U. & Van Dijck, P. *Candida albicans* Biofilm Development on Medically-relevant Foreign Bodies in a Mouse Subcutaneous Model Followed by Bioluminescence Imaging. *J. Vis. Exp.* e52239 (2015).

412 Nieminen, M. T. *et al.* DL-2-hydroxyisocaproic acid attenuates inflammatory responses in a murine *Candida albicans* biofilm model. *Clin Vaccine Immunol* **21**, 1240-1245 (2014).
413 Ghosh, S. *et al.* Arginine-induced germ tube formation in *Candida albicans* is essential for escape from murine macrophage line RAW 264.7. *Infect Immun* **77**, 1596-1605 (2009).
414 Cheng, S. C., Joosten, L. A., Kullberg, B. J. & Netea, M. G. Interplay between *Candida albicans* and the mammalian innate host defense. *Infect Immun* **80**, 1304-1313 (2012).
415 McKenzie, C. G. *et al.* Contribution of *Candida albicans* cell wall components to recognition by and escape from murine macrophages. *Infect Immun* **78**, 1650-1658 (2010).
416 Wellington, M., Koselny, K., Sutterwala, F. S. & Krysan, D. J. *Candida albicans* triggers NLRP3-mediated pyroptosis in macrophages. *Eukaryot Cell* **13**, 329-340 (2014).
417 Uwamahoro, N. *et al.* The pathogen *Candida albicans* hijacks pyroptosis for escape from macrophages. *MBio* **5**, e00003-00014 (2014).
418 Krysan, D. J., Sutterwala, F. S. & Wellington, M. Catching fire: *Candida albicans*, macrophages, and pyroptosis. *PLoS Pathog* **10**, e1004139 (2014).
419 Rizzetto, L., Weil, T. & Cavalieri, D. Systems Level Dissection of *Candida* Recognition by Dectins: A Matter of Fungal Morphology and Site of Infection. *Pathogens* **4**, 639-661 (2015).
420 Bain, J. M. *et al.* Non-lytic expulsion/exocytosis of *Candida albicans* from macrophages. *Fungal Genet Biol* **49**, 677-678 (2012).
421 Bain, J. M. *et al. Candida albicans* hypha formation and mannan masking of beta-glucan inhibit macrophage phagosome maturation. *MBio* **5**, e01874 (2014).
422 Nakagawa, Y., Kanbe, T. & Mizuguchi, I. Disruption of the human pathogenic yeast *Candida albicans* catalase gene decreases survival in mouse-model infection and elevates susceptibility to higher temperature and to detergents. *Microbiol Immunol* **47**, 395-403 (2003).
423 Frohner, I. E., Bourgeois, C., Yatsyk, K., Majer, O. & Kuchler, K. *Candida albicans* cell surface superoxide dismutases degrade host-derived reactive oxygen species to escape innate immune surveillance. *Mol Microbiol* **71**, 240-252 (2009).
424 Collette, J. R., Zhou, H. & Lorenz, M. C. *Candida albicans* suppresses nitric oxide generation from macrophages via a secreted molecule. *PLoS One* **9**, e96203 (2014).
425 Wagener, J., MacCallum, D. M., Brown, G. D. & Gow, N. A. *Candida albicans* Chitin Increases Arginase-1 Activity in Human Macrophages, with an Impact on Macrophage Antimicrobial Functions. *MBio* **8** (2017).
426 Ermert, D. *et al. Candida albicans* escapes from mouse neutrophils. *J Leukoc Biol* **94**, 223-236 (2013).
427 Zhang, X. *et al.* Different virulence of *Candida albicans* is attributed to the ability of escape from neutrophil extracellular traps by secretion of DNase. *Am J Transl Res* **9**, 50-62 (2017).
428 Cheng, S.-C. *et al. Candida albicans* Dampens Host Defense by Downregulating IL-17 Production. *The Journal of Immunology* **185**, 2450-2457 (2010).
429 Zelante, T. *et al.* Sensing of mammalian IL-17A regulates fungal adaptation and virulence. *Nat Commun* **3**, 683 (2012).
430 Xiong, J. *et al. Candida albicans* and *Candida krusei* differentially induce human blood mononuclear cell interleukin-12 and gamma interferon production. *Infect Immun* **68**, 2464-2469 (2000).
431 Cheng, S. C. *et al. Candida albicans* releases soluble factors that potentiate cytokine production by human cells through a protease-activated receptor 1- and 2-independent pathway. *Infect Immun* **78**, 393-399 (2010).
432 Sutmuller, R. P. *et al.* Toll-like receptor 2 controls expansion and function of regulatory T cells. *J Clin Invest* **116**, 485-494 (2006).
433 Dillon, S. *et al.* Yeast zymosan, a stimulus for TLR2 and dectin-1, induces regulatory antigen-presenting cells and immunological tolerance. *J Clin Invest* **116**, 916-928 (2006).
434 Reales-Calderon, J. A., Aguilera-Montilla, N., Corbi, A. L., Molero, G. & Gil, C. Proteomic characterization of human proinflammatory M1 and anti-inflammatory M2 macrophages and their response to *Candida albicans*. *Proteomics* **14**, 1503-1518 (2014).
435 Worthington, R. J. & Melander, C. Combination approaches to combat multidrug-resistant bacteria. *Trends Biotechnol* **31**, 177-184 (2013).
436 Pierce, C. G., Srinivasan, A., Ramasubramanian, A. K. & Lopez-Ribot, J. L. From Biology to Drug Development: New Approaches to Combat the Threat of Fungal Biofilms. *Microbiol Spectr* **3** (2015).
437 Roemer, T. & Boone, C. Systems-level antimicrobial drug and drug synergy discovery. *Nat Chem Biol* **9**, 222-231 (2013).

438 Butts, A. & Krysan, D. J. Antifungal drug discovery: something old and something new. *PLoS Pathog* **8**, e1002870 (2012).
439 Zhao, Y. *et al.* CD101: a novel long-acting echinocandin. *Cell Microbiol* **18**, 1308-1316 (2016).
440 Sandison, T., Ong, V., Lee, J. & Thye, D. Safety and Pharmacokinetics of CD101 IV, a Novel Echinocandin, in Healthy Adults. *Antimicrob Agents Chemother* **61** (2017).
441 Pfaller, M. A., Messer, S. A., Rhomberg, P. R., Jones, R. N. & Castanheira, M. Activity of a long-acting echinocandin, CD101, determined using CLSI and EUCAST reference methods, against *Candida* and *Aspergillus* spp., including echinocandin- and azole-resistant isolates. *J Antimicrob Chemother* **71**, 2868-2873 (2016).
442 Locke, J. B., Almaguer, A. L., Zuill, D. E. & Bartizal, K. Characterization of *In Vitro* Resistance Development to the Novel Echinocandin CD101 in *Candida* Species. *Antimicrob Agents Chemother* **60**, 6100-6107 (2016).
443 Clardy, J. & Walsh, C. Lessons from natural molecules. *Nature* **432**, 829-837 (2004).
444 Cos, P., Vlietinck, A. J., Berghe, D. V. & Maes, L. Anti-infective potential of natural products: how to develop a stronger *in vitro* 'proof-of-concept'. *J Ethnopharmacol* **106**, 290-302 (2006).
445 Odds, F. C. Antifungal agents: their diversity and increasing sophistication. *Mycologist* **17**, 51-55 (2003).
446 Pierce, C. G. & Lopez-Ribot, J. L. Candidiasis drug discovery and development: new approaches targeting virulence for discovering and identifying new drugs. *Expert Opin Drug Discov* **8**, 1117-1126 (2013).
447 Pierce, C. G. *et al.* A Novel Small Molecule Inhibitor of *Candida albicans* Biofilm Formation, Filamentation and Virulence with Low Potential for the Development of Resistance. *NPJ Biofilms Microbiomes* **1** (2015).
448 Reen, F. J. *et al.* Exploiting Interkingdom Interactions for Development of Small-Molecule Inhibitors of *Candida albicans* Biofilm Formation. *Antimicrob Agents Chemother* **60**, 5894-5905 (2016).
449 van de Veerdonk, F. L., Netea, M. G., Joosten, L. A., van der Meer, J. W. & Kullberg, B. J. Novel strategies for the prevention and treatment of *Candida* infections: the potential of immunotherapy. *FEMS Microbiol Rev* **34**, 1063-1075 (2010).
450 van de Veerdonk, F. L., Kullberg, B. J. & Netea, M. G. Adjunctive immunotherapy with recombinant cytokines for the treatment of disseminated candidiasis. *Clin Microbiol Infect* **18**, 112-119 (2012).
451 Casadevall, A. & Pirofski, L. A. Adjunctive immune therapy for fungal infections. *Clin Infect Dis* **33**, 1048-1056 (2001).
452 Ostrosky-Zeichner, L., Casadevall, A., Galgiani, J. N., Odds, F. C. & Rex, J. H. An insight into the antifungal pipeline: selected new molecules and beyond. *Nat Rev Drug Discov* **9**, 719-727 (2010).
453 Ravikumar, S., Win, M. S. & Chai, L. Y. Optimizing Outcomes in Immunocompromised Hosts: Understanding the Role of Immunotherapy in Invasive Fungal Diseases. *Front Microbiol* **6**, 1322 (2015).
454 Mochon, A. B. & Cutler, J. E. Prospects of vaccines for medically important fungi. Is a vaccine needed against *Candida albicans*? *Medical Mycology* **43**, 97-115 (2005).
455 Cassone, A. Development of vaccines for *Candida albicans*: fighting a skilled transformer. *Nat Rev Microbiol* **11**, 884-891 (2013).
456 Bistoni, F. *et al.* Evidence for macrophage-mediated protection against lethal *Candida albicans* infection. *Infect Immun* **51**, 668-674 (1986).
457 Quintin, J. *et al. Candida albicans* infection affords protection against reinfection via functional reprogramming of monocytes. *Cell Host Microbe* **12**, 223-232 (2012).
458 Saville, S. P., Lazzell, A. L., Chaturvedi, A. K., Monteagudo, C. & Lopez-Ribot, J. L. Efficacy of a genetically engineered *Candida albicans* tet-*NRG1* strain as an experimental live attenuated vaccine against hematogenously disseminated candidiasis. *Clin Vaccine Immunol* **16**, 430-432 (2009).
459 Stevens, D. A., Clemons, K. V. & Liu, M. Developing a vaccine against aspergillosis. *Med Mycol* **49** S170-176 (2011).
460 Wang, X. J. *et al.* Vaccines in the treatment of invasive candidiasis. *Virulence* **6**, 309-315 (2015).
461 Cutler, J. E., Deepe, G. S., Jr. & Klein, B. S. Advances in combating fungal diseases: vaccines on the threshold. *Nat Rev Microbiol* **5**, 13-28 (2007).
462 Cassone, A. Vulvovaginal *Candida albicans* infections: pathogenesis, immunity and vaccine prospects. *BJOG* **122**, 785-794 (2015).

463 Schmidt, C. S. *et al.* NDV-3, a recombinant alum-adjuvanted vaccine for *Candida* and *Staphylococcus aureus*, is safe and immunogenic in healthy adults. *Vaccine* **30**, 7594-7600 (2012).

464 Ibrahim, A. S. *et al.* NDV-3 protects mice from vulvovaginal candidiasis through T- and B-cell immune response. *Vaccine* **31**, 5549-5556 (2013).

465 Lin, L. *et al.* Th1-Th17 cells mediate protective adaptive immunity against *Staphylococcus aureus* and *Candida albicans* infection in mice. *PLoS Pathog* **5**, e1000703 (2009).

466 De Bernardis, F. *et al.* A virosomal vaccine against candidal vaginitis: immunogenicity, efficacy and safety profile in animal models. *Vaccine* **30**, 4490-4498 (2012).

467 Pachl, J. *et al.* A randomized, blinded, multicenter trial of lipid-associated amphotericin B alone versus in combination with an antibody-based inhibitor of heat shock protein 90 in patients with invasive candidiasis. *Clin Infect Dis* **42**, 1404-1413 (2006).

468 Hodgetts, S. *et al.* Efungumab and caspofungin: pre-clinical data supporting synergy. *J Antimicrob Chemother* **61**, 1132-1139 (2008).

469 Herbrecht, R., Fohrer, C. & Nivoix, Y. Mycograb for the treatment of invasive candidiasis. *Clin Infect Dis* **43**, 1083; author reply 1083-1084 (2006).

470 Fujibayashi, T. *et al.* Effects of IgY against *Candida albicans* and *Candida* spp. Adherence and Biofilm Formation. *Jpn J Infect Dis* **62**, 337-342 (2009).

471 Lechner, A. J., Lamprech, K. E., Potthoff, L. H., Tredway, T. L. & Matuschak, G. M. Recombinant GM-CSF reduces lung injury and mortality during neutropenic *Candida* sepsis. *Am J Physiol* **266**, L561-568 (1994).

472 Vazquez, J. A., Gupta, S. & Villanueva, A. Potential utility of recombinant human GM-CSF as adjunctive treatment of refractory oropharyngeal candidiasis in AIDS patients. *Eur J Clin Microbiol Infect Dis* **17**, 781-783 (1998).

473 Rokusz, L., Liptay, L. & Kadar, K. Successful treatment of chronic disseminated candidiasis with fluconazole and a granulocyte-macrophage colony-stimulating factor combination. *Scand J Infect Dis* **33**, 784-786 (2001).

474 Dignani, M. C. *et al.* Immunomodulation with interferon-gamma and colony-stimulating factors for refractory fungal infections in patients with leukemia. *Cancer* **104**, 199-204 (2005).

475 Roilides, E., Holmes, A., Blake, C., Pizzo, P. A. & Walsh, T. J. Effects of granulocyte colony-stimulating factor and interferon-gamma on antifungal activity of human polymorphonuclear neutrophils against pseudohyphae of different medically important *Candida* species. *J Leukoc Biol* **57**, 651-656 (1995).

476 Kullberg, B. J. *et al.* Recombinant murine granulocyte colony-stimulating factor protects against acute disseminated *Candida albicans* infection in nonneutropenic mice. *J Infect Dis* **177**, 175-181 (1998).

477 Kullberg, B. J., van de Veerdonk, F. & Netea, M. G. Immunotherapy: a potential adjunctive treatment for fungal infection. *Curr Opin Infect Dis* **27**, 511-516 (2014).

478 Tramsen, L. *et al.* Generation and characterization of anti-*Candida* T cells as potential immunotherapy in patients with *Candida* infection after allogeneic hematopoietic stem-cell transplant. *J Infect Dis* **196**, 485-492 (2007).

479 Bacci, A. *et al.* Dendritic Cells Pulsed with Fungal RNA Induce Protective Immunity to *Candida albicans* in Hematopoietic Transplantation. *The Journal of Immunology* **168**, 2904-2913 (2002).

480 Bakkali, F., Averbeck, S., Averbeck, D. & Idaomar, M. Biological effects of essential oils--a review. *Food Chem Toxicol* **46**, 446-475 (2008).

481 Raut, J. S. & Karuppayil, S. M. A status review on the medicinal properties of essential oils. *Industrial Crops and Products* **62**, 250-264 (2014).

482 Lang, G. & Buchbauer, G. A review on recent research results (2008-2010) on essential oils as antimicrobials and antifungals. A review. *Flavour and Fragrance Journal* **27**, 13-39 (2012).

483 Clarke, J. O. & Mullin, G. E. A review of complementary and alternative approaches to immunomodulation. *Nutr Clin Pract* **23**, 49-62 (2008).

484 Baser, K. & Buchbauer, G. Handbook of Essential Oils: Science, Technology and Applications. . *CRC Press, Taylor & Francis Group* (2010).

485 Hyldgaard, M., Mygind, T. & Meyer, R. L. Essential oils in food preservation: mode of action, synergies, and interactions with food matrix components. *Front Microbiol* **3**, 12 (2012).

486 Bona, E. *et al.* Sensitivity of *Candida albicans* to essential oils: are they an alternative to antifungal agents? *J Appl Microbiol* **121**(6), 1530-1545 (2016).

487 Carson, C. F., Hammer, K. A. & Riley, T. V. *Melaleuca alternifolia* (Tea Tree) oil: a review of antimicrobial and other medicinal properties. *Clin Microbiol Rev* **19**, 50-62 (2006).

488 Dewick, P. M. Medicinal natural products: a biosynthetic approach 3 ed. *Chichester : Wiley* (1997; 2009).
489 Palmeira-de-Oliveira, A. *et al.* The anti-*Candida* activity of *Thymbra capitata* essential oil: effect upon pre-formed biofilm. *J Ethnopharmacol* **140**, 379-383 (2012).
490 Girardot, M. I., C. Natural Sources as Innovative Solutions Against Fungal Biofilms. *Advances in experimental medicine and biology* **931**, 105-125 (2016).
491 Burt, S. Essential oils: their antibacterial properties and potential applications in foods--a review. *Int J Food Microbiol* **94**, 223-253 (2004).
492 Hammer, K. A., Carson, C. F. & Riley, T. V. *In vitro* activity of essential oils, in particular *Melaleuca alternifolia* (tea tree) oil and tea tree oil products, against *Candida* spp. *J Antimicrob Chemother* **42**, 591-595 (1998).
493 Tampieri, M. P. *et al.* The inhibition of *Candida albicans* by selected essential oils and their major components. *Mycopathologia* **159**, 339-345 (2005).
494 Behmanesh, F. *et al.* Antifungal Effect of Lavender Essential Oil (*Lavandula angustifolia*) and Clotrimazole on *Candida albicans*: An *In Vitro* Study. *Scientifica (Cairo)* **2015**, 261397 (2015).
495 Agarwal, V., Lal, P. & Pruthi, V. Prevention of *Candida albicans* biofilm by plant oils. *Mycopathologia* **165**, 13-19 (2008).
496 Tian, J. *et al.* Nerol triggers mitochondrial dysfunction and disruption via elevation of Ca2+ and ROS in *Candida albicans*. *Int J Biochem Cell Biol* **85**, 114-122 (2017).
497 Singh, S., Fatima, Z. & Hameed, S. Citronellal-induced disruption of membrane homeostasis in *Candida albicans* and attenuation of its virulence attributes. *Rev Soc Bras Med Trop* **49**, 465-472 (2016).
498 Tyagi, A. K. & Malik, A. *In situ* SEM, TEM and AFM studies of the antimicrobial activity of lemon grass oil in liquid and vapour phase against *Candida albicans*. *Micron* **41**, 797-805 (2010).
499 Doke, S. K., Raut, J. S., Dhawale, S. & Karuppayil, S. M. Sensitization of *Candida albicans* biofilms to fluconazole by terpenoids of plant origin. *The Journal of General and Applied Microbiology* **60**, 163-168 (2014).
500 Laird, K. & Phillips, C. Vapour phase: a potential future use for essential oils as antimicrobials? *Lett Appl Microbiol* **54**, 169-174 (2012).
501 Doran, A. L., Morden, W. E., Dunn, K. & Edwards-Jones, V. Vapour-phase activities of essential oils against antibiotic sensitive and resistant bacteria including MRSA. *Lett Appl Microbiol* **48**, 387-392 (2009).
502 Laird, K., Armitage, D. & Phillips, C. Reduction of surface contamination and biofilms of *Enterococcus* sp. and *Staphylococcus aureus* using a citrus-based vapour. *J Hosp Infect* **80**, 61-66 (2012).
503 Lopez, P., Sanchez, C., Batlle, R. & Nerin, C. Solid- and vapor-phase antimicrobial activities of six essential oils: susceptibility of selected foodborne bacterial and fungal strains. *J Agric Food Chem* **53**, 6939-6946 (2005).
504 Souza, C. M. *et al.* Antifungal activity of plant-derived essential oils on *Candida tropicalis* planktonic and biofilms cells. *Med Mycol* **54**, 515-523 (2016).
505 Boukhatem, M. N., Ferhat, M. A., Kameli, A., Saidi, F. & Kebir, H. T. Lemon grass (*Cymbopogon citratus*) essential oil as a potent anti-inflammatory and antifungal drugs. *Libyan Journal of Medicine* **9**, 25431 (2014).
506 Andes, D. R. *In Vivo Candida* Device Biofilm Models. *Candida albicans: Cellular and Molecular biology*, 93-113 (2017).
507 Drayton, D. L., Liao, S., Mounzer, R. H. & Ruddle, N. H. Lymphoid organ development: from ontogeny to neogenesis. *Nat Immunol* **7**, 344-353 (2006).
508 Gringhuis, S. I. *et al.* Dectin-1 directs T helper cell differentiation by controlling noncanonical NF-kappaB activation through Raf-1 and Syk. *Nat Immunol* **10**, 203-213 (2009).
509 Netea, M. G. *et al.* Immune sensing of *Candida albicans* requires cooperative recognition of mannans and glucans by lectin and Toll-like receptors. *J Clin Invest* **116**, 1642-1650 (2006).
510 Cambi, A. *et al.* Dendritic cell interaction with *Candida albicans* critically depends on N-linked mannan. *J Biol Chem* **283**, 20590-20599 (2008).
511 Murciano, C. *et al. Candida albicans* cell wall glycosylation may be indirectly required for activation of epithelial cell proinflammatory responses. *Infect Immun* **79**, 4902-4911 (2011).
512 Castillo, L., MacCallum, D. M., Brown, A. J., Gow, N. A. & Odds, F. C. Differential regulation of kidney and spleen cytokine responses in mice challenged with pathology-standardized doses of *Candida albicans* mannosylation mutants. *Infect Immun* **79**, 146-152 (2011).

513 Wagener, J. *et al.* Glycosylation of *Candida albicans* cell wall proteins is critical for induction of innate immune responses and apoptosis of epithelial cells. *PLoS One* **7**, e50518 (2012).
514 Netea, M. G., Quintin, J. & van der Meer, J. W. Trained immunity: a memory for innate host defense. *Cell Host Microbe* **9**, 355-361 (2011).
515 Newton, R. Molecular mechanisms of glucocorticoid action: what is important? *Thorax* **55**, 603-613 (2000).
516 Fontenot, J. D., Gavin, M. A. & Rudensky, A. Y. Foxp3 programs the development and function of CD4+CD25+ regulatory T cells. *Nat Immunol* **4**, 330-336 (2003).
517 Murphy, K. M. *et al.* T helper differentiation proceeds through Stat1-dependent, Stat4-dependent and Stat4-independent phases. *Curr Top Microbiol Immunol* **238**, 13-26 (1999).
518 Zhu, J. & Paul, W. E. CD4 T cells: fates, functions, and faults. *Blood* **112**, 1557-1569 (2008).
519 Farrar, J. D., Ranganath, S. H. & Murphy, K. M. Molecular mechanisms in T-helper phenotype development. *Springer Semin Immunopathol* **21**, 211-230 (1999).
520 Dunn, T. B. Normal and Pathologic Anatomy of the Reticular Tissue in Laboratory Mice, With a Classification and Discussion of Neoplasms. *JNCI: Journal of the National Cancer Institute* **14**, 1281-1433 (1954).
521 Murphy, K. T., P.; Walport, M.; Janeway, C. . Janeway's Immunobiology. *New York: Garland Science.* (2008).
522 Whibley, N. & Gaffen, S. L. Brothers in arms: Th17 and Treg responses in *Candida albicans* immunity. *PLoS Pathog* **10**, e1004456 (2014).
523 Mundt, S., Basler, M., Buerger, S., Engler, H. & Groettrup, M. Inhibiting the immunoproteasome exacerbates the pathogenesis of systemic *Candida albicans* infection in mice. *Sci Rep* **6**, 19434 (2016).
524 Benck, C. J., Martinov, T., Fife, B. T. & Chatterjea, D. Isolation of Infiltrating Leukocytes from Mouse Skin Using Enzymatic Digest and Gradient Separation. *J. Vis. Exp* e53638 (2016).
525 Clancy, C. J., Cheng, S. & Nguyen, M. H. Animal models of candidiasis. *Methods Mol Biol* **499**, 65-76 (2009).
526 Gillum, A. M., Tsay, E. Y. & Kirsch, D. R. Isolation of the *Candida albicans* gene for orotidine-5'-phosphate decarboxylase by complementation of *S. cerevisiae ura3* and *E. coli* pyrF mutations. *Mol Gen Genet* **198**, 179-182 (1984).
527 Brand, A., MacCallum, D. M., Brown, A. J., Gow, N. A. & Odds, F. C. Ectopic expression of *URA3* can influence the virulence phenotypes and proteome of *Candida albicans* but can be overcome by targeted reintegration of *URA3* at the RPS10 locus. *Eukaryot Cell* **3**, 900-909 (2004).
528 Absorption and emission spectra (consulted 2017, July 12). Retrieved from http://www.bdbiosciences.com/us/applications/s/spectrumguidepage
529 Payne, D. J., Gwynn, M. N., Holmes, D. J. & Pompliano, D. L. Drugs for bad bugs: confronting the challenges of antibacterial discovery. *Nat Rev Drug Discov* **6**, 29-40 (2007).
530 Roemer, T. *et al.* Confronting the challenges of natural product-based antifungal discovery. *Chem Biol* **18**, 148-164 (2011).
531 Adukwu, E. C., Bowles, M., Edwards-Jones, V. & Bone, H. Antimicrobial activity, cytotoxicity and chemical analysis of lemongrass essential oil (*Cymbopogon flexuosus*) and pure citral. *Appl Microbiol Biotechnol* **100**, 9619-9627 (2016).
532 Langeveld, W. T., Veldhuizen, E. J. & Burt, S. A. Synergy between essential oil components and antibiotics: a review. *Crit Rev Microbiol* **40**, 76-94 (2014).
533 Inouye, S., Uchida, K., Maruyama, N., Yamaguchi, H. & Abe, S. A novel method to estimate the contribution of the vapor activity of essential oils in agar diffusion assay. *Nihon Ishinkin Gakkai Zasshi* **47**, 91-98 (2006).
534 Kloucek, P. *et al.* Fast screening method for assessment of antimicrobial activity of essential oils in vapor phase. *Food Research International* **47**, 161-165 (2012).
535 Suhr, M. J. & Hallen-Adams, H. E. The human gut mycobiome: pitfalls and potentials--a mycologist's perspective. *Mycologia* **107**, 1057-1073 (2015).
536 Mandras, N. *et al.* Liquid and vapour-phase antifungal activities of essential oils against *Candida albicans* and non-*albicans Candida*. *BMC Complement Altern Med* **16**, 330 (2016).
537 Budzynska, A., Sadowska, B., Wieckowska-Szakiel, M. & Rozalska, B. Enzymatic profile, adhesive and invasive properties of *Candida albicans* under the influence of selected plant essential oils. *Acta Biochim Pol* **61**, 115-121 (2014).
538 Leite, M. C., Bezerra, A. P., de Sousa, J. P., Guerra, F. Q. & Lima Ede, O. Evaluation of Antifungal Activity and Mechanism of Action of Citral against *Candida albicans*. *Evid Based Complement Alternat Med* (2014).

539 Franchomme, P., Jollois, R., Pénoël, D. & Mars, J. L'aromathérapie exactement : encyclopédie de l'utilisation thérapeutique des huiles essentielles : fondements, démonstration, illustration et applications d'une science médicale naturelle. (2001).
540 Hili, P., Evans, C. S. & Veness, R. G. Antimicrobial action of essential oils: the effect of dimethylsulphoxide on the activity of cinnamon oil. *Lett Appl Microbiol* **24**, 269-275 (1997).
541 Li, J., Zhang, J., Han, B., Wang, Y. & Gao, L. Compressed CO2-enhanced solubilization of 1-butyl-3-methylimidazolium tetrafluoroborate in reverse micelles of Triton X-100. *J Chem Phys* **121**, 7408-7412 (2004).
542 Livermore, D. M., British Society for Antimicrobial Chemotherapy Working Party on The Urgent Need: Regenerating Antibacterial Drug, D. & Development. Discovery research: the scientific challenge of finding new antibiotics. *J Antimicrob Chemother* **66**, 1941-1944 (2011).
543 Fischbach, M. A. & Walsh, C. T. Antibiotics for emerging pathogens. *Science* **325**, 1089-1093 (2009).
544 Bassetti, M., Peghin, M. & Timsit, J. F. The current treatment landscape: candidiasis. *J Antimicrob Chemother* **71**, ii13-ii22 (2016).
545 Vale-Silva, L. A. & Sanglard, D. Tipping the balance both ways: drug resistance and virulence in *Candida glabrata*. *FEMS Yeast Res* **15**, fov025 (2015).
546 Moloney, M. G. Natural Products as a Source for Novel Antibiotics. *Trends Pharmacol Sci* **37**, 689-701 (2016).
547 Harvey, A. L., Edrada-Ebel, R. & Quinn, R. J. The re-emergence of natural products for drug discovery in the genomics era. *Nat Rev Drug Discov* **14**, 111-129 (2015).
548 Anderson, T. M. *et al.* Amphotericin forms an extramembranous and fungicidal sterol sponge. *Nat Chem Biol* **10**, 400-406 (2014).
549 Lewis, K. Platforms for antibiotic discovery. *Nat Rev Drug Discov* **12**, 371-387 (2013).
550 Sharifi-Rad, J. *et al.* Biological Activities of Essential Oils: From Plant Chemoecology to Traditional Healing Systems. *Molecules* **22** (2017).
551 Begnaud, F. & Chaintreau, A. Good quantification practices of flavours and fragrances by mass spectrometry. *Philos Trans A Math Phys Eng Sci* **374** (2016).
552 Waseem, R. & Low, K. H. Advanced analytical techniques for the extraction and characterization of plant-derived essential oils by gas chromatography with mass spectrometry. *J Sep Sci* **38**, 483-501 (2015).
553 Sanguinetti, M. & Posteraro, B. New approaches for antifungal susceptibility testing. *Clin Microbiol Infect* (2017).
554 Cuenca-Estrella, M. Antifungal drug resistance mechanisms in pathogenic fungi: from bench to bedside. *Clin Microbiol Infect* **20 Suppl 6**, 54-59 (2014).
555 Johnson, E. M. Issues in antifungal susceptibility testing. *J Antimicrob Chemother* **61 Suppl 1**, i13-18 (2008).
556 Feyaerts, A. F. *et al.* Assay and recommendations for the detection of vapour-phase-mediated antimicrobial activities. *Flavour and Fragrance Journal*, 1-7(2017).
557 Peters, B. M., Ward, R. M., Rane, H. S., Lee, S. A. & Noverr, M. C. Efficacy of ethanol against *Candida albicans* and *Staphylococcus aureus* polymicrobial biofilms. *Antimicrob Agents Chemother* **57**, 74-82 (2013).
558 Mazzola, P. G., Jozala, A. F., Novaes, L. C. d. L., Moriel, P. & Penna, T. C. V. Minimal inhibitory concentration (MIC) determination of disinfectant and/or sterilizing agents. *Brazilian Journal of Pharmaceutical Sciences* **45**, 241-248 (2009).
559 Benjamini, Y., Krieger, A. M. & Yekutieli, D. Adaptive linear step-up procedures that control the false discovery rate. *Biometrica* **93**, 491-507 (2006).
560 Palmeira-de-Oliveira, A. *et al.* Anti-*Candida* activity of essential oils. *Mini Rev Med Chem* **9**, 1292-1305 (2009).
561 Golus, J., Sawicki, R., Widelski, J. & Ginalska, G. The agar microdilution method - a new method for antimicrobial susceptibility testing for essential oils and plant extracts. *J Appl Microbiol* **121**, 1291-1299 (2016).
562 Muller, C., Binder, U., Bracher, F. & Giera, M. Antifungal drug testing by combining minimal inhibitory concentration testing with target identification by gas chromatography-mass spectrometry. *Nat. Protocols* **12**, 947-963 (2017).
563 Riedel, S. *et al.* Comparison of commercial antimicrobial susceptibility test methods for testing of *Staphylococcus aureus* and *Enterococci* against vancomycin, daptomycin, and linezolid. *J Clin Microbiol* **52**, 2216-2222 (2014).
564 Bueno, J. Models of evaluation of antimicrobial activity of essential oils in vapour phase: a promising use in healthcare decontamination. *Nat. Volatiles & Essent Oils* **2**(2), 16-29 (2015).

565 Almeida, L. d. F. D. d. *et al.* Efficacy of citronella and cinnamon essential oils on *Candida albicans* biofilms. *Acta Odontologica Scandinavica* **74**, 393-398 (2016).

566 Taguchi, Y., Hasumi, Y., Abe, S. & Nishiyama, Y. The effect of cinnamaldehyde on the growth and the morphology of *Candida albicans*. *Med Mol Morphol* **46**, 8-13 (2013).

567 Ooi, L. S. *et al.* Antimicrobial activities of cinnamon oil and cinnamaldehyde from the Chinese medicinal herb *Cinnamomum cassia* Blume. *Am J Chin Med* **34**, 511-522 (2006).

568 Teixeira, A. P., Duarte, T. M., Oliveira, R., Carrondo, M. J. & Alves, P. M. High-throughput analysis of animal cell cultures using two-dimensional fluorometry. *J Biotechnol* **151**, 255-260 (2011).

569 Wiegand, I., Hilpert, K. & Hancock, R. E. Agar and broth dilution methods to determine the minimal inhibitory concentration (MIC) of antimicrobial substances. *Nat Protoc* **3**, 163-175 (2008).

570 Simonetta, S. H. & Golombek, D. A. An automated tracking system for *Caenorhabditis elegans* locomotor behavior and circadian studies application. *J Neurosci Methods* **161**, 273-280 (2007).

571 Francis, G. W. & Bui, Y. T. Changes in the Composition of Aromatherapeutic Citrus Oils during Evaporation. *Evid Based Complement Alternat Med* **2015**, 421695 (2015).

572 Holm, S. A Simple Sequentially Rejective Multiple Test Procedure *Scand J Statist* **6**, 65-70 (1979).

573 Fischer, A. H., Jacobson, K. A., Rose, J. & Zeller, R. Hematoxylin and Eosin Staining of Tissue and Cell Sections. *Cold Spring Harbor Protocols* **2008**, pdb.prot4986 (2008).

574 Lazzell, A. L. *et al.* Treatment and prevention of *Candida albicans* biofilms with caspofungin in a novel central venous catheter murine model of candidiasis. *J Antimicrob Chemother* **64**, 567-570 (2009).

575 Amatya, N., Garg, A. V. & Gaffen, S. L. IL-17 Signaling: The Yin and the Yang. *Trends Immunol* **38**(5), (5), 10-322 (2017).

576 Tang, C., Chen, S., Qian, H. & Huang, W. Interleukin-23: as a drug target for autoimmune inflammatory diseases. *Immunology* **135**, 112-124 (2012).

577 Sato, K., Krist, S. & Buchbauer, G. Antimicrobial effect of trans-cinnamaldehyde, (-)-perillaldehyde, (-)-citronellal, citral, eugenol and carvacrol on airborne microbes using an airwasher. *Biol Pharm Bull* **29**, 2292-2294 (2006).

578 Ramarao, N., Nielsen-Leroux, C. & Lereclus, D. The insect *Galleria mellonella* as a powerful infection model to investigate bacterial pathogenesis. *J Vis Exp*, e4392 (2012).

579 Ames, L. *et al. Galleria mellonella* as a host model to study *Candida glabrata* virulence and antifungal efficacy. *Virulence*, **00** 1-9 (2017).

580 Brieland, J. *et al.* Comparison of pathogenesis and host immune responses to *Candida glabrata* and *Candida albicans* in systemically infected immunocompetent mice. *Infect Immun* **69**, 5046-5055 (2001).

581 Arendrup, M., Horn, T. & Frimodt-Møller, N. *In Vivo* Pathogenicity of Eight Medically Relevant *Candida* Species in an Animal Model. *Infection* **30**, 286-291 (2002).

582 Korzeniewski, C. & Callewaert, D. M. An enzyme-release assay for natural cytotoxicity. *J Immunol Methods* **64**, 313-320 (1983).

Appendix I: Gating flow cytometer

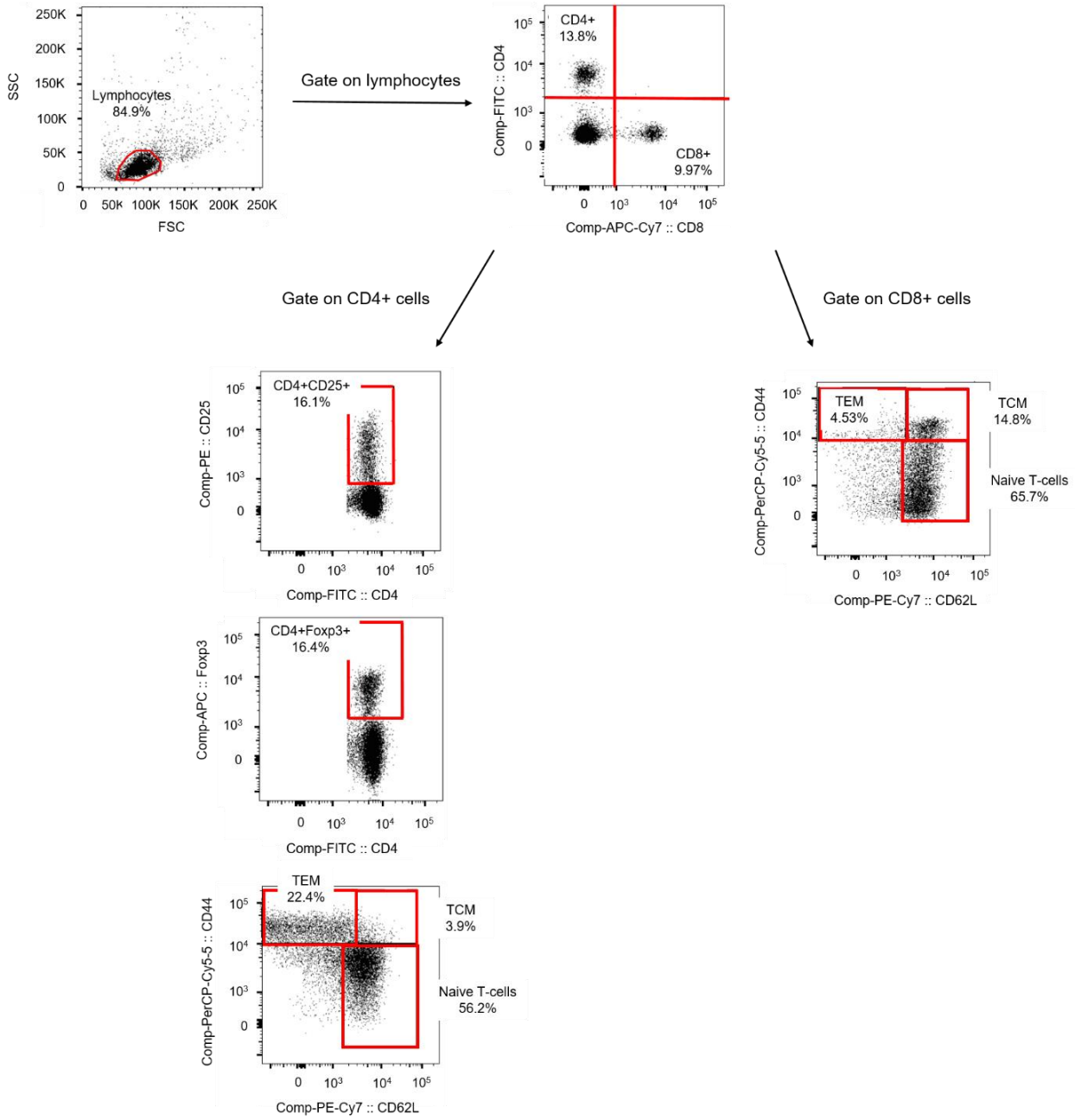

Figure A-I-1: Steps in gating used for the detection of T-cells. First, signals from the sideward scatter channel (SSC; proportional to the amount of cytosolic structures in the cell) and the forward scatter channel (FSC; proportional to the size of the cell) were plotted. Further analyses were performed using 3 x 10^5 cells acquired per organ (lymph nodes and spleen), based on the lymphocyte gate. Plotting CD4 and CD8 signals on the axes allows to gate on CD4+ and CD8+ cells. These were analyzed in subsequent steps, by plotting different markers on the axes. TEM = Effector memory T-cell. TCM = Central memory T-cell.

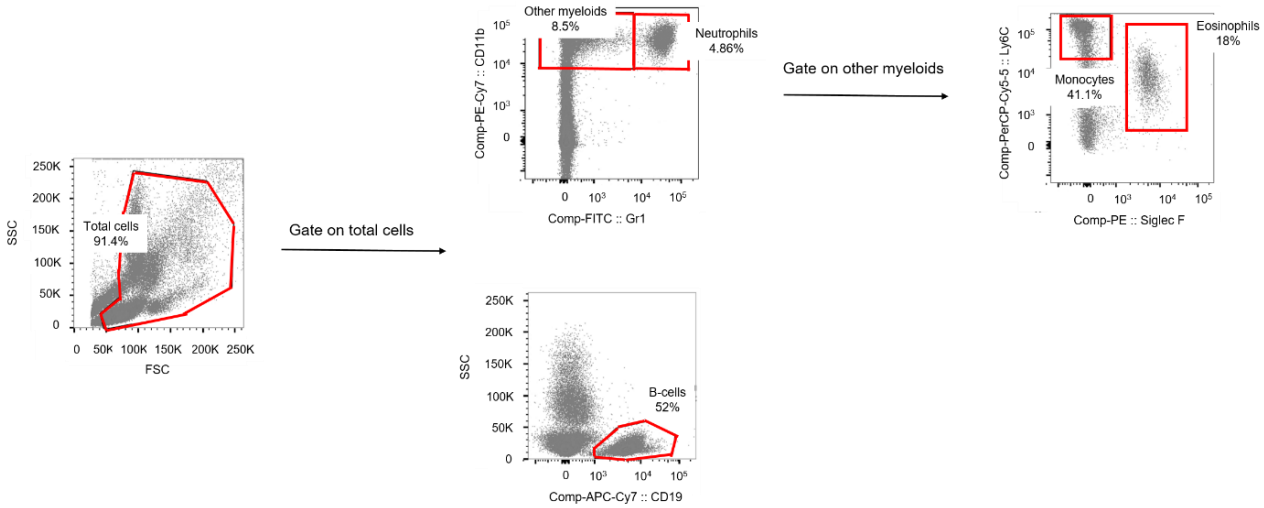

Figure A-I-2: Steps in gating used for the detection of myeloids and B-cells. First, signals from the sideward scatter channel (SSC; proportional to the amount of cytosolic structures in the cell) and the forward scatter channel (FSC; proportional to the size of the cell) were plotted. Further analyses were performed using 3 x 10^5 cells acquired per organ (lymph nodes, spleen and blood), based on the leukocyte (total cells) gate. These were analyzed in subsequent steps, by plotting different markers on the axes.

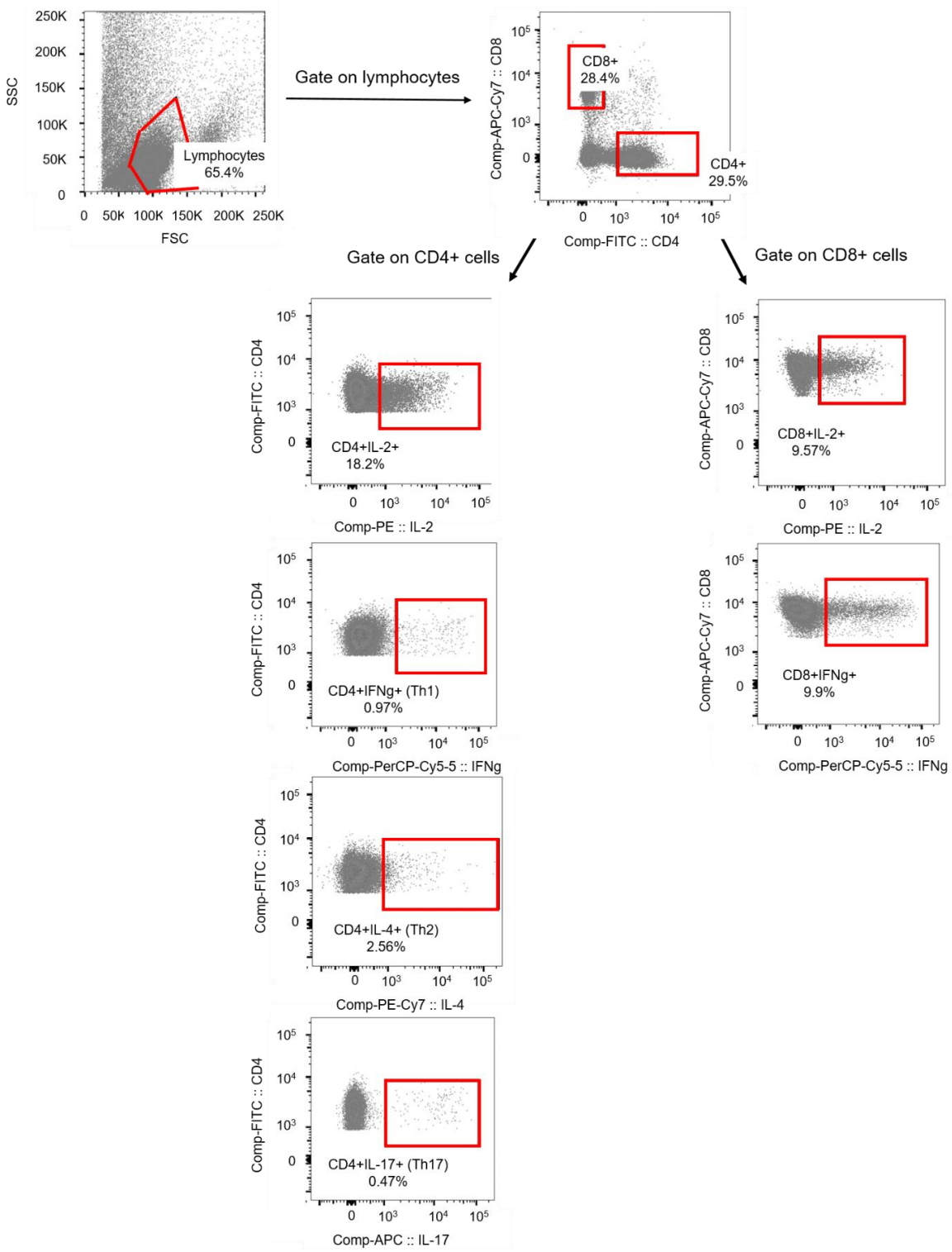

Figure A-I-3: Steps in gating used for the detection of cytokines. First, signals from the sideward scatter channel (SSC; proportional to the amount of cytosolic structures in the cell) and the forward scatter channel (FSC; proportional to the size of the cell) were plotted. Further analyses were performed using 3 x 10^5 cells acquired per organ (lymph nodes and spleen), based on the lymphocyte gate. Plotting CD4 and CD8 signals on the axes allows to gate on CD4+ and CD8+ cells. These were analyzed in subsequent steps, by plotting different cytokine markers on the x-axis.

Appendix II: Supplementary material manuscript 1

Table A-II: List of chemically defined essential oils with components (≥ 0.10%).

Artemisia dracunculus	**% (v/v)**
ESTRAGOLE	79,36
trans-β-OCIMENE	7,93
cis-β-OCIMENE	7,12
LIMONENE	2,38
α-PINENE	0,76
METHYLEUGENOL	0,40
EUGENOL	0,25
BICYCLOGERMACRENE + α-FARNESENE	0,21
ALLO-OCIMENE ISOMERE	0,14
β-MYRCENE	0,13
GERMACRENE D	0,12
METHYL CINNAMATE	0,12
β-PINENE	0,10
γ-TERPINENE	0,10
TOTAL	**99,12**

Cinnamomum camphora ct linalool	
LINALOOL	98,35
trans-LINALOOL OXIDE	0,28
cis-LINALOOL OXIDE	0,16
FENCHOL	0,16
TOTAL	**98,95**

Cinnamomum cassia	
trans-CINNAMALDEHYDE	78,45
trans-o-METHOXY-CINNAMALDEHYDE	10,75
CINNAMYL ACETATE	2,05
COUMARIN	2,01
BENZALDEHYDE	0,85
PHENYLETHYL ALCOHOL	0,59
BENZENE PROPANAL	0,58
2-METHOXY-BENZALDEHYDE	0,52
α-COPAENE	0,3
SALICYLALDEHYDE	0,23
BORNEOL	0,14

cis-CINNAMALDEHYDE		0,14
γ-MUUROLENE		0,13
2-PHENYLETHYL ACETATE		0,13
CINNAMYL ALCOHOL		0,13
β-CARYOPHYLLENE		0,12
δ-CADINENE		0,12
NEROLIDOL		0,11
STYRENE		0,1
β-BISABOLENE		0,1
BENZYLPROPANOL		0,1
SPATHULENOL		0,1
	TOTAL	**97,75**

Melissa officinalis	
β-CARYOPHYLLENE	23,46
GERANIAL	20,94
NERAL	15,82
GERMACRENE D	11,52
trans-β-OCIMENE	3,5
CITRONNELLAL	2,89
δ-CADINENE	1,65
α-HUMULENE	1,54
GERANYL ACETATE	1,27
GERANIOL	1,22
6-METHYL-5-HEPTEN-2-ONE	1,2
ISOPULEGOL + PHOTOCITRAL B	0,97
α-COPAENE	0,93
α-FARNESENE + BICYCLOGERMACRENE	0,73
CARYOPHYLLENE OXIDE	0,68
LINALOOL	0,6
NEROL	0,58
Z,E-α-FARNESENE ISOMERE	0,56
α-MUUROLENE	0,56
PHOTOCITRAL A	0,55
E-β-FARNESENE	0,48
β-ELEMENE	0,44
ISONERAL	0,4
CITRONELLOL	0,4
cis-β-OCIMENE	0,39

METHYL CITRONELATE		0,38
γ-CADINENE		0,38
α-CADINOL		0,38
β-BOURBONENE		0,36
1-OCTEN-3-OL		0,35
METHYL NERATE		0,35
ISOGERANIAL		0,31
γ-MUUROLENE + α-TERPINEOL		0,31
β1-CUBEBENE		0,27
β-MYRCENE		0,22
ε-CADINENE		0,21
β-CUBEBENE		0,21
α-MUUROLOL		0,21
LIMONENE		0,18
T-CADINOL		0,17
GERMACRA-1,5-DIEN-4-OL		0,15
3-OCTANONE		0,13
β-BISABOLENE		0,12
α-AMORPHENE		0,11
ALLO-AROMADENDRENE		0,1
ISOCARYOPHYLLENE OXIDE		0,1
GERANIC ACID		0,1
	TOTAL	**98,38**

***Origanum compactum* (Lot OCH13)**	
CARVACROL	39,95
THYMOL	19,51
γ-TERPINENE	16,23
p-CYMENE	10,86
β-CARYOPHYLLENE	1,93
α-TERPINENE	1,89
β-MYRCENE	1,63
LINALOOL	1,56
α-THUJENE	0,71
α-PINENE	0,61
TERPINENE-4-OL	0,53
1-OCTEN-3-OL	0,29
LIMONENE	0,27
α-TERPINEOL	0,27

β-PHELLANDRENE + 1,8-CINEOLE		0,23
α-PHELLANDRENE		0,21
CARYOPHYLLENE OXIDE		0,15
3-OCTANONE		0,13
trans-THUJANOL		0,13
β-PINENE		0,12
cis-LINALOOL OXIDE		0,12
TERPINOLENE		0,11
α-HUMULENE		0,11
p-CYMENE-8-OL		0,11
CAMPHENE		0,10
δ-CADINENE		0,10
CARVACROL ISOMERE		0,10
	TOTAL	**97,96**

Origanum compactum **(Lot OF10299)**	
CARVACROL	43,67
THYMOL	19,52
γ-TERPINENE + trans-β-OCIMENE	16,16
p-CYMENE	7,72
α-TERPINENE	1,88
β-CARYOPHYLLENE	1,69
β-MYRCENE	1,6
LINALOOL	1,46
α-THUJENE	0,75
α-PINENE	0,56
TERPINENE-4-OL	0,54
LIMONENE	0,26
cis-LINALOOL OXIDE + α,p-DIMETHYLSTYRENE	0,26
α-TERPINEOL	0,25
1,8-CINEOLE + β-PHELLANDRENE	0,24
α-PHELLANDRENE	0,21
BORNEOL	0,19
trans-THUJANOL	0,14
β-PINENE	0,12
3-OCTANONE	0,12
CAMPHENE	0,1
1-OCTEN-3-OL	0,1
METHYL CARVACROL ETHER	0,1

CARYOPHYLLENE OXIDE		0,1
ISOCARVACROL		0,1
	TOTAL	**97,84**

Pimenta racemosa		
EUGENOL		45,23
β-MYRCENE		25,92
CHAVICOL		10,60
LIMONENE		2,79
LINALOOL		2,55
GERANYLGERANIADIENE		1,12
1-OCTEN-3-OL		1,10
3-OCTANONE		1,06
trans-β-OCIMENE		1,02
1,8-CINEOLE + β-PHELLANDRENE		0,93
TERPINENE-4-OL		0,57
δ-CADINENE		0,57
3-OCTANOL		0,56
p-CYMENE		0,53
β-CARYOPHYLLENE		0,48
α-PHELLANDRENE		0,40
α-FARNESENE + CARVONE		0,39
GERANYLGERANIADIENE ISOMERE		0,38
α-PINENE		0,31
α-TERPINEOL		0,29
α-COPAENE		0,26
γ-MUUROLENE		0,22
TERPINOLENE		0,20
α-TERPINENE		0,16
α-HUMULENE		0,15
γ-CADINENE		0,13
γ-TERPINENE		0,12
β-BISABOLENE + α-MUUROLENE		0,11
GERANIAL		0,10
	TOTAL	**98,25**

Appendix III: Supplementary material manuscript 2

Table A-III-1: EOs used in this study with their major components (≥10%) and assigned chemical class of components. AP = aerial parts; AP-S = aerial parts - seeds; B = bark; BB = berry branches; F = fruits; FB = flower buds; FL = flowers; FT = flowering tops; H = herbs; L = leaves; LT = leafy twigs; N = needles; O = oleoresin; P = peels; R = roots; RH = rhizome; T = twigs; T + B = twigs + bark; TF = twigs flowers; W = wood. # = organic EO; ct = chemotype; ssp = subspecies; cv = cultivar; var = variety. When no EOCs present at >10% (n=2): only EOC at highest concentration shown.

Plant species	Part of plant	Lot number	Major components (≥ 10% v/v)	% (v/v)	Chemical class
Abies alba	N	OF11341	α-PINENE	34.30	monoterpenes
			LIMONENE	19.42	monoterpenes
			β-PINENE	17.71	monoterpenes
			CAMPHENE	12.90	monoterpenes
Abies balsamea[#]	N	OF11276	β-PINENE	33.96	monoterpenes
			δ3-CARENE	14.67	monoterpenes
			α-PINENE	12.80	monoterpenes
Abies sibirica	N	OF10586	BORNYL ACETATE	28.45	esters
			CAMPHENE	22.00	monoterpenes
			δ3-CARENE	12.91	monoterpenes
			α-PINENE + α-THUJENE	11.91	monoterpenes + monoterpenes
Achillea millefolium	FT	OF10749	SABINENE	17.78	monoterpenes
			GERMACRENE D	16.36	sesquiterpenes
			β-PINENE	14.92	monoterpenes
Ammi visnaga[#]	S	OF8569	LINALOOL	35.82	monoterpenols
			ISOAMYL 2-METHYLBUTYRATE	15.53	esters
			AMYL ISOBUTYRATE	10.80	esters
Anethum graveolens	F	OF8420	CARVONE	50.44	ketones
			LIMONENE	43.08	monoterpenes
Angelica archangelica	R	OF1127	α-PINENE	22.01	monoterpenes
			δ3-CARENE	16.42	monoterpenes
			α-PHELLANDRENE	11.32	monoterpenes
			β-PHELLANDRENE	10.76	monoterpenes
Apium graveolens	F	OF10289	LIMONENE	63.69	monoterpenes
			β-SELINENE	17.55	sesquiterpenes

Artemisia dracunculus	FT	OF10105	ESTRAGOLE	79.36	phenol methyl ethers
Artemisia herba alba	FT	OF11480	α-THUJONE	61.45	ketones
			CAMPHOR	12.47	ketones
			β-THUJONE	10.39	ketones
Cananga odorata extra	FL	OF10390	GERMACRENE D	14.61	sesquiterpenes
Cananga odorata totum[#]	FL	OF9867	GERMACRENE D	18.23	sesquiterpenes
			b-CARYOPHYLLENE	12.45	sesquiterpenes
Canarium luzonicum	O	OF9870	LIMONENE	51.76	monoterpenes
			α-PHELLANDRENE	12.87	monoterpenes
Carum carvi	F	000027	CARVONE	54.09	ketones
			LIMONENE	43.78	monoterpenes
Cedrelopsis grevei[#]	W	OF9859	ISHWARANE	21.35	sesquiterpenes
Cedrus atlantica	W	OF10992	β-HIMACHALENE	43.34	sesquiterpenes
			α-HIMACHALENE	16.75	sesquiterpenes
Cedrus atlantica[#]	W	OF10799	β-HIMACHALENE	42.39	sesquiterpenes
			α-HIMACHALENE	17.09	sesquiterpenes
			γ-HIMACHALENE	10.17	sesquiterpenes
Cedrus deodara	W	OF10214	β-HIMACHALENE	38.29	sesquiterpenes
			α-HIMACHALENE	16.76	sesquiterpenes
			γ-HIMACHALENE	10.16	sesquiterpenes
Chamaemelum nobile	FL	OF10863	ISOBUTYL ANGELATE + ISOAMYL METHACRYLATE	32.93	esters + esters
			ISOAMYL ANGELATE	17.40	esters
Chamaemelum nobile[#]	FL	OF11255	METHYLAMYL ANGELATE	17.16	esters
			METHALLYL ANGELATE	12.84	esters
Cinnamomum camphora ct cineole[#]	L	OF11065	1,8-CINEOLE	56.28	ethers
			SABINENE	13.19	monoterpenes
Cinnamomum camphora ct linalool	W	OF10369	LINALOOL	98.35	monoterpenols
Cinnamomum cassia	T	OF10584	E-CINNAMALDEHYDE	78.45	aldehydes
			trans-o-METHOXY-CINNAMALDEHYDE	10.75	phenol methyl ethers

Cinnamomum cassia[#]	T	OF10588	E-CINNAMALDEHYDE	82.39	aldehydes
Cinnamomum zeylanicum	B	OF10850	E-CINNAMALDEHYDE	61.69	aldehydes
Cinnamomum zeylanicum	L	OF9780	EUGENOL	74.35	phenol methyl ethers
Cinnamosma fragrans[#]	L	OF10651	1,8-CINEOLE	42.28	ethers
Cistus ladaniferus ct pinene[#]	T	OF10502	CAMPHENE	29.98	monoterpenes
			α-PINENE	15.47	monoterpenes
			BORNYL ACETATE	11.79	esters
Citrus aurantifolia	F	OF10400	LIMONENE	44.61	monoterpenes
			γ-TERPINENE + Trans-β-OCIMENE	12.67	monoterpenes + monoterpenes
Citrus aurantium ssp amara	L	OF10467	LINALYL ACETATE	52.94	esters
			LINALOOL	20.71	monoterpenols
Citrus aurantium ssp amara	P	OF10404	LIMONENE	93.37	monoterpenes
Citrus aurantium ssp amara[#]	L	OF11484	LINALYL ACETATE	46.65	esters
			LINALOOL	26.70	monoterpenols
Citrus aurantium ssp amara[#]	FL	OF10993	LINALOOL	46.47	monoterpenols
Citrus aurantium ssp bergamia	P	OF10862	LIMONENE	47.94	monoterpenes
			LINALYL ACETATE	23.60	esters
Citrus bergamia ssp bergamia[#]	P	OF11052	LIMONENE	46.80	monoterpenes
			LINALYL ACETATE	26.33	esters
Citrus limon	P	OF11188	LIMONENE	67.01	monoterpenes
			β-PINENE	11.85	monoterpenes
Citrus limon	L	OF3114	LIMONENE	41.19	monoterpenes
			β-PINENE	18.38	monoterpenes
			CITRAL	10.80	aldehydes
Citrus limon[#]	P	OF11178	LIMONENE	64.31	monoterpenes
			β-PINENE	13.88	monoterpenes
Citrus paradisii	P	OF9436	LIMONENE	93.79	monoterpenes
Citrus paradisii[#]	P	OF9722	LIMONENE	94.61	monoterpenes
Citrus reticulata	L	OF9239	METHYL N-METHYLANTHRANILATE	54.32	esters
			γ-TERPINENE	23.83	monoterpenes

Citrus reticulata	P	OF3457	LIMONENE	87.50	monoterpenes
Citrus reticulata[#]	P	OF10644	LIMONENE	70.74	monoterpenes
			γ-TERPINENE	18.31	monoterpenes
Citrus sinensis	P	OF9238	LIMONENE	95.10	monoterpenes
Citrus sinensis[#]	P	OF11321	LIMONENE	95.09	monoterpenes
Copaifera officinalis	O	OF10996	β-CARYOPHYLLENE	54.20	sesquiterpenes
Coriandrum sativum	F	OF11183	LINALOOL	70.83	monoterpenols
Corydothymus capitatus	FT	OF11481	CARVACROL	66.65	phenols
Crithmum maritimum[#]	FT	OF9373	γ-TERPINENE + Trans-β-OCIMENE	48.83	monoterpenes + monoterpenes
			β-PHELLANDRENE	19.70	monoterpenes
Cuminum cyminum	F	OF9607	CUMINAL	31.94	aldehydes
			γ-TERPINENE	18.32	monoterpenes
			β-PINENE	16.71	monoterpenes
			p-CYMENE	16.31	monoterpenes
Cupressus sempervirens var stricta	T	OF10218	α-PINENE + α-THUJENE	58.01	monoterpenes + monoterpenes
			δ3-CARENE	13.18	monoterpenes
Cupressus sempervirens var stricta[#]	T	OF10846	α-PINENE + α-THUJENE	49.83	monoterpenes + monoterpenes
			δ3-CARENE	15.19	monoterpenes
Curcuma longa[#]	R	OF10876	ar-TURMERONE	38.76	ketones
			ar-TURMERONE	23.37	ketones
Cymbopogon citratus	AP	OF10881	CITRAL	69.57	aldehydes
Cymbopogon flexuosus	H	OF9994	CITRAL	74.40	aldehydes
Cymbopogon giganteus[#]	L	OF9770	trans-p-1,7-MENTHA-8,9-DIEN-2-OL	19.60	monoterpenols
			cis-p-MENTHA-2,8-DIEN-1-OL	17.84	monoterpenols
			cis-p-1,7-MENTHA-8,9-DIEN-2-OL	15.20	monoterpenols
			LIMONENE	12.56	monoterpenes
Cymbopogon martinii var motia	AP	OF10011	GERANIOL	78.99	monoterpenols
Cymbopogon martinii var motia[#]	AP	OF9950	GERANIOL	77.78	monoterpenols
			GERANYL ACETATE	10.96	esters

Cymbopogon nardus	AP	OF2106	GERANIOL	22.63	monoterpenols
Cymbopogon winterianus	AP	OF10851	CITRONELLAL	36.42	aldehydes
			GERANIOL	20.25	monoterpenols
			CITRONELLOL	12.19	monoterpenols
Daucus carota var sativus	F	OF11585	CAROTOL	38.56	sesquiterpenols
Daucus carota var sativus[#]	AP	OF4113	α-PINENE	23.79	monoterpenes
			β-BISABOLENE + β-SELINENE	21.59	sesquiterpenes + sesquiterpenes
			trans-METHYLISOEUGENOL	16.93	phenol methyl ethers
Elettaria cardamomum	F	OF12267	TERPENYL ACETATE	35.60	esters
			1,8-CINEOLE	32.76	ethers
Eucalyptus citriodora ct citronellal[#]	L	OF10647	CITRONELLAL	80.02	aldehydes
Eucalyptus dives ct piperitone[#]	L	OF10872	PIPERITONE + BICYCLOGERMACRENE	39.04	ketones + sesquiterpenes
			α-PHELLANDRENE	22.20	monoterpenes
			1,8-CINEOLE + β -PHELLANDRENE	10.79	ethers + monoterpenes
Eucalyptus globulus	L	OF10646	1,8-CINEOLE	80.51	ethers
Eucalyptus globulus[#]	L	OF11274	1,8-CINEOLE	81.99	ethers
Eucalyptus polybractea ct cryptone[#]	L	OF11142	p-CYMENE	28.14	monoterpenes
			SPATHULENOL	10.98	sesquiterpenol
Eucalyptus radiata ssp radiata	L	OF10865	1,8-CINEOLE	71.80	ethers
Eucalyptus radiata ssp radiata[#]	L	OF10720	1,8-CINEOLE	71.93	ethers
*Eucalyptus smithii**	L	OF9370	1,8-CINEOLE	77.31	ethers
Eugenia caryophyllus	FB	OF9948	EUGENOL	83.33	phenol methyl ethers
			EUGENYL ACETATE	11.58	esters
Eugenia caryophyllus[#]	FB	OF10583	EUGENOL	81.78	phenol methyl ethers
			EUGENYL ACETATE	12.90	esters
Ferula gummosa	O	OF12273	β-PINENE	56.53	monoterpenes
			δ3-CARENE	11.97	monoterpenes
Foeniculum vulgare[#]	AP- S	OF10796	trans-ANETHOLE	85.18	phenol methyl ethers

Fokiena hodginsii	BB	OF11589	FOKIENOL	39.08	sesquiterpenols
			NEROLIDOL	31.65	sesquiterpenols
Gaultheria fragrantissima[#]	L	OF11051	METHYL SALYCATE	99.39	esters
Gaultheria procumbens	L	OF11068	METHYL SALYCATE	99.37	esters
Helichrysum italicum ssp serotinum	FT	OF9441	NERYL ACETATE	19.88	esters
			γ-CURCUMENE + γ-MUUROLENE	15.04	sesquiterpenes + sesquiterpenes
			α-PINENE	14.77	monoterpenes
Helichrysum italicum ssp serotinum[#]	FT	OF10622	NERYL ACETATE	20.25	esters
			α-PINENE	15.47	monoterpenes
			γ-CURCUMENE	11.55	sesquiterpenes
Hyssopus officinalis var officinalis	FT	OF11287	ISOPINOCAMPHONE	36.22	ketones
			PINOCAMPHONE	18.68	ketones
			β-PINENE	10.74	monoterpenes
Illicium verum[#]	F	OF10399	trans-ANETHOLE	89.22	phenol methyl ethers
Inula graveolens[#]	FT	OF11143	BORNYL ACETATE	43.47	esters
			BORNEOL	19.59	monoterpenols
Juniperus communis ssp communis[#]	T + B	OF10654	α-PINENE + α-THUJENE	40.12	monoterpenes + monoterpenes
Juniperus communis var alpina[#]	T	OF4120	LIMONENE	26.29	monoterpenes
			β-PHELLANDRENE	16.71	monoterpenes
Juniperus oxycedrus	T	OF9732	δ-CADINENE	25.01	sesquiterpenes
			CUBENOL	11.33	sesquiterpenols
Juniperus virginiana	W	OF9364	THUJOPSENE	27.41	sesquiterpenes
			α-CEDRENE	24.11	sesquiterpenes
			CEDROL	16.77	sesquiterpenols
Laurus nobilis	L	OF11039	1,8-CINEOLE	41.40	ethers
Lavandula angustifolia spp angustifolia	FT	OF10864	LINALOOL	37.79	monoterpenols
			LINALYL ACETATE	33.41	esters
Lavandula angustifolia spp angustifolia[#]	FT	OF10951	LINALOOL	41.87	monoterpenols
			LINALYL ACETATE	31.34	esters

Lavandula latifolia	FT	OF10007	LINALOOL	39.10	monoterpenols
			1,8-CINEOLE + β-PHELLANDRENE	26.97	ethers + monoterpenes
			CAMPHOR	12.54	ketones
Lavandula latifolia[#]	FT	OF9693	LINALOOL	43.88	monoterpenols
			1,8-CINEOLE + β-PHELLANDRENE	25.92	ethers + monoterpenes
			CAMPHOR	10.82	ketones
Lavandula stoechas[#]	FT	OF11591	CAMPHOR	29.48	ketones
			FENCHONE	24.41	ketones
Lavandula x burnatii clone abrialis[#]	FT	OF10059	LINALOOL	36.12	monoterpenols
			LINALYL ACETATE	19.34	esters
Lavandula x burnatii clone grosso	FT	OF1743	LINALYL ACETATE	33.11	esters
			LINALOOL	31.07	monoterpenols
Lavandula x burnatii clone grosso[#]	FT	OF6689	LINALOOL	37.06	monoterpenols
			LINALYL ACETATE	29.68	esters
Lavandula x burnatii clone reydovan	FT	OF9108	LINALOOL	52.58	monoterpenols
			LINALYL ACETATE	18.43	esters
Lavandula x burnatii clone super	FT	OF10869	LINALOOL	36.28	monoterpenols
			LINALYL ACETATE	33.98	esters
Lavandula x burnatii clone super[#]	FT	OF10745	LINALOOL	33.86	monoterpenols
			LINALYL ACETATE	33.44	esters
Ledum groenlandicum[#]	TF	OF9694	SABINENE	25.18	monoterpenes
Leptospermum petersonii	L	OF10212	CITRAL	56.97	aldehydes
			CITRONELLAL	18.72	aldehydes
Levisticum officinale	R	OF9237	LIGUSTILIDE	42.85	phtalides
			(Z)-BUTYLIDENE PHTHALIDE	41.96	phtalides
Lippia citriodora	L	OF9771	LIMONENE	20.92	monoterpenes
			CITRAL + PIPERITONE	16.91	aldehydes + ketones
Litsea citrata	F	OF10225	CITRAL	71.80	aldehydes
			LIMONENE	12.90	monoterpenes
Litsea citrata[#]	F	OF11261	CITRAL	71.80	aldehydes

			LIMONENE	11.05	monoterpenes
Matricaria recutita	FL	OF10999	trans-β-FARNESENE	43.60	sesquiterpenes
Melaleuca alternifolia	L	OF11248	TERPINENE-4-OL	41.35	monoterpenols
			γ-TERPINENE	20.64	monoterpenes
Melaleuca alternifolia[#]	L	OF10388	TERPINENE-4-OL	38.38	monoterpenols
			γ-TERPINENE	22.23	monoterpenes
			α-TERPINENE	11.07	monoterpenes
Melaleuca cajeputi	L	OF10662	1,8-CINEOLE	69.15	ethers
Melaleuca cajeputi[#]	L	OF11405	1,8-CINEOLE	61.09	ethers
			α-TERPINEOL + γ-MUUROLENE	11.13	monoterpenols + sesquiterpenes
Melaleuca quinquenervia ct cineol	L	OF10731	1,8-CINEOLE	57.07	ethers
Melaleuca quinquenervia ct cineol[#]	L	OF10956	1,8-CINEOLE	55.18	ethers
Melissa officinalis	AP	OF10300	β-CARYOPHYLLENE	23.46	sesquiterpenes
			CITRAL	36.76	aldehydes
			GERMACRENE D	11.52	sesquiterpenes
Mentha arvensis	AP	OF10883	MENTHOL	42.68	monoterpenols
			MENTHONE	18.42	ketones
Mentha arvensis[#]	AP	OF9728	MENTHOL	39.61	monoterpenols
			MENTHONE	13.59	ketones
Mentha citrata	AP	OF9449	LINALYL ACETATE	36.47	esters
			LINALOOL	31.71	monoterpenols
Mentha x piperita	AP	OF10867	MENTHOL	37.61	monoterpenols
			MENTHONE	23.98	ketones
Mentha x piperita[#]	AP	OF11594	MENTHOL	33.05	monoterpenols
			MENTHONE	23.80	ketones
Mentha pulegium	AP	OF9582	PULEGONE	84.14	ketones
Mentha spicata[#]	AP	OF12639	CARVONE	56.35	ketones
			LIMONENE	12.68	monoterpenes
			trans-CARVEOL	11.9	monoterpenols

Myristica fragrans	F	OF10590	α-PINENE + α-THUJENE	23.79	monoterpenes + monoterpenes
			SABINENE	15.01	monoterpenes
			β-PINENE	14.25	monoterpenes
Myroxylon balsamum var pereiras	O	OF1706	DMSO		
Myrtus communis ct cineole[#]	L	OF9864	α-PINENE	51.52	monoterpenes
			1,8-CINEOLE	23.87	ethers
			LIMONENE	10.36	monoterpenes
Myrtus communis ct myrtenyl acetate	L	OF9391	1,8-CINEOLE	29.37	ethers
			α-PINENE + α-THUJENE	22.40	monoterpenes + monoterpenes
			MYRTENYL ACETATE	18.59	esters
			LIMONENE	11.78	monoterpenes
Myrtus communis ct myrtenyl acetate[#]	L	OF10882	1,8-CINEOLE	30.33	ethers
			α-PINENE	22.81	monoterpenes
			MYRTENYL ACETATE	18.18	esters
			LIMONENE	11.63	monoterpenes
Nardostachys jatamansi[#]	R	OF11047	CALARENE	9.49	sesquiterpenes
Ocimum basilicum ssp basilicum[#]	FT	OF10861	ESTRAGOLE	71.57	phenol methyl ethers
			LINALOOL	19.59	monoterpenols
Ocimum sanctum	L	OF11260	EUGENOL	50.45	phenol methyl ethers
			β-CARYOPHYLLENE	22.47	sesquiterpenes
Origanum compactum	FT	OF10299	CARVACROL	43.67	phenols
			THYMOL	19.52	phenols
			γ-TERPINENE + Trans-β-OCIMENE	16.16	monoterpenes + monoterpenes
Origanum compactum[#]	FT	OF11283	CARVACROL	39.44	phenols
			THYMOL	23.17	phenols
			γ-TERPINENE + Trans-β-OCIMENE	13.70	monoterpenes + monoterpenes
			p-CYMENE	10.89	monoterpenes
Origanum heracleoticum	FT	OF11288	CARVACROL	66.96	phenols
Origanum majorana	FT	OF10217	TERPINEOL	22.90	monoterpenols

			γ-TERPINENE	14.85	monoterpenes
			cis-THUJANOL	11.39	monoterpenols
Origanum majorana[#]	FT	OF9776	TERPINEOL	23.01	monoterpenols
			cis-THUJANOL	15.11	monoterpenols
			γ-TERPINENE	13.77	monoterpenes
Origanum majorana ct thujanol	FT	OF10871	cis-THUJANOL	21.41	monoterpenols
			TERPINEOL	19.67	monoterpenols
			γ-TERPINENE	12.46	monoterpenes
Pelargonium x asperum cv Bourbon[#]	L	OF12053	CITRONELLOL + d-CADINENE	22.20	monoterpenols + sesquiterpenes
			GERANIOL + CALAMENENE	16.14	monoterpenols + sesquiterpenes
			CITRONELLYL FORMATE	10.96	esters
Pelargonium x asperum	L	OF9858	CITRONELLOL	32.40	monoterpenols
			GERANIOL	14.07	monoterpenols
Petroselinum crispum	L	OF11587	1,3,8-p-MENTHATRIENE	20.75	monoterpenes
			α-PINENE	18.76	monoterpenes
			MYRISTICINE	13.64	phenol methyl ethers
			β-PINENE	12.74	monoterpenes
Picea mariana[#]	N	OF10298	BORNYL ACETATE	28.58	esters
			CAMPHENE	19.09	monoterpenes
			α-PINENE	14.24	monoterpenes
Pimenta racemosa	F	OF9871	EUGENOL	46.32	phenol methyl ethers
			β-MYRCENE	25.87	monoterpenes
			CHAVICOL	10.35	phenols
Pinus pinaster	O	OF11277	α-PINENE + α-THUJENE	74.27	monoterpenes + monoterpenes
			β-PINENE	17.07	monoterpenes
Pinus ponderosa	N	OF11050	β-PINENE	38.12	monoterpenes
			ESTRAGOLE	18.91	phenol methyl ethers
			δ3-CARENE	17.47	monoterpenes
Pinus sylvestris	N	OF11339	α-PINENE	40.96	monoterpenes
			β-PINENE	20.22	monoterpenes

			δ3-CARENE	16.12	monoterpenes
Pinus sylvestris[#]	N	OF2115	α-PINENE	40.76	monoterpenes
			β-PINENE	24.62	monoterpenes
Piper nigrum	F	OF9540	β-CARYOPHYLLENE	20.83	sesquiterpenes
			LIMONENE	19.07	monoterpenes
			α-PINENE + α-THUJENE	15.23	monoterpenes + monoterpenes
			β-PINENE	13.10	monoterpenes
			δ3-CARENE	12.94	monoterpenes
Pistacia lentiscus[#]	LT	OF9359	β-MYRCENE	16.73	monoterpenes
			α-PINENE	16.58	monoterpenes
			LIMONENE	13.96	monoterpenes
Pogostemon cablin	FT	OF10211	PATCHOULOL	30.15	sesquiterpenols
			α-BULNESENE	18.00	sesquiterpenes
			α-GUAIENE	14.98	sesquiterpenes
Pogostemon cablin[#]	FT	OF9954	PATCHOULOL	28.99	sesquiterpenols
			α-BULNESENE	19.70	sesquiterpenes
			α-GUAIENE	15.47	sesquiterpenes
Ravensara aromatica	B	OF9044	ESTRAGOLE	90.01	phenol methyl ethers
Ravensara aromatica[#]	L	OF11431	LIMONENE	16.45	monoterpenes
Rosmarinus officinalis ct camphor[#]	FT	OF11044	α-PINENE	21.00	monoterpenes
			1,8-CINEOLE	19.05	ethers
			CAMPHOR	17.28	ketones
Rosmarinus officinalis ct cineole	FT	OF10655	1,8-CINEOLE	42.01	ethers
			α-PINENE	13.72	monoterpenes
			CAMPHOR	12.85	ketones
Rosmarinus officinalis ct cineole[#]	FT	OF10408	1,8-CINEOLE	44.38	ethers
			α-PINENE	10.76	monoterpenes
			CAMPHOR	10.07	ketones
Rosmarinus officinalis ct verbenone[#]	FT	OF10075	α-PINENE + α-THUJENE	42.70	monoterpenes + monoterpenes

Salvia lavandulifolia	FT	OF11046	CAMPHOR	29.99	ketones
			1,8-CINEOLE	26.41	ethers
Salvia officinalis	FT	OF10880	α-THUJONE	37.64	ketones
			β-THUJONE	12.74	ketones
Salvia officinalis[#]	FT	OF9241	α-THUJONE	24.73	ketones
			CAMPHOR	22.23	ketones
			1.8-CINEOLE	11.19	ethers
Salvia sclarea[#]	FT	OF9454	LINALYL ACETATE	71.98	esters
			LINALOOL	15.56	monoterpenols
Santalum austrocaledonicum var austrocaledonicum	W	OF11042	(Z)-α-SANTALOL	43.93	sesquiterpenols
			(Z)- β-SANTALOL	18.51	sesquiterpenols
Satureja hortensis	FT	OF3340	γ-TERPINENE	42.45	monoterpenes
			CARVACROL	29.95	phenols
			p-CYMENE	10.07	monoterpenes
Satureja montana	FT	OF11247	CARVACROL	43.51	phenols
			γ-TERPINENE + Trans-β-OCIMENE	16.62	monoterpenes + monoterpenes
			p-CYMENE	13.86	monoterpenes
Solidago canadensis[#]	AP	OF10723	GERMACRENE D	28.46	sesquiterpenes
			α-PINENE	12.87	monoterpenes
Tanacetum annuum	L	OF10287	SABINENE	16.87	monoterpenes
			CAMPHOR	12.87	ketones
Thuya occidentalis	T	OF9451	α-THUJONE	52.15	ketones
			FENCHONE	16.59	ketones
Thymus mastichina	FT	OF9049	1.8-CINEOLE	52.44	ethers
			LINALOOL	20.98	monoterpenols
Thymus satureioides	FT	OF10106	BORNEOL	28.01	monoterpenols
			α-TERPINEOL	12.64	monoterpenols
Thymus satureioides[#]	FT	OF10589	BORNEOL	28.36	monoterpenols
			α-TERPINEOL	14.25	monoterpenols
			CAMPHENE	10.73	monoterpenes

Thymus serpyllum	FT	OF10659	p-CYMENE	15.62	monoterpenes
			CARVACROL	14.69	phenols
			THYMOL	12.93	phenols
			GERANIOL	10.51	monoterpenols
Thymus vulgaris ct geraniol	FT	OF9453	GERANIOL	59.00	monoterpenols
			GERANYL ACETATE	15.73	esters
Thymus vulgaris ct linalool[#]	FT	OF12998	LINALOOL	62.19	monoterpenols
Thymus vulgaris ct thymol[#]	FT	OF10842	THYMOL	36.39	phenols
			p-CYMENE	22.71	monoterpenes
			γ-TERPINENE	12.77	monoterpenes
Thymus zygis	FT	OF9050	THYMOL	48.13	phenols
			p-CYMENE	21.22	monoterpenes
Trachyspermum ammi	F	OF9576	THYMOL	35.24	phenols
			γ-TERPINENE	34.65	monoterpenes
			p-CYMENE	22.41	monoterpenes
Tsuga canadensis[#]	N	OF10884	BORNYL ACETATE	31.43	esters
			α-PINENE	20.69	monoterpenes
			CAMPHENE	15.3	monoterpenes
Valeriana officinalis	R	OF9234	BORNYL ACETATE	35.57	esters
			CAMPHENE	23.79	monoterpenes
Vetiveria zizanoïdes	R	OF10233	β-VETIVENENE	8.32	sesquiterpenes
Zingiber officinalis[#]	RH	OF11621	α-ZINGIBERENE	24.00	sesquiterpenes
			β-SESQUIPHELLANDRENE	10.85	sesquiterpenes
			CAMPHENE	10.34	monoterpenes

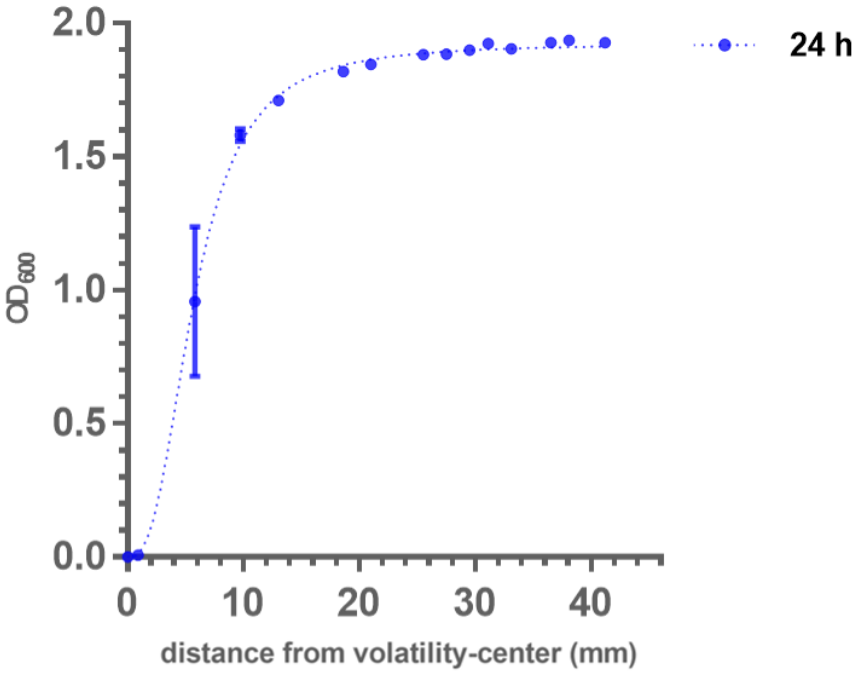

Figure A-III-1: The growth inhibitory effect of a volatile is largest in wells close to the volatility-center. Spectrophotometric assessment of *C. albicans* growth inhibition by *Litsea citrata* EO in the VMS assay after 24 hours of incubation. One data point represents the average of four to 12 wells, in accordance with number of wells per category shown in figure 6.1b. Error bars represent standard deviation.

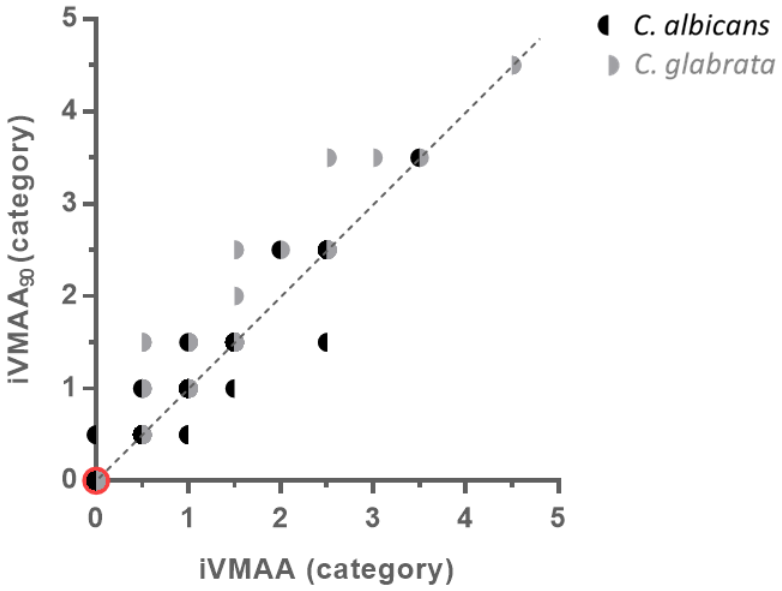

Figure A-III-2: There is a very strong correlation between iVMAA and iVMAA$_{90}$ for each *Candida* species. Scatterplot showing the correlation between iVMAA and iVMAA$_{90}$ of EO(C)s (n=212) against *C. albicans* (ρ=0.991, p<0.0001) and *C. glabrata* (ρ=0.991, p<0.0001). iVMAA = inhibitory vapor-phase-mediated antimicrobial activity (visual assessment). iVMAA$_{90}$ = iVMAA resulting in 90% reduction of growth as compared to control growth (spectrophotometric assessment).

Table A-III-2: Highly enriched EOCs used in this study with their purity and assigned chemical class.

EOC	Purity (%)	chemical class
trans-ANETHOLE	99	phenol methyl ethers
BENZYL BENZOATE	99	esters
(-)-BORNYL ACETATE	95	esters
CARVACROL	99	phenols
(-)-CARVONE	98	ketones
(+)-CARVONE	98	ketones
β-CARYOPHYLLENE	80	sesquiterpenes
1,8-CINEOLE	99	ethers
trans-CINNAMALDEHYDE	99	aldehydes
CITRAL	95	aldehydes
CITRONELLAL	95	aldehydes
CITRONELLOL	95	monoterpenols
p-CYMENE	97	monoterpenes
ESTRAGOLE	98	phenol methyl ethers
EUGENOL	99	phenol methyl ethers
FARNESOL	95	sesquiterpenols
FARNESYL ACETATE	NA	esters
GERANIOL	98	monoterpenols
GERANYL ACETATE	97	esters
(+)-LIMONENE	97	monoterpenes
(-)-LIMONENE	95	monoterpenes
LINALOOL	97	monoterpenols
LINALYL ACETATE	97	esters
METHYL EUGENOL	98	phenol methyl ethers
MYRCENE	90	monoterpenes
NEROL	97	monoterpenols
ALLO-OCIMENE	80	monoterpenes
β-OCIMENE	90	monoterpenes
α-PHELLANDRENE	NA	monoterpenes
α-PINENE	98	monoterpenes
(-)-β-PINENE	99	monoterpenes
(+)-PULEGONE	90	ketones
(-)-TERPINEN-4-OL	95	monoterpenols
γ-TERPINENE	97	monoterpenes
α-TERPINEOL	96	monoterpenols
TERPINYL ACETATE	95	esters
THYMOL (5:1 DMSO)	99	phenols

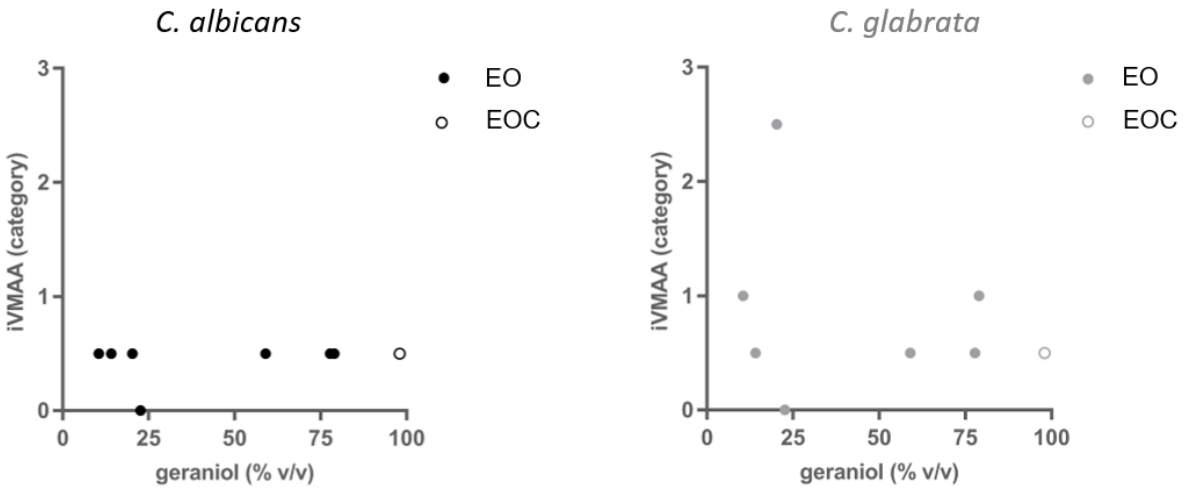

Figure A-III-3: No correlation could be observed between the geraniol concentration of an EO(C) and its iVMAA against each *Candida* species. Correlations between the iVMAA of an EO(C) and its geraniol concentration (>10%, n=8) for *C. albicans* (ρ=0.0825, p>0.99) and *C. glabrata* (ρ=-0.217, p=0.62).

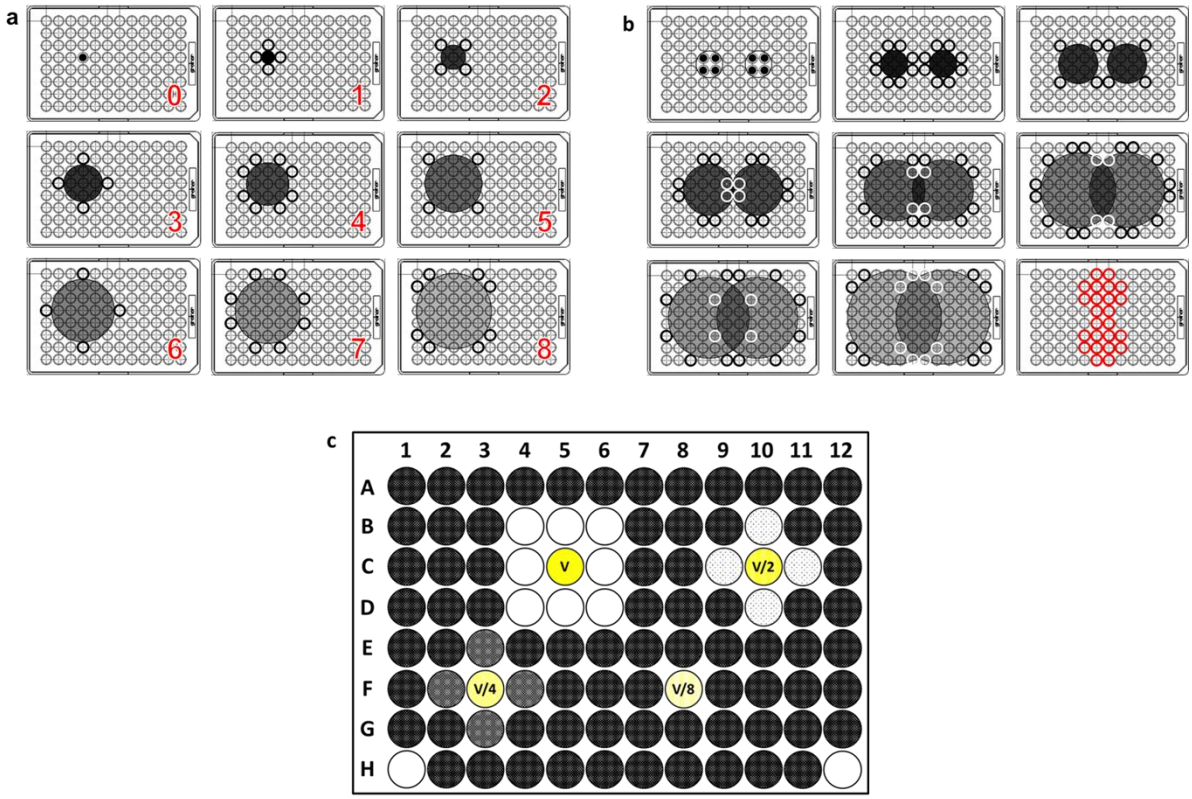

Figure A-III-4: The VMS assay is versatile as demonstrated by these examples of alternative set-ups. a: Changing the size of the volatility center affects the categories. Upper-left: volatility-center of one well. Upper-middle to bottom-right: First eight categories associated with a volatility-center of size one well. **b:** Using two volatility-centers allows for the detection of synergies between two volatiles. Upper-left: two volatility-centers; Upper-middle to bottom-middle: The first seven stages associated with using two volatility-centers of four wells; Bottom-right: The interaction zone between the two volatiles added in their respective volatility-center in which synergies can be detected. **c:** Testing multiple volumes of the same volatile using volatility-centers of one well allows for the determination of the minimal volume necessary to inhibit cell growth in all wells of the first category. V = volume.